THE MOLECULAR, GENETIC AND BIOCHEMICAL DISSECTION OF DEFENCE SIGNAL TRANSDUCTION IN *ARABIDOPSIS*

Mourad A. M. Aboul-Soud

Doctor of Philosophy

Institute of Cell & Molecular Biology

The University of Edinburgh

July 2002

بِسْمِ اللَّهِ الرَّحْمَٰنِ الرَّحِيمِ

وَقُلِ ٱعْمَلُوا۟ فَسَيَرَى ٱللَّهُ عَمَلَكُمْ وَرَسُولُهُۥ وَٱلْمُؤْمِنُونَ ۖ وَسَتُرَدُّونَ إِلَىٰ
عَٰلِمِ ٱلْغَيْبِ وَٱلشَّهَٰدَةِ فَيُنَبِّئُكُم بِمَا كُنتُمْ تَعْمَلُونَ ﴿١٠٥﴾

In the Name of Allâh, the Most Beneficent, the Most Merciful.

And say (Muhammad SAW): "Work (righteousness): Soon will Allah observe your work, and (so will) His Messenger, and the Believers. Soon you will be brought back to the All-Knower of what is hidden and what is open. Then, He will show you the truth of all what you used to do."

{Qura'n (9:105)}

Table of contents

Acknowledgements

First of all, I would like to thank Allah (SWT) for giving me the energy and health to begin and successfully accomplish this work.

I would like to take this opportunity to thank the following people:

I am grateful to the Darwin Trust of Edinburgh, and particularly Prof. K. Murray, for both the moral and financial support.

I would like to thank Dr. Gary Loake for his outstanding kindness, patience, guidance, and continuous support shown to me while working at his lab.

I would like to acknowledge the significant contribution of Dr. Xinwei Chen, Loake's lab, in mapping the *pcd1* gene.

I am thankful to Dr. Byung-Wook Yun, Loake's lab, for the help with in-gel MAPK assay.

I am also thankful to Dr. Lucy Harrier, Scottish Agricultural College, for her help in *Fusarium* transformation.

I am grateful to Luc-Jan Laarhoven, University of Nijmegen, for his help with the set-up of photoacoustic CO-laser for detection of NO emissions.

I am grateful to John Findlay and Patrick Hickey for their assistance with fluorescence and confocal microscopy, respectively.

I am grateful to the gardeners Bob and Bell for taking care of my plants

Last but not least, I would like to thank all my lab colleagues for their extraordinary spirit of teamwork, co-operation and assistance shown towards me.

Dedication

I would like to dedicate this thesis to my mother. This is in memory of her noble and unconditional love and continuous giving over the years.

Abstract

Systemic acquired resistance (SAR) is a pivotal defence response to pathogen attack that results in a broad-spectrum, long-lasting immunity throughout challenged plant tissues. However, little is known about the signal transduction events leading to the establishment of SAR in plants. To facilitate the identification of novel signal transduction components that are involved in the regulation of *p*athogenesis-*r*elated (*PR*) gene expression and the establishment of SAR, I have undertaken a T-DNA activation tagging approach. Chapter III presents and describes the results obtained during the identification and characterisation of one potential mutant. Thus, homozygous *Arabidopsis PR1a::luciferase* transgenic lines were transformed with the activation tagging vector SKI15. Hence, we generated and screened 8000 T-DNA activation tagged lines for dominant gain-of-function mutants that exhibit constitutive luciferase expression. One putative mutant was identified that exhibited high luciferase activity; constitutive hypersensitive response (HR)-like lesions in the absence of pathogen; and accelerated cell death; hence it was designated *p*otentiated *c*ell *d*eath *1* (*pcd1*). Moreover, histochemical and molecular analyses revealed that *pcd1* leaves accumulate high levels of hydrogen peroxide (H_2O_2) and constitutively express a battery of antioxidant and defence-related genes. Furthermore, biochemical analyses indicated that *pcd1* plants contain high constitutive levels of the signal compound salicylic acid (SA) and elevated peroxidase and constitutive mitogen activated protein kinase (MAPK) activities. Interestingly, *pcd1* plants exhibited heightened resistance against biotrophic bacterial and fungal pathogens. Importantly, epistasis analysis indicated that the HR-like lesions and H_2O_2 accumulation, characteristic to the *pcd1* phenotype, are dependent on SA but independent of ethylene and jasmonic acid. The *pcd1* mutation was mapped to the lower arm of chromosome I.

Recently, nitric oxide (NO) importance during plant disease resistance has been highlighted. In chapter IV, I present and discuss the results obtained during the investigation of the ability of NO to trigger increases in cytosolic calcium concentration ($[Ca^{2+}]_{cyt}$). During the course of this investigation, transgenic *Arabidopsis* plants expressing the luminescent Ca^{2+}-sensitive protein aequorin have been employed. In chemiluminometer and *in vivo* Ca^{2+} imaging assays, the NO-donor sodium nitroprusside (SNP) brought about a strong, instantaneous, reproducible, and dose-dependent rise in $[Ca^{2+}]_{cyt}$. Moreover, the observed rise in $[Ca^{2+}]_{cyt}$ was shown to be NO-specific and not associated to its decomposition products. Interestingly, $_L$-arginine, the substrate for nitric oxide synthase (NOS), led to an instantaneous elevation in $[Ca^{2+}]_{cyt}$ that was stronger than that obtained with SNP. Plants treated with the avirulent bacterial pathogen *Pseudomonas syringae* DC3000 carrying the avirulent gene *AvrB* {*Pst*DC3000 (*AvrB*)} exhibited no HR-specific rise in $[Ca^{2+}]_{cyt}$. Moreover, using photoacoustic CO-laser spectroscopy I failed to detect any NO emissions from *Pst*DC3000 (*AvrB*) treated plants. Furthermore, I successfully engineered transgenic plants containing the bacterial gene nitric oxide dioxygenase (*NOD*), encoding an enzyme known to oxidise NO to nitrate, under the control of the 35S constitutive promoter from cauliflower mosaic virus (CaMV). Moreover, molecular analyses, performed on *35S::NOD* transgenic plants, revealed that the *NOD* gene is correctly transcribed and translated to constitutive levels. Interestingly, no significant difference in the level of resistance of *35S::NOD* plants, compared to wild-type plants, was observed against the bacterial virulent pathogen *Pseudomonas syringae* DC3000.

Currently, gene transfer studies in *Fusarium* are hampered by the absence of an efficient transformation system. Recently, particle bombardment technology has been successfully employed to transform a number of filamentous fungal pathogens. In chapter V, we present and discuss the results of transforming the vascular wilt *Fusarium oxysporum* via particle bombardment. We utilised this approach to introduce a chimeric gene comprising the *Aspergillus nidulans g*lyceraldehyde *p*hospho*d*ehydrogenase *p*romoter (*Pgpd*) fused to a green fluorescent protein (GFP) reporter gene. A transformation efficiency of 45 transformants per µg of plasmid DNA was routinely achieved. Moreover, the *Pgdp* promoter directed a strong cytoplasmic expression of the GFP marker in transformed *F. oxysporum* monitored via fluorescence and confocal microscopy. Importantly, a pathogenicity assay undertaken on *Arabidopsis* seedlings with a selected transformant revealed that virulence was retained following transformation. Furthermore, in a similar fashion to wild-type *F. oxysporum*, this transformant activated an *Arabidopsis* defence gene promoter::*luciferase* fusion, as reported by ultra low-light imaging.

List of Abbreviations

λ	wavelength
°C	degrees Celsius
μCi	microcurie
μl	microlitre
ABA	abscisic acid
ACC	1-aminocyclopropane-1-carboxylic acid
ATP	adenosine triphosphate
bar	Basta resistance gene
BSA	bovine serum albumin/ bulked segregant analysis
CaMV	cauliflower mosaic virus
CAT	catalase`
CC	Coiled coil domain
cfu	colony forming units
cm	centimetre
cM	centimorgan
Col-0	*Arabidopsis* ecotype Columbia
CP	capsid protein
DAB	3,3-diaminobenzidine
DMSO	dimethylsulphoxide
DNA	deoxyribonucleic acid
DTT	dithiothreitol
eds	enhanced disease susceptibility mutant
EDTA	ethylenediaminetetraacetic acid
EGTA	ethylene glycol-bis (beta-aminoethyl ether) N,N,N',N'-tetraacetic acid
EEs	endogenous elicitor
ET	ethylene
g	gram
GFP	green fluorescent protein
HABS	high affinity binding site
H_2O_2	hydrogen peroxide
hph	hygromycin B resistance gene
HPLC	high-performance liquid chromatography
HR	hypersensitive response
hr	hour
hrp	hypersensitive reaction and pathogenicity
HRT	hypersensitive response to TCV
ICS	isochorismate synthase

IPM	integrated pest management
JA	jasmonic acid
kb	kilobasepairs
KB	King's B medium
kD	kilodalton
KPB	potassium phosphate buffer
l	litre
LB	Luria Broth medium
L*er*	*Arabidopsis* ecotype Landsperg *erecta*
LRR	Leucine-rich repeat
luc	luciferase
M	molar
MAPK	mitogen activated protein kinase
MBP	myelinbasic protein
MBq	megabecquerel
Me-JA	methyljasmonate
mg	milligram
min	minute
ml	millilitre
mM	millimolar
MS	Murashige and Skoog medium
ng	nanogram
nm	nanometre
NBS	nucleotide binding site
OB	oxidative burst
OD	optical density
PAGE	polyacrylamide gel electrophoresis
PAL1	phenylalanine-ammonia lyase 1
pcd1	potentiated cell death 1 mutant
PCR	polymerase chain reaction
PDA	potato dextrose agar
PGs	endopolygalacturonases
PGIPs	endopolygalacturonase-inhibiting proteins
pH	-log $[H^+]$
POD	peroxidase
psi	pound per square inch
Pst	*Pseudomonas* syringae pv. *tomato*
R	resistance gene
RFU	relative fluorescence units
RIL	recombinant inbred lines

RLU	relative light units
RNA	ribonucleic acid
ROS	reactive oxygen species
RPW8	resistance to powdery mildew 8 gene
rpm	revolutions per minute
s	second
SA	salicylic acid
SA:CC	signal anchor:coiled coil
SAG	salicylic acid glucoside
SAR	systemic acquired resistance
sdH_2O	sterile distilled water
SNP	single nucleotide polymorphism/ sodium nitroprusside
SSLP	simple sequence length polymorphism
TCA	trichloroacetic acid
TIR	Toll-Interleukin receptor domain
TMV	tobacco mosaic virus
Uk-4	*Arabidopsis* ecotype Umkirch 4
UV	ultraviolet
V	volts
v/v	volume/volume
w/v	weight/volume

List of Figures

List of Tables

CHAPTER I

1 LITERATURE REVIEW

" We see our cattle fall and our plants wither without being able to render them assistance, lacking as we do understanding of their condition"

(J. C. Fabricius, 1745-1808)

1.1 Devastation of plant diseases worldwide

Like animals and humans, plants are continually exposed to pathogen attack. The range of phytopathogenic organisms that attack plants is diverse and includes viruses, mycoplasma, bacteria, nematodes, protozoa, and parasites. Plant diseases affect the productivity of all kinds of plants, and thereby affect one of the basic prerequisites for a healthy life for humans. Destruction of food and feed crops by diseases has been an all too common occurrence in the past. Indeed, ancient chronicles of famine, plagues, and epidemics show that some of the more serious plant diseases, such as rusts, smuts and mildews, were recognised soon after the emergence of organised agriculture (Agrios, 1997). Plant disease has resulted in malnutrition, starvation, and migration of people and animals on numerous occasions, several of which are well documented in history. The devastating epidemics of late blight of potato in the 1840s in Northern Europe and particularly Ireland, which was caused by the fungus *Phytophthora infestans* (Now classified as an Oomycetes), is an example. Late blight absolutely destroyed the potato crop in Ireland which caused widespread famine that resulted in the death of at least a quarter of a million people and the emigration of more than one and a half million people from Ireland to the United States (Agrios, 1997). Some examples of plant diseases that have caused severe losses and health hazards in the past are shown in Table 1.1.

Table 1.1.: Examples of severe losses caused by plant diseases worldwide (Adapted from Agrios, 1997)

Disease	Location	Comments
Fungal diseases		
1. Cereal rusts	Worldwide	Frequent severe epidemics; huge annual losses
2. Cereal smuts	Worldwide	Continuous losses on all grains
3. Ergot of rye and wheat	Worldwide	Poisonous to humans and animals
4. Late blight of potato	Cool, humid climates	Annual epidemics, e.g. the great Irish famine (1845-1846)
5. Brown spot of rice	Asia	Epidemics, e.g., the great Bengal famine (1943)
6. Southern corn leaf blight	U.S.A	Epidemic 1970, $1 billion lost
7. Powdery mildew of grapes	Worldwide	European epidemics (1840s-1850s)
8. Downy mildew of grapes	U.S.A., Europe	European epidemic (1870s-1880s)
9. Downy mildew of tobacco	U.S.A., Europe	European epidemic (1950s-1960s); epidemic in North America (1979)
10. Chestnut blight	U.S.A.	
11. Dutch elm disease	U.S.A. Europe	Destroyed American elm trees (1930 to date)
12. Coffee rust		Destroyed all coffee in Southeast Asia (1870s-1880s)
13. Banana leaf spot (Sigatoka) disease	Worldwide	Great annual losses
14. Rubber leaf blight	South America	Destroys rubber tree plantations
Viral diseases		
15. Sugarcane mosaic	Worldwide	Great losses on sugarcane and corn
16. Sugar beet yellows	Worldwide	Great losses every year
17. Citrus quick decline (tristeza)	Africa, Americas	Million of tree being killed
18. Swollen shoot of cacao	Africa	Continuous heavy losses
19. Pulm pox or sharka	Europe	Spreading severe epidemics on plums, peaches, apricots
20. Barley yellow dwarf	Worldwide	Important on small grains worldwide
21. Tomato yellow leaf curl	Mediterranean, Caribbean basin	Severe losses of tomatoes, beans, etc.
22. Tomato spotted wilt virus	Worldwide	On tomato, tobacco, peanuts, ornamentals, etc.
Bacterial diseases		
23. Citrus canker	Asia, Africa, Brazil, U.S.A.	Caused eradication of millions of trees in Florida in 1910s and again in the 1980s and 1990s
24. Fire blight of pome fruits	North America, Europe,	Kills numerous trees annually
25. Soft rot of vegetables	Worldwide	Huge losses of fleshy vegetables
Phytoplasmal diseases		
26. Peach yellows	Eastern U.S.A., Russia	10 million peach trees killed
27. Pear decline	Pacific coast and Canada (1960s), Europe	Millions of pear trees killed
Nematode diseases		
28. Root knot	Worldwide	Continuous losses on vegetables and most other plants
29. Sugar beet cyst nematode	Severe in Northern Europe and western U.S.A.	Continuous severe annual losses on sugar beets

During the twentieth century there has been a dramatic explosion in the human population. Inspite of recent efforts to reduce the rate of population growth, the increase in the world population each year and the additional demand for food, energy, and other resources from our planet are frightening. At the current growth rate of 1.70% annual growth, the world population has reached 6.2 billion on the year 2000 (double of that of 3.2 billion in the mid sixties). Currently the world population increases by 1 billion every 11 years. Paradoxically, the developing countries, in which from 50 to 80% of the population is engaged in agriculture, have the lowest agricultural output, their people are living on a substandard diet, and they have the highest population growth rates (2.64%) (FAO, 1993).

It is estimated that even today some two billion people suffer from hunger or malnutrition or both. To feed these people and the additional millions to come in the next few years, all possible methods of increasing the world food supply are currently being pursued, including (1) expansion of crop acreage, (2) improved methods of cultivation, (3) increased fertilisation, (4) use of improved varieties of crops, (5) increased irrigation, and (6) improved crop protection. There is no doubt that the first five of the above measures must provide the larger amounts of food needed. Crop protection from pest and diseases can only reduce the amount lost after the potential for increased food production has been attained by proper utilisation of all means possible. Worldwide, a total of **33.7 %** (one-third) of the potential preharvest crop production is destroyed due to diseases (Table 1.2), including the 9-20% postharvest losses to pests brings the total (preharvest and postharvest) food losses to pests for the entire world to about **48%** of all food crops, inspite of all types of pest controls used. It is estimated that the annual production for all agricultural crops worldwide is about $1,250 billion (1995). Of this, about **$500 billion** worth of produce is lost annually. An additional loss of about **$300 billion** would occur annually, but is averted by the use of various crop protection practices (Oerke *et al.*, 1994 and FAO, 1993).

Table 1.2: Estimated percentages of world crop production preharvest losses to disease, insects and weeds of the year 1993 (Adapted from Agrios, 1997).

Crops	Crop % lost to			Total of crop lost (%)
	Disease	Insects	Weeds	
Cereals	9.2	13.9	11.4	34.5
Potatoes	21.8	6.5	4.0	32.3
Other root crops	16.7	13.6	12.7	43.0
Sugar beets	10.4	8.3	5.8	24.5
Sugarcane	19.2	20.1	15.7	55.0
Legumes	11.3	13.3	8.7	33.3
Vegetables	10.1	8.7	8.9	27.7
Fruits	12.6	7.8	3.0	23.4
Coffee-cocoa-tea	17.7	12.1	13.2	42.4
Oil crops (oil equiv.)	9.8	10.5	10.4	30.7
Fibre crops	11.0	12.9	6.9	30.8
Tobacco	12.3	10.4	8.1	30.8
Natural rubber	15.0	12.2	9.7	25.0
AVERAGE	**11.8**	**12.2**	**9.7**	**33.7**

Agricultural systems are in many ways the opposite of natural biological communities. Modern crop husbandry entails growing huge numbers of genetically uniform plants crowded together over large areas. Nutrients, water or both are applied in quantities sufficient to ensure vigorous crop growth. Any pest, pathogen or weed able to thrive under these ideal conditions therefore has the potential for explosive multiplication and spread, free from the usual constraints encountered in a diverse natural community. One important aspect of crop production is to prevent such disease outbreaks, or if they occur to restrict population of the pathogens or pests to levels which do not adversely affect the performance of the crop (Jarosz and Davelos, 1995).

1.2 Approaches to disease management

A number of different approaches are available to the grower to prevent or limit the damage caused by plant pathogens. These include: (1) exclusion of the pathogen by using pathogen-free area, clean seed material and applying quarantine, (2) reduction of inoculum by soil treatment, treatment of seed materials, rotation, and biological control, (3) reduce rate of pathogen multiplication by using rate-reducing plant resistance, chemical control and biological control, (4) integrated control programmes combining several approaches. From a historical perspective, many of the problems encountered in crop protection have arisen from a 'quick-fix' approach, in which a simple strategy has been used, often intensively, to control a disease or pest. The recent history of breeding for disease resistance has interesting parallels with developments in chemical control. 'Boom-and bust' apply equally well to resistance genes and selective fungicides. The variability and adaptability of pathogens demands a more subtle approach to disease control, in which more than one strategy is deployed.

The most cost effective, durable and environmentally acceptable strategies for disease management usually entail the use of several, co-ordinated complementary approaches in what is called **I**ntegrated **P**est **M**anagement (**IPM**). Pressures to look for novel alternative and/or complementary approaches driven the introduction of the technology of engineering plant disease resistance based on transgenic plants. The development of techniques for the stable transformation of plants has opened up apparently limitless opportunity for engineering novel pest- and disease-resistant crops. It is now possible to introduce genes from unrelated plants, or more exotic sources such as animals or even microorganisms. The technology is still in its infancy, and for some crops, such as cereals, is not yet routine, but the first generation of transgenic crops are now being tested in the field and, apart from the legislative questions concerning release of recombinant organisms, there is no reason why this approach should not become a normal part of the breeding process. There are now numerous examples of plants engineered for improved resistance to pathogens (Table 1.3); they include genes

conferring resistance to fungi, bacteria or viruses. The large majority are still at an experimental stage, and are being tested in model plants such as tobacco and potato. Nevertheless, in the next phase commercial crops and species less amenable to transformation, such as major cereals, will become available. Identifying novel genes encoding defence functions would make it possible to clone such genes and transfer them to new host species. This approach will undoubtedly be of value in extending the genetic option for disease control to the plant breeder, but has yet to be exposed on a large scale in the field. Once this been accomplished, this approach offers a promising potential as a component of an IPM strategy (Lucas, 1998).

Table 1.3: Some examples of genetically engineered crops with enhanced resistance to pathogens (Lucas, 1998).

Introduced gene(s)	Plant	Target pathogen(s)
		Fungi
Chitinase	Tobacco	*Rhizoctonia solani*
Chitinase + glucanase	Tobacco	*Cercospora nicotianae*
PR-1	Tobacco	*Peronospora tabacina*
Ribosome-inactivating protein	Tobacco	*Rhizoctonia solani*
Stilbene synthase	Tobacco	*Botrytis cinerea*
		Bacteria
Hordothionin	Tobacco	*Pseudomonas tabaci*
Lysozyme	Potato	*Erwinia carotovora*
		Viruses
Virus coat protein	Tobacco	Tobacco mosaic virus
	Potato	Potato viruses X and Y
Virus replicase	Tobacco	Tobacco mosaic virus
	Potato	Potato viruses X and Y
		Potato leaf roll virus
Antisense RNA	Potato	Potato virus Y
		Potato leaf roll virus
Antiviral protein	Tobacco	Cucumber mosaic virus
	Potato	Potato viruses X and Y

1.3 Plant defence strategies employed against pathogens

1.3.1 Constitutive versus inducible defence strategies

Although plants are constantly exposed to a vast arrays of phytopathogenic organisms, both above and below the ground, disease rarely develops from these contacts. In fact, resistance is the rule in plants, and susceptibility to infection is a rare exception. This observation suggests that plants must possess highly effective mechanisms for preventing parasitism and predation, or at least limiting their effects. Because plants lack a circulatory system and antibodies, they have evolved a defence mechanism that is distinct from the vertebrate immune system (Staskawicz *et al.*, 1995). In contrast to animal cells, each plant cell is capable of defending itself by means of a combination of passive (constitutive) and active (inducible) defence systems. Passive defence mechanisms include: anatomical and physical barriers (e.g. cell wall, cuticle, trichomes), preformed chemical inhibitors (e.g. phenols, alkaloids, saponins, tannins, cyanogenic glycosides and glucosinolates) and plant defence proteins (e.g., antifungal peptides, enzyme inhibitors, and hydrolases) (reviewed in Osbourn, 1996). Active defence mechanisms include: changes in host cell wall or wall appositions (e.g. deposition of callose, suberin, and lignin; oxidative cross-linking of cell wall proteins; and impregnation of oxidised phenols, e.g. melanins); hypersensitive response (HR), the production of pathogenesis-related (PR) proteins, and phytoalexin biosynthesis (reviewed in Lamb *et al.*, 1989; Hammond-Kosack & Jones, 1996).

1.3.2 Pathogen recognition

When a plant pathogen interacts with a potential host, it may successfully colonise the host and cause disease, in which case the pathogen is said to be virulent, the host is susceptible, and the interaction is compatible. Alternatively, the plant may respond to the

pathogen by rapidly activating a battery of defence responses, interfering with pathogen multiplication, and preventing disease. In this case, the pathogen is said to be avirulent, the host is resistant and the interaction is incompatible (Figure 1.1).

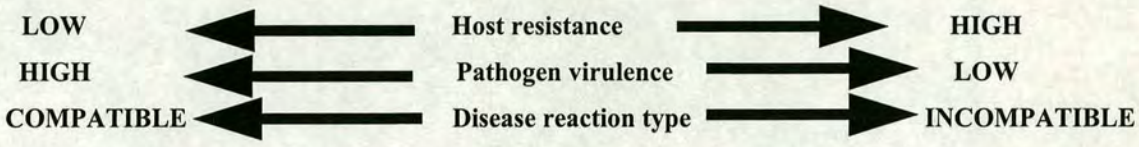

Figure 1.1: Relationship between host, pathogen and disease reaction type.

The outcome of plant-pathogen interactions often fits a "gene-for-gene", i.e. *R*-for-*Avr*, model proposed by HH Flor in the 1940s using flax (*Linum usitatissimum*) and its fungal rust pathogen *Melamposora lini*. In this model, resistance (incompatibility) results only when the pathogen carries a particular avirulence (*Avr*) gene that corresponds to a cognate resistance gene (*R*-gene) in the host. *R* and *Avr* genes are normally dominant. According to this model, it is an absolute prerequisite for resistance to occur that both *R* and *Avr* genes must present. If either gene is mutated or missing, compatibility or disease occurs (Figure 1.2) (Glazebrook, 1997a).

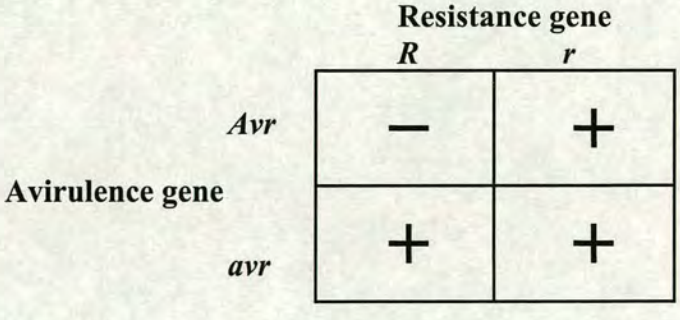

Figure 1.2: The quadratic check depicting the interaction between alleles of a host resistance gene (*R*) and a pathogen avirulence gene (*Avr*). *R* and *Avr* are dominant; *r* and *avr* are recessive or mutated; (+) is a compatible interaction; (-) is an incompatible interaction.

1.3.3 Avirulence (Avr) genes

1.3.3.1 Avirulence gene products versus non-specific elicitors

It is well established that microbial culture filtrates, or extracts from microbial cells, can act as potent inducers of plant defence responses. The active components of such extracts are generally referred to as elicitors. Thus, the term elicitor denotes any molecule which is able to induce any plant defence response, including the accumulation of pathogen-related (PR) proteins (section 1.4), cell-wall changes, and hypersensitive cell death (sections 1.3.5 and 1.3.6). Studies of the chemical nature of elicitors revealed that they are chemically diverse, and include polysaccharides, glycoproteins and proteins. Partial hydrolysis of fungal cell walls by host-endcoded hydrolytic enzymes (e.g. glucanase and chitinase) releases a mixture of breakdown oligosaccharide products, some of which are highly active in switching on host defence. Analysis of the glucans extracted from the soybean pathogen *Phytophthora megasperma* f. sp. *glycinea* identified the presence of a potent elicitor of phytoalexins. This elicitor has been shown to be a branched oligosaccharide containing seven sugars, termed a heptaglucoside. Radiolabelling experiments have detected a high-affinity binding site in soybean cell membranes. Thus, a specific ligand-receptor binding mechanism appears to be present in this type of interaction (Lucas, 1998).

Enogenous elicitors formulate another class of oligosaccharide elicitors that originate from the host cell wall, rather than from the pathogen, derived via the action of pathogen cell-wall-degrading enzymes {e.g. endopolygalacturonases (PGs)} during tissue colonisation. Fragments of pectic polymers (known as oligosaccharins), ranging from 10 to 13 sugar residues in size, are very effective elicitors of plant defence (Darvill *et al.*, 1994; Lucas, 1998). Fungal PGs catalyse the fragmentation and solubilization of pectic polymers by cleaving the internal bonds of homogalacturonan, which is the constituent of the "smooth region" of pectin. Intriguingly, the complete hydrolysis of homogalacturonan by fungal PGs can be hampered by polygalacturonase-inhibiting

proteins (PGIPs), localised in the cell wall of many plants. PGIPs, members of the large family of leucine-rich repeat (LRR) proteins, inhibit and modulate the activity of fungal PGs, thereby favouring the release of elicitor-active oligogalacturonides and prolonging its half-life (De Lorenzo *et al.*, 2001).

The specificity of elicitors varies widely. Thus, not all elicitors are regarded as avirulence gene products. For an elicitor to fulfil the gene-for-gene model (section 1.3.2), it must be the specific product of a pathogen avirulence gene which is recognised by the product of the appropriate host resistance gene to activate defence. Moreover, it should display activity on plants containing the complementary *R* gene, and be inactive on plants lacking this gene (Figure 1.2). Most of the elicitors described to date are non-specific in action, inducing defence responses in both resistant and susceptible hosts. Indeed, potent elicitors have been isolated from non-pathogens, such as the yeast *Saccharomyces cerevisiae* (Lucas, 1998). Thus, most elicitors cannot be classified as avirulence factors.

1.3.3.2 Bacterial *Avr* genes

The first *Avr* genes to be successfully isolated were all from bacterial pathogens. Superimposed on the basic capacity of a bacterium to be pathogenic, *Avr* genes determine the inability of a given bacterial strain to invade a host plant carrying the corresponding *R* gene. To date more than 30 bacterial *Avr* genes in pathovars of *Pseudomonas syringae* and *Xanthomonas* spp. (the most common bacterial phytopathogens) have been identified. Generally, *Avr* bacterial genes are either chromosomal or plasmid-borne, do not share sequence homology, and encode hydrophilic, soluble proteins that do not contain a classic signal peptide (Dangl, 1994; Hammond-Kosack & Jones, 1996). These *Avr* genes were identified by mutations which altered host range, followed by testing of random clones from genomic libraries to find those which restored the original host specificity (Lucas, 1998).

Compelling evidence suggests that the delivery of avirulence factors from bacteria is accomplished by their active secretion into the plant cell via a cluster of genes known as *hrp* gene (for *h*ypersensitive *r*esponse and *p*athogenicity). Like *Avr* genes, *hrp* genes are not expressed when the bacteria are grown in nutrient-rich culture media but are switched on when the pathogen grows under low nutrient media, conditions typical of the environment encountered within the apoplast of the host plant. *hrp* genes are localised in 20-25 kb gene clusters, have been found in all major Gram-negative genera of plant pathogenic bacteria and encode a type III protein secretion machinery that is highly conserved and was found first in mammalian pathogens (Lindgren *et al.*, 1986; He, 1996; Alfano & Collmer, 1997; Huek *et al.*, 1998). Several experiments strongly advocate the notion that Avr and probably other type-III effector proteins are directly translocated into the host cell. Firstly, transient expression of *Avr* genes within plant cells, in the absence of the pathogen, induced *R*-gene specific HR (Bonas & Van den Ackerveken, 1999). Secondly, the fact that recognition of the Avr proteins takes place within the plant cell implies that the signal molecule is the Avr protein itself that is transferred into the plant cell via the *hrp* type III secretion system. Moreover, type III secretion of the Avr proteins AvrB and AvrPto has been achieved by the heterologous expression of the *E. chrysanthemi hrp* gene cluster in *E. coli* (Ham *et al.*, 1998). Finally, using *in situ* immunogold labelling procedure, the extrusion of the effector protein AvrPto from the tip of the Hrp pilus has been visualised (Jin & He, 2001).

Mechanistically, it is presumed that a pilus-like surface appendage provides the link between the bacterial cell surface and the plant plasma membrane, through which Avr and other type-III effector proteins travel from the bacterium to be directly delivered into the plant cell cytoplasm. This hypothesis is advocated by the finding that among the protein of *P. syringae* secreted by the type III system is the subunit of a pilus-like bacterial surface structure, HrpA (Roine *et al.*, 1997).

It was not until recently that insights into the possible functions of *Avr* genes in pathogenic bacteria have been gained. It is intriguing to know that selective pressure exerted by the frequently occurring *R*-gene does not cause pathogens to shed off their *Avr* genes. Hence, the maintenance of *Avr* genes in pathogen population suggests that these genes play a role in virulence on susceptible hosts and losing them entails a high fitness cost (Table 1.4). This assumption is now supported strongly with numerous experiments (reviewed in Kjemtrup *et al*, 2000). It is assumed that Avr proteins contribute to virulence of the pathogen through direct interaction with host proteins resulting in inhibition of the host proteins required for establishing basal or specific defences. Accordingly it has been suggested that one plausible function of *R* genes is to guard virulence targets and to intercept incoming Avr proteins at, or close to, their cognate virulence target (Nimchuk *et al.,* 2001).

Table 1.4 summarises the functions and properties of selected Avr proteins. To achieve effective interception of Avr proteins, R proteins must be localised to similar cellular locations as their putative ligands (i.e. Avr proteins). Experimental evidence has been recently produced supporting this prediction. For example, myristoylation sequences in the *P. syringae* AvrRpm1, AvrB, and AvrPphB proteins are required for their localisation to the plasma membrane (Nimchuk *et al.*, 2001). Moreover, these sequences are required for bacteria expressing AvrRpm1 and AvrB to elicit a resistance response by plants expressing the cognate RPM1 protein, a plasma membrane-associated protein (Boyes *et al.*, 1998). AvrPto has also been shown to require N-myristoylation sites to localise to the host plasma membrane and trigger Pto function. Pto, the cognate R protein to AvrPto, also carries putative N-myristoylation sequences, indicating that Pto may be associated with the plasma membrane (Shan *et al.*, 2000). However, experimental evidence has not been presented, showing that Pto localises to the membrane, as yet.

Table 1.4: Properties of selected Avr proteins (from Nimchuk *et al.*, 2001 with modifications).

Avr Protein	Pathogen	Homology with and/or possible virulence function	Location in the plant cell*	Common domain for avirlulence and virulence function*	Location of the matching R gene product*
AvrPphC	*P. syringae* pv. *phaseolicola*	Interferes with the plant defence response	NR	NR	NR
AVRpt2	*P. syringae* pv. tomato	Interferes with the plant defence response	NR	NR	NR
AvRpm1	*p. syringae* pv. *maculicola*	Enhances growth	PM	No	PM
AvrPto	*P. syringae* pv. tomato	Enhances growth	PM	No	NR
AvrBst	*X. campestris* pv. *campestris*	Ubiquitin-like protease	NR	Yes	NR
AvrBs2	*X. campestris* pv. *vesicatoria*	Agrocinopine synthase from *A. tumefaciens*	NR	Recognition region localised in the portion with the highest homology to synthase	NR
AvrBs3	*X. campestris* pv. *glycinea*	Transcriptional activation domain required for virulence	Nucleus	Yes	NR
AvrXa7	*X. oryzae* pv. oryzae	Transcriptional activation domain required for virulence	Nucleus	Yes	NR
AvrPitA	*M. grisae*	Protease	NR	NR	NR
Avr9	*C. fulvum*	NR	PM	NR	PM
NIa	Potato Virus Y	Protease	NR	Yes	NR

• On the basis of experimental data; * on the basis of sequence analysis and experimental data; PM= plasma membrane; NR= not reported.

Consistent with the possible role of R proteins in intercepting their cognate Avr ligands, it has been recently shown that some of these proteins physically interact either inside or outside the host cell, using yeast two hybrid systems, leading to race-specific resistance. These include the interaction between the Pto and the AvrPto (Tang *et al.*, 1996). *Xa1* and *Xa21* are *R* genes that are important in conveying *Avr*-dependent resistance to the bacterial leaf pathogen *Xanthomonas oryzae* pv. *oryzae*. *Xa1*, a member of the CC-NBS-LRR (coiled coil-nucleotide binding site-leucine rich repeat) class (section 1.3.4), is predicted to reside within the cytoplasm, whereas *Xa21*, a member of the LRR-kinase

class, is likely to be a transmembrane protein with the LRRs exposed extracellularly. This suggests that recognition events of *X. oryzae* determinants can occur both extra- and intracellularly. For other proteins encoded by *R* genes there is no evidence for a direct interaction with the corresponding Avr protein; this implies that a third putative protein could make the physical link between the *Avr*- and *R* gene-encoded proteins. Recent reports highlight the fact that there is a continuous evolutionary war between pathogens and their host plants. Consistent with this concept, is the observation that some bacterial pathogens encode additional proteins that mask the presence of a particular Avr effector. As a classic example, in *Pseudomonas syringae* pv. *phaseolicola*, the type-III effector AvrPphF masks an unknown *Avr* gene. As a counter attack, hosts have developed the ability to recognise the masking effector. Moreover, the avirulence activity of AvrPphF can itself be masked by yet a third type-III effector, AvrphC, which is an avirulence determinant on soybean (Jackson *et al.*, 1999; Tsiamis *et al.*, 2000).

1.3.3.3 Fungal *Avr* genes

The most known and thoroughly-studied phytopathogenic fungal system, with regard to *R-Avr* interactions, is *Cladosporium fulvum* which causes leaf mould of tomato (*Lycopersicon esculentum* Mill.). *C. fulvum* enters via stomata and grows in the intercellular spaces of the leaf, eventually sporulating on the surface. The interaction between tomato and *C. fulvum* is based on a typical gene-for-gene relationship, implying that for each dominant *C. fulvum R* gene in tomato (*Cf*) there is a matching *Avr* gene in the fungus (de Wit & Joosten, 1999). The availability of plants carrying the *Cf R* genes *Cf-4* and *Cf-9* allowed the isolation of the matching fungal avirulence factors Avr4 and Avr9. Initial experiments focused on the interaction between the tomato gene *Cf-9* and races of the fungus possessing the putative *Avr9* gene. Pierre de Wit and colleagues (Wageningen University) employed an elegant experimental approach that led to the first successful cloning of an avirulence gene from a fungal pathogen. First, the pathogen

was inoculated onto a susceptible cultivar lacking the *Cf-9* to allow for the expression of the putative *Avr* gene product. Recovered intercellular fluids were then injected into leaves containing *Cf-9.* Thus, a necrotic HR reaction was observed. Interestingly, fluids recovered from compatible races did not induce necroses. Moreover, the fluids inducing a positive HR on *Cf-9* tomato were inactive on cultivars lacking this gene, or containing alternative *R* genes. This observation indicated that races of the fungus incompatible with *Cf-9* cultivars produced a specific elicitor recognised by this host gene. Next, the specific elicitor, i.e. *Avr9*, was purified and was found to be a peptide containing 28 amino acids. A specific oligonucleotide probe was designed, based on the amino acid sequence, to screen a cDNA library prepared from leaves infected with a *C. fulvum* race containing *Avr9*. A cDNA clone was identified and the cDNA could then be used to screen genomic DNA extracted from *C. fulvum* and to identify the *Avr9* sequence (Van Kan *et al.*, 1991). A similar approach was employed for the cloning of the *Avr4* gene; *Avr4* is a protein of 86 amino acids. The three dimensional structure of the Avr9 peptide revealed the presence of three anti-parallel beta-sheets, two solvent-exposed loops and three disulfide bridges typical for cystine-knotted peptides. In addition to all the Cys residues, the hydrophobic residue Phe21, present in one of the solvent-exposed loops, is essential for HR-inducing activity. To avoid recognition by tomato genotypes carrying the *Cf-4* or *Cf-9*, *C. fulvum* employs two distinct mechanisms. Natural strains that circumvent *Cf-4* recognition contain a single point mutation in the *Avr4* gene, resulting in virulent *avr4* alleles. Most of these mutations involve Cys residues. Secondly, strains of *C. fulvum* that circumvent the *Cf-9* resistance gene lack the complete *Avr9* gene in their genome; this does not seem to entail parasitic fitness cost. Little is known about the interaction between *Avr-* and *Cf* -encoded proteins. Binding studies have shown that both resistant and susceptible tomato genotypes contain a high affinity binding site (HABS) for the Avr9 peptide in plasma membranes of mesophyll cells, indicating that the Cf9 protein is not the primary receptor for Avr9. Thus, a model is presented in which the Cf9 protein could represent a molecule that interacts with the HABS-Avr9 complex. According to this model, HABS might represent a transmembrane LRR-receptor-like kinase (LRR-RLK), similar to the rice *R* gene product X*a21* (Table 1.5). Thus, such a

three component receptor complex is reminiscent of the complex encoded by the *CLAVATA* family of genes implicated in development of *Arabidopsis* (de Wit & Joosten, 1999).

Further *Avr* genes have now been cloned, including from *Magnaporthe grisea*, causal agent of the destructive blast disease of rice. This hemibiotrophic pathogen penetrates directly through the cuticle and outer cell wall into epidermal cells of the host. The fungus grows interacellularly , filling individual plant cells with fungal mycelium before moving on to the next cell. However, it is unknown whether the intracellular hyphae of this pathogen are enveloped with plant plasma membrane, as is the case for haustoria produced by biotrophic fungi, or if the pathogen breaches the plasma membrane. (Valent, 1997). Intense research has led to the isolation of the matched pair of resistance gene *Pi-ta* and avirulence gene *Avr-Pita* (previously referred to as *Avr-YAMO*) (Bryan *et al.*, 2000; Orbach *et al*, 2000). Avr-Pita is hypothesised to be a neutral zinc metalloprotease, although direct biochemical evidence is lacking (Orbach *et al.*, 2000). Avr-Pita has been shown to act as an elicitor molecule that directly binds the Pi-ta protein and triggers a signal transduction cascade leading to resistance. Moreover, a specific physical interaction between Avr-Pita and Pi-ta has been demonstrated in yeast two-hybrid system. Thus, it has been suggested that Avr-Pita is translocated from the fungus into the cytoplasm of the plant cell where it specifically binds to Pi-ta to initiate a *Pi-ta*-mediated defence response (Jia *et al.*, 2000).

1.3.3.4 Viral *Avr* genes

Comparatively little is known about *Avr* genes in phytopathogenic viruses. A classical model system for the study of gene-for-gene disease resistance is the interplay between tobacco mosaic virus (TMV) and tobacco plants bearing the *R* gene *N* was first described by F. O. Holmes (Holmes, 1938). The *N* gene, originally derived from *Nicotiana glutinosa*, a member of the TIR-NBS-LRR class of *R* genes (section 1.3.4),

confers resistance to TMV by mediating defence responses that function to limit viral replication and movement (Whitham *et al.*, 1994). A 126 kD replicase protein has been identified as the avirulence factor that triggers *N*-mediated HR (Padgett *et al.*, 1997). Moreover, using *Agrobacterium*-mediated expression strategies, it has been demonstrated that the putative helicase region of the replicase protein, termed TMV elicitor domain, is sufficient to elicit *N*-mediated defences (Erickson *et al.*, 1999). A second *R* gene, *N'*, derived from another related tobacco species, *N. Sylvestris*, also confers HR-mediated resistance to most strains of TMV. In contrast to the *N* gene, the TMV coat protein has been shown to act as an elicitor of the *N'* gene (Beachy, 1999).

In potato, the dominant *Ry R* gene, a member of the NBS-LRR class of *R* genes (Section 1.3.4), confers extreme resistance to all strains of potato virus Y (PVY) (Ross, 1952). The *Ry*-mediated resistance is similar to the resistance conferred by the potato *Rx* gene to potato virus X (PVX) in that resistant plants do not develop visible symptoms. The PVX coat protein has been implicated as the elicitor of the *Rx*-mediated resistance (Bendahmane *et al.*, 1995). In contrast, an intact active site of the NIa proteinase from PVY is required for *Ry*-mediated resistance response. Thus, NIa has been hypothesised to function either via releasing an endogenous elicitor by cleavage of a host-encoded protein or inactivating a negative regulator of *Ry*-mediated resistance (Mestre *et al.*, 2000).

The study of susceptibility and resistance responses of *Arabidopsis* to turnip crinkle virus (TCV) has been of particular interest because TCV is one of the few well-characterised plant viruses known to infect this model plant (Simon *et al.*, 1992). It has been previously established that a single dominant locus, termed *HRT*, is responsible for local HR formation in and the establishment of systemic resistance in *Arabidopsis* Di-17 plants inoculated with TCV (Dempsey *et al.*, 1997). Additionally, the TCV capsid protein (CP), in addition to having an obvious role in virulence, has been implicated as the elicitor of this resistance response. Moreover, the avirulence determinant of TCV has been mapped to the N-terminus of the CP (Wobbe & Zhao, 1998). The TCV CP triggers

the NBS-LRR (section 1.3.4) *HRT* gene in *Arabidopsis*. However, no direct interaction between TCV CP and *HRT* has been demonstrated yet. Interestingly, the *HRT*-mediated resistance of TCV CP has been shown to require a third factor, termed TCV-interacting protein (TIP). TIP, a member of the NAC-family of transcriptional activators that are implicated in the regulation of development of plant embryos and flowers, interacts with the TCV CP in yeast two-hybrid system. TCV expressing CP mutants that no longer interact with TIP are virulent on *HRT* plants (Ren *et al.*, 2000).

1.3.4 Resistance genes

While the identification and isolation of pathogen *Avr* genes controlling host range is an important advance in understanding the molecular basis of specificity, an even greater prize is to clone the corresponding host *R*-genes. This is because *R*-genes are the raw material selected by plant breeders, and isolation of such genes will create novel possibilities for their use in practice. Furthermore, understanding of how such genes work should suggest alternative ways of engineering crop resistance, and hopefully of improving the durability of resistance in the field. To date, a number of2 *R*-genes have been cloned and thoroughly characterised. The classes of the reported *R* genes so far from *Arabidopsis*, tomato, and rice are summarised in Table 1.5 (reviewed in Hammond-Kosack & Jones,1997; Bonas & Vanden Ackerveken, 1999; Jones, 2001).

Table 1.5: The major *R*-gene classes (Compiled from Bonas & Van den Ackerveken, 1999; and Jones, 2001 with modifications).

R-gene class	Member	Pathogen	Cognate *avr* gene	Protein structure	Predicted localisation	Arabidopsis homologs
LRR kinase	*Xa21* (Rice)	*X. oryzae*	?	LRR-TM-PK	MS, E	~ 174
eLLRs	*Cf-9* (Tomato)	*C. fulvum*	*avr9*	TM-eLRR	MS, E	~ 30
Pto	*Pto* (Tomato)	*P.s.* pv *tomato*	*avrPto*	PK	C	~ 100
TIR:NB:LRR	*RPS4* (Arabidopsis)	*P.s.* pv *pisi*	*avrRps4*	TIR-NBS-LRR	C	~ 100
CC:NBS:LRR	*RPS2* (Arabidopsis)	*P.s.* pv *tomato*	*avrRpt2*	CC-NBS-LRR	C	~ 65
SA:CC	*RPW8.1*, *RPW8.2* (Arabidopsis)	*Erysiphe* sp.	*?*	SA-CC	?	~ 5

LRR, leucine-rich repeats; NBS, nucleotide binding site; CC, coil-coil domain; TIR, similar to cytoplasmic signalling domains of Toll and Interleukin-1 receptor homology domain; PK, protein kinase; TM, transmembrane domain; C cytoplasmic; MS, membrane spanning; e, extracellular.

R genes isolated until now belong to one of six classes (Table 1.5). The vast majority of *R* genes encode proteins containing an amino-terminal nucleotide binding site (NBS) and carboxy-terminal leucine-rich repeats (LRRs). In animal systems, LRRs mediate protein-protein interactions in ligand-receptor models (AGI, 2000).The NBS-LRR R proteins can be further subdivided into two major classed on the basis of their amino-terminal sequences, featuring either a coiled coil (CC) or Toll-Interleukin receptor (TIR) homology domain. In *Arabidopsis*, there are around 150 sequences that have homology to the NBS-LRR class of genes. There are more TIR-NBS-LRR genes (approximately 60%) than CC-NBS-LRR (approximately 40%). Resistance gene evolution may involve duplication and divergence of linked gene families (Ellis *et al.*, 2000). However, most of the *R* genes (46) are singletons with 25 doubletons, seven loci with three *R*-gene copies and individual loci with four, five, seven, eight and nine NB-containing genes. *R* homologues are unevenly distributed among chromosomes, with 49 on chromosome 1, 2 on chromosome 2, 16 on chromosome 3, 28 on chromosome 4 and 55 on chromosome 5. Some *R* homologues have unexpected structures. Two *R* genes encode, in addition to a TIR-NBS-LRR structure, a WRKY domain that is likely to confer DNA-binding capacity (AGI, 2000). The sixth class of *R* genes encodes an entirely novel R-protein structure. The *RPW8* genes encode relatively short proteins that carry a putative signal

anchor and then a coiled-coil domain (SA:CC) (Table 1.5). Despite its lack of resemblance to known *R* genes, *RPW8* provides resistance that is associated with a hypersensitive response, SA-dependent and surprisingly requires a functional *EDS1* gene (known to be required for signalling from the TIR-NBS-LRR class of *R* genes) (Xiao *et al.*, 2001).

Recently, insights into the *R* gene domains that are required for specificity of Avr recognition have been gained, using gene shuffling and domain swapping approaches. Experimental evidence suggests that the highly variable LRRs in *R* genes have a major role in recognition of pathogen determinants encoded by *Avr* genes. In tomato Cf-4 and Cf-9, specificity has been mapped to amino acids 10-18 in the LRRs region (Van der Hoorn *et al.*, 2001; Wulff *et al.*, 2001). Another interesting piece of evidence came from the study of the flax L protein, which indicated that along with the LRR domains, another subdomain of the amino-terminal TIR region is required for specificity and is also under diversifying selection (Ellis *et al.*, 1999; Luck *et al.*, 2000).

1.3.5 The oxidative burst

Following the infection by an avirulent necrotising pathogen, gene-for-gene recognition occurs. This causes a rapid activation of plant defence responses, and triggering of a cell death response (i.e., the hypersensitive response, HR) at the site of infection. The hypersensitive response is characterised by rapid generation of reactive oxygen species (ROS) including superoxide radical ($O_2^{\cdot-}$), hydroxyl radical ($OH^{\cdot}$) and accumulation of H_2O_2; it has been termed the oxidative burst (OB). Emerging data indicate that the oxidative burst may reflect activation of a membrane-bound NADPH oxidase, closely resembling that operating in activated neutrophils responsible for the generation of reactive oxygen species. Similar to in human macrophages or neutrophils, ROS are believed to function in plant defence by either directly killing the pathogen, or indirectly by triggering a cell death program, or both (Levine *et al.*, 1996).

Homologues of *gp91phox* (the major subunit of the mammalian NADPH oxidase complex) were identified in both monocots and dicots (Groom *et al.*, 1996; Keller *et al.*, 1998; Torres *et al.*, 1998). Recently, evidence supporting a functional role for this H_2O_2-generating complex in pathogen defence has been presented. The human Rac protein is one out of three cytosolic factors which, together with two-membrane-bound proteins-P22phox and gp91phox, control the activity of the neutrophil multicomplex enzyme NADPH oxidase (Bokoch, 1994). The recombinant rice OsRac1 was shown to have both GTP-binding activity and GTPase activities. Overexpression of the OsRac1 led to: 1) the formation of HR-like discrete spontaneous lesions; 2) resistance against the rice blast fungus and bacterial blight; 3) enhanced production of a phytoalexin and defence-related genes. Moreover, the constitutively active form of OsRac1 was also shown to mediate a constitutive and DPI (diphenyleniodonium; a suicidal inhibitor for NADPH-oxidase) sensitive H_2O_2 generation. Transgenic expression of a dominant-negative form of OsRac1 significantly compromised *R*-gene dependent resistance upon challenge with an avirulent *M. grisea* isolate (Ono *et al.*, 2001; Kawasaki *et al.*, 1999). *Arabidopsis* was found to encode least eight functional *gp91phox* homologs, called *Atrboh* (for respiratory burst oxidase homologe) (AGI, 2000). Intriguingly, unlike *gp91phox*, they all carry an N-terminal EF-hand Ca^{2+}-binding domain (Keller *et al.*, 1998). Unexpectedly, no Rac, Ras, NADPH oxidase subunits (i.e. p22, p47, p67, p40) proteins are found in *Arabidopsis* (AGI, 2000). These findings highlight some apparent mechanistic differences as to the function and regulation of the *Atrboh* responsible for H_2O_2 generation in *Arabidopsis*.

Several findings indicate that H_2O_2 from the oxidative burst plays a central role in the orchestration of the HR: (1) as the substrate driving the cross-linking of cell wall structural proteins to slow microbial ingress prior to the deployment of transcription-dependent defences and to trap pathogens in cells destined to undergo hypersensitive cell death, (2) as a local threshold trigger of this programmed cell death in challenged cells, and (3) as a diffusible signal for the induction in adjacent cells of genes encoding

cellular protectants such as glutathione S-transferase and glutathione peroxidase (Tenhaken *et al.*, 1995; reviewed in Lamb & Dixon, 1997).

1.3.6 The hypersensitive response

Cell death in higher plants has been widely observed in predictable patterns throughout development and in response to pathogenic infection (Greenberg, 1996). There appear to be two types of plant cell death associated with pathogen infection: a rapid, hypersensitive cell death localised at the site of infection during an incompatible interaction between a resistant plant and an avirulent pathogen, and a slow plant cell death that spreads beyond the site of infection during some compatible interactions involving a susceptible plant and a virulent, necrogenic pathogen. Hypersensitive cell death is accompanied by the induction of multifaceted defence responses, including production of active oxygen species and antimicrobial compounds (phytoalexins), rapid cross-linking of cell-wall proteins and ultimately resistance to pathogens (Dixon *et al.*, 1994). Several observations suggest that the HR is a form of programmed cell death (PCD) in plants: (1) the appearance of the HR is genetically controlled (as evident from the mutants *acd* and *lsd* that constitutively show HR lesions in the absence of pathogens); (2) purified HR-inducing factors from bacteria called harpins will not induce the HR unless the plant tissue is transcriptionally active; (3) HR-inducing bacteria will not cause the HR if protein synthesis is blocked in the plant (He *et al.*, 1993; Keen *et al.*, 1981); (4) it was shown that cell death associated with the HR in several plant-pathogen systems not only shares morphological similarities to animal apoptosis (Ryerson & Heath, 1996), but also some mechanistic similarities. Evidence exists for the presence of caspase-like proteins {caspases are cysteine proteases that regulate animal PCD} in tobacco tissues that were developing HR following infection with tobacco TMV (del Pozo & Lam, 1998). Moreover, overexpressed *bcl-*x_L,which encodes a mammalian suppressor of PCD, in tobacco plants, suppressed cell death induced by UV-B irradiation, paraquat treatment or the HR to TMV infection. Similar enhanced resistance

to cell death was found in transgenic tobacco plants overexpressing the *ced-9* gene, a *C. elegans* homologue of *bcl-x_L*, indicating that Bcl-x_L and Ced-9 can function to inhibit cell death in plants (Mitsuhara *et al.*,1999). Recent analysis of the *Arabidopsis* genome sequence revealed no clear homologues of many mammalian defence and cell-death control genes. No similarities were found to proteins involved in the control of apoptosis in animal cells, such as caspases and BCL/CED9. However, eight homologues of a newly-defined metacaspase family were identified (AGI, 2000).

Although the HR is well-known as a central feature of gene-for-gene resistance and is usually associated with the activation of other locally or systemic responses, there is some evidence showing that the HR may be uncoupled from the downstream signal transduction gene activation process. This evidence includes: (1) plants mutated in the *DND1* (*d*efence, *n*o *d*eath) locus are defective in HR cell death but retain the characteristic induction of PR gene expression and strong restriction of pathogen growth in response to avirulent bacteria (Yu *et al.*, 1998); (2) Caspase-specific peptide inhibitors could abolish bacterial-induced plant PCD but did not significantly affect the expression of defence genes (del Pozo & Lam, 1998).

1.4 Systemic acquired resistance

The events of OB and HR are often accompanied by synthesis of salicylic acid (SA) in both local and systemic tissues, which causes systemic expression of defence genes, leading to *s*ystemic *a*cquired *r*esistance (SAR). The phenomenon of SAR in plants has been reported for over 90 years. In 1933, KS Chester reviewed 201 studies dealing with " the problem of acquired physiological immunity in plants" (Chester, 1933). Ross coined the term SAR to refer to the inducible systemic resistance (Ross, 1961a) and localised acquired resistance to describe the resistance induced in inoculated leaves (Ross, 1961b). This induced resistance, or SAR, results in broad-spectrum, long-lasting immunity in non-infected tissues which provides protection not only against the

inducing pathogen but to a broad spectrum of pathogens including viruses, bacteria and fungi. Since the days of Chester, the SAR phenomenon in plants has been extensively studied and is a well-established response of plants to pathogen infection (reviewed in Shirasu *et al.*, 1996; Hunt *et al.*, 1996; and Ryals *et al.* 1994).

Three of the best characterised biological models for the study of SAR are tobacco, cucumber, and *Arabidopsis*. Using the tobacco/TMV model system, it was shown that the development of SAR is associated with expression of a number of SAR marker genes belonging to at least nine families. A protein can be classified as a SAR protein when its presence or activity correlates tightly with maintenance of the resistance state. Analysis of SAR-related proteins showed that many of these proteins belong to the class of pathogenesis-related (PR) proteins (Ward *et al.*, 1991). These include: PR-1 from tobacco and tomato showing growth-inhibiting activity against *Phytophthora infestans* (Cohen *et al.*, 1992); PR-2 (β-1,3-Glucanase) and PR-3 (chitinase) are glycanoendohydrolases with *in vitro* activity that catalyse the hydrolysis of the cell wall constituents of phytopathogenic fungi; PR-4 is an antifungal protein as well; and PR-5 is a thaumatin-like Cys-rich protein with antifungal activity that appear to reside in disrupting membrane integrity- which is the basis of calling this class of proteins permatins, more commonly known as osmotins (reviewed in Linthorst, 1991).

The constitutive overexpression of an SAR gene in some cases can convey enhanced protection against at least some pathogens, indicating that these genes may potentially play direct roles in SAR. For example, transgenic tobacco constitutively expressing *PR-1a* are resistant to *Peronospora tabacina* and *Phytophthora parasitica.* Though statistically significant the resistance was not strong as observed in chemically immunised plants, suggesting that *PR-1* might act in concert with other SAR-related proteins (Alexander *et al.*, 1993; Liu *et al.*, 1994). Coexpression of a chitinase and glucanase in tobacco enhances protection against *Cercospora nicotianae* (Zhu *et al.*, 1996).

A chemical is considered as a compound that induces SAR when it fulfils the following three criteria: (1) induction of resistance to the same spectrum of pathogens as in biologically induced SAR; (2) induction of expression of the same set of biochemical markers as by a necrogenic pathogen; and (3) if the chemical (possibly after modification *in planta)* has a direct antimicrobial effect, then induced resistance against pathogens that are genetically resistant to the antimicrobial effects must be demonstrated. The chemical compound 2,6-dichloro-isonicotinic acid (INA), a functional analogue of salicylic acid (SA), is an example of a non-plant-derived SAR-inducing chemical. In tobacco, INA induced the same nine families of SAR genes as TMV and SA (Kessmann *et al.*, 1994).

SA importance and necessity in SAR induction was documented. A large body of evidence suggests that SA is required for SAR signal transduction. Pathogen infection results in a significant increase in SA by several hundred-fold in cucumber and tobacco, and this increase was shown to correlate with SAR (Malamy *et al.*, 1990; Metraux *et al.*, 1990; Yalpani *et al.*, 1991). Compelling evidence supporting this idea comes from the analysis of transgenic plants expressing the bacterial *nahG* gene encoding salicylate hydroxylase, an enzyme that catalyses the conversion of SA to catechol. These plants are not only unable to accumulate free SA, but they are incapable of mounting a SAR response to pathogens (Gaffney *et al.*, 1995). However, whether SA itself is the primary systemic signal or merely transported with the primary systemic signal remains a matter of debate (Mauch-Mani & Métraux, 1998). Two lines of evidence, coming from the work on cucumber, suggest that SA is not likely to be the translocated signal that triggers SAR in distal plant organs (Vernooij *et al.*, 1994; and Rasmussen *et al.*, 1991).

SA biosynthesis has been reported to take place either via the conversion of phenylalanine to trans-cinnamic acid (t-CA) catalysed by phenylalanine ammonia-lyase (PAL) (Yalpani *et al.*, 1993) or via isochorismate catalysed by isochorismate synthase (ICS), a mechanism similar to that in bacteria (Wildermuth, 2001).

As to the SA mechanism of action, the data available suggest the existence of more than one mode of action of SA in resistance responses. In infected leaves, high concentrations of SA around the site of infection may inhibit catalase and other oxidoreductases. Inhibition of catalase activity could prolong the half-life of H_2O_2 and lead to an amplification of the oxidative burst which in turn may trigger a variety of local defence responses, including programmed cell death during the HR as well as defence gene expression and synthesis of SA in adjacent cells (Hammond-Kosack & Jones, 1996). This would create a runaway cycle leading to high levels of both SA and H_2O_2 at the site of pathogen attack. In this model, inhibition of oxidoreductases represents a low-affinity perception mechanism that transduces local SA levels into local defence responses (Hammond-Kosack & Jones, 1996).

Genetic dissection of the basis of microbial pathogenicity and host resistance is made easier by *Arabidopsis thaliana*. *Arabidopsis* is a useful model plant because of its small genome size (~120 MB) and rapid generation time (6 to 12 weeks) (Baker *et al.*, 1997; AGI; 2000). In 1996, the *Arabidopsis* Genome Initiative (AGI) was established for the purpose of coordinating large-scale sequencing efforts of the *Arabidopsis* genome. This effort has just been successfully completed (AGI, 2000).

One powerful approach for the dissection of complex signal transduction processes is the application of mutant analysis. The simple procedures for chemical and insertional mutagenesis, efficient methods for performing crosses and introducing DNA through plant transformation, extensive collection of mutants with diverse phenotypes, and a variety of chromosome maps of mutant genes and molecular markers (Meinke *et al.*, 1998) facilitated the isolation and identification of several mutants in the SAR signal transduction pathway. These mutants can be classified as either constitutively activated in SAR (e.g. *lsd1, lsd2, lsd3, lsd4, lsd5, lsd6, lsd7, acd2, cim2, and cim3)* or compromised in their ability to launch the SAR response (e.g. *npr1/nim1*) (section 1.8.2) (Table 3.5) (Ryals *et al.*, 1996). Currently, efforts are being made to discover more mutants and genes implicated in this SA-dependent pathway.

1.5 Jasmonate as a defence signalling plant hormone

Jasmonic acid (JA) is a cyclopentanone derivative of linolenic acid that exhibits features of a plant hormone. Jasmonate is thought to be an important signal molecule in plant responses to various biotic and abiotic stresses. Wounding, osmotic stress, touch of tendrils, and pathogen attack led to an accumulation of jasmonate or its precursors, followed by the expression specific genes coding for proteinase inhibitors, enzymes of phytoalexin synthesis, and defence antifungal proteins such as thionins and defensins. The biosynthesis and functions of jasmonates in plants have been elucidated (Creelman & Mullet, 1997; Sembdner & Parthier, 1993). A JA-dependent pathway was shown to be particularly important for resistance against insects and necrotrophic fungi. Jasmonate acts as an inducer of some genes known collectively as Jasmonate responsive genes (JR). Among which are protease inhibitor (*Pin2*), osmotin, thionins (*Thi2.1*), and defensins (*PDF.1.2*). The induction of JA by wounding, and the subsequent accumulation of proteinase inhibitors, help in protecting plants against insect damage (Creelman & Mullet, 1997). The *PDF1*.2 (Penninckx *et al.*, 1996) and *Thi2.1* genes (Epple *et al*, 1995) are induced by JA or ethylene (ET) but not by SA. Systemic inducion of the *PDF1.2* gene by *Alternaria brassicicola* was unaffected in transgenic *Arabidopsis nahG* plants or the mutants *npr1* and *cpr1,* which are affected in SA response. In contrast, *PDF1.2* expression was strongly reduced in the *Arabidopsis* mutants *ein1* and *coi1* that are blocked in their response to ET and JA, respectively. These results indicate that the systemic pathogen-induced expression of the *PDF1.2* (Penninckx *et al.*, 1996) *Thi2.1* (Epple *et al.*, 1995) genes, in *Arabidopsis*, is independent of SA but require components of the ethylene and JA response (Penninckx *et al.*, 1996). Furthermore, several lines of evidence support the involvement of the JA-dependent signal transduction pathway in resistance against necrotrophic fungi. *Arabidopsis* triple mutants, *fad3-2, fad7-2 and fad8* (*f*atty *a*cid *d*eficient mutants that can not accumulate JA), were extremely susceptible to root rot caused by the fungal root pathogen *Pythium mastophorum* and they were substantially protected by exogenous application of JA (Vijayan *et al.*, 1998). During a screen of several *Arabidopsis* ecotypes, Mt-0 and Uk-4

showed high expression of *Thi2.1* that correlated well with the resistance against the necrotrophic fungi *Fusarium oxysporum* f. sp. *matthiolae*. The *Thi2.1* transcript level after infection correlates with resistance, being 5 to 10 times higher in the resistant Mt-0 and Uk-4 *Arabidopsis* ecotypes than in the susceptible Col-2, Ler, and Ws ecotypes. The β-glucuronidase (GUS) expression of *Thi2.1*-promoter-*uidA* fusion (with a promoter derived from Col-2) is on average almost 10 times higher in the Uk-4 background than in the Col-2 background. This indicates that Uk-4 might have a more sensitive recognition system for *F. oxysporum* f. sp. *mathiolae* or might have a signal transduction system that gives a higher amplification of the original recognition signal (Epple *et al.*, 1998). Constitutive overexpression of an endogenous *Thi2.1* enhanced resistance of the susceptible ecotype Col-2 against attack by *Fusarium oxysporum* f. sp. *matthiolae.* Transgenic lines had a reduced loss of chlorophyll after inoculation and supported significantly less fungal growth on the cotyledons, as evaluated by trypan blue staining. Moreover, fungi on cotyledons of transgenic lines had more hyphae with growth anomalies, including hyperbranching, than on cotyledons of the parental line (Epple *et al.*, 1997).

The current model indicates that both the SA-dependent and the JA-dependent pathways are distinct and lead to the induction of genes upon pathogen attack. HH Flor's gene-for-gene resistance concept was shown to be applicable also for necrotrophic fungi; tomato plants preimmunised with an avirulent strain of *F. oxysporum* resulted in cross protection against a virulent race. Cross protection was found to be mediated by recognition of a specific elicitor from the avirulent race by the resistance gene product and by subsequent induction of the plant defence response (Huertas *et al.*, 1999).

There is now compelling evidence that an SA-dependent pathway is important for mounting resistance in *Arabidopsis* to some microbial pathogens (e.g. *Pseudomonas syringae. tomato*) and biotrophic fungi (e.g. *Peronspora parasitica*); *nahG*-expressing *Arabidopsis* plants were found to be considerably more sensitive to these pathogens compared to wild-type plants (Delaney *et al.*, 1994).

On the other hand, the JA-dependent pathway is believed to be involved in mounting systemic defence responses to insect herbivory and necrotrophic fungi (McConn *et al.*, 1995; Penninckx *et al.*, 1996). Emerging evidence, presented by Felton *et al.* (1999), supports the notion that there is a significant cross-talk between SA-dependent and JA-dependent pathways. Silencing the expression of PAL reduces SAR to tobacco mosaic virus, whereas overexperession of PAL enhances SAR. Tobacco plants with reduced SAR exhibited more effective grazing-induced systemic resistance to larvae of *Heliothis virescens,* but larval resistance was reduced in plants with elevated PAL levels. Furthermore, an inverse relationship between SA and JA levels was revealed as a result of the genetic modification of PAL (Felton *et al.*, 1999).

Unlike SAR, our knowledge of the JA signal transduction pathway is limited. It is presumed that jasmonate interacts with receptors in the cell that activate a signalling pathway resulting in changes in transcription, translation, and other responses mediated by JA. Receptors for JA and other components of the signal transduction pathway are more likely to be discovered via mutant analysis through uncovering plants that are insensitive or altered in their response to JA. One class of mutants, that are insensitive to JA, have been identified that include *coi1, jar1, jin1* and *jin4* (Creelman & Mullet, 1997; Xie *et al.*, 1998). Another class of mutants, isolated through their constitutive expression of vegetative storage protein 1(*VSP1*), *PDF1.2* and *Thi2.1*, known as *cev* and *cex*, have recently been described (Ellis & Turner, 2001; Xu *et al.*, 2001).

1.6 Induced systemic resistance

In *Arabidopsis*, non-pathogenic, root-colonising *Pseudomonas fluorescens* bacteria trigger an induced systemic resistance (ISR) response against infection by the bacterial leaf pathogen *P. syringae pv tomato*. In contrast to classic, pathogen-induced SAR, the rhizobacteria-mediated ISR response is independent of SA accumulation and *PR* gene activation. *Pseudomonas fluorescens* strain WCS417r (WCS417r) has been shown to

activate the ISR pathway in several plant species (Van Peer *et al.*, 1991; Leeman *et al.*, 1995; Duijff *et al.*, 1995) including *Arabidopsis thaliana* (Pieterse *et al.*, 1996). In *Arabidopsis*, like SAR, WCS417r-mediated ISR is effective against a broad-spectrum of pathogens including: the fungal root pathogen *Fusarium oxysporum* f. sp. *raphani* (Pieterse *et al.*, 1996); the oomycete leaf pathogen *Pernospora parasitica*; and the bacterial leaf pathogens *Xanthomonas campestris* pv. *campestris* (Van Wees *et al.*, 2000) and *Pseudomonas syringae* pv. *tomato* (Pieterse *et al.*, 1996). Using the JA response mutant *jar1*, the ethylene response mutant *etr1*, and the SAR regulatory mutant *npr1*, it was demonstrated that the ISR signal transduction pathway requires responsiveness to JA and ethylene and is dependent on NPR1. The JA and ET response components were shown to engage successively to trigger a defence reaction that, like SAR, is regulated by NPR1 (Pieterse *et al.*, 1998). The induction of ISR by WCS417r is not normally accompanied by increase in ethylene production in roots or leaves, or in the expression of the genes encoding ethylene biosynthetic enzymes. However, ethylene responsiveness is required at the site of application of inducing rhizobacteria (Knoester *et al.*, 1999). Interestingly, it was shown that the processes downstream of NPR1 in the establishment of ISR are divergent from those in the SAR pathway, indicating that NPR1 differentially regulates defence responses, depending on the signals that are elicited during induction of resistance (Figure 1.3) (Pieterse *et al.*, 1998). Moreover, despite the requirement of the same regulatory component NPR1, no apparent cross-talk (either positive or negative) was reported between SAR and ISR. Furthermore, an additive protective effect was observed when both pathways are simultaneously activated. These observations have led to the conclusion that these two pathways are fully compatible and contribute to an enhanced level of protection via parallel activation of complementary, NPR1-dependent defence responses (Van Wees *et al.*, 2000).

Recent evidence in support of the notion that ISR-mediated signalling employs a distinct battery of genes that are different from those induced during SAR, has been provided. In *Arabidopsis*, known defence-related genes, i.e. the SA-responsive genes *PR-1*, *PR-2*, and *PR-5*, the ethylene-inducible gene *Hel*, the ET- and JA-responsive genes *ChiB* and

PDF1.2, and the JA-inducible genes *Atvsp*, *Lox1*, *Lox2*, *Pal1*, and *Pin2*, are neither induced locally in the roots nor systemically in the leaves upon ISR induction (Van Wees *et al.*, 1999) In the hunt for genes that are up or down regulated during ISR, the recent technology of Affymetrix GeneChip® microarrays has recently been employed. In ISR-expressing leaves, only a few genes (~ 8) were up or down regulated. These genes were found to encode transcription factors, stress-related proteins and proteins with miscellaneous functions which are not directly related to defence reactions. Therefore, it was concluded that, unlike SAR, ISR is not associated with major changes in gene expression, but nevertheless has a great potential and effectiveness against different types of pathogens (Verhagen *et al.*, 2001).

Not much is known about signalling components that are specific and important for the establishment of the ISR-mediated signal transduction defence responses. No reported mutants that define ISR-specific genes have been identified as yet. The only reported ISR-related locus came from the efforts of screening *Arabidopsis* ecotypes for perturbed ISR responses after root treatment with WCS714r. Two accessions were identified, namely Ws and RLD, that failed to develop ISR but still expressed normal levels of SAR response. Furthermore, the WCS417r-non-responsive phenotype of RLD and Ws was associated with a relatively high levels of susceptibility to *Pst*. Genetic analysis revealed that the ability to express ISR, as well as the relatively high levels of basal resistance against *Pst*, are controlled by single dominant locus (*ISR1*) that maps on chromosome III. It was concluded that the *ISR1* locus is involved in both the expression of rhizobacteria-mediated ISR and basal resistance against *Pst* (Ton *et al.*, 1999). *ISR1* locus has been recently shown to be involved in ethylene signalling. In contrast to Col-0 (*ISR1*), accessions RLD and Ws (having the recessive mutation *isr1*) showed an affected expression of the triple response and a reduced expression of ethylene responsive genes *Hel* and *PDF1.2* after exogenous application of the ethylene precursor 1-aminocyclopropane-1-carboxylate (ACC). Interestingly, RLD and Ws were blocked in the resistance to *Pst* after treatment of leaves with ACC. Taken together, it was

suggested that the *ISR1* locus encodes an essential component for the ethylene response which is required for the expression of a fully-functional ISR (Ton *et al.*, 2001).

1.7 SAR-independent resistance

Based on the complexity of defence signalling transduction data, it is generally believed that plants possess several other pathways that have not been identified as yet. Therefore, extensive attempts are being made to uncover these novel pathways. One approach is being conducted by T. Delaney and his co-workers. Their research is focused on the identification of novel components that are independent of the SAR key positive regulator *NIM1/NPR1*, termed SAR independent resistant (SIR) (Figure 1.3). It is worth pointing out that the SIR is completely distinct from the JA/ET/*NPR1*-dependent ISR pathway (section 1.6) that is primarily induced by non-pathogenic, root-colonising bacteria (Figure 1.3).

Based on the observation that mutations in *NIM1/NPR1* gene diminish the expression of resistance against avirulent pathogens, but do not abolish it, it has been suggested that while SAR may contribute to resistance, other defence pathways are essential for full manifestation of race-specific resistance. In an effort to identify genes that are required for expression of SIR, a mutant screen was conducted in a *nim1/npr1* (Ws) background in the search for mutants with increased susceptibility to the normally avirulent oomycete *Peronospora parasitica* Noco2. Due to the fact the Ws-0 resistance is mediated by several resistance genes, the authors believe that this pathosystem is efficient in uncovering novel SIR components (Argueso & Delaney, 2001).

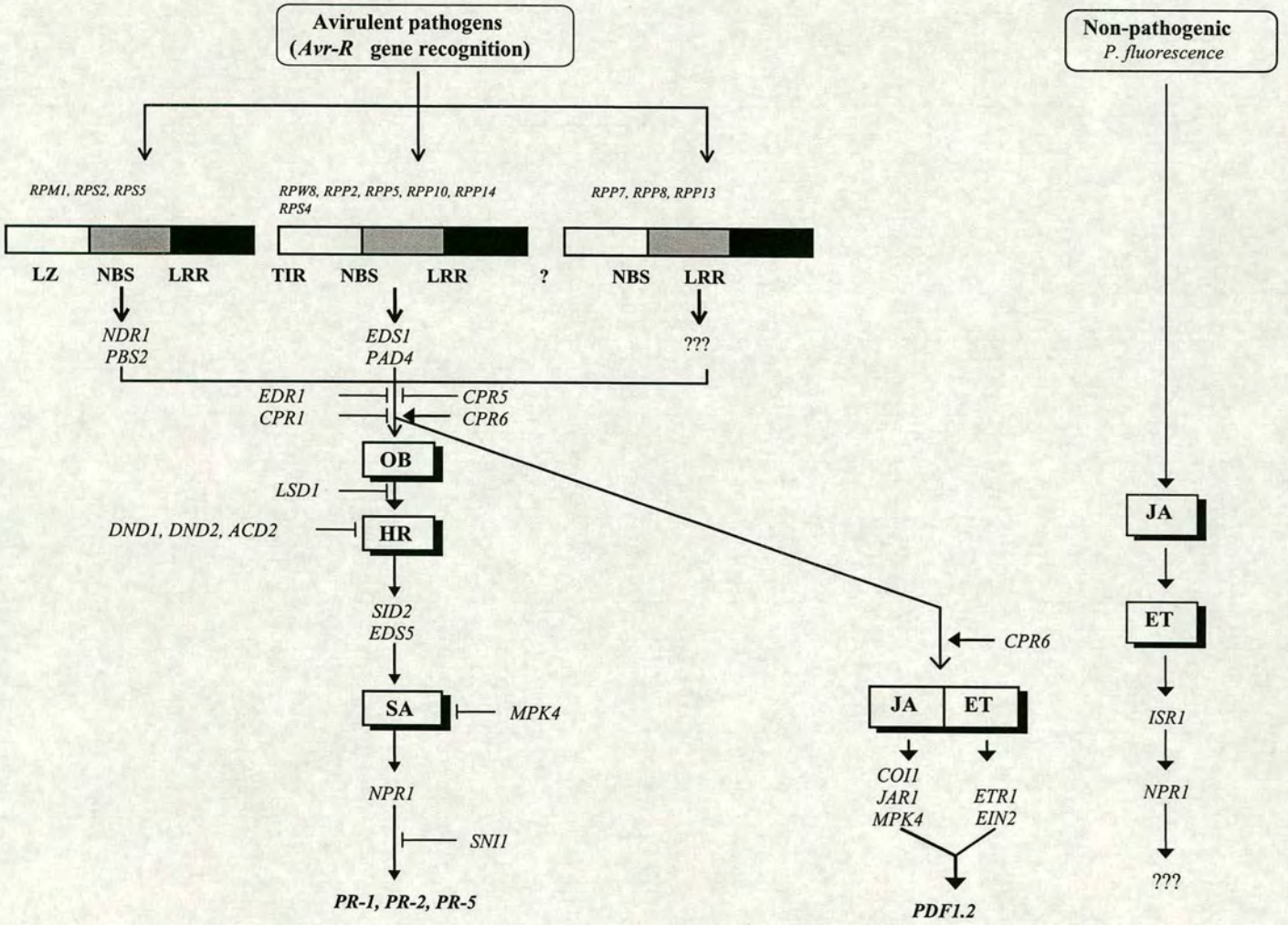

Figure 1.3: Schematic representation illustrating our current understanding of defence signal transduction networks in the model plant *Arabidopsis thaliana* (Based on Dong, 1998; Glazebrook, 1999; Feys & Barker, 2000; Glazebrook, 2001).

1.8 Signal transduction networks

One approach to understanding and dissecting signal transduction networks controlling defence mechanisms is to employ genetic analyses to identify signalling components and pinpoint their roles within these networks. Recent genetic and phenotypic analyses of plant mutants, with compromised or enhanced disease resistance have contributed significantly to the advancement of our understanding of the mechanisms of plant-pathogen recognition and resistance pathway utilisation in *Arabidopsis*-pathogen model systems.

In the light of the recent progress made in the dissection of the disease signal transduction network, the following section highlights efforts made in identifying genes that affect regulation of defence gene expression and their roles and relative positions in the signal transduction network. Figure 1.3 depicts a model of our current understanding on how the network might be arranged in *Arabidopsis*.

1.8.1 R gene-dependent signal transduction

First evidence on the presence of ancillary signalling genes that are necessary for the function of a particular Avr-R interactions came from mutation analysis of the interaction between barely and the powdery mildew fungus *Erisiphe graminis* f. sp. *hordei*. Two genes, namely *Rar1* and *Rar2*, were found to be essential for the function of the *R* gene *Mla12* (Torp & Jorgensen, 1986; Freialdenhoven *et al.*, 1994). The *rar1* mutations compromise the function of many other, but not all, *R* genes recognising different powdery mildew isolates, placing wild-type *Rar1* at a point of pathway convergence for a subset of barley *R* genes (Jorgensen, 1996; Peterhänsel *et al.*, 1997). *Rar1* was cloned and shown to encode a member of a novel class of eukaryotic zinc-binding proteins (Shirasu *et al.*, 1999).

In *Arabidopsis*, mutations in *PBS1*, *PBS2*, *NDR1*, *EDS1*, and *PAD4* block gene-for-gene resistance that is mediated by some *R* genes (Figure 1.3). The only *R* gene known to be affected by *PBS1* mutation is *RPS5* (Warren *et al.*, 1999). *NDR1* (for *n*on-race-specific *d*isease *r*esistance) and *EDS1* (for *e*nhanced *d*isease *s*usceptibility) are required for gene-for-gene mediated resistance to avirulent strains of *Pseudomonas syringae* and *Peronospora parasitica*. Interestingly, *ndr1* and *eds1* mutants are susceptible to a different set of avirulent pathogens. *R* genes that require *EDS1* belong to the TIR-NBS-LRR class, whereas *R* genes that require *NDR1* belong to the LZ-NBS-LRR class (Aarts *et al.*, 1998). *R* genes that require *EDS1* seem to also require *PAD4* (for *p*hyto*a*lexin *d*efficient) (Glazebrook *et al.*, 1997b). Similarly, most *R* genes that require *NDR1* also require *PBS2* with few exceptions (Warren *et al.*, 1999).

Recent data suggest that some *R* genes that belong to the LZ-NBS-LRR class do not require either *NDR1* or *EDS1*. Using *eds1::ndr1* double mutant analysis, *RPP7*, *RPP8*, and *RPP13* were found to condition an *Avr-R* reaction that is independent on both *NDR1* and *EDS1* (McDowell *et al.*, 2000; Bittner-Eddy & Beynon, 2001; Bittner-Eddy *et al.*, 2001). These data support a model including at least three signal transduction cascades acting downstream of *R* genes: first is *NDR1*-dependent, second is *EDS1*-dependent, and a third for which no genetic components have been defined yet (Figure 1.3). However, there are a few reported cases that do not comply to this proposed model. For example, resistance mediated by *RPP8* is SA-independent (McDowell *et al.*, 2000). Moreover, Despite that fact the *R* gene *HRT* is more than 90% identical to *RPP8* (Cooley *et al.*, 2000), *HRT*-mediated resistance is yet SA-dependent (Kachroo *et al.*, 2000). Furthermore, the novel *RPW8* gene has been reported to belongs to the novel class of *R* genes SA:CC that encodes a coiled-coil domain with very little similarity to the LZ-NBS-LRR class of *R* genes. However, *RPW8*-mediated resistance required *EDS1* and is SA-dependent (Xiao *et al.*, 2001). Therefore, based on these two observations and despite the importance of the structural features of a given *R* gene in determining the pathway used by this *R* gene, apparently other factors are also involved.

Few of the above mentioned genes that condition *R*-gene signal transduction have been cloned. *NDR1* was found to encode a protein with two predicted transmembrane domains. One putative function for this protein is to hold R proteins close to the membrane (Century *et al.*, 1997). *EDS1* and *PAD4* encode proteins with similarity to triacyl glycerol lipases (Falk *et al.*, 1999; Jirage *et al.*, 1999). Mutations in either gene can cause a defect in SA accumulation and expression of both genes can be induced by SA or pathogen infection, suggesting that they act upstream of SA and possibly as part of a signal amplification loop (Figure 1.3) (Falk *et al.*, 1999; Jirage *et al.*, 1999). *pbs1* (for *avrPphB* susceptible) mutation of *Arabidopsis* is characterised by susceptibility to *Pseudomonas syringae* DC3000 expressing *avrPphB* and lack of a hypersensitive response elicited by the *avrPphB* gene when expressed *in planta*. *PBS1* gene has been cloned recently and was found to encode a serine/threonine protein kinase with 65% similarity to Apk1a kinase (Swiderski & Innes, 2001a). *In vitro* studies revealed that PBS1 protein has autophosphorylation activity and that it is able to phosphorylate the RPS5 protein in both the NBS and LRR regions but not in the N-terminal LZ domain (Swiderski & Innes, 2001b). The *PBS2* gene has been also cloned and was found to be allelic to the *RAR1* locus of barley (Merritt *et al.*, 2001).

1.8.2 SAR signalling network

1.8.2.1 SA binding proteins

In tobacco, *Arabidopsis*, and cucumber, an increase in SA concentration locally in response to pathogen attack and systemically in response to SAR-inducing signal, is necessary and sufficient for the activation of PR gene expression and enhanced disease resistance (Malamy *et al.*, 1990; Métraux *et al.*, 1990; Uknes *et al.*, 1993). Biochemical strategies employed to identify SA-binding components involved in the transduction of the SA signal have resulted in interesting candidates. SA-binding proteins identified include an SA binding protein 2 (SABP2) which has a 150-fold higher affinity for SA than catalase . Catalase (SABP) was the first SA-binding

protein isolated using ^{14}C-labeled SA (Du & Klessig, 1997). Interestingly, SABP3 has recently been isolated and it have been reported to be the chloroplastic carbonic anhydrase (CA). The identification of SABP3 as CA has been confirmed by the fact that the recombinant protein produced in *E. coli* has both SA binding and CA activities (Slaymaker *et al.*, 2001).

Protein phosphorylation and dephosphorylation play a key role in early defence signal transduction events and SA-regulated *PR* gene expression (Conrath *et al.*, 1997). In this context, using an in-gel kinase assay, Mitogen activated protein kinase (MAPK) has been shown to be activated rapidly and transiently in an SA-induced tobacco cell suspension culture. The sequence of this SA-induced protein kinase (SIPK) is distinct from other plant MAPKs previously implicated in stress responses (Zhang & Klessig, 1997). SIPK interacting proteins (SIIPs) have been recently identified using a new cytosolic-based two-hybrid system identified in which SIPK was used as a bait. SIPKK, a MAPK kinase (MAPKK) which was previously identified (Liu *et al.*, 2000), was pulled out as a SIIP. Another class of SIIP, identified in this screen, was the nuclear-encoded RPL12, which is a part of the chloroplast large ribosome subunit (Minke & Klessig, 2001).

1.8.2.2 SAR compromised mutants

In addition to biochemical approaches, genetic screens performed in *Arabidopsis* have uncovered one locus: *NPR1*(for nonexpressor of *PR-1*)*/NIM1* (for non-inducible immunity)*/SAI1*(for salicylic acid insensitive) that is required downstream of SA to activate the defence genes *PR-1*, *PR-2* (*BGL-2*), and *PR-5* in response to SA (Figure 1.3) (Cao *et al.*, 1994; Delaney *et al.*, 1995; Shah *et al.*, 1997). *NPR1* has been cloned independently by two different research groups (Cao *et al.*, 1997; Ryals *et al.*, 1997) and it was shown to encode a protein with an ankyrin-repeat domain which could be involved in protein-protein interactions. The carboxyl end of NPR1 was found to contain a nuclear localisation signal (NLS) important for its function. Using NPR1-GFP fusion protein analysis, the NLS has been recently shown to be an absolute requirement for its *bona fide* nuclear localisation and the activation of *PR-1*

expression (Kinkema *et al.*, 2000). Overexpression of NPR1 in *Arabidopsis* confers significant resistance to bacterial and oomycete pathogens (Cao *et al.*, 1998). NPR1 interacts with TGA-type transcription factors in yeast two-hybrid assays and promotes the binding of TGA2 to its binding site (Zhang *et al.*, 1999; Zhou *et al.*, 2000; Despres *et al.*, 2000). Interestingly, the upstream regulatory region of the *PR-1* gene has been characterised with some details and was shown to contain two positive regulatory elements. The consensus pentanucleotide *cis* element (TGACG) for the recognition by a subgroup of the TGA family of basic leucine zipper (bZIP) transcription factors and the recognition element of NF-kB (which is a vertebrates transcription factor of the Rel family) (Lebel *et al.*, 1998).

Taken together, these data suggest that NPR1 regulates defence gene expression by interacting with bZIP transcription factors. In an *npr1* suppresser screen, SA-inducible *PR-1* expression is restored in *npr-1::sni1* plants. Using transient expression assays in onion epidermal cells, SNI1 (for suppresser of NPR1 inducible) has been identified as a nuclear-localised protein with no substantial homology to any known protein. A model has been proposed in which SNI1 acts as a negative regulator of SAR. According to this model, the transcriptional repression of *PR-1* by SNI1 takes place via the action of *NPR-1* in response to SA, thereby allowing transcription factors of the TGA family to drive *PR-1* gene expression. However, no direct interaction between NPR1 and SNI has been reported (Li *et al.*, 1999).

It is also worth noting that another independent screen for <u>s</u>uppressers <u>o</u>f <u>nim1</u> (*son*) has been recently undertaken by T. Delany (Cornell University) and co-workers. EMS mutagenesis and screening in a *nim1* background resulted in the identification of *son1*. The mutant *son1* was found to exhibit complete restoration of pathogen, SA, and INA induction of *PR-1* that is normally suppressed in a *nim1/npr1* background. Interestingly, *son1* was shown to have a high resistance level to *Peronospora parasitica* that is independent of HR, SAR genes or *PDF1.2* transcripts (Kim *et al.*, 2001).

Recently, mutations in *EDS5* (also known as *SID1*) and *SID2* (for *s*alicylic acid *i*nduction *d*eficient) (also known as *EDS16*) where identified and shown to abolish the increase in SA levels observed in infected plants. Therefore, *EDS5* and *SID2* are assumed to function upstream of SA (Figure 1.3) (Dewdney *et al.*, 2000; Nawrath & Métraux., 1999). Recently, *EDS5* was cloned and was found to encode a protein with 12 predicted membrane-spanning domains and a coiled-coil domain at the N-terminus. EDS5 shows homology to DINF of *E. coli*, whose transcription is induced after treatment with DNA-damage inducing agents and UV-C light. Based on homology, DINF and EDS5 have been grouped to the MATE transporter family (for *m*ulti-drug *a*nd toxic *c*ompound *e*xtrusion). *EDS5* transcription after UV-C light exposure or pathogen inoculation is dependent on both PAD4 and EDS1 (Nawrath *et al.*, 2001). A mutation in *EDS4* causes reduced SA accumulation and reduced sensitivity to SA (Gupta *et al.*, 2000). Intriguingly, although *eds5*, *sid2*, *eds4*, *eds1*, and *pad4* mutations, as well was *nahG*, reduce SA levels and expression of *PR-1*, only *pad4* and *nahG* actually reduce production of the phytoalexin camalexin (Nawrath & Métraux, 1999; Gupta *et al.*, 2000; Zhou *et al.*, 1998). It can be concluded, therefore, that low SA production does not cause the camalexin defect in these plants, and that *pad4* and *nahG* may affect signalling pathways in addition to the SA-dependent pathway.

1.8.2.3 SAR constitutive mutants

Many mutants in which constitutively high levels of SA, defence gene expression, and disease resistance have been isolated that display a lesion-mimic phenotype (i.e. exhibit spontaneous cell death in the absence of pathogen attack). Several lines of evidence support the idea that HR cell death is a form of programmed cell death (Mittler & Lam, 1996; Morel & Dangl, 1997). The best evidence so far comes from the lesion-mimic mutants. Such mutants have been found in maize (Walbot *et al.*, 1983), barley (Wolter *et al*, 1993), and other species (Dangl *et al.*, 1996). In *Arabidopsis*, *acd* (Greenberg & Ausubel, 1993; Greenberg *et al.*, 1994) and *lsd* (*l*esion *s*imulating *d*isease resistance) mutants (Dietrich *et al.*, 1994) have been identified. These mutants exhibit several constitutive plant defence responses, such

as the expression of defence genes, leading to disease resistance. Based on their phenotypic analysis, two classes of *lsd* mutations were identified. The first is the initiation class that exhibits controlled lesions the do not spread once initiated. The vast majority of *lsd* mutants belong to this class (e.g. *lsd5*). Generally these mutations represent defects in genes involved in the triggering of the HR (Dangl *et al*, 1996; Mittler & Lam, 1996). The second class is a propagation class which represents mutations with uncontrolled lesions spread once they have been initiated. Genetic analysis of some of these mutants revealed that these mutations might function as negative regulators of cell death. As an example, *LSD1* gene of *Arabidopsis* encodes a novel class of zinc finger protein that could act as a negative regulator of cell death. Recessive mutation is *LSD1* results in a lack of up-regulation of a CuZnSOD (a copper zinc superoxide dismutase) that is responsible for detoxification of accumulating superoxide radical (Dietrich *et al.* 1997; Kliebenstein *et al.*, 1999). The maize *LLS1* gene encodes a putative dioxygenase that could be responsible for the detoxification of signals generated during the HR (Gray *et al.*, 1997). Finally, the *MLO* resistance gene from barley encodes a putative transmembrane protein (Buschges *et al.* 1997).

On the other hand, several reports attribute the lesion mimic phenotype to a mere perturbation in cellular homeostasis and metabolic functions leading to cell death, which then triggers the SAR signal transduction cascade. Examples of these cases include overexpression of a bacterio-opsin proton pump (Mittler *et al.*, 1995), antisense expression of protoporphyrinogen oxidase (Molina *et al.*, 1999). Moreover, the *ACD2* gene of *Arabidopsis* has been recently cloned and shown to encode a protein that is similar to red chlorophyll catabolite reductase, an enzyme responsible for the proper catabolism of the porphyrin component of chlorophyll (Mach *et al.*, 2001).

In *acd2*, the loss of enzyme possibly results in the accumulation of toxic catabolites that induce cell death (Mach *et al.*, 2001). *dnd1* and *dnd2* mutants (for *d*efence, *n*o *d*eath) display lesions under certain growth conditions. *DND1* gene encodes a cyclic

nucleotide-gated ion channel whose loss of function leads to the acceleration of cell death (Clough *et al.*, 2000; Yu *et al.*, 2000).

The close examination of constitutive expressor of *PR* genes (*cpr*) class of mutants has contributed significantly to our understanding of the SAR pathway. Three non-allelic *cpr* mutants have been reported: *cpr1* (Bowling *et al.*, 1994); *cpr5* (Bowling *et al.*, 1997) and *cpr6-1* (Clarke *et al.*, 1998). *cpr1* exhibits constitutive expression of *PR* genes, high level of SA and resistance to both bacterial and oomycete pathogens; epistasis analysis places *cpr1* upstream of SA. *cpr5* is a lesion-mimic mutant with similar characteristics to *cpr1*; epistasis analysis places *cpr5* upstream of both the HR and SA. Unlike *cpr1* and *cpr5* which are recessive, *cpr6-1* is a dominant mutant. *cpr6-1* exhibits constitutive expression of *PR-1* and *PDF1.2* and resistance to both bacterial and oomycete pathogens (Bowling *et al.*, 1994; Bowling *et al.*, 1997; Clarke *et al.*, 1998). Recently, double mutant analysis of *cpr1* and *cpr6-1* revealed that these phenotypes are blocked by mutations in *eds5* (Clarke *et al.*, 2000), *eds1* (Clarke *et al.*, 2001), or *pad4* (Jirage *et al.*, 2001); which places the *cpr* mutations on *SA*-dependent signalling upstream of *PAD4* (Figure 1.3). However, the disease resistance phenotypes of *cpr1* and *cpr6* are only partially blocked by mutations in *npr1*, demonstrating the existence of an SA-dependent, *NPR1*-independent resistance mechanism (Clarke *et al.*, 2000). In a similar fashion, *dnd1::pad4* or *dnd2::pad4* double mutants still retain characteristic *PR-1* expression and SA accumulation but the resistance to *Pseudomonas syringae* is lost, suggesting the existence of a *PAD4*-dependent, but SA-independent component of resistance (Jirage *et al.*, 2001).

Further support for the existence of SA-dependent, *NPR-1*-independent resistance mechanisms comes from the observation that responses that are blocked by *nahG* are not necessarily blocked by *npr1*. Recently, a mutation that may function in an SA-dependent, NPR1-independent pathway has been identified. Plants carrying the *dth9* mutation express *PR* genes in response to SA treatment but fail to develop resistance. Therefore, it is suggested that DTH9 is required downstream of SA to activate SAR, but is not required for the expression of known SAR-related genes (Mayda *et al.*, 2000). In *cpr5*, however, SA levels and *PR-1* expression and disease resistance are

partially reduced by *eds1* and *pad4* mutations, and are completely blocked by *eds5* mutation. Hence, it can be concluded that in *cpr5* whereas the accumulation of SA does not strictly require *EDS1/PAD4*, a functional *EDS5* is an absolute requirement (Clarke *et al.*, 2001; Jirage *et al.*, 2001; Clarke *et al.*, 2000). It would be interesting to characterise the numerous lesion-mimic mutants that have been isolated with regard to their requirements for *PAD4/EDS1* and dependency of SA accumulation on *EDS5/SID2*.

1.8.2.4 MAPK cascade components

It has been recently shown, from several mutations in MAPK cascade components, that they negatively regulate the SA-dependent pathway. A null mutation in *EDR1*, that was found to encodes a MAPK kinase kinase (MAPKKK), enhances resistance to *Pseudomonas syringae* and *Erisyphe cichoracearum*, possibly via the rapid expression of defence-related genes after attempted infection. This enhanced resistance is blocked by *nahG*, *pad4*, or *npr1* mutations, indicating that the *edr1* mutation requires SA-dependent signalling. The *EDR1* is suggested to negatively regulate SA signalling acting upstream of *pad4* and *eds1* (Figure 1.3) (Frye *et al.*, 2000; Frye & Innes, 1998).

1.8.3 JA/ET-dependent signalling network

The wound response pathway has been extensively studied in the context of induced resistance to insect predation in tomato and tobacco and more recently in *Arabidopsis*. It is triggered by wounding and insect feeding resulting in the induction of *p*roteinase *i*nhibitor (*Pin*) genes in solanaceous species. The PIN proteins interfere with digestion in the insect gut and stop the insect from further feeding. Signalling in the wound response pathway is mediated by JA and ET, which act synergistically to induce wound response genes in addition to stimulating the biosynthesis of each other (McConn *et al.*, 1997; Ryan *et al.*, 1990; Creelman & Mullet, 1997; Xu *et al.*, 1994; O'Donnell *et al.*, 1996). Over the past few years, accumulating evidence has

been produced implicating JA and ET as important signals in the induction of systemic defence responses that are distinct from the SA-mediated SAR. Both JA and ET are rapidly produced when the plant is attacked by a pathogen, particularly during necrotrophic pathogens where the rise in JA levels extends to systemic tissues (Penninckx *et al.*, 1996). Moreover, exogenous application of these signalling molecules induces a set of defence genes that are also activated upon pathogen infection. Among these genes are *PDF1.2* and *Thi2.1* (which encode small, cysteine-rich, basic proteins with anti-microbial activity) (Terras *et al.*, 1995; Epple *et al.*, 1995). In *Arabidopsis*, the *Thi2.1* and *PDF1.2* genes are locally and systemically activated after infection with the necrotrophic fungal pathogen *Fusarium oxysporum* f. sp. *matthiolae* or exogenous application of methyl jasmonate (a volatile form of JA), but not after treatment with SA. In *Arabidopsis nahG* plants (defective in SA-signalling), pathogen-induced *PDF1.2* is unaffected (Epple *et al.*, 1995; Epple *et al.*, 1997). Moreover, *nahG* and *npr1* mutants do not show enhanced susceptibility towards the necrotrophic soft rot fungus *Botrytis cinerea*. On the contrary, the *e*thylene-*in*sensitive (*ein2*) mutant and the JA insensitive mutant *coi1* display enhanced susceptibility towards this fungus, indicating that this pathway is SA-independent and JA-/ET-dependent (Thomma *et al.*, 1998; Thomma *et al.*, 1999a). Furthermore, *PDF1.2* gene expression is blocked in the *e*thylene-*in*sensitive (*ein2*) mutant and the jasmonic acid insensitive mutant *coi1*, demonstrating a further evidence that the signalling pathway involved in *PDF1.2* induction requires components of the ET and JA response (Penninckx *et al.*, 1998). In addition, it was shown that JA and ET signalling pathways need to be activated concomitantly to induce *PDF1.2* upon pathogen attack (Penninckx *et al.*, 1998). In addition to *PDF1.2* (also known as *PR-12*), JA and ET co-regulate a subset of *PR* genes including *PR-3* and *PR-4* that also encode antimicrobial proteins (Penninckx *et al.*, 1998; Thomma *et al.*, 1998).

The only cloned defence regulatory gene in the JA defence pathway is *COI1*, which encodes a protein containing 16 LRRs and an F-box protein. COI1 has similarity to the F-box proteins: *Arabidopsis* TIR1, human Skp2, and yeast Grr1 which function by targeting repressor proteins for removal by ubiquitination. It is hypothesised that

COI1 might bind negative regulators of the JA response (Xie *et al.*, 1998). In the ET pathway, *EIN2* has been recently cloned and it encodes a membrane-associated signal transduction component of which the amino terminus shows homology to the Nramp family of metal ion transporters. As it is demonstrated that the expression of the carboxyl terminus leads to activation of ethylene response, it is concluded that EIN2 might act as a bifunctional signal transducer in which the amino terminus senses a cation as a signal and the carboxyl terminus is involved in downstream responses (Alonso *et al.*, 1999).

1.8.4 Defence pathways specificity and spectrum of effectiveness

It is believed, based on experimental evidence, that the SA-dependent defence responses seem to be effective against biotrophic pathogens such as *Peronospora parasitica*. Moreover, resistance against this type of pathogen is quite often associated with an HR reaction that is confined to the infected cells whereby nutrient deprivation of the pathogen is accomplished. As another example, the SA-dependent, but not the JA-/ET-dependent, defence response has been shown to be effective in protecting the plant against the powdery mildew biotrophic fungus *Erysiphe orontii* (Reuber *et al.*, 1998). In contrast, JA-/ET-dependent defence seem to be more effective against necrotrophic pathogens such as *B. cinerea*. This is supported by genetic evidence showing that both a JA-deficient *fad* triple mutant *fad3::7::8*, which fails to synthesise JA, and a JA-insensitive (*jar1*) mutant display higher susceptibility to the necrotrophic pathogen *Pythium irregulare* (Vijayan *et al.*, 1998; Staswick *et al.*, 1998). Similarly, defects in SA signalling lead to enhanced susceptibility towards strains of the hemi-biotrophic bacterium *Pseudomonas* (Delaney *et al.*, 1994), whereas insensitivity towards either JA or ET compromises defence against the necrotrophic bacterium *Erwinia carotovora* (Norman-Setterblad *et al.*, 2000). Taken together, it seems more likely that the type of pathogenicity and pathogen life style (i.e. biotrophic or necrotrophic), rather than the phylogeny (i.e. bacteria or fungi), that dictates the effectiveness of the plant's resistance mechanism. Recent genetic evidence providing further support for this concept comes from the study of disease responses of the *dnd1* mutant. It has been demonstrated that in the *dnd1* mutant

(Clough *et al.*, 2000), the growth of the necrotrophic pathogens *Botrytis* and *Sclerotinia* is suppressed. This finding indicates that where the HR is important in restricting the growth of biotrophs, it represents an added advantage for necrotrophic pathogens whereby facilitating the infection and successful colonisation of the host (Govrin & Levine, 2000). Consequently, it is possible that plants might have evolved the two separate SA- and JA-/ET-dependent defence responses to operate selectively against biotrophs and necrotrophs, respectively.

1.8.5 Cross talk between the SA- and JA/ET-dependent pathways

Most biological signal transduction pathways ate integrated in complex and highly sophisticated communication networks (Bhalla & Iyengar, 1999; Genoud & Metraux, 1999). Thanks to the recent use of cDNA microarray analysis of gene expression in response to pathogens and defence signalling molecules, it is now believed that plant defence signalling networks exhibit a considerable degree of complexity, interplay and cross-talk (Schenk *et al.*, 2000). As mentioned before, there is a clearly evident antagonistic relationship between SA- and JA/ET-dependent signalling. This is supported by many observations including the antagonistic effect of SA application on wound- and/or JA-induced gene expression (Penacortes *et al.*, 1993; Doares *et al.*, 1995). Additionally, further genetic evidence for the antagonism between the two pathways comes from the analysis of *Arabidopsis* defence mutants. Many lesion-mimic mutants, including *cpr5*, *cpr6*, *dnd1*, *dnd2* and *ssi1*, display constitutively high expression of both *PR-1* and *PDF1.2*, suggesting that the SA- and JA-dependent signalling pathways share common activating signal. Genetic and molecular analysis of mutants involved in the SA-dependent pathway indicated that the expression of the JA-dependent gene *PDF1.2* is modulated. This evidence include the *PDF1.2* strong induction in response to the *PDF1.2*-inducing agent rose bengal in *pad4* mutants (Gupta *et al.*, 2000); increased *cpr6*-dependent *PDF1.2* expression in *cpr5:: eds5*, *cpr6:: pad4*, and *cpr6:: eds1* double mutants (Clarke *et al.*, 2001; Jirage *et al.*, 2001; Clarke *et al.*, 2000); enhanced *PDF1.2* expression in *sid2* plants infected with *Erisyphe orontii* (Dewdney *et al.*, 2000); and enhanced *PDF1.2* expression in *npr1* or *nahG* plants treated with rose bengal or infected with *Alternaria brassicicola*

(Penninckx *et al.*, 1996; Clarke *et al.*, 1998). Moreover, the ability of JA to repress the expression of SA-induced *PR-1* gene in response to ozone treatment, has been also demonstrated (Rao *et al.*, 2000).

Alongside the mechanism of mutual antagonistic cross-talk, synergistic cross-talk between signalling pathways has been reported. A striking example is the ability of *Arabidopsis* plants to simultaneously activate both SAR and JA/ET-dependent ISR responses, resulting in increased resistance against the virulent *P. syringae* pv. *tomato* strain DC3000 (Van Wees *et al.*, 2000). The shared requirement of NPR1 by both ISR and SAR is a further demonstration of this positive interplay. Identification of novel signalling components in *Arabidopsis* has indicated the existence of several branches within a pathway and additional defence pathways. Experiments using *pad4* and *sid* mutants have shown that *PR-2* and *PR-5* can also be induced independently of *PR-1* by an SA-independent pathway (Zhou *et al.*, 1998; Nawrath & Métraux, 1999), which also provides further evidence supporting the existence of an SA-dependent NPR1-independent defence pathway. The dominant mutant *ssi1* constitutively expresses both *PR-1* and *PDF1.2* genes and was found to completely bypass the requirement for *NPR1*; implicating SSI1 in a NPR1-independent signal transduction pathway (Figure 1.3). SSI1 is suggested to be a genetic switch acting as a negative regulator of SA-dependent responses (Shah *et al.*, 1999; Greenberg, 2000). The dominant *acd6* mutant is only partially suppressed by *npr1*, suggesting that ACD6 acts in both an NPR1-dependent and NPR1-independent pathway perhaps as a positive regulator of SA-dependent responses (Rate *et al.*, 1999).

The complexity of *Arabidopsis* defence signalling against different pathogens is depicted in Figure 1.4.

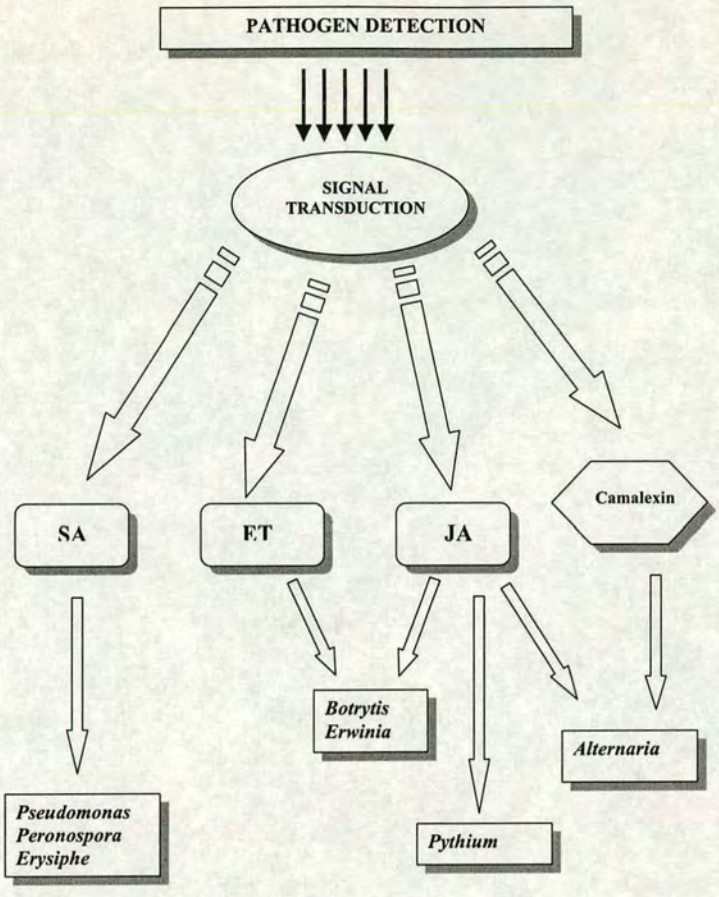

Figure 1.4: Schematic representation of the complexity of disease signalling network in *Arabidopsis*. This model is meant to emphasis the fact that plants often recruit components of different pathways in order to successfully restrain a particular pathogen. (After Thomma *et al.*, 2001 with modifications).

Analysis of the complexities of *Arabidopsis* defence signalling responses against *A. brassicicola* reveals the plant's capacity of integrating various pathways depending on the type of pathogen it is encountering. *pad3* mutants show enhanced susceptibility towards *A. brassicicola* (Thomma *et al.*, 1998; Thomma *et al.*, 1999b). This mutant is deficient in the production of the phytoalexin camalexin, owing to a mutation in a gene encoding P_{450} mono-oxygenase (Zhou *et al.*, 1999). Camalexin biosynthesis is not directly controlled by SA, ET or JA. The *pad3* mutant does not show enhanced susceptibility towards *P. syringae*, *P. parasitica*, *E. orrontii*, or *B. cinerea*. While *coi1* mutant is susceptible towards *A. brassicicola*, whereas *ein2* is

not. Taken together, it can be concluded that resistance against this fungus is controlled by an ET-independent branch of the JA/ET-dependent defence pathway (Thomma *et al.*, 1998; Thomma *et al.*, 1999a).

This apparent complexity no doubt equips the plant with the flexibility required to respond to a particular pathogen by activating appropriate subsets of defences and suppressing inappropriate responses. Another important lesson to be learned, is that sometimes the plant resorts to the use of more than one pathway in order to achieve the ultimate goal, that is to successfully contain and restrain a particular pathogen. Examples include the use of both camalexin-dependent pathway together with JA-dependent pathway to contain *A. brassicicola*, the use of both SA-dependent together with JA-dependent pathway to contain *Plectosphaerella cucumerina* (Figure 1.4) (Thomma *et al.*, 2000).

1.9 The role of nitric oxide in defence signalling in plants

1.9.1 NO biosynthesis in mammalian cells

In mammalian systems, the highly reactive radical nitric monoxide (NO) has been implicated in the control of a number of diverse physiological processes. At low concentrations, around 10^{-7} M, NO functions in the control of smooth muscle relaxation, blood pressure homeostasis, inhibition of platelet aggregation, neurotransmission and immune system regulation (Schmidt & Walter, 1994; Cooper, 1999). On the other hand, at higher concentrations, NO plays an essential defensive and cytotoxic role in the immunological reaction against invading microbes (Stamler, 1992; Beck *et al.*, 1999). With a half-life of less than a second, NO exhibits one of the most rapid and complicated chemical reactions. NO reactions of biological significance include those with (di)oxygen and its various redox forms and with transition metal ions. Reminiscent of ROI ($O_2^{\cdot-}$, $OH^{\cdot}$ and H_2O_2), NO forms an array of interrelated redox forms collectively known as reactive nitrogen intermediates (RNI) that arise in physiological environments including the nitric oxide radical ($NO^{\cdot}$), nitrosonium cation (NO^+), nitroxyl anion (NO^-), NO_2^-, N_2O_3, N_2O_4, peroxynitrite $OONO^-$, S-nitrosothiols and dinitrosyl-iron complexes (Stamler *et al.*, 1992).

In vertebrates, NO biosynthesis is primarily accomplished by the enzyme nitric oxide synthase (NOS, EC 1.14.13.39). Three isoforms have been identified and named on the basis of their tissue of origin: neuronal NOS (nNOS), inducible NOS in macrophages (iNOS) and endothelial NOS (eNOS) (Nathan & Xie, 1994). Both nNOS and eNOS are constitutive, whereas iNOS gene expression is inducible in macrophages and other cell types. Each NOS is a bidomain enzyme consisting of an N-terminal oxygenase and a C-terminal reductase. The C-terminal oxygenase domain, contains a P-450 type heme centre and a binding site for the cofactor tetrahydrobiopterin. The reductase domain contains NADPH, FAD and FMN binding sites with high homology to NADPH cytochrome P-450 reductase.

Both domains are connected by a calmodulin (CaM) binding site. In their active form, NOSs oxidise L-arginine to L-citrulline and NO (Figure 1.5). The activity of constitutive NOSs is strictly dependent on the elevation of intracellular free Ca^{2+} and resultant binding of the Ca^{2+}-CaM complex, whereas, the activity of iNOS is independent of free Ca^{2+} concentration, with CaM remaining tightly bound to the enzyme even in the absence of elevated intracellular Ca^{2+} (Mayer & Hemmens, 1997; Marletta, 1994). NO generated by NOS together with the NADPH oxidase product O_2^- can form the powerful cytotoxic species peroxynitrite ($OONO^-$) which is implicated in several pathophysiological processes including apoptosis and the killing of invading pathogens (Brüne *et al.*, 1998).

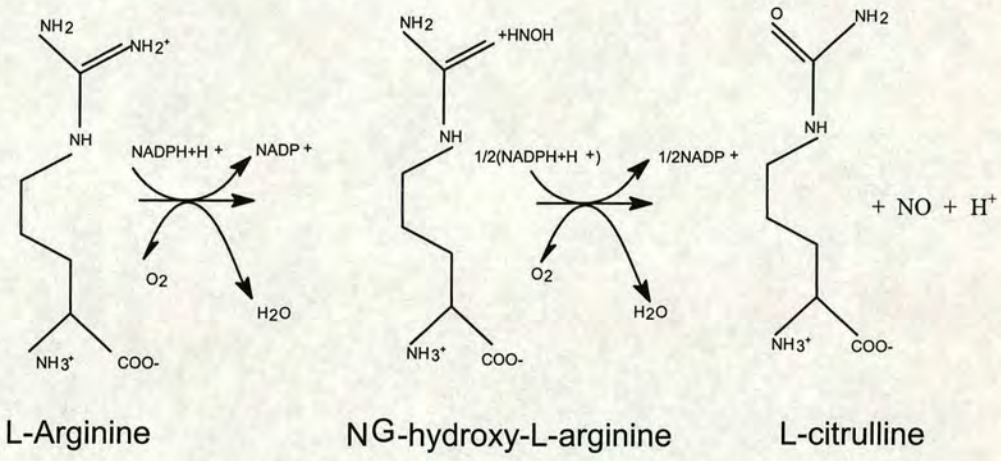

Figure 1.5: Schematic representation of the biosynthetic reaction mediated by NOS leading to the generation of NO in animal cells.

It is generally conceived that NO has the ability to freely diffuse from endothelium to vascular smooth muscle and platelets and across neural synapses to evoke biological responses (Lancaster, 1994). NO signalling pathways in animal cells are typically classified as either cyclic GMP (cGMP) -dependent or -independent (Nathan & Xie, 1994). The cGMP-dependent pathway is initiated by NO-induced activation of guanylate cyclase by binding to the heme iron resulting in a transient increase in cGMP which is involved in smooth muscle relaxation, inhibition of platelet aggregation and in sensory systems. Several downstream cGMP targets are implicated in this pathway including cGMP-dependent protein kinase, cyclic nucleotide-gated channels, phosphodiestrases, ryanodine-sensitive calcium channels

and the potent Ca^{2+} mobilising second messenger cyclic ADP ribose (cADPR) (Willmott *et al.*, 1996; Beck *et al.*, 1999). On the other hand, the cGMP-independent pathway seems to function through nitrosation. Nitrosation is the process through which NO modulates the biological activity of proteins by direct interaction with either their metal centres or thiols forming S-nitrosothiols (RS-NO). Metal- and thiol- containing NO signalling target proteins include: membrane proteins (e.g. NADPH oxidase, G proteins, protein kinase C, and K_{ca}^{+} channel); cytosolic proteins (e.g. GADPH, guanylate cyclase, aconitase/IRE-BP, and cytochrome P-450s) and transcription factors (e.g. AP-1 and NF-kB) (Stamler, 1994).

1.9.2 NO signalling in plants

ROS appear to play key roles in early and later stages of the plant response against pathogens. During the hypersensitive response, a massive production of ROS takes place leading to the induction of host cell death and pathogen containment. However, the role of ROS in host cell death seems to necessary but not sufficient for the induction of cell death, implying the involvement of other factors (Dangl, 1998). In animals, ROS (mainly the superoxide radical) produced by NADPH oxidase, collaborates with NO (produced by NOS) to regulate apoptosis and pathogen killing. In this regard, the recent discovery of plant homologues of the NADPH oxidase (Groom *et al.*, 1996; Keller *et al.*, 1998) prompted scientists to investigate whether NOS, and indeed NO, also play roles during plant-pathogen interactions. The ability of plants to accumulate and metabolise NO has been known for some time (Nishimura *et al.*, 1986). Several physiological responses in plants are associated with NO including growth and development (Leshem & Kuiper, 1996; Leshem & Haramaty, 1996; Beligni & Lamattina, 2000), and phytoalexin production (Noritake *et al.*, 1996). Moreover, recent evidence suggests that NO plays a prominent role in plant defence against pathogens. In *Arabidopsis* and soybean cells the treatment with avirulent bacteria resulted in an elevated NOS activity and the subsequent release of NO. Interestingly, NOS inhibitors were able to compromise the resistance response in *Arabidopsis* and the induction of hypersensitive response in pathogen-treated soybean suspension cells (Delledonne *et al*, 1998). Similarly, infection of tobacco

with TMV resulted in enhanced NOS-like activity (Durner *et al.*, 1998). Reminiscent of the oxidative burst during the hypersensitive response, very recent studies suggest the formation of a NO burst that could be detected in the cytosol and chloroplasts and is sensitive to NOS inhibitors (Pedroso *et al.*, 2000). Similarly, in epidermal tobacco cells treated with a fungal elicitor, a very fast NO burst was reported to occur within minuets of the elicitor treatment using fluorophore-based *in vivo* imaging (Foissner *et al.*, 2000). As mentioned previously, Ca^{2+}/CaM-dependent activation of NOS and its production of NO play a key regulatory role in both plant and animal cell function. Point mutations in the plant calmodulin SCaM-1, which shares 91% identity to mammalian CaM, resulted in the inhibition of mammalian NOS (Kondo *et al.*, 1999).

Taken together, these data clearly demonstrate and shed some light on the remarkable similarities between plant and animal NO signal transduction pathways. Figure 1.6 is a schematic representation summarising our current understanding of NO signalling components and its physiological effects in plants. Bacterial NO detoxifying components are also included in the schematic representation.

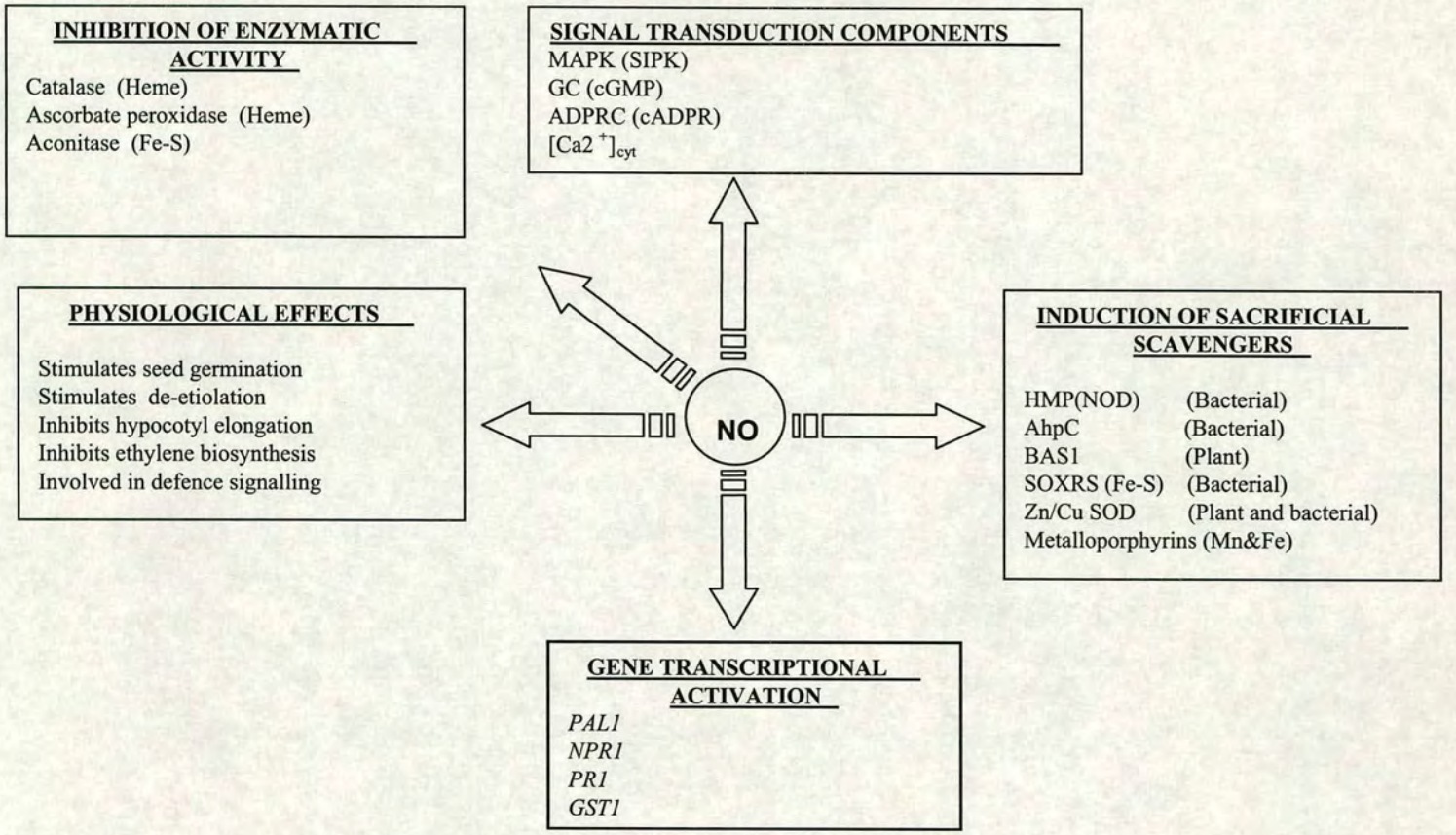

Figure 1.6: Schematic representation depicting the signal transduction network and physiological effects of NO in plants.

An accumulating body of evidence revealed that plants share great similarities with their animal counterparts with regard to NO signal transduction pathways and signalling components. For example, the second messenger cGMP was discovered to be present in plants (Brown & Newton, 1992) and it was shown to be responsible for the control of several physiological processes including, the induction of the stress responsive genes chalcone synthase and the production of secondary metabolites (Bowler *et al.*, 1994). Moreover, NO treatment was shown to mimic gibberellic acid and light stimulation (Penson *et al.*, 1996) in their ability to induce a transient increases in cGMP levels in plants (Pfeiffer *et al.*, 1994). Administration of NO donors or recombinant mammalian NOS to tobacco plants or cell suspensions resulted in the induction of the expression of defence genes encoding the PR1 protein and PAL. These tobacco defence genes were also induced by cGMP and cADPR. Moreover, PAL gene activation by NO was blocked by specific guanylate cyclase inhibitors (Durner *et al.*, 1998). Furthermore, NO treatment of plants results in the inhibition of ethylene production, which is a natural plant hormone that controls senescence and fruit ripening (Leshem & Pinchasov, 2000). Other experiments revealed that administration of the commercial drug Viagra®, a specific and potent inhibitor of cGMP-degrading phosphodiestrases (i.e. blocks NO signalling), resulted in more dramatic inhibition of ethylene production and the prevention of wilting in flowers (Siegel-Itzkovich, 1999). These observations clearly implicate NO as an important maturation and senescence regulating factor in plants.

In mammals, many insights into the understanding of NO functions came from the identification of NOS. NOS-like activity, based on the formation of $_{L}$-citrulline from $_{L}$-arginine and/or sensitivity to mammalian NOS inhibitors, has been detected in several plants (Wendehenne *et al.*, 2001). However, despite continuous search efforts neither the gene nor the protein responsible for NOS activity has been isolated from plants. Recently, indirect evidence for presence of a plant NOS homologue has been presented including the identification of a plant cDNA sequence with pronounced similarity to a mammalian NOS inhibitor (Jaffrey & Snyder, 1996) and the detection of immunoreactive proteins in plant extracts using antibodies raised against mammalian

NOSs (Barroso *et al.*, 1999; Ribeiro *et al.*, 1999). To add to the difficulty of finding a plant NOS homologue, an alternative enzymatic pathway for NO production based on the reduction of nitrite (NO_2^-) to NO by the enzyme nitrate reductase has been reported (Yamasaki *et al.*, 1999).

1.9.3 NO defence components

Study of bacterial responses to NO stress have contributed significantly towards our understanding of NO stress defence mechanisms. Bacterial cells are well equipped with tightly regulated genes conferring resistance to NO and oxidative stress in general, the expression of which is controlled by either thiol- or metal-containing proteins that sense changes in redox states (Nathan & Shiloh, 2000). Several candidate reactive nitrogen intermediates (RNI) resistance and detoxification gene products have been found to functions in microorganisms. For example, those blunting the action of NO. By reducing the levels of superoxide, *E. coli* Cu, Zn-SODs decrease the extent to which superoxide combines with NO to form the more cytotoxic product peroxynitrite resulting in protection against RNI (Hausladen *et al.*, 1996). NO can activate the transcription factor SoxR that in turn induce the SoxS regulon controlling SOD expression (Ding & Demple, 2000). *Salmonella* typhimurium OxyR, a cysteine-dependent transcription factor, is activated by intramolecular disulphide bond formation upon oxidation by hydrogen peroxide. Oxidised OxyR induces a stress regulon that includes catalase and alkylhdroperoxide reductase (Ahp) (Zheng *et al.*, 1998). The small subunit of Ahp (AhpC) was found to belong to the ubiquitous peroxiredoxin family several members of which have been shown to reduce hydrogen peroxide or alkyhydroperoxides. Recently, persoxiredoxins were shown to confer protection against RNI. An *ahpC* deficient *Salmonella typhimurium* strain was significantly more susceptible than the wild-type to RNI killing. Moreover, expression of a*hpC* from *Mycobacterium tuberculosis* conferred marked resistance against RNI generated by NOS2 (Chen *et al.*, 1998). In *E. coli*, NO-resistant mutants were isolated that rapidly consumed NO. A flavohemoglobin (*hmp*)

was shown to be responsible for the NO-converting, cyanide-sensitive, O_2-dependent and aconitase-protecting activity. The HMP enzyme dioxygenates NO to NO_3^- according to the following NADPH- and O_2-dependent reaction:

$$2NO^{\cdot} + 2O_2 + NAD(P)H \xrightarrow{\textbf{NOD}} 2\,NO_3^- + NADP^+ + H^+$$

Therefore, *HMP* has also been named nitric oxide dioxygenase (NOD). Interestingly, *HMP/NOD* is induced by RNI. Moreover, *HMP/NOD*-deficient mutants whave been reported to be sensitive to growth inhibition exerted by NO (Gardner *et al.*, 1998).

Other RNI-defence mechanisms are involved in the repair of RNI-dependent lesions. The DNA repair proteins RecB and RecC are important for survival of *S. typhimurium* in mice and macrophages. The growth of a *recBC* mutant of *S. typhimurium* was attenuated in both wild-type and NOS2-deficient mice, but regained partial virulence in phox-deficient mice and complete virulence in mice deficient in both NOS2 and phox (Shiloh *et al.*, 1999). Therefore, it seems vital for bacteria to have a functional repair system in order to be able to withstand the RNI and ROS defence mechanisms mounted against them during attempted invasion.

In plants, apart form SOD and peroxiredoxin homologoues (Baier & Dietz, 1997), very little is known about RNI defence. Therefore, more efforts are required in order to identify novel plant candidates for RNI resistance and detoxification.

1.10 Phytopathogenic fungi

1.10.1 Economic significance of filamentous phytopathogenic fungi

Most notorious diseases of humans and other animals are caused by bacteria and viruses. By contrast, the majority of plant pathogens are fungi. This can be explained partly on the basis of several differences between plants and animals as habitats for microbial growth. Bacteria generally prefer warm, alkaline conditions with high nitrogen levels. Because bacteria are unicellular their spread within the host is enhanced by a circulatory system. The cell wall and cuticle in plants represent the physical barriers that keep most organisms from developing an intimate contact with plants. Unlike bacteria, filamentous fungi are more effective pathogens because they are capable of directly penetrating through the surface layers of plants and they require acid pH high carbon level (as in plant cells). Consequently, fungi play the dominant role not only by causing devastating epidemics, but also through the less spectacular although persistent and significant annual crop yield losses that have made fungal pathogens of plants a serious economic factor, attracting the attention of farmers, plant breeders, and scientists alike (Knogge, 1996).

Fungi constitute a highly versatile group of organisms that are small, generally microscopic; eukaryotic, usually filamentous, branched, spore-bearing organisms that lack chlorophyll. Fungi have cell walls that contain chitin and glucans as skeletal components, which are embedded in a matrix of polysaccharides and glycoproteins. The vast majority of the 100,000 known fungal species are strictly saprophytic, that is, they live on dead organic matter which they help decompose. More than 10, 000 species of fungi can cause disease in plants. All plants are attacked by some kinds of fungi and each of the parasitic fungi can attack one of many kinds of plants. Some fungi, known as obligate parasites or biotrophs, can grow and multiply only by remaining, during their entire life, in association with their host plants. Others, known are non-obligate parasites or necrotrophs, require a host plant for part of their life cycles but can complete their

cycles on dead organic matter, or they can grow and multiply on dead organic matter as well as on living plants. The fungi that cause diseases on plants are a diverse group. The true fungi (i.e. chtridiomycetes, zygomycetes, ascomycetes, basidiomycetes, and deuteromycetes) belong to the kingdom Fungi (earlier called Euycota or Mycetae) (Agrios, 1988).

Ascomycetes and the asexual Fungi Imperfecti (Deuteromycetes) are two groups of fungi that closely resemble one another: both produce a haploid mycelium that has cross walls, both produce conidia in identical types of conidiophores or fruiting bodies, and both cause the same kinds of plant diseases. The only difference is that Ascomycetes also produce sexual spores, known as ascospores, whereas imperfect fungi do not. In many ascomycetes, however, ascospores are seldom found in nature. Therefore, such Ascomycetes reproduce, spread, cause disease, and overwinter as mycelium or conidia, or both so that they actually behave as imperfect fungi. Ascomycetes (the sac fungi) produce sexual spores that are called ascospores because they form within a sac called ascus. They also produce asexual spores known as conidia. The ascus or sexual stage of Ascomycetes is often called teleomorph or perfect stage, whereas the conidial or asexual stage is the anamorph or imperfect stage. Asomycetes, during the growing season the fungus exists as mycelium and reproduces and causes most infections with its asexual stage, that is conidia. The sexual or perfect stage is produced on or in infected leaves, fruits, or stems only at the end of the growing season or when food supply is diminishing. The perfect stage is usually the overwintering stage. Generally, ascospores act as the primary inoculum and cause the first (primary) infections in the spring. The primary infections then produce conidia, which act as the secondary inoculum and cause all subsequent infections during the growing season (Agrios, 1988).

Fungi cause local or general symptoms on their hosts and such symptoms may occur separately or concurrently, or may follow one another. In general, fungi cause local or general necrosis or killing of plants, and they often result in reduced growth (stunting) of plant organs or entire plants. The most common necrotic symptoms include: leaf spots,

blight, cankers, dieback, root rot, basal stem rot, soft and dry rots, anthracnose, scab, and decline. Almost all of those may also cause pronounced stunting of the infected plants. In addition, certain other symptoms such as rusts, mildews, and wilts may cause stunting of the plants as a whole (Agrios, 1988).

1.10.2 Vascular wilts caused by Fusarium oxysporum infection

An economically important group of plant fungal pathogens is the group of vascular wilts. Vascular wilts are considered to be one of the most widespread, devastating and destructive plant fungal diseases. There are four general of fungi that cause vasculat wilts: *Ceratocystis*, *Ophiostoma*, *Fusarium*, and *Verticillium*. In particular, *Fusarium* is one of the four fungal genera that cause vascular wilts that results in substantial annual yield losses in vegetables, flowers, plantation crops and perennial ornamentals. Disease symptoms appear as rapid wilting, browning, and dying of leaves and succulent shoots of plants followed by death of the whole plant. Wilts occur as a result of the presence and activities of the pathogen in the xylum vessels of the plant. Entire plants may die within a matter of weeks. As long as the infected plant is alive, the wilt-causing fungi remain in the vascular (xylem) tissues and a few surrounding cells. Only when the infected plant is killed by the disease do these fungi move into other tissues and sporulate at or near the surface of the dead plant. Each of them causes diseases on several important crops, forest, and ornamental plants. Most of the wilt-causing *Fusarium* belong to the highly ubiquitous species *Fusarium oxysporum*. Different host plants are attacked by special forms (i.e. *forma specialis*) or races of the fungus; e.g. the fungus that attacks tomato is designated as *F. oxysporum* f. sp. *lycopersici* (Agrios, 1997).

1.11 Aims

1.11.1 Chapter III: characterisation of T-DNA activation tagged Arabidopsis SAR mutants identified by luciferase imaging

The aim of this work is to employ the T-DNA activation tagging approach in combination with luciferase imaging technology for the identification and characterisation of SAR mutants. In this chapter, the molecular, biochemical and genetic characterisation of an identified *bona fide* SAR mutant is covered. In the light of current knowledge of plant defence signalling responses, discussion of the results obtained and its significance to crop protection and biotechnology is also considered.

1.11.2 Chapter VI: Nitric oxide and calcium signal transduction in Arabidopsis

The aims of this work are two-fold. Firstly, investigation of the ability of the NO donor SNP and NO produced during avirulent plant-bacterial interactions to elicit $[Ca^{2+}]_{cyt}$ transients using *Arabidopsis* transgenics expressing the Ca^{2+}-sensitive photoprotein aequorin. In this, a chemiluminometer assay and *in vivo* Ca^{2+} imaging are employed. Moreover, the specificity and dose-dependency of the $[Ca^{2+}]_{cyt}$ transients induced by NO are closely examined. Furthermore, the results obtained using a novel photocoustic-based CO laser spectroscopic approach are discussed. Secondly, generation and characterisation of NO-deficient *Arabidopsis* transgenic plants overexpressing the bacterial gene *HMP/NOD*. Characterisation of 35S::*NOD/HMP* lines include molecular (i.e. northern and western) analyses and bacterial pathogenicity assays.

1.11.3 Chapter V: Transformation of Fusarium oxysporum with GFP via particle bombardment

Despite its economic importance and widespread, reports describing the genetic transformation of *Fusarium oxysporum* are limited. Therefore, the aims of this work are two-fold. Firstly, to investigate the utility of particle bombardment as a tool for genetic transformation of *Fusarium oxysporum* using the green fluorescent protein (GFP) as a vital marker. Secondly, to assess the potential use of GFP-transformed *Fusarium oxysporum* in the quantification of fungal biomass on leaf surfaces. The results obtained are discussed. The results obtained and its utility are discussed.

CHAPTER II

2 MATERIALS AND METHODS

Unless otherwise stated, all chemicals were purchased from Sigma (Sigma-Aldrich, UK).

2.1 Growth of *Arabidopsis thaliana* plants on soil

Arabidopsis thaliana seeds of the accession Columbia (Col-0) and Landsberg (L*er*) were used. For *Agrobacterium* transformation, homozygous *Arabidopsis PR1::LUC* seeds were used. *PR1::LUC* plants are transgenic Col-0 lines that were transformed with the fire fly luciferase reporter gene (*LUC*) under the control of the *PR1* promoter of tobacco followed by the transcription termination and polyadenylation signals of the *oc*topine *s*ynthase (*ocs*) (Murray *et al.*, submitted). Routinely, seeds were placed on potting medium consisting of peat moss, vermiculite and sand (4:1:1), and allowed to vernalise for 48 hrs at 4°C after which they were transferred to 20°C. Two weeks old seedlings were transferred 4 per pot, watered by sub-irrigation and fertilised once a week with Phosphogen®. In order to promote healthy vegetative growth, plants were placed under short day length conditions (10 hrs light, 14 hrs dark) at 20°C. Plants destined for *Agrobacterium* transformation, were placed in the greenhouse under longer day length conditions (16 hrs light, 8 hrs dark).

2.2 Bacterial growth and inoculation

Pseudomonas syringae pv. *tomato* (*Pst*) DC3000 expressing the gene *AvrB* was grown on King's broth (KB) (King *et al.*, 1954) supplemented with 50 $mg.l^{-1}$ rifampicin and 50 $mg.l^{-1}$ kanamycin. Liquid cultures were grown on a shaker at 30 °C, and cells were harvested at $OD_{600} \cong 0.2$ (equivalent to 10^6 colony forming units (cfu).ml^{-1}). Cells were pelleted by centrifugation and re-suspended for plant inoculation in 10 mM $MgCl_2$. For inoculation, 6 µl of the *Pst*DC3000 (*AvrB)* suspension were forced under the abaxial epidermis using a 1 ml syringe. Successful inoculations were visualised by the

appearance of a watery area under the epidermis. Inoculated plants were placed back in to the growth room. Infiltrated leaf tissues were collected, 48 hrs post-inoculation, frozen in liquid nitrogen and stored at -70°C for further analysis.

2.3 T-DNA mutagenesis

Transformation of homozygous *PR1::Luc* plants was undertaken according to Clough & Bent (1998). *Agrobacterium tumefaciens* GV3101 strain, harbouring the SKI15 activation tagging binary vector, was grown at 28°C on overnight on LB medium supplemented with 50 $mg.l^{-1}$ kanamycin (to select for the helper plasmid) and 50 $mg.l^{-1}$ ampicillin (to select for the SKI15 binary vector). The bacterial culture was spun down and re-suspended to a final density of $OD_{600} \cong$ 0.8 in 5% sucrose solution. Before dipping, Silwet (Union Carbide) was added to a concentration of 0.001% in order to decrease surface tension thereby increasing the accessibility of the bacteria to plant tissues, hence increasing the transformation efficiency. The procedure is schematically represented in Figure 2.1.

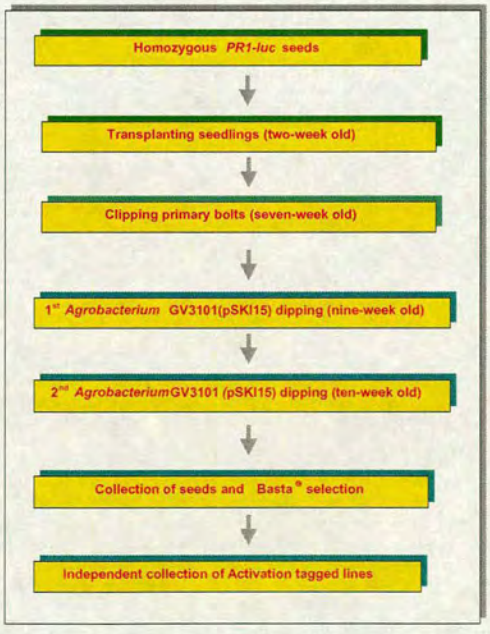

Figure 2.1: Strategy for the generation of activation tagged lines.

Soil grown mature homozygous *Arabidopsis* plants were used for transformation. Primary bolts of these plants were cut (2-10 cm high) one week before the transformation day in order to encourage the proliferation of secondary bolts and increase the transformation efficiency. Plants were briefly dipped in the *Agrobacterium* solution and placed in a humid environment under a plastic cover for at least 24 hrs. Ideally, plants were dipped twice with at least one week interval (to avoid any phytotoxicity and allow them to recover) in order to increase the transformation efficiency. After transformation, plants were kept in the greenhouse, watered by sub-irrigation and left to set seeds. After silique formation, watering was stopped to allow for seed maturation and drying. Arial parts of plants were cut and run through several sieves to remove unwanted debris. Then, seeds were collected and maintained well aerated, in order to avoid fungal growth, awaiting the process of transformants selection.

2.4 Selection of *bona fide* activation tagged T1 transformants

Approximately 36000 seeds were evenly spread on large rectangular pots filled with water pre-wetted soil. After incubation at 4°C for 48 hrs, to allow for vernalisation to take place, pots they were transferred to the greenhouse under long day growth conditions. Two weeks old seedlings were sprayed with Basta® solution at a concentration of 100 $\mu g.l^{-1}$. Spraying for two times with a one-week interval was found optimal for transformants selection. After seed maturation, seeds from each line were collected independently and stored under aerated conditions for further analysis.

2.5 Screening strategy for gain-of-function mutants via an ultra-low light luciferase imaging camera

Seeds from activation T-DNA tagged lines (~ 10-20 seeds each) were surface sterilised in sterile water containing 10% (v/v) bleach with a drop of Triton® X-100 (Sigma) for 20 min. Seeds were then washed four times with sterile distilled water. Seeds were resuspended in 0.1% (w/v) agarose and plated out on MS plates containing 1X MS (M5519), 0.3% sucrose (w/v), 0.8% agar, cefotaxine 200 $mg.l^{-1}$ and rovral 20 $mg.l^{-1}$ (Rhone-Poulenc Ltd). After allowing for agarose to dry out, plates were sealed with medical tape and vernalised at 4°C for 48 hrs, and incubated in a growth room at 20°C under continuous fluorescent light. Ten day old seedling were sprayed with 1 mM luciferin (Biosynth AG) (the substrate for luciferase) in a 100 mM Na-citrate buffer (pH 5.8) containing 0.001% (v/v) Silwet. Plates were then placed in the dark for 30 min in order to allow for luciferin to dry, hence minimising the autofluorescence during subsequent imaging steps. Imaging was performed using an EG&G Berthold Luminograph fitted with an ultra-low light camera. Bioluminescence images were routinely collected over a 10-second period. Images were processed using Adobe Photoshop® 5.5.

2.6 Real time *in planta* luciferase imaging using *PDF1.2::Luc* plants

Col-0 *Arabidopsis* transgenic *PDF1.2::LUC* plants (Basu *et al.*, unpublished) were used. Transgenic 4 weeks old soil-grown plants were leaf-inoculated with *Fusarium oxysporum* spore supsension of 10^6 spores ml^{-1}. Leaves were inoculated with sterile water as a negative control. Two days post inoculation, leaves were painted with a solution containing 1 mM Luciferin (Biosynth AG), 0.01% Triton® X-100 (Sigma), 0.001% Silwet (Union Carbide) in a 100 mM Na-citrate buffer pH 5.8. Following painting, plants were placed in the dark for 30 min to minimise autofluorescence and to allow for luciferin to dry. Leaves were then excised and imaged using an EG&G

Berthold Luminograph 980 equipped with an ultra-low-light imaging camera. Images were collected over a period of 10s, converted into a tiff format and processed further using Adobe® Photoshop® software.

2.7 Measurement of *in vitro* luciferase enzymatic activity

Luciferase activity was measured in the EG&G Berthold MicroLumat LB96P luminometer, which is attached to an ELISA plate reader. Luciferase enzymatic activity was assayed using the Luciferase Assay System kit (Promega). Crude protein extractions were made by grinding a leaf in a 1x lysis buffer (25 mM Tris-phosphate pH 7.8, 2 mM DTT, 2 mM 1,2-diaminocyclohexane-N,N,N',N'-tetraacetic acid, 10% glycerol, 1% Triton® X-100) in an eppendorf tube. The whole mixture was centrifuged at 4000 rpm for 10 min at 4°C. The total protein content in the supernatant was measured using bovine serum albumin (BSA) as a standard according to Bradford (1976). Then, to 100 µl luciferase assay substrate (containing 1mM luciferin and 2 mM ATP), 10 µl protein extract was added. Specific luciferase activity was calculated as relative light units (RLU) per microgram total protein.

2.8 Trypan blue staining

Leaf samples were boiled for 2 min in lactic acid-phenol-trypan blue solution (2.5 $mg.ml^{-1}$ trypan blue, 25% lactic acid (v/v), 23% phenol (v/v), 25% glycerol (v/v) and water) (Bowling *et al.*, 1997). After allowing the solution to cool to room temperature, the trypan blue staining solution was replaced with a chloral hydrate solution (25 g in 10 ml water) for de-staining overnight. Then, the chloral hydrate solution was poured off and the samples were equilibrated in 70% glycerol (v/v) in water and mounted onto microscopic slides. Stained leaves were viewed for micro-lesions or fungal hyphae and spores using the Leica Wild M3C microscope.

2.9 *In situ* H_2O_2 detection by the DAB-uptake method

In situ H_2O_2 detection in epidermal leaf tissue was performed according to the protocol of Thordal-Christensen *et al.* (1997). This is based on 3,3-*dia*mino*b*enzidine (DAB) ability to polymerise instantly as soon as it comes into contact with H_2O_2 in the presence of peroxidase. The peroxidase-based H_2O_2-mediated oxidation of DAB results in the local formation of a brown oxidation product enabling the localisation of H_2O_2. Detached leaves were placed in DAB-HCl solution (1 $mg.ml^{-1}$, pH 3.8) overnight. Then, leaves were cleared of their chlorophyll content by boiling in ethanol 96% for 10 min. Cleared leaves were mounted on 7% glycerol and H_2O_2 was visualised as reddish-brown colouration.

2.10 Examination of leaf autofluorescence

Leaves were examined for accumulating of aromatic and phenolic compounds by virtue of their ability to fluoresce under UV illumination (Dietrich *et al.*, 1994). Leaves were boiled for 2 min in alcoholic lactophenol (95% ethanol:lactophenol, 2:1), rinsed in 50% ethanol, and then rinsed in water. Cleared leaves were mounted on slides in 70% glycerol in water. Autofluorescence was observed using UV epifluorescence microscopy (excitation filter, 365 nm; dichroic mirror, 395; and barrier filter, 420 nm).

2.11 Northern analysis

Northern analysis was conducted according to standard protocols (Sambrook *et al.*, 1989). Total RNA was extracted from 5 weeks *Arabidopsis* plants using the guanidinium thiocyanate (GTC) phenol/chloroform extraction method. Basically, leaf tissue (approx. 0.1-0.2 g) was ground in liquid nitrogen using a pestle and mortar, poured into a 1.5 ml eppendorf tube and 0.45 ml GTC solution (4M guanidinium thiocyanate, 25 mM Na-

citrate, 0.5% (w/v) sarcosyl, 0.1 M β mercaptoethanol) was added. Following mixing by vortexing for 30 s, 0.05 ml 2 M Na-acetate pH 4.0, 0.45 ml phenol, and 0.1 ml chloroform:isoamylalcohol (49:1) were added. After further mixing, the tubes were placed on ice for 15 min. The samples were centrifuged at 10 000 rpm for 20 min, the supernatant was removed carefully from each tube and transferred to a new tube. An equal volume of isopropanol was added to each tube, mixed and left at -20°C for at least 2 hrs or overnight in order to precipitate the RNA. After incubation, the RNA was recovered by centrifugation at 10 000 rpm for 20 min. The pellet was re-dissolved in 0.15 ml GTC solution, and re-precipitated by the addition of o.15 ml isopropanol and keeping at -20°C for 1 hr. Following centrifugation, the RNA pellet was washed twice in 70% ethanol, dried under vacuum and dissolved in 100 µl DEPC-treated water. The absorbance of each sample was measured at 260 nm, and used to calculate the concentration of RNA. Approx. 10 µg RNA of each samples were loaded and separated on denaturing formaldehyde-agarose gels (Sambrook *et al.*, 1989) transferred to a Hybond™-N hybridisation membrane according to the supplier's instructions (Amersham Lifesciences) and hybridised with the corresponding probe. DNA probes were routinely labelled with α-32P-dCTP by random priming using the Prime-a-Gene® labeling system (Promega). Dextran sulphate (10%) was included in the pre-hybridisation/hybridisation solution in order to allow for efficient binding of the probe (Sambrook *et al.*, 1989). Blots were washed twice for 30 min each at 65 °C in 4X SSC, 1% (w/v) SDS, which was followed by two washes at 65°C in 4X SSC, 0.5% (w/v) SDS. Blots were exposed to X-Omat-ART™ imaging film (Kodak) overnight.

DNA probes were prepared either by PCR amplification and directly purified using a kit for PCR product purification (Promega) or by digestion with relevant restriction enzymes, identified by gel electrophoresis, and purified from the gel by freeze-thaw extraction. Several probes were used namely: *PR1*, *PR2*, *PR5* (Ukness *et al.*, 1992), *GST1* (Sharma *et al.*, 1996; Yang *et al.*, 1998), *PDF1.2* (Penninckx *et al.*, 1996), *CAT3* (Zhong & McCLung, 1996), *GER3* (Membre *et al.*, 1997), *RbohA* (Keller *et al.*, 1998),

PAL1 (Wanner *et al.*, 1995), *HMP/NOD* (Gardner *et al.*, 1998a) and *r18S* (Pruite & Meyerowitz, 1986) as an RNA loading control.

2.12 Southern analysis

Genomic DNA was prepared using a midi-scale plant DNA-Easy Kit (Promega). DNA was digested with the appropriate restriction enzyme at 37°C overnight. The quality of the digests was assessed by briefly running a few microliters of each samples on a 1% agarose gel (a good quality DNA digest is visualised as clear banding). Digested DNA samples were run on 1% agarose gel overnight. Gels were depurinated 2X15 min in a 0.25 M HCl with agitation. Southern blot analysis was performed according to the Church & Glibert (1984) protocol. Briefly, gels were denatured 2X30 min in 0.5 M NaOH with agitation. Gels were neutralised 2X30 min in 25 mM Na-phosphate buffer, pH 6.5. DNA was blotted onto nylon membrane overnight by capillary action in 25 mM Na-phosphate, pH 6.5. DNA was cross-linked to the membrane by exposure to short UV light at 0.4 $J.cm^{-2}$. Membranes were rinsed in water and pre-hybridised (1% BSA, 1 mM EDTA, 0.5 M Na_2HPO_4 pH 7.2 and 7% SDS) for 15 min at 65°C. Following the addition of the appropriate probe, membranes were hybridised at 65°C overnight. Membranes were washed 2X5 min at 65°C in washing solution I (0.5% BSA, 1 mM EDTA pH 8, 40 mM Na_2HPO_4 pH 7.2 and 5% SDS) then 4X5 min in washing solution II (1 mM EDTA pH 8, 40 mM Na_2HPO_4 pH 7.2 and 1% SDS) at 65°C. Membranes were exposed for 24 hrs at -70°C with a kodak film. Then, films were developed.

2.13 Western analysis

Total protein extracts were prepared from T1 35S::*NOD* candidates in 50 mM K-phosphate buffer (KPB) pH 7. Total soluble protein concentration was quantified in these extracts according to Bradford (1976) using a BSA standard curve. Approx. 40 µg

total protein per sample were denatured in SDS loading buffer for 3 min at 95°C. Samples were loaded individually and run in a 10% SDS-PAGE at 100 volts for 1 hr. Electrophresis-run protein samples were electroblotted on a Hybond™-P membrane (Amersham) at 12 volts for 1 hr according to standard protein blotting procedures (Sambrook *et al.*, 1989).

2.14 Pathogenicity assays

2.14.1 Bacterial disease resistance assay

The bacterial strain *P. syringae* pv *tomato* DC3000 (*Pst* DC3000) (Whalen *et al.*, 1991) was used. *Pst* DC3000 was grown in King's broth liquid media (King *et al.*, 1954) supplemented with a 50 $mg.ml^{-1}$ rifampicin. Five weeks old soil-grown plants were impregnated with a suspension of *Pst* DC3000 (OD600= 0.0002) in 10 mM MgCl2 in the abaxial side of the leaf with a 1 ml syringe (Cao *et al.*, 1994). As a negative control, leaves of wild-type Col-0 grown at the same conditions and at the same age were mock inoculated with sterile 10 mM MgCl2 solution. Three days post inoculation, three leaves of each treatment were weighed and ground in 900 µl 10 mM $MgCl_2$ with a pestle and mortar. Serial dilutions were made from the resulting bacterial suspension, and 100 µl of each dilution was used to inoculate King's B agar Petri dishes supplemented with 50 mg.l-1 rifampicin. The plates were inverted and incubated at 30°C for 2 days. Then, the number of colony forming units (CFU) was recorded. Each experiment were repeated at least two times. Data were further processed in Excel (MS Office, Microsoft®) to calculate the means and the standard error on the mean.

2.14.2 Fungal pathogenicity assay

2.14.2.1 Disease resistance against *Peronospora parasitica* Noco2

The *Peronospora parasitica* Noco2 biotrophic oomycete pathogen (Parker *et al.*, 1993) was maintained on Col-0 seedlings grown under humid conditions and conidiophores were transferred to new seedlings weekly by dusting infected seedlings onto healthy seedlings. For the *P. parasitica* disease resistance assays, conidiophores were harvested by vortexing infected seedlings in water. The spore concentration was determined using a haemocytometer, and adjusted to $1X10^5$ spores ml^{-1}. Four-week old plants grown under short day conditions (10 hrs light, 14 hrs dark) were sprayed with the conidiophore solution and maintained under humid conditions. Results were taken 10 days post-inoculation, and infected plants were scored for the extent of downy mildew growth (visualised as conidiophore growth) based on Bowling *et al.* (1997). Scoring was as follows: 0= no infection, 1= < 25% of one leaf covered with conidiophores, 2= 25-50% of one or two leaves covered with conidiophores, 3= 25-50% of three to four leaves covered with conidiophores, 4= 25-50% of all leaves covered with conidiophores, 5= all leaves covered with conidiophores. Plants in different replicates were assigned a disease index as follows: D.I.= $\Sigma iXj/n$, where i= infection class, j= the number of plants scored for that infection class and n= the total number of plants in the replicate.

2.14.2.2 Disease resistance against *Erysiphe* spp.

An untypified powdery mildew strain that is endemic to the Edinburgh University greenhouse was used in this assay. The fungal strain was maintained on Col-0 plant (susceptible host). Plants were inoculated via rubbing infected land covered with powdery mildew against the leaf surface of the plants to be infected. In order to ensure reliability of results interpretation, the infection technique was made sure to be

consistent in all plant treatments. Then 7-10 days post-inoculation plants were scored for visible fuzzy-looking conidiphore formation and chlorotic leaves. Furthermore, trypan blue assay was undertaken for intracellular visualisation of spores and hyphal growth.

2.14.2.3 *Fusarium oxysporum* f. sp. *matthiolae* pathogenicity assay

Fusarium oxysporum f sp *matthiolae* (strain 247.61; Centraalbureau voor Schimmecultures, Baarb-Delft, The Netherlands) was kindly provided by K. Apel of the Swiss Federal Institute of Technology (ETH), Switzerland. The fungus conidiophores were ideally long-term stored at -70°C in 25% glycerol under sterile conditions. Conidia were allowed to germinate on potato dextrose agar (PDA) (Sigma) in a growth chamber at room temperature under continuous fluorescent light. Pathogenicity assays with GFP-transformed *Fusarium oxysporum* on *Arabidopsis* seedlings ecotype Col-0 (i.e. an ecotype which was shown to exhibit a susceptible interaction towards *Fusarium oxysporum* f. sp. *matthiolae*) were carried out according to Epple *et al.* (1997). Basically, seeds of *Arabidopsis* Col-0 ecotype were surface sterilised, sown on MS medium (Sigma) containing nutrients (glycine {2 mg l^{-1}}, nicotinic acid {0.5 mg l^{-1}}, pyridoxine-HCl {0.5 mg l^{-1}}thiamine-HCl {0.1 mg ml^{-1}}), 0.5% sucrose, and 0.8% agar, vernalised at 4°C for 48 h and then grown in a growth chamber under continuous illumination for 12-15 days. Spores suspension at a density of 10^6 spores ml^{-1} was prepared from *bona fide* GFP expressing transformants and sprayed candidate as described before. Then, 2 weeks old Col-0 seedlings were pipetted by means of a pipetman (10 µl at a time) with the spore suspension. A systematic pattern of pipetting was followed and generalised for all treatments. Petri dishes containing the inoculated seedlings were closed immediately, sealed with a medical tape and incubated in the same growth chamber under the same conditions. As a negative control, seedlings were simultaneously pipetted with sterile water and incubated under similar conditions to those plates sprayed with fungal spore suspension. In addition, seedlings sprayed with spores of wild-type *Fusarium* at the same spore density were also included to be able to

compare the disease symptoms between GFP-transformed colonies and untransformed wild-type.

2.15 Genetic analysis of identified mutants

Crosses were performed by dissecting and emasculating unopened buds two days prior to anthesis, and using the pistils as recipients for pollen from open donor flowers (Koorneef & Stam, 1992). In order to determine the mode of inheritance of the mutation in the identified putative mutants, pollen from the mutant lines was used to pollinate wild-type parental *PR1::Luc* plants. In cases where the mutation has a characteristic visible phenotype (i.e. *pcd1* mutation), close phenotypic examination of the backcross F1 and F2 was conducted to infer the mode of inheritance. Alternatively, in cases where the mutant has no clear visible phenotypes (i.e. *cpe1* mutation), constitutive *PR1::Luc* expression using an ultra low-light imaging camera of the F1 and F2 progeny was examined. For epistasis analysis, pollen from homozygous *pcd1* was routinely used to pollinate *nahG*, *coi1*, *etr1*. To select for *pcd1 nahG*, *pcd1 coi1* and *pcd1 etr1* double mutants, F1 or F2 seedlings (depending whether the mutant was dominant or recessive) were tested on MS plate supplemented with the appropriate selective agent. To select for the dominant *nahG* phenotype, F1 seeds were germinated on MS plates supplemented with 0.5 μM SA. *nahG* seedlings were visualised by the appearance of brown roots. To select for the recessive *coi1* phenotype, F2 seeds were germinated on MS plates supplemented with 100 μM Me-JA. Homozygous *coi1* plants were visualised by their insensitivity to Me-JA and healthy growth. To select for the dominant *etr1* phenotype, seeds were germinated on MS plates supplemented with 10 μM 1-aminocyclopropane-1-carboxylic acid (ACC) in the dark. Homozygous or heterzygous *etr1* seedlings, were visualised by their insensitivity to ACC and elongated hypocotyl. To select for the *pcd1* phenotype, seedlings were transferred to soil and examined for the appearance of the characteristic HR-like lesions.

2.16 In-gel kinase assay

In-gel kinase assay was essentially conducted according to Romeis *et al.* (1999). Basically, leaves were ground in liquid nitrogen, thawed in 2 volumes of extraction buffer (50 Hepes pH 7.4, 5 mM EDTA, 5 mM EGTA, 5 mM DTT, 10 mM NaF, 10 mM Na_3VO_4, 50 mM β-glycerophosphate, 1 mM 4-[2-aminoethyl]-benzenesulfonyl fluoride [AEBSF, Pefablock], 2 $\mu g.ml^{-1}$ antipain, 2 $\mu g.ml^{-1}$ aprotinin, and 2 $\mu g.ml^{-1}$ leupeptin), and centrifuged at maximum speed for 20 min at 4°C in a microcentrifuge. The supernatant was stored at -70°C. The protein concentration was determined using Bradford protein assay kit with BSA as a standard. Ca. 20 µg total protein per lane was separated on an 10% SDS-polyacrylamide gel embedded with 0.25 $mg.ml^{-1}$ myelinbasic protein (MBP) as a kinase substrate. After electrophoresis, the SDS was removed by two washings (30 min each) in buffer A (50 mM Tris-HCl, pH 8.0, and 20% isopropanol) followed by two washings in buffer B (50 mM Tris-HCl, pH 8 and 5 mM β-mercaptoethanol). The proteins in the gel were dentatured in buffer C (50 mM Tris-HCl, pH 8, 5 mM β-mercaptoethanol and 6 M guanidinium chloride) for 1 hr at room temperature and were renatured overnight at 4°C in buffer D (50 mM Tris-HCl, pH 8, 5 mM β-mercaptoethanol and 0.04% Tween 20). After equilibration in buffer E (40 mM Hepes, pH 7.4, 2 mM DTT, 15 mM $MgCl_2$ and 0.1 mM EGTA) for 30 min at room temperature, the gel was incubated in 10 ml of buffer E including 40 µM ATP plus 1.85 MBq (50 µCi) [γ-^{32}P]-ATP (3000 Ci/mmol; Amersham UK) for 90 min at room temperature. The reaction was stopped by transferring the gel into 5% trichloroacetic acid (w/v) and 1% sodium phosphate (w/v). Unincorporated [γ-^{32}P]-ATP was removed by an intensive washing for 3 hr with at least five changes of the same solution. The gels were dried onto Whatman 3MM paper and exposed to Kodak X-OMAT film. The size of protein kinases was estimated by using different prestained molecular mass markers.

2.17 Determination of POD and CAT enzymatic activity

A pyrogallol-based method was conducted to measure peroxidase (POD) activity (Kwak *et al.*, 1995). Leaves were frozen in liquid nitrogen and ground in 0.1 M KPB pH 7.0. After centrifugation at 8000 rpm for 10 min at 4°C, the supernatant was taken to measure the soluble POD activity. After several washes in KPB, treatment of the pellet with high ionic strength (3 M NaCl) and centrifugation, the supernatant was used to measure the ionically bound POD activity. Protein concentration was determined according to Bradford (1976). A 0.1 ml enzyme solution was added to 2.9 ml assay buffer (10 mM KPB pH 7.0, 8.0 mM H_2O_2, and 0.5% (w/v) pyrogallol) and the change in absorbance (ΔOD_{420}) was measured over 20 s. The specific POD activity was expressed as $U.\mu g^{-1}$ total protein. One unit will form 1.0 mg purpurogallin from pyrogallol in 20 s at pH 6.0 at 20°C.

Similarly, catalase (CAT) activity was measured in the supernatant after the addition of 0.1 ml enzyme solution to 2.9 assay buffer (10 mM KPB and 150 mM H_2O_2) and observing the ΔOD_{240} for 70 s (Abei, 1984). Specific CAT activity was expressed as $U.\mu g^{-1}$ total protein. One unit of CAT will decompose 1.0 μmol of H_2O_2 per min at pH 7.0 at 25°C, while the H_2O_2 concentration falls from 10.3 to 9.2 mM, measured by the rate of decrease of OD_{240}. For the CAT native gel assay, approx. 100 μg protein was run in a native Ready-Gel (10% Tris-HCl pH 7.0) (Bio-Rad®) for 1 hr at 100 V. Gel was soaked for 45 min in the dark at room temperature in a solution of horseradish POD (50 $\mu g.ml^{-1}$) in 50 mM KPB pH 7.0. Then, gels were incubated in KPB containing 5.0 mM H_2O_2 for 10 min. After rinsing twice with KPB, gels was placed into 0.5 $mg.ml^{-1}$ of DAB in KPB until staining is completed. CAT activity was visualised as achromatic bands in a darkly-stained background.

2.18 Determination of chlorophyll content

Total chlorophyll content was determined in 5-week old plants according to Lichtenthaler (1987). Briefly, leaves were frozen in liquid nitrogen and ground in 100% acetone using a pestle and mortar. Extracts were centrifuged at maximum speed for 10 min and spectrophotometric absorption of the supernatants was measured at 661.6 nm and 644.8 nm. Then, the total chlorophyll content (a + b) was quantified according to the following equations:

Ca = 11.24 A661.6 - 2.04 A664.8

Cb = 20.13 A664.8 - 4.19 A661.6

where Ca and Cb are chlorophyll a and b in $\mu g.ml^{-1}$, respectively.

2.19 Determination of SA levels

SA measurements were performed using 5-week old plants according to Bowling *et al.* (1994). Briefly, ~1 g of leaf tissue was collected, frozen in liquid nitrogen and homogenized in 3 ml of 90% methanol. After centrifugation, the pellet was re-extracted with 100% methanol. The combined supernatants were dried in a rotary evaporator at 40°C. The residue was resuspended in 2.5% trichloroacetic acid . SA was separated from its conjugated SA (SAG) through organic extraction with 2 volumes of ethylacetate-cyclopentane-isopropanol (50:50:1). The organic phase containing the free SA was then dried out in a rotary evaporator at 40°C. The dried extract was suspended in 0.5 ml of 0.01 N H_2SO_4, filtered and stored at –70°C for SA quantification. For analysing SAG, the aqueous phase, containing SAG, was acidified with HCl to pH 1.0 and boiled for 30 min to release SA from any acid-labile conjugated forms. The release of free SA was then extracted with the organic mixture as previously described. SA was quantified by high-performance liquid chromatography (HPLC).

In collaboration with Ken Cook, Dionex (UK) Ltd., HPLC analysis was performed on an inert Dionex DX600 system, composed of a GP50 PEEK quaternary gradient pump, CD25 conductivity detector, PDA-100 diode array detector and an RF2000 fluorescence detector. Samples were introduced to the system with an inert AS50 variable volume autosampler. Ion exchange was performed on an IonPac AS11 4mm separator and guard column at a flow rate of 1.0ml/min. Starting eluent conditions were 10mM NaOH, 5% acetonitrile with a gradient from 3 to15 minutes to 60mM NaOH, 30% acetonitile. The final eluent concentrations were held for a further 5 minutes before re-equilibration at the starting eluent conditions. Immediately after the column the eluent passes through an on-line anion self regenerating suppressor [Dionex ASRS Ultra suppressor]. This converts the NaOH in the eluent to water by flowing the eluent across a membrane continually regenerated into the H+ form [Joachim Weiss, Ion Chromatography, VCH Verlagsgesellschaft mbH]. This allows the use of increasing NaOH gradients with conductivity and low UV detection. The eluent then passes though the conductivity, diode array and fluorescence detectors in that order. The diode array 3D field was scanned between 190 and 400nm and the fluorescence excitation and emission were set at 303 and 407 respectively.

2.20 Salinity and abscisic acid tolerance assay

Salinity tolerance of plants was determined by growing surface-sterilised seeds on MS plates supplemented with either an increasing range of NaCl (0-400 mM) or 5 μM abscisic acid. Germination rate was then scored 10 days after sowing.

2.21 Gene mapping

Mapping experiments were performed on F2 *pcd1::*L*er* recombinant inbred lines (RIL). In order to obtain a rough map position for the *pcd1* mutant allele, a bulked segregant analysis (BSA) approach was undertaken (Michelmore *et al.*, 1991). A combination of single sequence length polymorphisms (SSLP) (Bell & Ecker, 1994) and single nucleotide polymorphisms (SNPs) (Cho *et al.*, 1999) markers that are polymorphic between Col-0 and L*er* were used. Both protocols are based on PCR analysis of polymorphic DNA amplified fragments. The description of SSLP and SNP markers is now publicly available at The *Arabidopsis* Information Resource (TAIR) data base (http://www.arabidopsis.org). Using a Peltier 200 thermal cycler, the following universal PCR programme was applied for the SSLP/SNPs markers: 94C 2 min, 10x (94C 1 min, 65-1C 30 sec, 72C 1 min), 35x (94C 50 sec, 46C 1 min, 72C 40 sec), and 72C 1 min. Alternatively, in some cases, a temperature gradient decrease in the annealing temperatures from 65-1C to 51-1C and from 46-1C and 41-1C, was deployed. Figure 2.2 lists the SSLP markers used and their chromosomal location in cM.

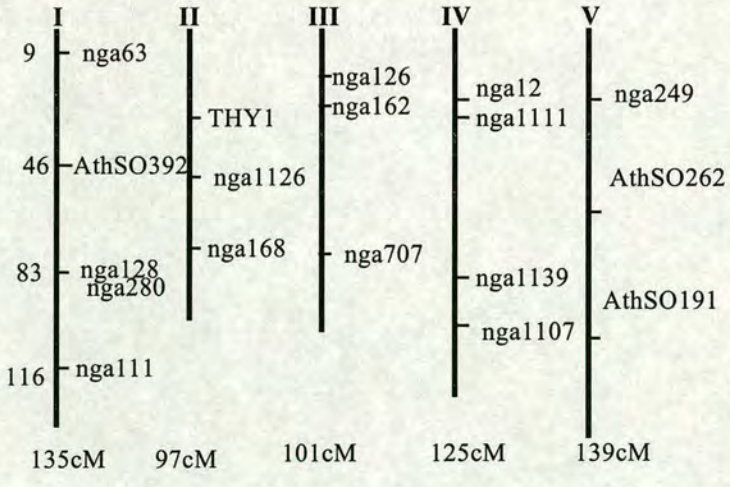

Figure 2.2: List of SSLP markers and their corresponding map position in cM tested for linkage to the *pcd1* mutation in bulked segregant analysis.

2.22 *E. coli* transformation

Briefly, a starter 5 ml *E. coli* LB culture was grown overnight. Another 20 ml of LB was inoculated with 200 µl of the overnight culture. Cells were harvested after 2-3 hrs of incubation at 37°C when their optical density at wave length 550 nm (OD_{550}) was 0.2-0.4. Culture was spun down at 4000 rpm for 10 min on a benchtop centrifuge. Supernatant was discarded and the pellet resuspended in 10 ml RbCl solution 1 (10 mM MOPS pH 7.0, 10 mM RbCl). After spinning, pellet was resuspended in 10 ml of RbCl solution 2 (10 mM MOPS pH 6.5, 10 mM RbCl, 50 mM $CaCl_2$). To make cells transformation-competent, they were incubated on ice for 30-90 min. After the incubation period, cells were spun down and pellet resuspended in 1 ml of RbCl solution 2. Then, 20 µl of dimethylsulphoxide were added and aliquots of 300 µl each were put in sterile 1.5 ml eppendorf tubes. At this stage bacterial cells were ready for transformation. pALTER(*HMP*) plasmid DNA was added, mixed well by gentle flicking of competent cells and incubated on ice for 1 hr. Cell suspension plus DNA was heat-shocked in a water path at 55°C for 30 sec and placed immediately on for 2 min. One ml of LB was added to the cell suspension and incubated for 1 hr at 37°C with shaking. Cells were then spundown and resuspended in 200 µl LB gently. Approx. 100 µl of the cell suspension were then aliquoted per each LB agar Perti dishes supplemented with 12.5 µg/ml tetracycline as a selective pressure. Aliquots were evenly distributed gently across the plate surface using a disposable sterile streaker and then incubated, upside-down, in an incubator at 37°C overnight.

2.23 Plasmid preparation and constructs

The plasmid pALTER, containing the flavohemoprotein/nitric oxide dioxygenase gene (*HMP/NOD*), was kindly provided by Paul Gardner of the Children's Hospital Medical Centre, University of Cincinnati, USA. The pALTER(*HMP/NOD*) plasmid was tranformed into the bacterial strain *E. coli* J109 according to a standard rubidium

chloride (RbCl) transformation protocol (Sambrook *et al.*, 1989). Freshly-emerging tetracycline-resistant *E. coli* colonies were picked up individually and miniscale pALTER(*HMP/NOD*) plasmid DNA preparation, using standard alkali lysis Qiagen miniprep. protocol and restriction enzyme analysis were conducted in order to confirm that the plasmid prepared was the correct size (~ 7.0 Kb). Then, a promoterless 1.2 Kb *HMP* was polymerase chain reaction (PCR)-amplified using the following oligo primer sequence pair: forward HMP4 (5'-CCAT**GAATTC**ATGCTTGACGCTCAAACCAT-3') and reverse HMP5 (5'-C**AAGCTT**GCATGCCTGCAGGTCGACTCT-3') (Severn.Biotech Ltd., UK). In order to facilitate the downstream cloning steps, unique restriction enzymes sites for *EcoR* I and *Hind* III (boldfaced-bases) were introduced in both HMP4 and HMP5 oligo primers, respectively. A 100 µl PCR reaction cocktail was prepared in a 200 µl capacity, thin-walled, and DNase- & RNase-free PCR tubes as follows: 81.2 µl distilled water (dH_2O), 10X buffer (containing 200 mM Tris-HCl, 20 mM $MgSO_4$, 100 mM KCl, 100 mM $(NH_4)_2SO_4$, 1% Triton X-100, 1 mg/ml nuclease-free BSA), dNTPs (25 mM each NTP), pALTER(*HMP.NOD*) (100 ng/µl), primers HMP4&5 (100 ng/µl each), and high-fidelity *Pfu* DNA polymerase (2.5. U/µl) (Stratagene®). The following PCR programme was used: 1X (94°C for 30 sec); 35X (94°C for 1 min, 50°C for 1 min, 72°C for 1.5 min), and 72°C for 10 min. Sticky-end cloning of the *EcoR* I/*Hind* III double-digested ~1.2 kb HMP insert was then cloned into *EcoR* I/*Hind* III double-digested, and dephosphorylated pART7 binary vector (Gleave, 1992) using T4 Ligase according to the standard cloning protocols (Sambrook *et al*, 1989). Then, pPART7(*HMP/NOD*) plasmid DNA was transformed in *E.coli* DH5α strain, mini-scale prepared, *EcoR* I/*Hind* III restriction-enzyme to confirm the HMP insert size as previously described. A *Not* I pART7 derived-fragment containing the 1.2 Kb promoterless *HMP/NOD* gene under the control of the 35S full-length promoter, from the cauliflower mosaic virus (CaMV), followed by *Agrobacterium nos* terminator was subsequently subcloned into *NotI*-digested binary vector pGREEN (John Innes Centre, Norwich UK).

The gGFP plasmid (Maor *et al.*, 1998) containing a codon-optimised *sGFP(Ser65T)* gene under the control of the *Aspergillus nidulans* P*gdp* promoter and the *hph* gene conferring resistance to hygromycin B as a selectable marker was used for particle bombardment of *Fusarium oxysporum* f. sp. *matthiolae*. The gGFP plasmid was obtained from A. Sharon of the Cereal Crop Improvement Institute; Tel Aviv University, Israel. Plasmid propagation was done in the bacterial strain *E. coli* DH5∝. A standard alkali lysis Qiagen kit protocol was carried out for plasmid isolation and purification according to the manufacturer procedures

2.24 *Agrobacterium* transformation with pGREEN(HMP)

pGREEN(*HMP/NOD*) construct was transformed into *Agrobacterium tumefaciens* harbouring the helper plasmid JIC according to a standard freeze and thaw protocol. Basically, the *Agrobacterium* strain was grown in LB medium incorporated with rifampicin, tetracyclin, and gentamycin at 30°C overnight until the culture's OD600 reached 0.5-1.0. Cultures were chilled on ice and briefly centrifuged at 1500 rpm to remove unwanted cell clumps. The suspension was poured into two sterile falcon tubes, 50 ml each, and kept on ice. Cell suspension was centrifuged at 4000 rpm for 10 min at 4°C. Supernatant was decanted and the cells resuspended in a total volume of 2.5 ml of ice-cold 20 mM $CaCl_2$ by gently pipetting up and down. Aliquots of 300 µl were dispensed into pre-chilled sterile 1.5 ml capacity eppendorf tubes, one tube per one transformtion. Approx. 5 µg pGREEN(*HMP/NOD*) plasmid DNA was added to the cells and, as a negative control, 5 µl of sterile distilled water (sdH_2O) was added to a separate eppendorf tube. Lids of eppendorf tubes were firmly closed and tubes flicked gently. Eppendorf tubes were snap-frozen in liquid nitrogen and allowed to thaw by incubating the tubes in an incubator at 37°C for 10 min. One ml of LB medium was added to each tube, gently mixed and incubated for 2-4 hrs at 30°C with gentle shaking. After the incubation period tubes were centrifuged for 10 min at 4000 rpm, supernatant discarded and pellet resuspended in 200 µl LB. Appox. 100 µl of cell suspension of each tube were

spread into LB agar Petri dishes supplemented with rifampicin, gentamycin, tetracyclin as well as kanamycin (for the selection of pGREEN). Plates were inverted and incubated at 30°C for 2-3 days. several transformed colonies were picked up randomly and a colony PCR screening for the *HMP/NOD* gene was conducted to confirm its presence as mentioned before.

2.25 Generation of *Arabidopsis* transgenic *35S::HMP/NOD* lines

The generation of *Arabidopsis 35S::HMP/NOD* transgenics was conducted according to an *Agrobacterium*-mediated floral dip protocol (Clough & Bent, 1998). *HMP* PCR-positive single *Agrobacterium* colony was grown overnight at 30°C on LB medium supplemented with the all appropriate antibiotics (as above). The bacterial culture was spun down and resuspended in 5% sucrose to $OD_{600} \cong 0.8$. Before dipping, Silwet L-77 was added to a final concentration of 0.05%. Plants were briefly dipped in the *Agrobacterium* solution and then placed in a humid environment under a plastic cover for at least 24 hrs in the green house. Then, the cover was lifted and plants placed in the green house and let to set seeds. Plants were regularly watered by sub-irrigation when necessary and fertilised once a week with the nutrient mixture Phosphogen®. After siliques formation watering was stopped in order to promote seeds maturation. Then seeds were collected. Ten days old seedlings were sprayed with Basta® solution at a concentration of 100 $\mu g.l^{1-}$ two times over two weeks period in order to select for transformants. Basta-resistant seedlings were then transferred individually, confirmed to contain the *HMP* gene by leaf PCR as above and let to set seeds. Seeds of T1 transformants were collected individually from each plant and were kept for further analysis.

2.26 NO quantitation by photoacoustic laser spectroscopy

Specific CO-based laser lines were used at which NO is known to absorb maximally. Four-week old coelentrazine-reconstituted *35S::AEQUORIN* leaves were infiltrated with *Pst* DC300 (*AvrB)*, *Pst* DC3000 (OD= 0.2), or $_{L}$-arginine (10 mM). After the treatment, plants where gently freed of their soil and floated on a column of water in the measuring cuvette. Then, NO emission was monitored over a period of approx. 6 hrs. Similarly, SNP solutions, prepared in dH_2O pH 5.5. and 7.4, were allowed to accumulate NO for one hour in sealed glass vials. Then, NO released was quantified in the same way as above. General CO-laser operation and data processing were conducted according to Bijnen *et al.* (1992).

2.27 Aequorin chemiluminescence measurement

Transgenic Col-0 *Arabidopsis* plants genetically transformed with a chimeric gene in which the cauliflower mosaic virus 35S promoter was fused to the apoaequorin coding region were used. Two-week old homozygous 35S::*APOAEQUORIN* seedlings were aequorin-reconstituted by floating into a cuvette containing 0.5 ml of 10μM coelenterazine solution (prepared in sterile water) at room temperature in the dark overnight (Knight *et al.*, 1993). Then, reconstituted seedlings, floating in the cuvette, were treated with either the NO donor sodium nitroprusside (SNP), at different concentrations, or 10 mM $_{L}$-arginine. Chemicals such as lanthanum chloride ($LaCl_3$) (a general plasma membrane channel blocker (Tester, 1990), potassium ferrocyanide {$K_4Fe(CN)_6$}, and 2-4-carboxyphenyl-4,4,5,5-tetramethylimidazoline-1-oxyl-3oxide (C-PTIO) (Calbiochem®) (Delledonne *et al.*, 1998), were added to the coelenterazine-reconstituted seedlings 4 hrs before the treatment with SNP. To check whether SNP interacts with apoaequorin producing inappropriate luminescence, apoaequorin was reconstituted *in vitro*. Apoaequorin was *in vitro* reconstituted and extracted from *35S::APOAEQUORIN Arabidopsis* seedlings in a buffer containing 0.5 M NaCl, 5 mM

β-mercaptoethanol, 5 mM EDTA, 0.1% gelatine (w/v), 10 mM Tris-HCl pH 7.4 and 10 μM coelenterazine in the darkness for 4 hours.

Luminescence measurements were made using a digital chemiluminometer with a photomultiplier, model 9757 AM (THORN EMI Electron Tubes Limited, Ruislip, Middlesex, U.K.) at 1 kV with a discriminator (Campbell, 1988). In order to minimise background counts, temperature of the cuvette chamber was continuously kept at approximately -30 °C by means of an installed cooler. The cuvette temperature was kept at room temperature.

2.28 *In vivo* Ca^{+2} imaging

Four-week old *Arabidopsis 35S::APOAEQOURIN* plant were reconstituted by infiltrating the abaxial side of the leaf with 10 μM coelenterazine solution and incubation in the dark overnight. The next day, reconstituted leaves were infiltrated with either SNP or a suspension of avirulent *Pst* DC3000 (*AvrB*) in 10 mM $MgCl_2$ (OD600=0.2). Immediately after infiltration, leaves were detached and placed in the dark box for imaging. Leaves were imaged within 1 min after infiltration and placement in the darkbox. Imaging was conducted by means of a low-light camera. Pictures settings were: 3 min accumulation and 1.5 min integration.

2.29 Preparation of fungal conidia and microprojectiles, and biolistic transformation

Aseptic potato dextrose broth media were inoculated with freshly-harvested fungal spores. Then liquid media were incubated at 24°C with continuous shaking at 150 rpm for 7-10 days. After the incubation period, cultures were vortexed, filtered through Miracloth and the final spore density was adjusted to 10^9 spores ml^{-1}. Spore suspension

was then aliquoted onto PDA Petri dishes supplemented with 50 μg ml^{-1} hygromycin for the selection of antibiotic-resistant transformants. Dose response experiments had revealed that concentrations of 50 μg ml^{-1} hygromycin were sufficient to prevent the growth of wild-type *Fusarium oxysporum*. Before transformation, spores aliquots were allowed to slowly dry first in a laminar flow. Particle bombardment of *Fusarium oxysporum* spores was carried out using the PDF-1000/He device (Bio-Rad® Laboratories) (Kikkert, 1993). The PDS-1000/He is powered by a burst of helium gas that accelerates a macrocarrier, upon which millions of DNA coated inert microcarriers (gold particles) have been dried. The preparation of biolistic microparticles was conducted essentially as previously described (Forbes *et al.*, 1998). Basically, 60 mg of gold particles (1μm in diameter) were weighed into an eppendorf tube containing 1 ml of 70% ethanol. Then, the suspension was vortexed and left to soak for 15 min. The gold particles were pelleted by centrifugation at high speed for 5 min, followed by the removal of the supernatant and addition of 1 ml of sterile water and mixing. Particles were then spun down as above and supernatant discarded. A further 1 ml of sterile water was added followed by spinning and supernatant removal. At the stage, the particles were stored in 1 ml of sterile 50% glycerol. To an aliquot of 50 μl gold particles in a sterile eppendorf tube, ~5 μg gGFP plasmid was added followed by the addition of 50 μl of 2.5 M $CaCl_2$ and 20 μl of 0.1 M spermidine and vortexing. The mixture was then incubated on ice for 1 min followed by centrifugation at maximum speed for 1 min and supernatant removal. The plasmid-coated particles were then washed in 250 μl of 100% ethanol and spun for 30s. After removal of the supernatant, 60 μl of 100% ethanol were added to the gold pellet and followed by thorough vortexing. Six μl of this suspension was then carefully loaded onto the centre of a clean surface-sterilised kaplon disc. Hygromycin-containing PDA plates aliquoted with the now dried *Fusarium oxysporum* spores were then placed on the platform within the PDS-1000/He device. After several experimental trials, optimal configuration parameters were found to be: platform setting 2, stage settings 5, rupture disc at 1350 pounds per square inch (*psi*). At lower (i.e. 1110 *psi*) or higher pressure (i.e. 1500 *psi*) a dramatic decrease in transforamtion efficiency

was observed. After bombardment, plates were immediately covered, parafilm-wrapped and incubated under continuous fluorescent illumination at room temperature in a growth chamber. Four days after transformation, putative transformants started to emerge. Then, transformants were transferred individually to a fresh PDA Petri dishes supplemented with 50 μg ml^{-1} hygromycin B for further analysis.

2.30 Fluorescence and confocal microscopy

Screening of hygromycin-resistant transformants for GFP expression was carried out by means of a Leica MZFL III fluorescence microscope equipped with the following GFP plant filter sets: excitation filter 470-490 nm and barrier filter 525-550 nm. Under these conditions, GFP expressing fungal colonies would appear as bright emerald-green. PDA Petri dishes with emerging hygromycin-resistant transformants were directly examined without prior modification or manipulation. *Bona fide* transformants were further examined by a confocal microscope to compare the intensity of their GFP expression. Confocal imaging was performed on a BioRad MRC600 confocal system mounted on a Nikon Diaphot. Transformants were streaked on a fresh PDA agar using a sterile inoculation needle. Then, transformants were allowed to grow overnight. For hyphal staining, a 25 μM FM4-64 (Molecular Probes) was used. FM4-64 is internalised by endocytosis and with time stains hyphal components. 30 μl of liquid medium containing 25 μM FM4-64 was placed on a clean glass coverslip. Then, an agar block ~1 cm^2 was cut from the lading edge of the colony and inverted in a "mycelium sandwich".

2.31 GFP fluorescence measurements

A Perkin-Elmer Luminescence Spectrometer LS-5 was used to measure the intensity of GFP fluorescence in selected *bona fide* transformants. In a 50 ml Falcon tubes, 10 ml culture of selected transformants were grown for 72 h with shaking at 24°C. The tubes

were subsequently centrifuged at 4000 rpm and the pelleted mycelium was macerated by vortexing in 5 ml 10 mM Tris pH 7.4, 1 mM $CaCl_2$ in the presence of 2 mm glass beads. Mycelial debris was removed by further centrifugation and the supernatant was assayed for GFP relative fluorescence units (RFU). RFU were measured using a 488 nm and 512nm wavelengths for excitation and emission, respectively. Protein concentrations were measured using Coomassie blue binding in the Biorad protein assay kit with bovine serum albumin as standard. RFU values were then normalised against the supernatant's protein content of each sample.

CHAPTER III

3 CHARACTERISATION OF T-DNA ACTIVATION TAGGED *ARABIDOPSIS* SAR MUTANTS IDENTIFIED BY LUCIFERASE IMAGING

" Ours is a military campaign against agents that destroy our plants. We can not wage this campaign successfully without knowing the measure of the enemy's ability to destroy"

{K. S. Chester, 1959}

3.1 Introduction

3.1.1 Activation tagging

Historically, transposon and T-DNA tagging, as well as chromosome walking have all proved to be valuable means for the isolation of plant genes (Gibson & Somerville, 1993). The mutants generated by these strategies generally involve disruption of a transcription unit (i.e. based on loss-of-gene function) resulting in a recessive mutation. Moreover, both the presence of multigene families and the generation of lethal mutations are major drawbacks of these techniques lowering the chance of isolating vitally important genes.

Alternatively, another T-DNA tagging approach was developed where the mutation is not a consequence of gene disruption, but rather the activation of the tagged gene. This was known as activation tagging (Walden *et al.*, 1994) in which mutation is based on a gain of function of the tagged gene. Consequently, the resulting mutant phenotype is dominant which allows a direct selection for a desired phenotype (i.e. in our case fungus resistant) from the population of primary transformants. In addition, unlike EMS mutagenesis, the activation-tagged gene can be cloned with a relatively simple plasmid rescue approach, without having to apply the lengthy and laborious map-based cloning or chromosome walking.

Walden *et al.*(1994) engineered a T-DNA tag to contain the transcriptional enhancer sequence of the cauliflower mosaic virus (CaMV) 35S RNA promoter cloned as tandem repeats near the right border of the T-DNA. *Agrobacterium* harbouring this vector was used to transform plants in order to isolate mutants affected in the action of the plant growth hormones auxins and cytokinins.

A further refinement of this approach was sought mainly for several reasons: Firstly, to overcome the problem of somaclonal variation, one of the major drawbacks of root tissue culture and plant regeneration (Valvekens *et al.*, 1988); Secondly, to allow for high-throughput activation-tagged line production. This was achieved by the

construction of an activation tagging binary vector called SKI15 (Weigel *et al.*, 2000) derived from pPCVICEnHPT (Walden *et al.*, 1994). The SKI15 vector contains many distinctive features between the left and right borders of *Agrobacterium* T-DNA. These include: (1) four tandem repeats, cloned near the right border of the T-DNA, of the CaMV 35S RNA promoter; (2) a pBluescript fragment containing the origin of replication for maintenance in *E. coli* and amp^r as a selectable marker; (3) *bar* (for *ba*sta *r*esistance) gene, from *Streptomyces hygroscopicus*, encoding the phosphinothricin acetyltransferase (PAT) conferring resistance against the tripeptide antibiotic phosphinothricin (PPT), under the regulation of the *mas5'* promotor, followed by fragments encoding termination and polyadenylation signals of *3'ocs*. PPT is the active ingredient in the commercially available pesticides bialaphos (Herbiace®) and Basta®. PPT is a natural analogue of L-glutamic acid and acts as a potent inhibitor of *g*lutamine *s*ynthetase (GS). Inhibition of GS by PPT causes rapid accumulation of ammonia which leads to death of plant cells (Block *et al.*, 1987). Therefore, transformed plants would be easily selected on soil by Basta® spraying. Recently, this approach has been employed for the isolation of a conserved regulator of the phenylpropanoid pathway. Transcriptional activation of a MYB transcription factor resulted in a massive accumulation of lignin, hydroxycinnamic acid esters, and flavonoids (Borevitz *et al.*, 2000).

3.2 Results

3.2.1 Generation of activation-tagged lines

The activation tagging binary vector SKI15 (Figure 3.1) was used for the transformation of homozygous *PR1::LUC* transgenic plants.

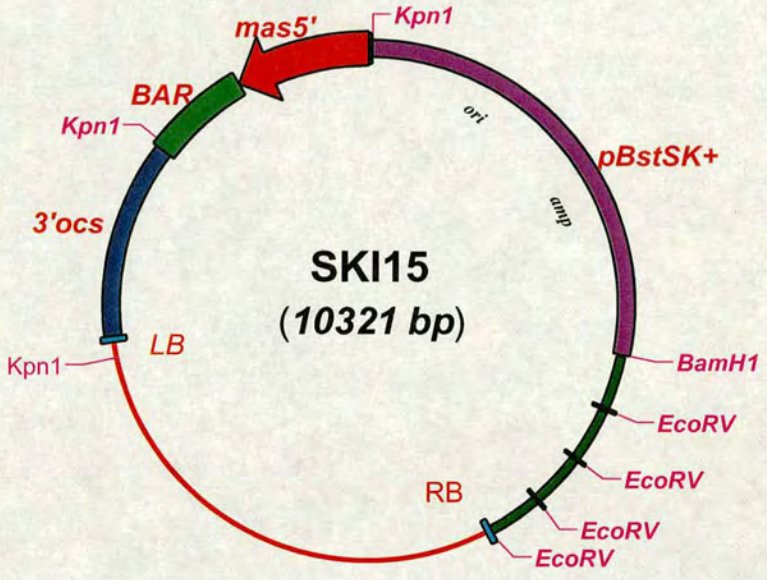

Figure 3.1: The activation tagging binary vector SKI15 employed in the generation of activation tagged *Arabidopsis* lines (Weigel *et al.*, 2000)

The SKI15 activation tagging binary vector was utilised in the generation of T-DNA transgenic lines (Figure 3.1). Over a period of three months, from October 1998 till January 1999, 12 *Agrobacterium*-mediated transformation experiments were undertaken. A total of 9000 homozygous *PR1::LUC* plants were transformed in a sequential fashion with a rate of 750 plants per week. The process of seed collection, selection of *bona fide* Basta-resistant T1 transformants, transplanting independent T-DNA lines, and collecting their seeds upon maturation continued on a regular basis up until Summer 1999 (Figure 3.2).

(A) (B) (C)

Figure 3.2: Sequence of events followed in the generation of activation tagged lines. Selection of *bona fide* transformants on soil via Basta spraying (A). Individual transplantation of Basta resistant lines on soil (B). Matured activation tagged lines awaiting seed collection (C).

I managed to successfully generate 9000 T0 independent T-DNA activation tagged lines (library I). Ten Basta selection experiments, each is composed of 36,000 seeds, were used to calculate the overall average of the transformation efficiency. The transformation efficiency was found to range between 0.4 to 0.8% with an overall average of 0.6%. Although the 0.6% average transformation rate is three times less than that reported by (Clough & Bent, 1998), it proved satisfactory in obtaining a reasonable number of lines to allow for a large-scale mutant screen. Additionally, 200 g (10^7 seeds) of non-selected seeds was harvested. Theoretically, based on the 0.4% transformation rate figure, ca. 4 x 10^4 lines would be obtained. In an independent simultaneous experiment, conducted by other lab co-workers, these 200 g of seeds yielded only ~10,000 T-DNA lines (library II) (four times less than expected). This can be ascribed to a large extent to the inherent variations in transformation efficiency found between different independent transformation experiments. The following sections will only deal with the screening of library I.

3.2.2 Phenotypic screening of T-DNA lines

By careful visual examination of the phenotypes of T1 plants of library I, I could identify several visible alterations. These included developmental mutants, e.g. late flowering; and morphological mutants, e.g. lost apical dominance, albino, and reduced stature. Thus, the morphological alterations observed in these lines

confirmed that the inserted T-DNA had resulted in some perturbations of gene function, presumably by activating certain genes. In agreement with Feldmann *et al.* (1991), the mutational spectrum derived from screening the 9000 T1 lines, for visible phenotypes, indicated that T-DNA inserts are not preferentially integrating into a small number of loci.

3.2.3 Optimisation of real-time luciferase imaging screening

The *PR1::LUC* plants (Murray *et al.*, submitted) provided the genetic background for activation tagging. The utilisation of such a "designer" genetic background, in the generation of the activation-tagged lines, facilitated a rapid high-throughput screen of the generated library of T-DNA mutants via luciferase imaging. Furthermore, this luciferase imaging screen should facilitate the identification of mutants that function not only in the SA-dependent and/or JA-dependent pathways but also in any novel pathway. The screening for both gain-of-function and loss-of-function mutants was developed in an EMS-mutagenised *PR1::LUC* background (Murray *et al.*, submitted). In this project, due to the use of the activation tagging vector SKI15, the screen for gain-of-function mutants was more relevant. Therefore, I focused on screening for gain-of-function mutants.

Before I embarked on the screen, it was essential to optimize the best possible strategy for the identification of gain-of-function mutants. Our optimization efforts led us to conclude that screening of seedlings grown on MS plates was more favorable to use than screening plants grown on soil. This was because the growth and accommodation of seedlings on MS plates does not demand significant space availability. Moreover, it is much more economic in luciferin consumption. Additionally, the chance of pathogen contamination of soil-grown plants is realistically much higher, which could lead to many false positives during the luciferase imaging screen. I found that 25 independent T-DNA lines per plate convenient for the screening. Seedlings of independent T-DNA lines, between 10-15 days old, were sprayed with 1 mM luciferin and screened for constitutive luciferase expression (Figure 3.3).

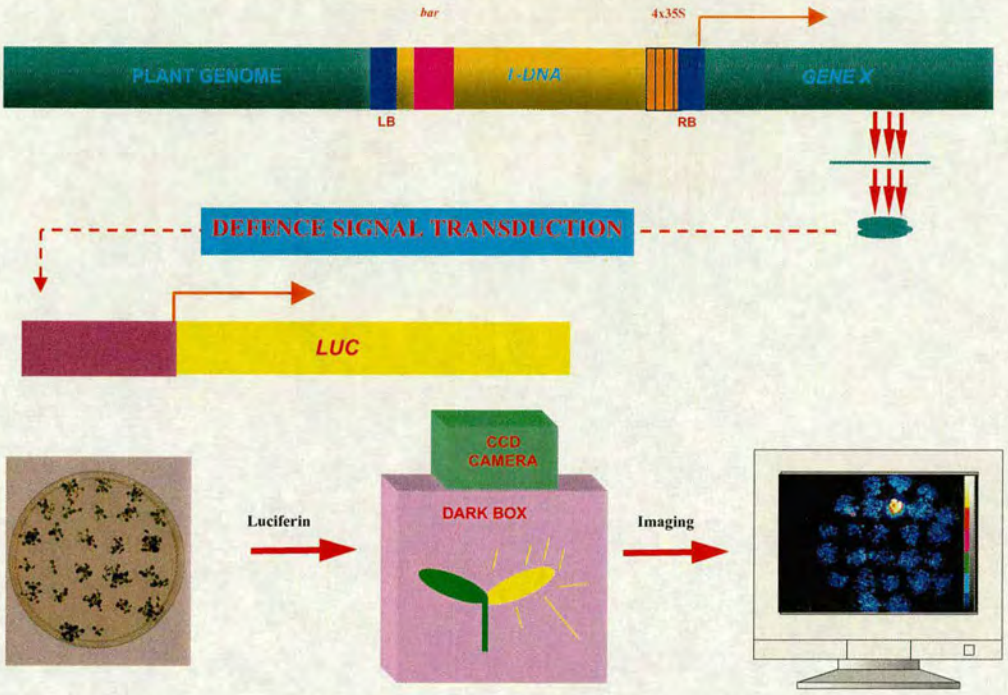

Figure 3.3: Strategy of screening for T-DNA gain-of-function SAR mutants. Approximately, 8000 lines were screened for constitutive *PR1::LUC* expression via a low-light imaging camera. The screening was conducted on 10 weeks old seedlings grown on MS plates (25 lines per plate). Routinely, images were taken over a 10s period.

3.2.4 T-DNA SAR mutants identified by luciferase imaging

During the primary round of screening, ~300 putative mutants showing constitutive expression of luciferase activity were identified. In order to confirm these primary results, these mutant plants were subjected to several secondary and tertiary rounds of screening. The outcome of these screening rounds enabled me to identify two confirmed mutants. Both mutant lines sustained high levels of *PR1::LUC* expression throughout all their developmental stages (Figure 3.4 A&B).

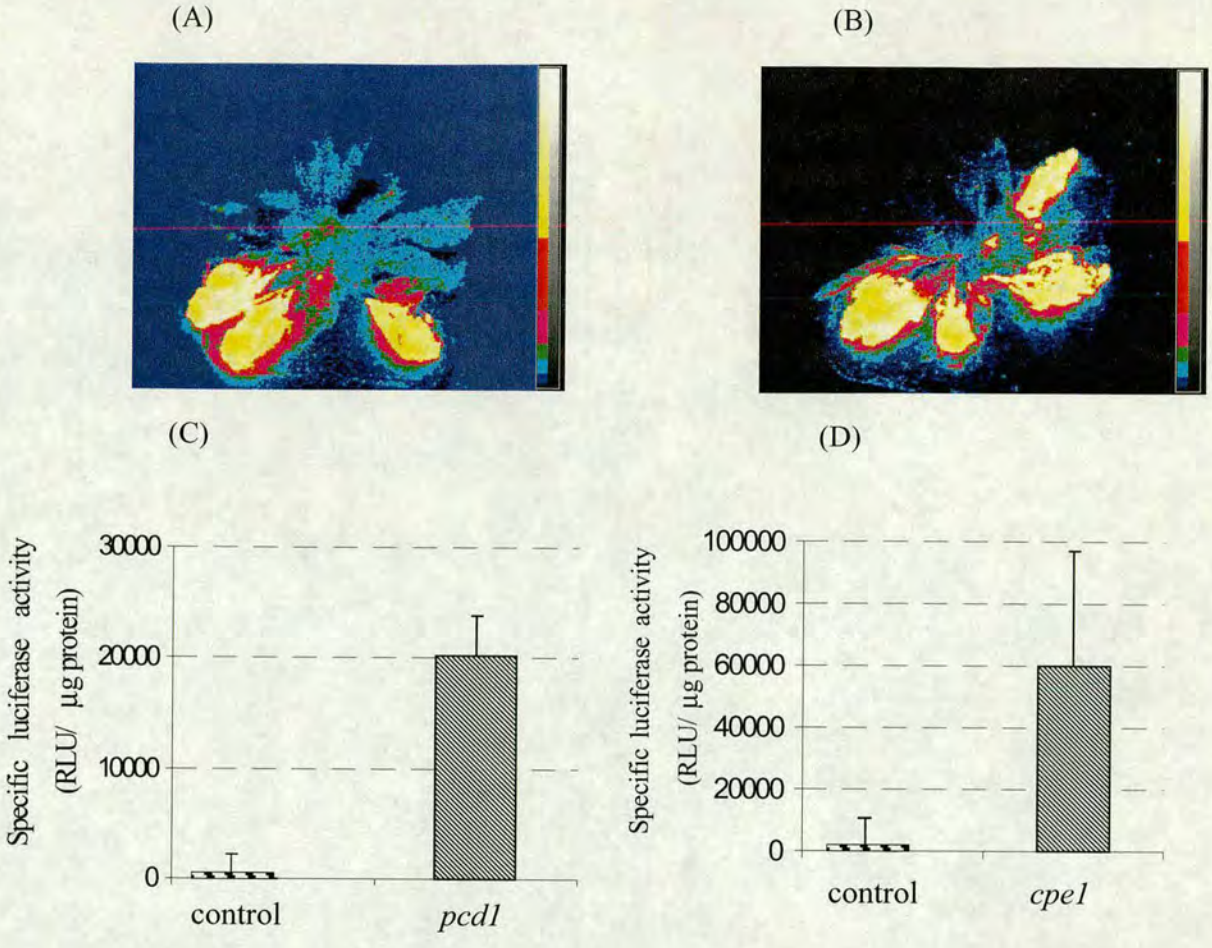

Figure 3.4: Identification of two putative mutants that constitutively express *PR1::LUC* activity. Luciferase imaging of *pcd1* (A) and *cpe1* (B). Pictures were taken at a 10 s period. The colour index, on the right of each image denotes the intensity of bioluminescence: yellow (high), blue (low). Measurement of luciferase enzymatic activity in *pcd1* (C) and (*cpe1*) (D) revealed that both mutants exhibit high luciferase activity compared to transgenic *PR1::LUC* plants(control). Each data point represents the mean of luciferase activity recorded in three independent experiments. Luciferase activity is represented as relative light units (RLU) per microgram of total protein. Error bars represent the standard error on the mean (n=3).

Interestingly, the spatial pattern of *in vivo* luciferase activity was found to be uniform and strong in cotyledons and all true leaves of both mutants (Figure 3.4 A&B). The luciferase imaging and pseudo-coloured images in Figure 3.4 A&B represent a tertiary screen performed on adult plants confirming the stability of the mutant phenotype in the T1 stage. Furthermore, *in vitro* luciferase enzymatic assays confirmed that both mutants constitutively express significantly high luciferase activity (Figure 3.4 C&D).

Both mutants were subjected to careful phenotypic examination. The *cpe1* mutant (*c*onstitutive *PR1* *e*xpresser), appeared normal in size and displayed an apparent crinckly-leaf phenotype. The *pcd1* mutant (*p*otentiated *c*ell *d*eath 1) is stunted in stature compared to wild-type Col-0 plants and was found to exhibit macroscopic HR-like lesions that are characteristic of the plant cell death response to an avirulent pathogen (Figure 3.5 A). Growth of this mutant under sterile pathogen-free conditions, confirmed that the appearance of these lesions is pathogen-independent. The lesions gave a predominant mosaic-like appearance to the *pcd1* leaves. Interestingly, the HR-like lesions were more dramatic on homozygous than heterozygous *pcd1* plants (Figure 3.5 B). The lesion distribution pattern was found to be uniform, emerging first at the tip of the leaf and progressing gradually towards the leaf origin, and covering all leaf area. Eventually, leaves turned yellow due to chlorophyll degradation and died. This natural process of senescence was strikingly accelerated in the mutant compared to wild-type Col-0 plants grown under the same conditions, hence the name of the mutant (Figure 3.5 C).

3.2.5 Histochemical examination of pcd1

3.2.5.1 *pcd1* cells accumulate high level of H_2O_2 but not O_2^-

One of the earliest responses following successful recognition of an avirulent pathogen is the OB generating O_2^- and H_2O_2 leading to the HR (Baker & Orlandi, 1995). Therefore, I examined the possibility that the HR and ROS accumulation might play are role in the *pcd1* phenotype. In this regard, trypan blue staining performed on *pcd1* leaves, revealed that the observed macroscopic HR-like lesions are predominantly formed of clusters of dead cells that are spread over the leaf surface (Figure 3.5 D).

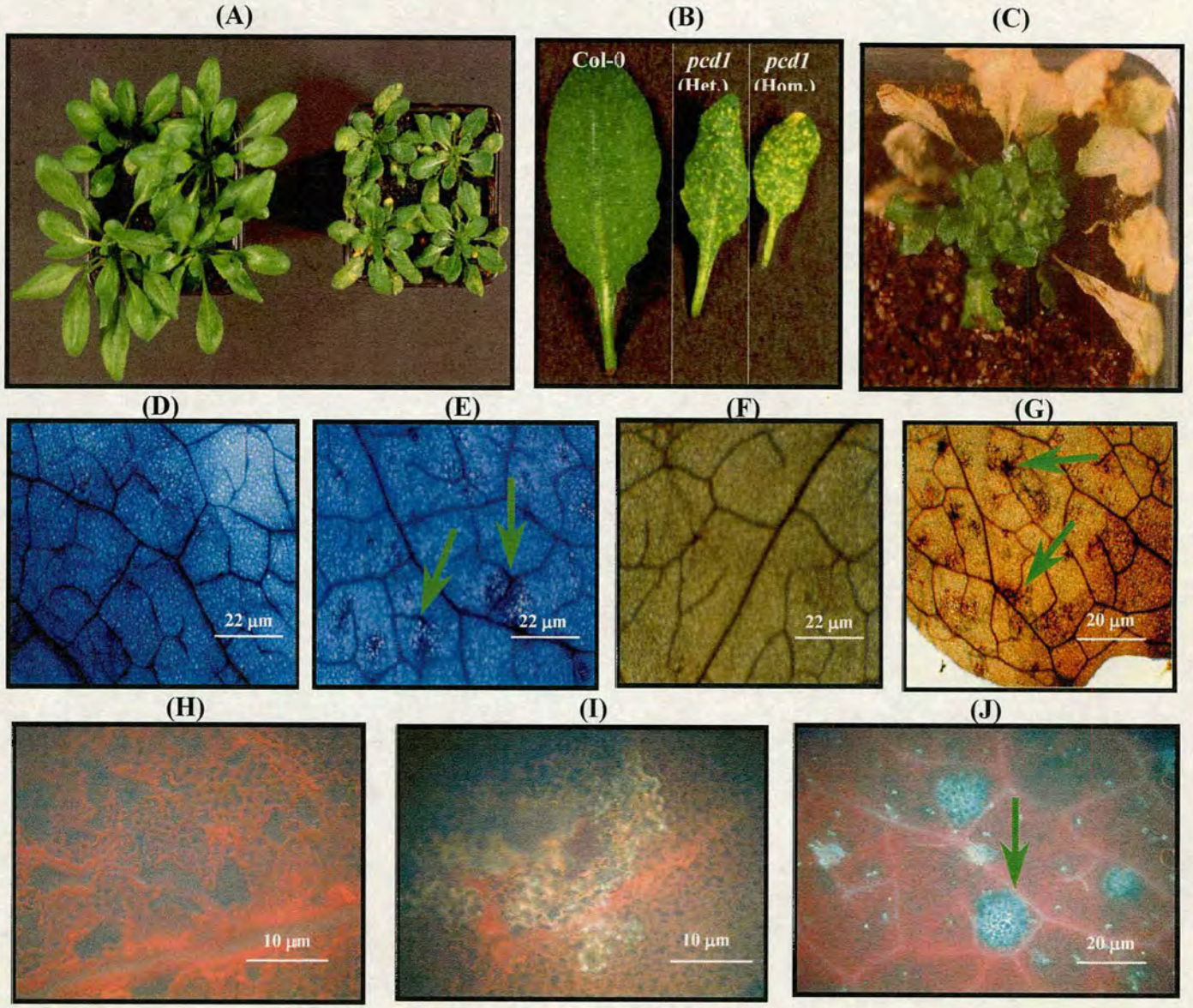

Figure 3.5: Phenotypic and histochemical characterisation of *pcd1*. (A-C) Phenotypic analysis of *pcd1* plants. (A) *pcd1* plants display a stunted stature compared to wild-type Col-0 plants. (B) *pcd1* leaves show constitutive HR-like lesions that are much more dramatic in homozygous than in heterozygous *pcd1* leaves. (C) *pcd1* plants exhibit an accelerated cell death phenotype. (D&E) Trypan blue staining of col-0 and *pcd1* leaves. Note the pattern of clustered dead cells that is absent from wild-type Col-0 leaves (D) and present in *pcd1* leaves (E). (F&G) Hydrogen peroxide detection by the peroxidase-based DAB-uptake method. *pcd1* leaves (G) were found to accumulate high levels of hydrogen peroxide (arrows) compared to wild type Col-0 leaves (F). (H-J) Autofluorescence examination. Autofluorescence examination was performed according to chapter II section 2.10. *pcd1* leaves accumulate autofluorescent phenolic compounds in the absence of pathogens. Phenolic compounds accumulation was found at lesion sites. Wild-type Col-0 leaf (H), Col-0 challenged with *Pst* (*AvrB*) (30 hrs post-inoculation) (I), *pcd1* leaf (J). Experiments were repeated twice with similar results.

I next examined whether this constitutive formation of HR-like lesions was accompanied by an oxidative burst. If yes, I wanted to find an answer as to what type of ROS is involved in *pcd1*. Histochemical staining of *pcd1* leaves with the superoxide radical specific dye nitroblue tetrazolium (NBT), resulted in negative staining. Leaves from *cpr5* (a mutant that constitutively accumulates superoxide radicals) and Col-0 plants were used as positive and negative controls, respectively (data not shown). Therefore, I concluded that the superoxide radical may not play a role in *pcd1*.

In order to investigate the role of hydrogen peroxide in *pcd1*, histochemical staining for H_2O_2 was performed. The peroxidase-based DAB-uptake method was employed. Interestingly, *pcd1* leaves were shown to have a strong DAB staining. Therefore, I concluded that *pcd1* accumulated high levels of H_2O_2. This strong DAB staining was completely missing from the Col-0 leaves used as a negative control (Figure 3.5 F&G). Furthermore, close examination of the DAB staining pattern indicated that H_2O_2 accumulation is not confined to the HR-like lesion sites but rather uniformly distributed in *pcd1* leaves. Additionally, this strong DAB staining was obtained with *pcd1* leaves in both the presence and absence of lesions. Taken together, these observations indicate that the accumulation pattern of H_2O_2 in *pcd1* is spread throughout the leaves, irrespective of the sites of macrolesion development. It can also be concluded that the *pcd1* mutant mimics the plant defence response to an avirulent pathogen by constitutively displaying HR-like cell death and H_2O_2 accumulation.

3.2.5.2 *pcd1* accumulates phenolic compounds and phytoalexins

One of the best and extensively-studied defence response of plants to infection is the induced accumulation of antimicrobial, low-molecular-weight secondary metabolites known as phytoalexins (Hammerschmidt, 1999). Accumulating evidence suggests that phytoalexins accumulate rapidly in response to avirulent pathogens and act as broad-spectrum antibiotics against bacterial and fungal pathogens *in vitro* (Glazebrook & Ausubel, 1994). In this context, I next investigated whether *pcd1*

accumulates phenolic and aromatic compounds. Phenolic compounds are generally synthesised via the phenylpropaniod pathway (Dixon *et al.*, 1996). These compounds share the possession of aromatic rings that characteristically fluoresce upon exposure to UV light. Examination of UV exposed *pcd1* leaves, that had first been cleared of their chlorophyll, indicated the presence of bright blue fluorescence that is missing from the corresponding Col-0 leaves (Figure 3. 5 H-J). This bright fluorescence was mainly confined to the HR-like lesion sites. Hence, the accumulation of phenolic compounds in *pcd1* leaves appears to be dependent on cell death. The most predominant class of phytoalexins in *Arabidopsis* is camalexin (i.e. a derivative of the amino acid tryptophan; 3-thiazol-2'-yl-indole; contains an aromatic ring) (Hammerschmidt & Dann, 1999). I used thin-layer chromatography (TLC) to separate organic compounds present in *pcd1* leaf extracts. Qualitative analysis of TLC-separated compounds revealed that *pcd1* accumulates significant amounts of camalexin and other unidentified phenolics (data not shown). Camalexin was identified by its characteristic blue fluorescence. Moreover, *pcd1* plants were found to accumulate significantly more camalexin than Col-0 plants inoculated with *Pst* (*AvrB*).

3.2.6 Biochemical analysis of pcd1

3.2.6.1 *pcd1* cells exhibit high POD but not CAT enzymatic activities

The constitutive accumulation of H_2O2 in *pcd1* leaves has led us to speculate on whether this would trigger the expression of antioxidant defence mechanisms. More specifically, I investigated the activity of POD and CAT in *pcd1* plants. Quantification of soluble POD activity in crude protein extracts of *pcd1* compared to wild-type Col-0 plants revealed a significant difference. Interestingly, *pcd1* protein extracts were found to possess ca. 14 times more soluble POD activity than Col-0. Moreover, ionically-bound POD (i.e. POD bound to membranes of intracellular compartments) activity was found to be ca. 10 times higher in *pcd1* than in Col-0 plants (Figure 3.6). I also observed that *pcd1* cell-wall-containing fractions exhibit

strong POD activity, as judged from the rapid conversion of the colourless pyrogallol to yellow purpurogallin. However, the spectrophotometric quantification of POD activity in cell-wall-containing fractions was technically difficult.

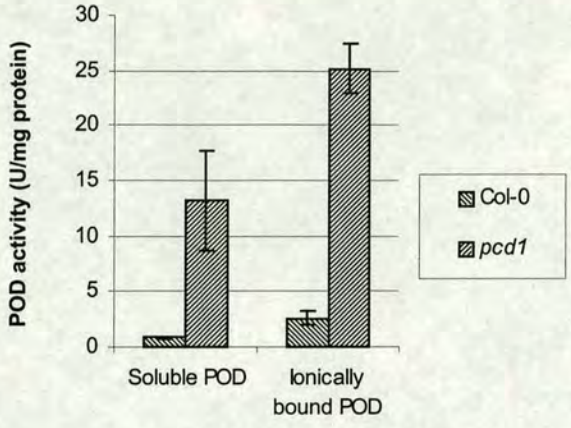

Figure 3.6: Quantification of peroxidase activity in homozygous *pcd1* plants. POD activity in protein extracts was assayed using a pyrogallol-based protocol. Each data point represents the mean of three independent POD activity measurements from three different plants. The experiment was repeated twice with similar results. POD activity is represented as U/ mg protein.

Thus, this observation suggests that, in *pcd1* leaves, H_2O_2 is probably being constitutively generated not only in the cytosol and within intracellular compartments (e.g. mitochondria, chloroplasts, endoplasmic reticulum) but also in the cell wall area. Taken together, it appears that one way for *pcd1* plants to protect themselves against the destructive oxidative stress, exerted by high H_2O_2 levels, is by having a significantly high soluble, ionically-bound and cell wall POD activity.

Catalase was another antioxidant enzyme whose activity was examined in *pcd1*. Catalases are one group of many enzymes that are subject to a tight circadian rhythm regulation. Therefore, I was interested in investigating catalase activity both during the day and night in *pcd1* plants. Unexpectedly, no significant differences in *in vitro* CAT activity was found in *pcd1* plants, either during the day or night, when compared to Col-0 plants. On average, day/night CAT activity in *pcd1* was around 0.9 U/ mg protein compared to ~ 0.8 U/ mg protein in Col-0 plants. These values

were not significantly different from each other according to the Tuckey test for difference between means at a 0.05 significance level (Figure 3.7 A).

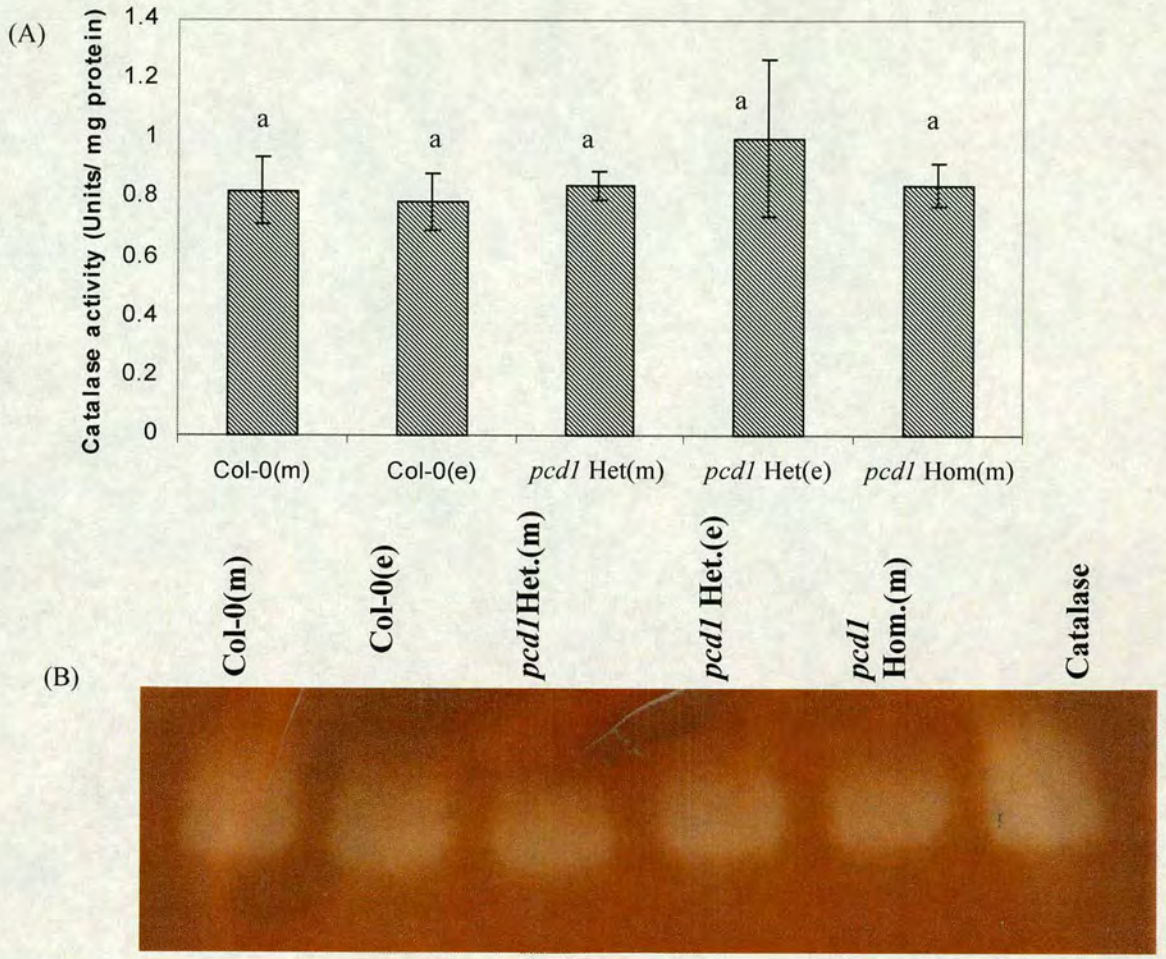

Figure 3.7: Biochemical analysis of catalase activity in *pcd1* as compared to Col-0 wild-type plants. (A) Catalase activity in the soluble protein extracts of *pcd1* compared to Col-0 wild-type. Abbreviations: m, leaf tissue collected in the morning; e, evening; Het, heterozygous *pcd1*; Hom., homozygous *pcd1*. Error bars represent the standard deviation on the mean (n=3). Similar letters (a) above bars represent no significant differences between means according to Tuckey test (P= 0.05). Catalase activity is represented as U/ mg protein. (B) Catalase native gel assay. In the last lane, 100 U of catalase were loaded as a positive control. Gel was negatively stained with 0.5 mg/ml DAB staining solution after pre-incubation for 10 min in a solution of 5 mM H_2O_2. Catalase activity is represented by the achromatic bands.

Similarly, no significant difference was found in in-gel CAT activity in *pcd1* compared to Col-0 (Figure 3.7B). Therefore, it can be concluded that in wild-type Col-0 plants, regardless of the circadian regulation of CAT genes, no apparent changes in the overall CAT enzymatic activity in the absence of oxidative stress could be detected. Moreover, it was rather surprising to observe that the high oxidative stress, represented by H_2O_2, in *pcd1* plants, does not trigger a corresponding upregulation in CAT enzymatic activity. Two explanations for this situation might be possible. Firstly, in the presence of high H_2O_2, such as in *pcd1*, cells respond by up-regulating activities of a battery of antioxidant enzymes, e.g. POD, but not necessarily CAT activity. Another plausible explanation is that in *pcd1* plants, there is a strong inhibition of CAT enzymatic activity. This possibility is discussed later in this chapter.

3.2.6.2 *pcd1* exhibits constitutive MAPK activity

MAPK activity was previously shown to be elevated in response to oxidative stresses such as H_2O_2 (Grant *et al.*, 2000). Therefore, I predicted that MAPK activity might be enhanced in a *pcd1* background due to elevated H_2O_2. Hence, in collaboration with Byung-Wook Yun, I examined MAPK activity in *pcd1* protein extracts. As expected, *pcd1* protein extracts were found to contain high MAPK activity according to in-gel kinase assays (Figure 3.8). Two MBP-phosphorylating activities of 46 and 48 kD, were detected. Moreover, constitutive *pcd1* MAPK activity could be mimicked by infiltrating Col-0 leaves with an H_2O_2-generating solution containing gucose/glucose oxidase (G/GO) within 15 min after infiltration (Figure 3.8). Furthermore, the MAPK activity induced by H_2O_2 could be totally blocked by co-infiltrating PD98059 (Figure 3.8), a well-known mammalian MAPK inhibitor (Romeis *et al.*, 1999).

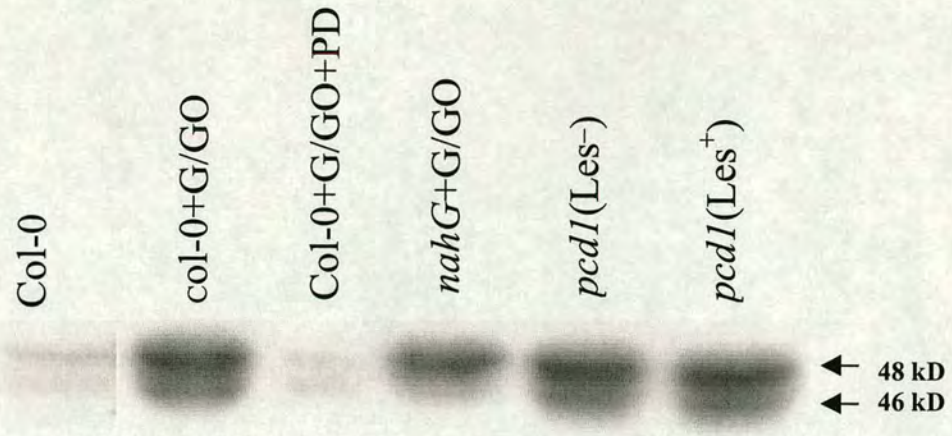

Figure 3.8: In-gel kinase assay performed on *pcd1* leaves with or without lesions. As a positive control Col-0 leaves were treated with the H_2O_2 generating system glucose/glucose oxidase (G/GO) (250 mM G/250 U.ml^{-1} GO) and samples were collected after 15 min. *pcd1*(Les$^-$) and *pcd1*(Les$^+$) are leaf samples from *pcd1* plants that are either have or have not macroscopic lesions; PD is a MAPK inhibitor type 98059. The two MAP kinase activities detected were detected of 48 and 46 kD, respectively.

No MAPK activity was detected in wild-type Col-0 protein extracts. Interestingly, MAPK activity could be equally detected in *pcd1* leaves in the absence or presence of HR-like lesions (Figure 3.8). Taken together, it can be concluded that the constitutive MAPK activity is uncoupled from visible macroscopic HR-like lesion development. The appearance of HR-like lesions on older *pcd1* leaves may therefore generate a systemic signal that leads to the expression of MAPK activity in younger leaves which have not yet developed lesions. The involvement of microbursts and micro-HRs, however, in the induction of constitutive MAPK activity in younger leaves can not completely be ruled out (Alvarez *et al.*, 1998).

3.2.6.3 *pcd1* accumulates high SA and SAG levels

The dwarfed phenotype of appreciable number of previously identified SAR mutants is often associated with the accumulation of SA. Therefore, in collaboration with Ken Cook (Dionex UK Ltd.), I investigated whether the stunted *pcd1* phenotype is associated with accumulation of endogenous SA and its conjugated form salicylic acid glucoside (SAG). Indeed, *pcd1* leaves were found to accumulate ~8 and ~15 times more SA and SAG, respectively, than wild-type Col-0. Moreover, 95% of SA in *pcd1* plants was present as SAG (Figure 3.9). Accumulation of SA in *pcd1* plants was significantly blunted in a SA-degrading *nahG* (section 1.4) background. More interestingly, the dwarfism and macroscopic HR-like lesions associated with *pcd1* were completely absent in *pcd1::nahG* plants. Therefore, based on this genetic and biochemical evidence, it can be concluded that the phenotypic characteristics of *pcd1* plants are primarily dependent on high SA or SAG levels. These observations strongly suggest that the *PCD1* functions through an SA-dependent signal transduction pathway.

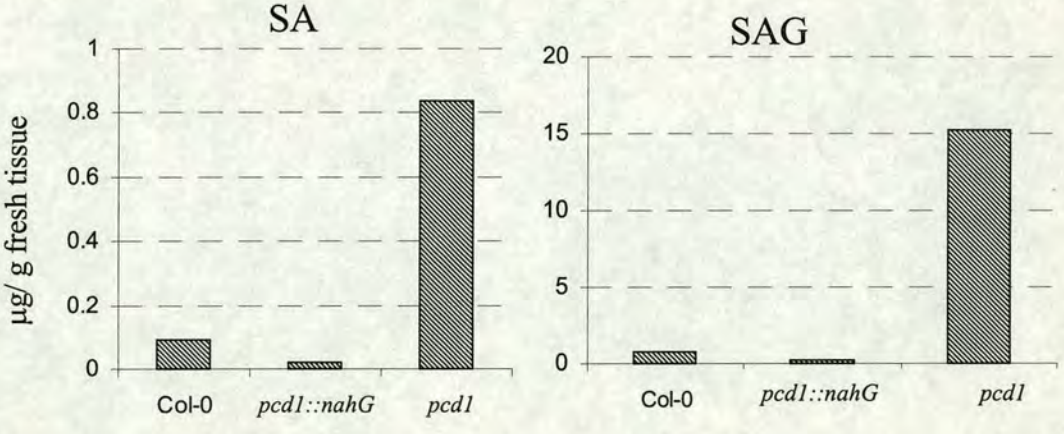

Figure 3.9: Quantification of the level of endogenous salicylic acid (SA) and its glucoside form, salicylic acid glucoside (SAG), in *pcd1* plants compared to wild-type Col-0 and *pcd1::nahG* plants. SA extraction was conducted according to Bowling *et al.* (1994). Samples were run on a Dionex IonPac® AS11, 4 mm column and guard column at a flow rate of 1.0 ml/min. As an eluent, a gradient of 10 mM NaOH/5% acetonitrile from 3 to 15 min to 60 Mm NaOH/30% acetonitrile was used. Suppressed conductivity/AutoSuppression™ mode was employed to improve signal/noise ratio. SA and SAG were quantified using conductivity and diode array, and fluorescence detectors in series. SA and SAG leaves are expressed as µg per gram fresh leaf tissue.

3.2.6.4 The chlorophyll content of *pcd1* decreases in response to HLI

I noticed qualitative phenotypic differences in *pcd1* plants grown under different light intensities. When first grown under high light intensity (HLI) (> 200 μEinstein. $m^{-2}.min^{-1}$) and then shifted to low light intensity (LLI) (~150 μEinstein.$m^{-2}.min^{-1}$), *pcd1* plants displayed characteristic changes which included the disappearance of defined macroscopic HR-like lesions and the development of an undefined pattern of large cholorotic patches (Figure 3.10 A). These changes were not observed in Col-0 plants. These observations led me to speculate that these changes are probably associated with changes in chlorophyll content. Therefore, I next examined the effect of changes in light intensity on chlorophyll content in *pcd1* plants. Indeed, a ~50% reduction in chlorophyll content was observed in *pcd1* plants that were first grown under HLI and then shifted to LLI (Figure 3.10 B). Interestingly, Col-0 or *pcd1* plants that were kept under LLI conditions had similar chlorophyll content. Moreover, Col-0 plants grown under HLI then LLI displayed no visible changes in chlorophyll content (pictures not shown). Therefore, I concluded that chlorophyll degradation in *pcd1* plants is enhanced in response to increases in light intensity.

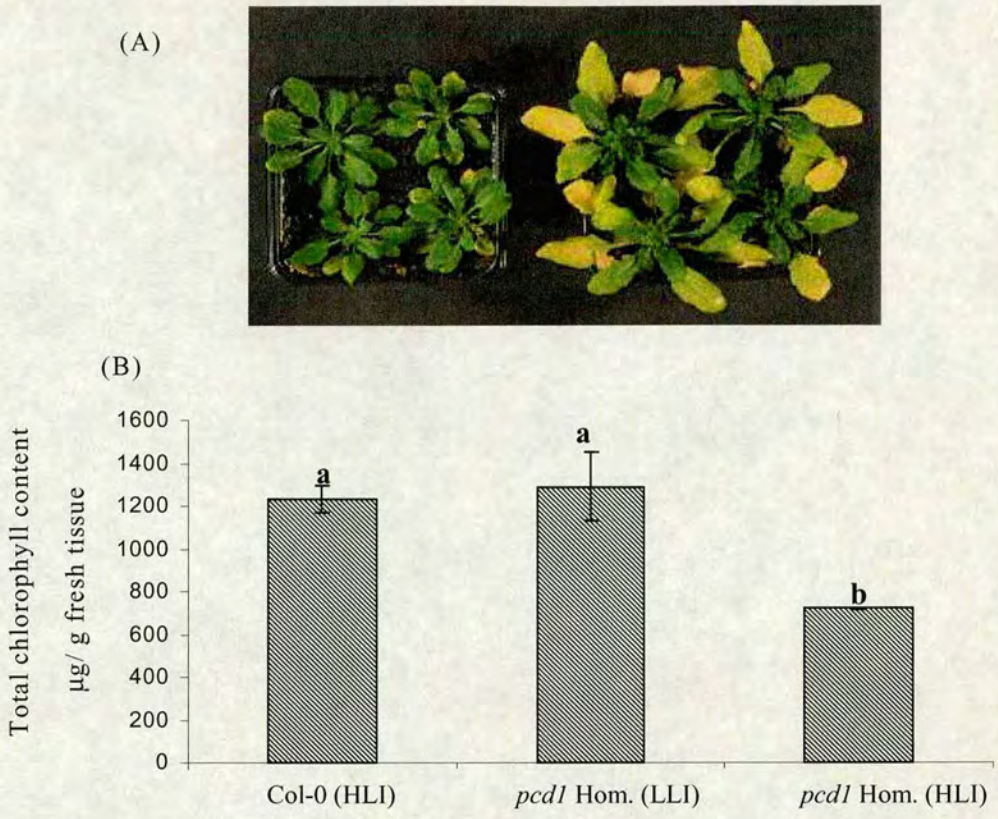

Figure 3.10: Phenotypic analysis and quantification of chlorophyll content in *pcd1* and Col-0 plants in response to changes in light intensity. LLI, low light intensity (~150 µEinstein.m^{-2}.min^{-1}); HLI, high light intensity (> 200 µEinstein.m^{-2}.min^{-1}). (A) Phenotypic analysis of *pcd1* plants in response to changes in light intensity. Note the appearance of chlorotic leaves on *pcd1* plants that were first grown under HLI and then transferred to LLI conditions (right). No chlorotic leaves were observed on leaves of *pcd1* plants that were kept under LLI conditions (left). (B) Quantification of chlorophyll content in *pcd1* plants in response to changes in light intensity. Chlorophyll content is represented as total chlorophyll (a and b) per µg fresh leaf tissue. Similar letter above the error bar represents no significant difference between the means, whereas different letters represent significant differences between the means according to Tuckey test (P=0.05).

3.2.7 *pcd1 constitutively expresses a battery of key defence and antioxidant genes*

Northern analysis revealed that *pcd1* plants express an array of key defence and antioxidant genes. Antioxidant genes such as *GST1* and *CAT3* were found to be expressed constitutively in *pcd1* (Figure 3.11 A).

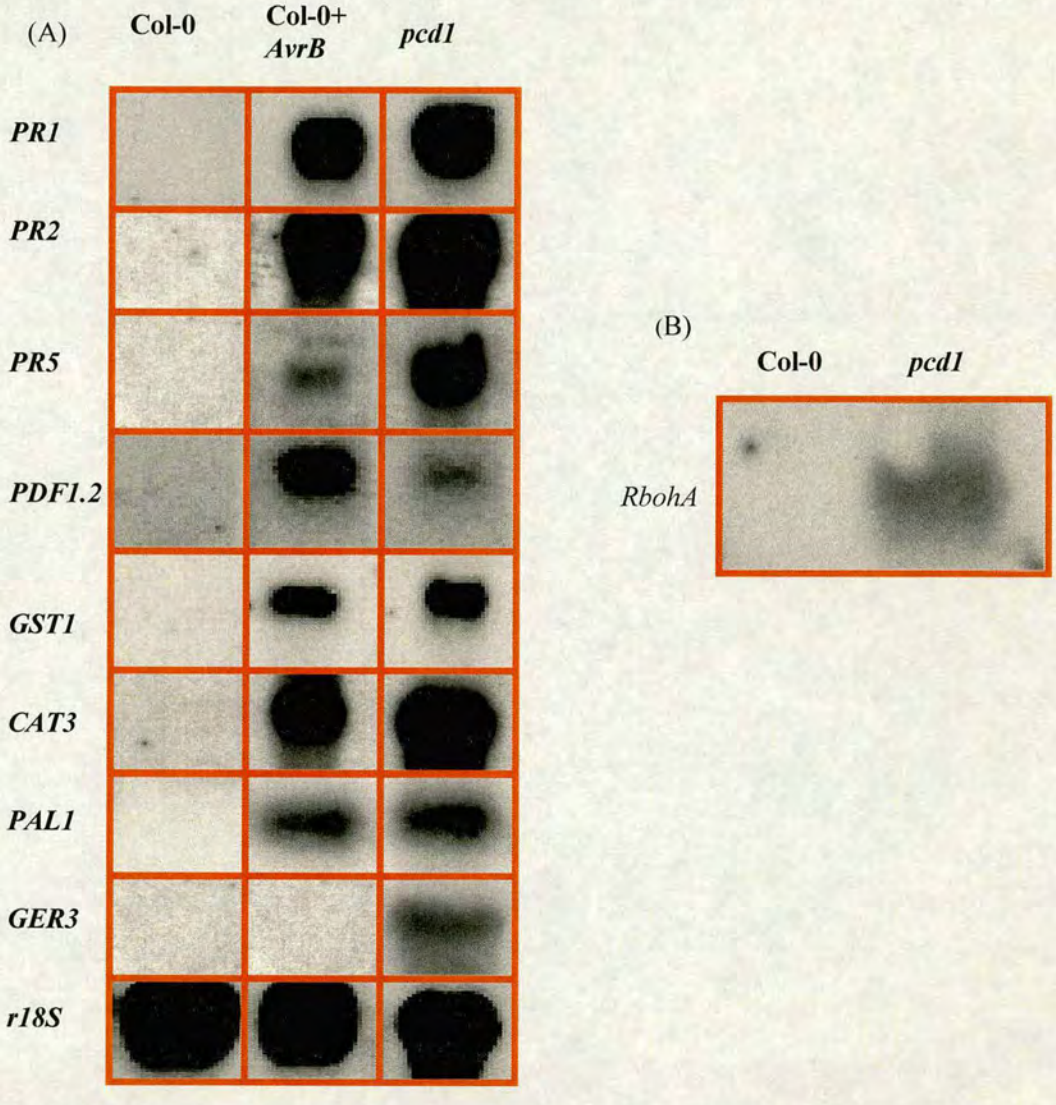

Figure 3.11: Northern analysis of *pcd1* plants. (A) Total RNA analysis in *pcd1*. ca. 10 µg total RNA was used for each sample. As a positive control, wild-type Col-0 leaves were infiltrated with *Pst* DC3000 (*AvrB)* and leaf tissue samples were collected 24 hrs post-infiltration. In the case of *PAL1*, samples were collected 2 hrs post-infiltration. *R18S* was used as an RNA loading and transfer control. (B) Analysis of *RbohA* expression in *pcd1* plants. ca. 1 µg of polyA-enriched RNA was loaded per each sample. All X-ray films were developed after exposure at –70°C for 24 hrs. Gene probes: *PR1,2&5*, pathogenesis-related 1,2&5; *PDF1.2*, plant defensin 1.2; *GST1*, glutathion S-transferase; *CAT3*, catalase 3; *PAL1*, phenylalanine-ammonia lyase 1; *GER3*, germine-like 3; *RbohA*, respiratory burst oxidase homologue A; *r18S,* ribosomal RNA gene encoding the 18S subunit.

In spite of the constitutive expression of *CAT3*, no overall change in CAT enzymatic activity was detected in *pcd1* plants. This observation suggests that there might be a posttranscriptional or indeed posttranslational regulation of *CAT* genes and/or CAT enzymatic activities, respectively. Alternatively, CAT inhibition by signal molecules, such as SA, could serve as a plausible explanation (Conrath *et al.,* 1995).

In order to identify the source of H_2O_2 generation in *pcd1*, I checked the expression of the NADPH oxidase gp^{phox91} subunit homologue *RbohA*. A constitutive level of expression for *RbohA* was detected in *pcd1* but not in Col-0 plants. Therefore, *RbohA* may contribute to the observed H_2O_2 accumulation in *pcd1* plants via the reductive conversion of O_2 to O_2^-. Moreover, it can also be concluded that despite the expression of several antioxidant genes for the detoxification of H_2O_2 in *pcd1* plants, cells fail to avert the occurrence of cell death.

Germin-like genes (*GER*) have previously been found in *Arabidopsis*. Germins are important proteins that are found in monocots and have been shown to exhibit oxalate oxidase activity leading to the generation of H_2O_2 (Berna & Bernier, 1999). I found that the *GER3* mRNA is constitutively expressed in *pcd1* leaves. Therefore, despite the fact that *Arabidopsis* GER proteins have not been shown to exhibit oxalate oxidase activity yet, I speculate that GER3 may participate together with RbohA in the production of H_2O_2 in *pcd1* plants. Taken together, the presented evidence suggests that there could be at least two distinct enzymatic sources for the generation of H_2O_2 in *pcd1*.

PR1, *PR2* and *PR5*, important key genes that convey resistance against a wide spectrum of bacterial and fungal pathogens, were found to be constitutively expressed in *pcd1*. Moreover, the JA-dependent gene *PDF1.2* was also detected. These observations suggest that the *pcd1* mutation engages both SA- and JA-dependent signalling pathways. I therefore speculate that *PCD1* resides at the branch point of at least two distinct signal transduction pathways. Furthermore, the expression of *PAL1*, which encodes the first enzyme for the phenylpropanoid pathway, was also detected. Therefore, I believe that SA and phytoalexin

accumulation in *pcd1* is predominantly due to an upregulation in the phenylpropanoid pathway.

3.2.8 pcd1 is significantly resistant to bacterial, fungal and oomycete pathogens

The constitutive expression of key resistant genes has led us to speculate that *pcd1* might be more resistant against pathogens than wild-type Col-0. Therefore, we next examined the response of *pcd1* to several biotrophic phytopathogens. The growth of the hemi- biotrophic bacterial pathogen *Pst* DC3000 was significantly decreased in *pcd1* compared to Col-0 leaves. At the third day post-inoculation, *pcd1* plants were at least half a log more resistant than Col-0 plants (Figure 3.12).

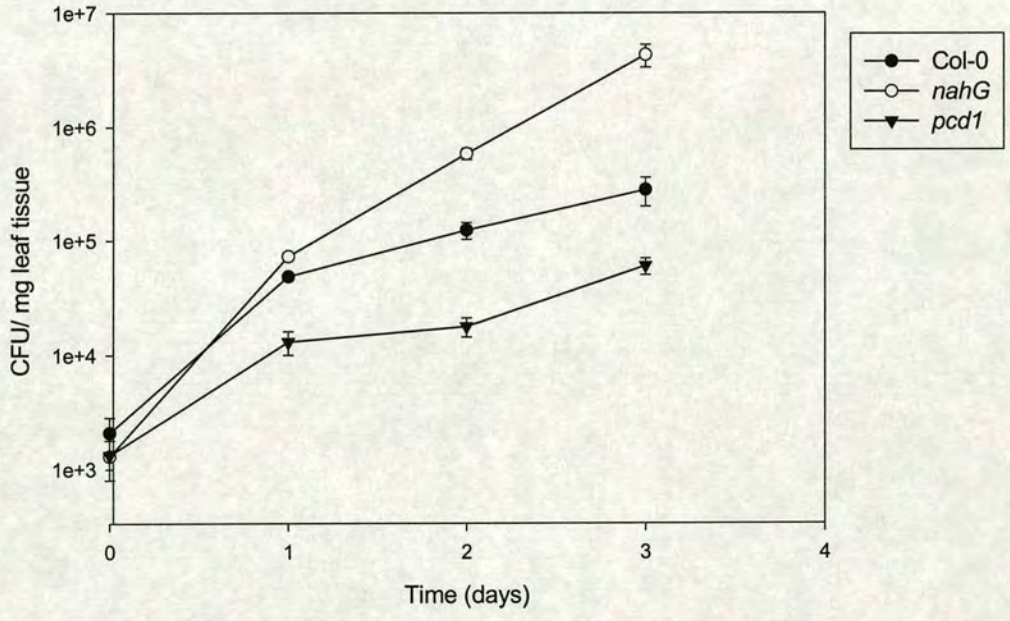

Figure 3.12: Growth of *P. syringae* pv. *tomato* DC3000 in *pcd1* compared to wild-type Col-0 leaves. Leaves of corresponding plants where inoculated with 0.0002 OD_{600} bacterial suspension in 10 mM $MgCl_2$. Leaf samples were assays for bacterial growth at the indicated time points. Bacterial growth is represented as CFU per mg leaf tissue. The experiment was repeated twice with similar results.

Therefore, the overexpression of *PR* genes, phenolic compounds and perhaps several other yet unidentified factors in *pcd1* significantly contribute to the observed heightened level of resistance compared to wild-type plants. Moreover, *pcd1* plants exhibited significant level of resistance to the biotrophic fungal pathogen *Erysiphe* (unclassified species). *pcd1* plants displayed no visible hyphal growth and germinating spores as confirmed by trypan blue staining (Figure 3.13).

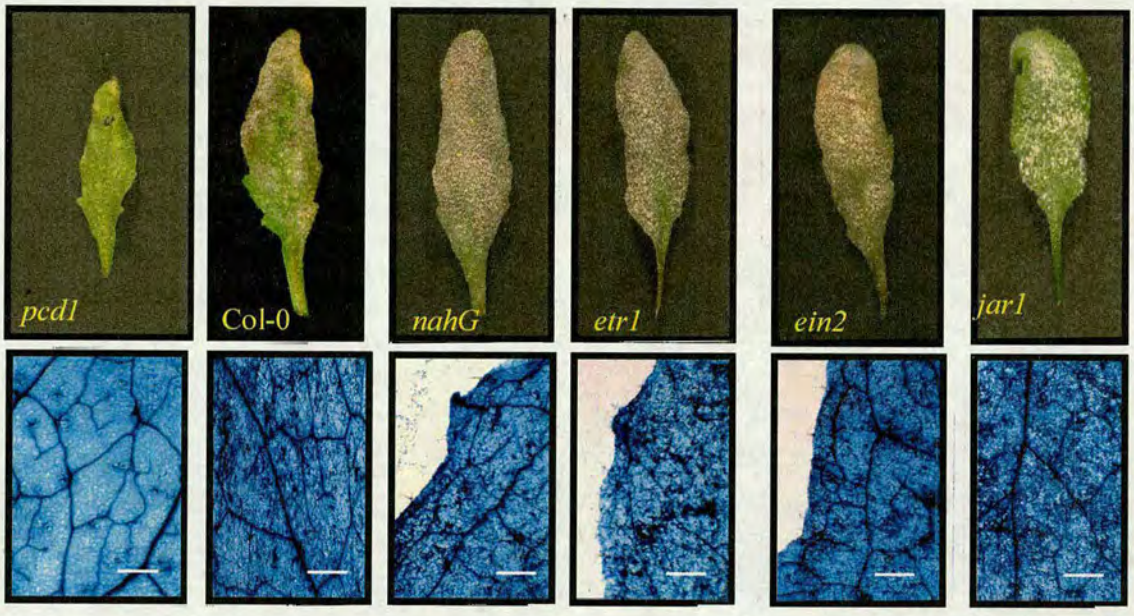

Figure 3.13: Growth of the biotrophic fungus *Erysiphe* (powdery mildew) on *pcd1* leaves compared to other defence signalling mutants. Plants of the genotypes noted above were uniformly dusted with spores of powdery mildew obtained from previously infected plants (section 2.14.2.2). Pictures were taken 10 days post-inoculation. Additionally, samples were collected for trypan blue staining to examine internal hyphal growth and sporulation. Scale bars are 10 μm.

Therefore, the high level of resistance observed in *pcd1* plants is probably attributed to the ability of *pcd1* plants to block internal spore germination and successful colonisation. Furthermore, resistance against the biotrophic oomycete pathogen *Pronospora parasitica* NOCO2 was also examined. *pcd1* plants displayed absolutely no growing conidiophores on their leaves. In terms of disease index, *pcd1* plants were at least 1.5 times more resistant than Col-0 plants (Figure 3.14).

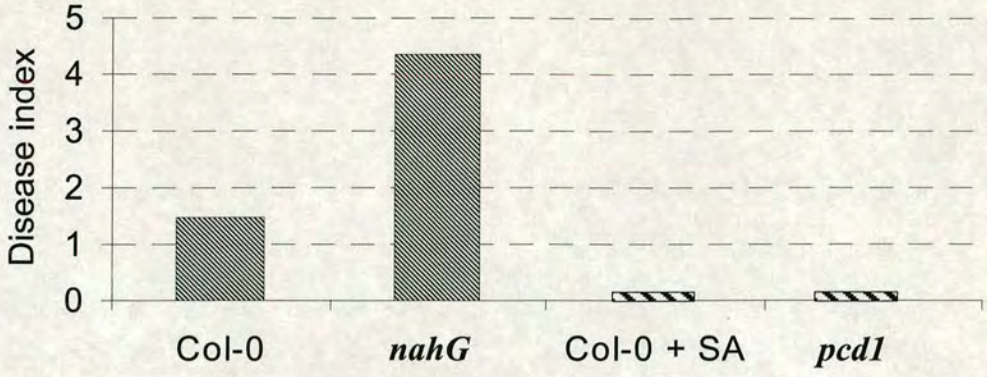

Figure 3.14: Growth of the oomycete *P. parasitica* NOCO2 on *pcd1* leaves compared to wild-type Col-0. Plants were sprayed with an oomycete suspension at a density of 10^5 spores.ml^{-1}. Plants were examined for *P. parasitica* growth on day 10 post-infection and a disease index was assigned (section 2.14.2.1) for each group of plants. Each group consisted of 10 plants.

This high level of resistance could only be mimicked by wild-type Col-0 plants painted with SA. Hence, SA accumulation in *pcd1* plants plays a central role in the observed heightened resistance against downy mildew.

3.2.9 pcd1 does not display increased salt tolerance or ABA insensitivity

I next investigated whether there is a cross-talk between abiotic and biotic stress responses in *pcd1*. Salinity and ABA tolerance were two responses that were particularly examined. *pcd1* plants displayed germination rates that mirrored Col-0 seeds when grown on MS plates incorporating increasing NaCl concentrations. *pcd1* exhibited a gradual decrease in germination rate with increasing salt concentration (0-200 mM) (Figure 3.15).

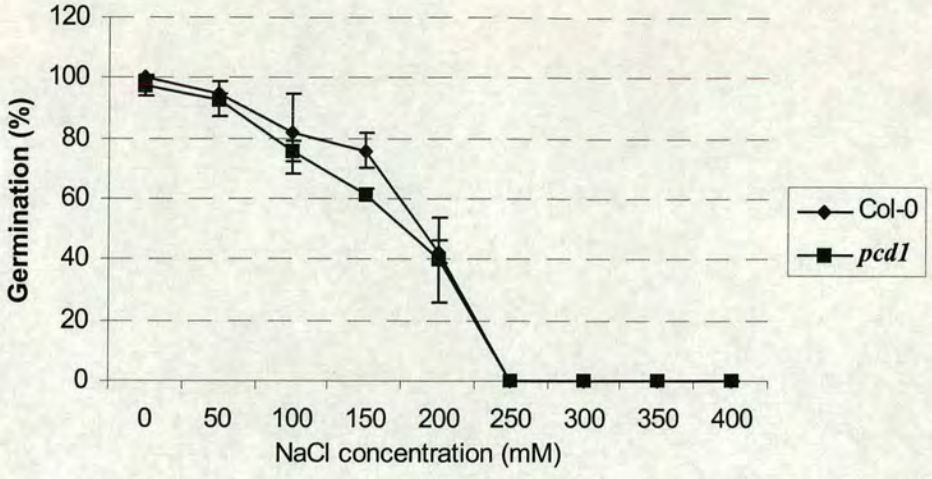

Figure 3.15: Germination rate of *pcd1* seeds and wild-type Col-0 on MS media containing increasing NaCl concentrations. Seeds representing Hom. *pcd1* and Col-0 were grown on MS media supplemented with an increasing range of NaCl (0-400 mM). Germination rate was scored 10 days after sowing. No difference in germination rate was found beyond 10 days.

Furthermore, similar to Col-0, *pcd1* seeds completely failed to germinates on higher salt concentrations (250-400 mM). Therefore, *pcd1* plants display a similar level of salt tolerance to wild-type plants in response NaCl. Moreover, *pcd1* seeds also failed to germinate on MS plates incorporating 5 μM ABA (Table 3.1). Hence, *pcd1* seeds display no ABA insensitivity. Taken together, it can be concluded that in *pcd1* the high biotic stress tolerance does not impact on abiotic stress tolerance to salt and ABA.

Table 3.1: Comparison of the germination rate of Col-0, *abi1*, and *pcd1* in response to abscisic acid. Germination was scored 10 days after seed were vernalized.

Genotype	Germination (%)	
	Without ABA	ABA (5 μM)
Col-0	100	0
abi1	100	100
pcd1	100	0

3.2.10 Genetic and molecular analysis of pcd1 and cpe1 mutants

3.2.10.1 Genetic analysis of *pcd1*

In order to determine the mode of inheritance of the *pcd1* mutation, homozygous *pcd1* plants were backcrossed to wild-type Col-0. The characteristic *pcd1* phenotype, HR-like lesions, H_2O_2 accumulation, and *PR1::LUC* activity were sustained in the F1 progeny of *pcd1*::Col-0. Moreover, the F2 progeny of *pcd1*::Col-0 plants segregated in a 3:1 Mendelian fashion (Table 3.2).

Table 3.2: Genetic analysis of *pcd1*.

Cross	Progeny	Total plants	Phenotype *pcd1*	Phenotype Wild-type	Ratios	#X^2
**pcd1::PCD1* (Col-0)	F1	12	12	0		
	F2	40	32	8	3:1	0.032 (P>0.9)
pcd1::PCD1 (L*er*)	F1	8	0	8		
	F2	632	152	486	1:3	0.47 (P>0.5)
	F2+BTH	42	32	10	3:1	0.023 (P>0.5)
pcd1::nahG	F1	16	0	16		
pcd1::coi1	F2	40	30	10		
pcd1::etr1	F1	8	8	0		

* *pcd1* was used as a pollen donor in all the crosses
# The Chi-square test for goodness-of-fit was used to test the hypothesis whether the observed segregation ratios fit to Mendelian patterns for recessive or dominant traits (Snedecor & Cochran, 1989).

Hence, the *pcd1* mutation segregates as a dominant monogenic Mendelian trait. Interestingly, *pcd1* behaved as a recessive trait when crossed to L*er*. The recessive nature of *pcd1* could be overridden when the F2 *pcd1*::L*er* progeny sprayed with the SAR inducing chemical BTH (Table 3.2). Moreover, the ability of *pcd1* plants to accumulate H_2O_2 was also lost in the L*er* background. Therefore, I suggest that this phenomenon is probably due to the low penetrance of the *pcd1* mutation in the L*er* background.

I next examined the phenotypic appearance of *pcd1*::*nahG*, *pcd1*::*coi1* and *pcd1*::*etr1* double mutants. I carefully checked these double mutants for the characteristic HR-like lesions. Lesion formation was apparent on *pcd1*::*coi1* and *pcd1*::*etr1* double mutants. Moreover, these double mutants maintained H_2O_2 accumulation in a similar fashion to homozygous *pcd1* plants. Interestingly, HR-like lesions and H_2O_2 accumulation were completely lost in *pcd1*::*nahG* double mutants (Figure 3.16).

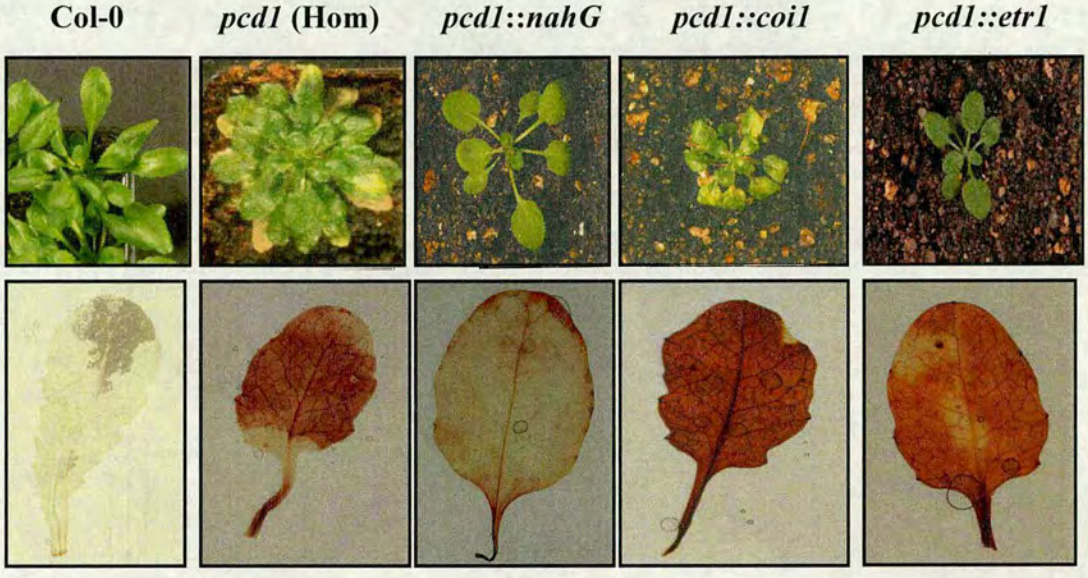

Figure 3.16: Phenotypic and histochemical analysis of *pcd1* double mutants with *nahG*, *coi1*, and *etr1*. Upper panels represent pictures of Col-0, *pcd1*, *pcd1*::*nahG*, *pcd1*::*coi1* and *pcd1*::*etr1*. Lower panels display DAB-stained leaves of representative plants.

Hence, based on this phenotypic and histochemical evidence, HR-like lesion formation and H_2O_2 production in *pcd1* plants are probably SA-dependent but JA- and ET-independent.

3.2.10.2 Molecular analysis of *pcd1*

One major advantages of using T-DNA mutagenesis is the ease with which the mutated gene can be rescued via a simple plasmid rescue protocol, provided that it is tagged by a linked T-DNA. In this context, we wanted to ascertain that the *pcd1* phenotype was the result of an activation/interruption of the *PCD1* gene by a single T-DNA. One way of verifying this was by analysing the co-segregation of the *pcd1* phenotype with Basta resistance. To my surprise, some Basta sprayed *pcd1* plants of the F2 *pcd1*::Col-0 progeny were susceptible to the pesticide. Basta resistance segregated in a 3(resistance):1(sensitive) fashion with ~50% of the Basta sensitive fraction comprised of *pcd1* plants.

This observation has led me to speculate that: 1) the *pcd1* mutation is probably not tagged by a T-DNA; and 2) there is a second functional unlinked T-DNA, that is probably segregating leading to the Basta resistant phenotype observed in some *pcd1* plants. In order to investigate the validity of this hypothesis, I embarked on an intensive molecular analysis performed on F2 *pcd1*::Col-0 progeny employing PCR and Southern strategies. In the screen for the presence of intact 35S enhancers and pBlueScript DNA, no PCR products were obtained in PCR reactions performed on DNA from Basta sensitive *pcd1* plants (Figure 3.17 A&B).

In the screen for the presence of an intact *bar* gene at least 3 different PCR products were detectable in PCR reactions performed on the same susceptible *pcd1* plants (Figure 3.17 C). Moreover, in Southern analysis using the *bar* DNA as a probe, a similar banding pattern was observed in Basta sensitive *pcd1* plants compared to T3 non-segregating homozygous *pcd1* plants (Figure 3.17 D). In contrast, Basta resistant *pcd1* plants, used as a positive control, gave the expected precise PCR products in the screen for 35S enhancer and pBlueScript (Figure 3.17 A&B).

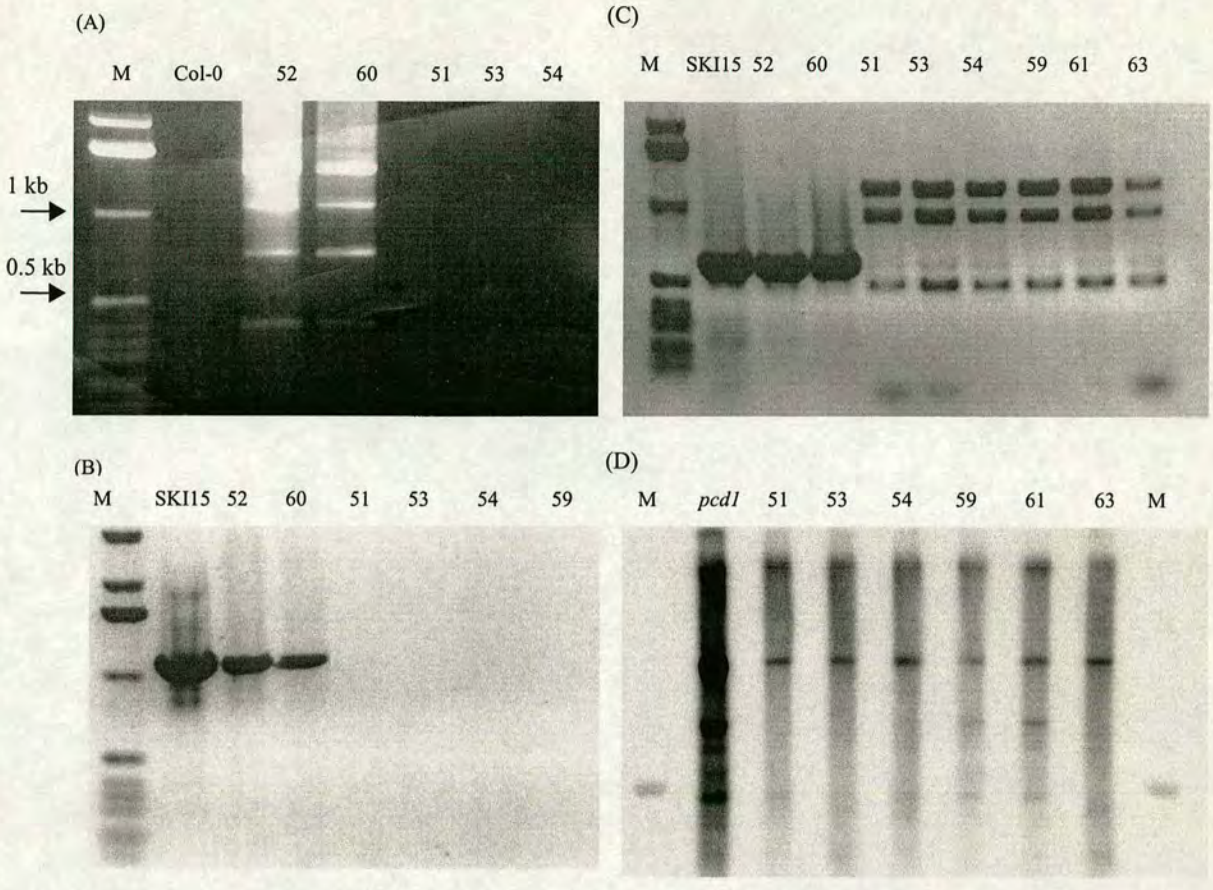

Figure 3.17: Molecular characterisation of *pcd1*. (A), (B) and (C) PCR analysis of the 35S CaMV enhancer sequence, the pBlueScript fragment and the *bar* gene in the T-DNA in *pcd1* plants of the F2 *pcd1*xCol-0 progeny, respectively. PCR conditions were conducted according to materials and methods (Chapter II). (D) Southern analysis for the *bar* gene in *pcd1* plants of the F2 *pcd1*xCol-0 progeny. Blots were probed with a full length 0.6 kb *bar* DNA fragment, exposed for 4 hrs and then films were developed. Abbreviations: M, 1 kb ladder; SKI15, binary vector plasmid DNA used as a positive control; *pcd1*, homozygous T3 *pcd1* plants that are Basta resistant; 52 and 60, *pcd1* plants from the F2 *pcd1*xCol-0 progeny that are Basta resistant; 51, 53, 54, 61, 62, and 63, *pcd1* plants from the F2 *pcd1*xCol-0 progeny that are Basta sensitive.

Taken together, I conclude that the T-DNA linked to the *pcd1* has probably undergone severe truncations resulting in the total loss of 35 enhancer region and pBlueScript DNA. Furthermore, evidence from PCR and Southern analyses (Figure 3.17) indicates that the *bar* gene region of the T-DNA is highly rearranged. The rearrangement in the *bar* gene could probably be taken as an explanation for the observed Basta sensitive phenotype of some *pcd1* plants, whereas the observed Basta

resistant phenotype of some of the *pcd1* plants could possibly be attributed to the presence of an extra segregating unlinked T-DNA copy. Unfortunately, due to the severe truncations and rearrangements in the T-DNA that is linked to the *PCD1* gene, alternative approaches for gene cloning, such as inverse PCR and TAIL PCR, could not be employed. Therefore, a map-based cloning approach has been adopted for the isolation of the *pcd1* gene instead.

3.2.10.3 Genetic and molecular analysis of *cpe1*

The *cpe1* mutant was also identified in our screen. I therefore examined the mode of inheritance of this mutation. The *PR1::LUC* activity screen was employed to screen for the *cpe1* phenotype. In the F1 progeny resulting from a *cpe1::PR1::LUC* cross, no constitutive bioluminescent plants were found (Table 3.3). The F2 *cpe1::*Col-0 progeny segregated according to a Mendelian 1:3 fashion (Figure 3.18 A). Hence, I concluded that the *cpe1* mutation conforms to the expected segregation of a monogenic recessive trait. In northern analysis, *cpe1* plants were confirmed to have constitutive *PR1* expression (Figure 3.18 B).

Table 3.3: Genetic analysis of *cpe1*.

Cross	Progeny	Total plants	*PR1::LUC expression*		Comments
			Yes	No	
cpe1::PR1::LUC	F1	8	0	8	Recessive
	F2	40	8	32	~1:3

Accordingly, this result was taken as a confirmation for the *PR1::LUC* imaging analysis indicating that the *cpe1* mutation segregates as a recessive monogenic trait. However, in two consecutive northern analyses I failed to reproduce the constitutive *PR1* expression of *cpe1* plants. Therefore, I terminated any further work with this mutant. The loss of the *PR1* expression in *cpe1* plants may be due to the instability of this mutation.

(A)

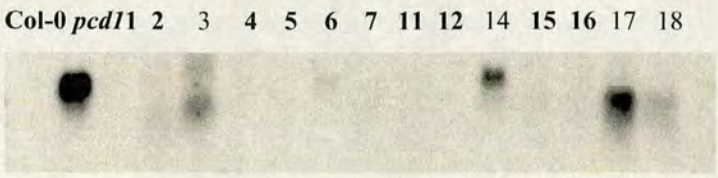

(B)

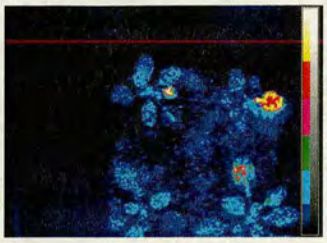

Figure 3.18: (A) Northern analysis performed on *cpe1::PR1::LUC* F2 progeny. The membrane was hybridised with a *PR1* probe. Total RNA of *pcd1* was used as a positive control. ca 10 µg total RNA was loaded for each sample. The membrane was developed after exposure at –70° C for 24 hrs. (B) Luciferase imaging of selected *cpe1 ::PR1::LUC* F2 plants. Image was taken over a period of 10 s.

3.2.11 pcd1 maps to the lower arm of chromosome I

In an attempt to map-based clone the *pcd1* gene, in collaboration with Xinwei Chen, we have generated recombinant inbred lines (RIL) of F2 *pcd1*x*Ler* cross. To assign a rough map position to the *pcd1* gene, several SSLP markers that are evenly spread over all five chromosomes were used (section 2.21). The bulked segregant analysis (BSA) approach was employed mainly for its ease, rapidity and simplicity. Approximately 24 F2 plants that were homozygous for *pcd1* were used in the BSA analysis.

All plants tested were confirmed to be homozygous for *pcd1* in the F3 generation. In our initial BSA analysis, linkage of the *pcd1* phenotype to the SSLP marker nga128 (83.3 cM) on chromosome I was detected. Next we attempted to identfy a genetic interval flanked by two markers to which the *pcd1* phenotype is closely linked. Therefore, we made use of the public availability of several Cereon SNPs markers, that are located near the SSLP marker nga128, of the type INDEL in order to accomplish this task. In this regard, a 14 cM genetic interval could be assigned to the *pcd1* mutation (Table 3.4).

Table 3.4: Mapping of *pcd1* to SSLP and SNP markers on chromosome I

Plant No.#	Outcome of molecular analysis of RILs								
	nga128 (83.3 cM)	T12P18 (~90 cM)	SNP213 (92.7 cM)	F5I14 (~102 cM)	T1F15 (~109 cM)	SNP177 (110.7 cM)	nga111 (115.5 cM)	nga692 (119.3 cM)	SNP95 (129.5 cM)
51	C		C					H	H
55	C		C	C	C	C	C	C	C
59	H	C	C	C	C	C	C	C	C
60	C		C		C	C	C	C	C
61	C		C	C		C	C	C	C
62	C		C	C	C	C	C	C	C
63	C		C	C	C	C	C	H	H
65	C		C		C	C	C	C	C
68	C		C	C	C	C	C	C	C
69	C		C	C	C	C	C	C	C
70	C		C	C	C	C	C	C	C
71	C		C			C	C	C	C
72	C		C		C	C	C	C	C
74			C	C	C	C	C	C	C
75	H	C	C	C	C	C	C	C	C
83	C		C		C	C	C	C	C
85	C		C				H	H	C
87	C	C	C	C	C	H	H	H	H
88	C	C	C	C	C	C	C	H	H
90	C		C		C	C	H	H	H
97	C		C		C	H	H	H	H
102	C	C	C	C	C	C	C	C	C
106	C	C	C	C		C	H	C	C
109	C	C	C	C	C	C	C	C	C

* Initials: C, Col-0 homozygous; H, heterozygous.

Plants tested here were all confirmed to be homozygous for *pcd1* in the F3 progeny of *pcd1*x*Ler* RIL. SNP, denote markers the Stanford Genome Center (SGC) SNPs. Information on these SGCSNPs markers and its sequence are available at the TAIR web page (http://www.arabidpsis.org/SNPs.html), whereas T12P18, F5I14 and T1F15 are Cereon SNPs of the type insertions/deletions (INDELs) that were generated by Cereon Genomics (http://www.arabidopsis.org/Cereon/index.html). The map position of these Cereon SNPs was estimated in cM using the AGI and Lister & Dean RI maps.

Fine linkage analysis indicates that the *pcd1* mutation is located between T12P18 (88 cM) and T1F15 (102 cM) in an approximate 14 cM genetic interval near the lower arm of chromosome I.

3.3 Discussion

3.3.1 pcd1 is a novel mutation

Genetic and molecular analyses of the *pcd1* mutant indicated that the *pcd1* gene is not tagged by a T-DNA insert (Figure 3.17). Therefore, we have alternatively undertaken a map-based cloning strategy to isolate the *pcd1* gene. Thus, the *pcd1* mutation was assigned to a genetic interval of approximately 14 cM, on the lower arm of chromosome I, between the SNP (INDEL) markers T12P18 and T1F15 (Table 3.4). Next we analysed the 14 cM genetic interval to which the *pcd1* mutation was mapped for any interesting annotated genes using the *Arabidopsis* database search facility provided by TAIR (www.arabidopsis.org). Our search identified several annotated genes of interesting functions. A sugar-metabolism related gene known as *G*DP-4-keto-6-deoxy-D-mannose-3,5-*e*pimerase-4-*r*eductase (*GER1*) was found. GER1 is an enzyme involved in pathway for *de novo* synthesis of GDP-L-fucose. A lipid-metabolism related gene similar to triacylglycerol biosynthesis defect 1 (*TAG1*) has also been found. Mutating the *TAG1* gene, in the *as11* mutant, affects diacylglycerol acyltranseferase activity resulting in alteration of seed fatty acid composition, namely reduction in very long-chain fatty acids content in seed (Katavic *et al.*, 1995). Similarly, a putative gene involved in C-26 fatty acylcoenzyme A elongation was identified. Interestingly, two genes with putative protein kinase activity and phosphatase activity were identified. Additionally, an annotated gene encoding a putative lipoxygenase with high similarity to *Solanum tuberosum* lipoxgenase was also found. Moreover, to our knowledge, with the exception of *lsd6*, no other previously identified *lsd* or other dominant defence-related mutations have been mapped to the *pcd1* region of chromosome I. (Table 3.5). Several *Arabidopsis* mutants displaying constitutive lesion formation phenotype have previously been described including *lsd*, *acd*, and *cpr5* and *cpr6* mutants (Dietrich *et al.*, 1994; Weymann *et al.*, 1995; Greenberg *et al.*, 1994; Bowling *et al.*, 1997; Clarke *et al.* 1998).

Table 3.5: *Arabidopsis* mutants with altered disease resistance.

Mutant	Ecotype	Mutagen	Chromosome	Mode of inheritance	Comments	Reference
SAR CONSTITUTIVES						
cpr1	Col-0	EMS	4	Recessive	BGL2::GUS screen	Bowling *et al.* (1994)
cpr5	Col-0	EMS	5	Recessive	BGL2::GUS screen	Bowling *et al* (1997)
cpr6	Co-0	EMS	1	Dominant	BGL2::GUS screen	Clarke *et al* (1998)
cpr22	Col-0	T-DNA	2	Recessive	Identified through *PR-1* expression	Yoshioka *et al* (2001)
*ACD2**	Col-0	EMS	4	Recessive	*ACD2* encodes a red chlorophyll catabolite reductase.	Mach *et al.* (2000)
acd5	Col-0	EMS	5	Recessive	SA-dependent HR is uncoupled from disease resistance.	Greenberg *et al.* (2000)
acd6	Col-0	EMS	4	Dominant gain-of-function	Functions in both *NPR-1*-dependent and –independent pathways.	Rate *et al.* (1999)
*LSD1**	Ws-0	T-DNA	4	Recessive	*LSD1* encodes a zinc finger protein that is a negative regulator of HR	Dietrich *et al.* (1997)
lsd2	Col-0	EMS	ND	Dominant	HR is SA-independent	Dietrich *et al.* (1994)
lsd3	Ws-0	T-DNA	ND	Recessive	HR is SA-dependent	ibedem
lsd4	Ws-0	T-DNA	ND	Dominant	HR is SA-independent	ibedem
lsd5	Ws-0	T-DNA	ND	Recessive	HR is SA-dependent	ibedem
lsd6	Col-0	EMS	1	Dominant	HR is SA-dependent	Weymann *et al.* (1995)
lsd7	Col-0	EMS	ND	Dominant	Not linked to chromosome 1	ibedem
ADR1*	Col-0	T-DNA activation tagging	1	Dominant	*ADR1* is possibly a novel class of *R* genes with CDPK domains.	Grant *et al.* (unpublished)
cep1	Ws-0	T-DNA	4	Recessive	*PR-1* mRNA analysis	Silva *et al.* (1999)
pcd1	Col-0	T-DNA activation tagging	1	Dominant	*PR-1::luc* screen	Aboul-Soud *et al.* (unpublished)
*SSI1**	Nossin	EMS	4	Dominant haploinsufficient	*PR-1* mRNA analysis	Shah *et al.* (1999)
*SSI2**	Nossin	EMS	2	Recessive	*SSI2* encodes an S-ACP-DES	Kachroo *et al.* (2000)
*SNI1**	Col-0	EMS	4	Recessive	SNI1 has no homology to any known proteins. It functions as SAR negative regulator	Li *et al.* (1999)
*EDR1**	Col-0	EMS	1	Recessive	*EDR1* encodes a MAPKKK that is a negative regulator of SAR	Frye *et al.* (2001)
clr1	Col-0	EMS	1	Recessive	*PR-1::luc* screen	Murray *et al.* (unpublished)
*MPK4**	L*er*	Transposon tagging	ND	Recessive	*MPK4* encodes a MAPK that negatively regulate SAR	Petersen *et al.*(2000)
SAR COMPROMISED						
*NPR1**	Col-0	EMS	1	Reccessive	*NPR1* encodes a protein with ankyrin-repeats	Cao *et al.* (1997)
sid1	Col-0	EMS	4	Recessive	Blocked in SA accumulation after *pst avrRpm1* treatment	Nawarth & Metraux (1999)
*SID2-1/EDS5**	Col-0	EMS	1	Recessive	*EDS5* encodes a protein with homology to DINF family in E. *coli*	ibedem
*SID2-2/EDS16-1**	Col-0	Fast neutrons	1	Recessive	*EDS2-2* encodes a protein with homology to isochorismate synthase that is required for SA synthesis in plants	Wildermuth *et al.* (2001)
*NDR1**	Col-0	Fast neutrons	3	Recessive	*NDR1* encodes a membrane-associated protein	Century *et al.* (1997)
*EDS1-2**	L*er*	Fast neutrons	3	Recessive	*EDS1* encodes a protein with homology to eukaryotic lipases	Falk *et al.* (1999)
pad1	Col-0	EMS	4	Recessive	Mutant deficient in camalexin	Gleazebrook *et al.* (1994)
pad2	Col-0	EMS	4	Recessive	ibedem	ibedem
*PAD3**	Col-0	EMS	3	Recessive	*PAD3* encodes a protein with homology to cytochrome P450	Zhou *et al.* (1999)
PAD4	Col-0	EMS	3	Recessive	*PAD4* encodes a protein with homology to eukaryotic lipases	Jirage *et al.* (1999)
ET MUTANTS						
*CTR1**	Col-0	EMS		Recessive	*CTR1* encodes a member of the RAF family of Ser/Thr kinases	Kieber *et al.* (1993)
*ETR1**	Col-0	EMS	1	Dominant	*ETR1* encodes a protein with homology to prokaryotic two-component sensors	Chang *et al.* (1993)
*EIN2**	Col-0	EMS	5	Recessive	*EIN2* encodes a protein with homology to Nramp family of metal-ion transporters	Alonso *et al.* (1999)
JA MUTANTS						
jar1	Col-0	EMS	2	Recessive	Insensitive to JA	Staswick *et al.* (1998)
*COI1**	Col-0	EMS	2	Recessive	*COI1* encodes a protein with homology to F-box proteins	Xie *et al.* (1998)
cev1	Col-*gl1*	EMS	5	Recessive	Isolated via constitutive expression of *VSP1::Luc*	Ellis & Turner (2001)

* Uppercase indicates that the gene has been cloned. An underlined, boldfaced mutant name indicates that the mutant has been isolated in our lab.

Of the previously published lesions mimics, only *acd6*, *lsd2*, *lsd4*, *lsd6* and *lsd7* are dominant (Table 3.5). The *acd6* maps to chromosome I in a different region to *pcd1*. Moreover, the *acd6* display some phenotypic that are distinctly different from those observed in *pcd1*; *acd6* leaves display a few punctate cell death patches as opposed to the uniformly-distributed mosaic-like lesions that are associated with the *pcd1* phenotype. Therefore, I believe that the *pcd1* mutation is not allelic to *acd6*. Unlike *pcd1*, the spontaneous lesion formation phenotypes associated with the *lsd2* and *lsd4* mutations have previously been shown to be SA-independent (Hunt *et al.*, 1997). Moreover, when compared to *pcd1*, both *lsd2* and *lsd4* display completely different HR-like lesion appearance and distribution on their leaves. Therefore, despite the fact that no map position has previously been assigned to these mutations, I conclude that the *pcd1* mutation is not allelic to either *lsd2* or *lsd4*. In contrast, unlike *lsd2* and *lsd4*, lesion formation on *lsd6* and *lsd7* leaves has previously been reported to be SA-dependent (Weymann *et al.*, 1995). The *lsd7* phenotype is associated with very small lesions that became evident when visualised microscopically by trypan blue staining. Moreover, the *lsd7* mutations has been shown not to be linked to chromosome I (Wemann *et al.*, 1995). Hence, I conclude the *pcd1* mutation is not allelic to lsd7. The *lsd6* phenotype is characterised by spontaneous formation of punctate necrotic lesions are not affected by day length (i.e. lesion formation appears similar under both short- and long-day conditions. Moreover, *lsd6* leaves have been shown to constitutively express the key defence genes *PR1*, *PR2* and *PR5*. Interestingly, the spontaneous lesion formation on *lsd6* leaves was blocked under high humidity. The *lsd6* mutation has been mapped to the same *pcd1* region of the lower arm of chromosome I, within an approximately 25 cM region, between the SSLP markers nga111 and nga128 (Weymann *et al.*, 1995). Thus, allelism analysis between *lsd6* and *pcd1* is essential to be conducted to ascertain that the *pcd1* mutation is novel. In this, examination of the lesioned-leaf phenotype segregation in the F2 progeny of *pcd1::lsd6* will be informative.

3.3.2 Dissection of H_2O_2-mediated signal transduction in pcd1

3.3.2.1 Source of H_2O_2 generation in *pcd1*

ROS play a prominent role in early and later stages of the plant defence responses, putatively acting as both cellular signalling molecules and direct antipathogen agents (Baker & Orlandi, 1995; Levine *et al.*, 1994; Alvarez *et al.*, 1998). The ability of plants of accumulating ROS in responses to several biotic and abiotic stress stimuli is believed to involve the activation of different ROS-generating mechanisms including: plasma membrane-bound NADPH oxidase, pH-dependent cell-wall peroxidase, extracellular germin-like oxalate oxidase, amine oxidases and *xanthine* oxidase (reviewed in Bolwell & Wojtaszek, 1997). In this work, I demonstrated that *pcd1* leaves accumulate high level of H_2O_2 (Figure 3.5 H). In order to identify the H_2O_2 -generating sources in *pcd1*, we employed biochemical enzymatic assays as well as northern analysis.

Analysis of peroxidase enzymatic activity revealed that *pcd1* leaves exhibit 12 and 10 times higher of both soluble and ionically-bound peroxidase activity, respectively, when compared to Col-0 plants (Figure 3.6). Classical secretory plant peroxidases (donor: H_2O_2 oxidoreductase, E.C. 1.11.1.7) are monomeric, heme-containing proteins that are usually glycosylated, the majority of which are believed to be localised in the cell wall or the vacuole (Welinder, 1992). Classical peroxidases have been implicated in several primary and secondary metabolic processes, including hormone catabolism (Kenten, 1955), pathogen defence (Moerschbacher, 1992), phenol oxidation (Lagrimini, 1991), cross-linking of cell wall-structural proteins and polysaccarides (Fry, 1986; Lamport, 1986), and particularly in lignin polymerisation (McDougall, 1992; Wallace & Fry, 1999). *In planta* peroxidase genes are highly redundant and most of them oxidise a wide range of substrates at the expense of H_2O_2. For example, the *Arabidopsis* genome is estimated to encode more than 40 different ER-targeted peroxidases grouped in families of high homology (Welinder *et al.*, 1996).

Although peroxidases usually function to dissipate H_2O_2, they have also been implicated in H_2O_2 generation taking place during alkalisation of the apoplast (Bowell *et al.*, 1995), which has been shown to accompany pathogen recognition (Viard *et al.*, 1994; Salzer *et al.*, 1996). Therefore, a peroxidase mechanism is probably involved in the heightened H_2O_2 levels observed in *pcd1* leaves. Moreover, isoperoxidases, arising from the transcription of different genes or from posttranslational modification, are widely distributed within both the intra-and extracellular environment (Ievinsh, 1992; Jackson & Ricardo, 1994). Therefore, whether the observed increase in pyrogallol-based peroxidase activity is attributed to posttranscriptional and posttranslational, or only posttranslational regulation remains to be determined. Furthermore, both intra- and intercellular peroxidases have been implicated in the generation of H_2O_2 through the oxidation of various compounds including certain phenols, NADPH, NADH, and indoleacetic acid (Bolwell & Wojtaszek, 1997). Therefore, determining the nature of the *in vivo* reductant for POD-catalysed generation of H_2O_2 in *pcd1* is both an interesting and challenging question.

Using northern analysis, I demonstrated that *pcd1* leaves express both *rbohA* and *GER3* at constitutive levels (Figure 3.11). In mammals, the neutrophil oxidative burst is believed to involve the reduction of molecular oxygen to O_2^- , followed by its dismutation to H_2O_2, a reaction catalysed by a plasma membrane-bound NADPH oxidase. In *Arabidopsis*, the *rbohA* gene encodes a putative 108 kD protein, with a C-terminal that shows pronounced similarity to the 69 kD apoprotein of the the $gp91^{phox}$ subunit of the neutrophil respiratory burst NADPH ocidase. Interestingly, N-terminal domain of RbohA contains two Ca^{2+}-binding EF hand motifs, which are not found in its mammalian counterpart, and has extended similarity to the human RanGTPase-activating protein 1 (Keller *et al.*, 1998). Thus, I propose that a NADPH oxidase-mediated H_2O_2-generating mechanism, similar to that found in human neutrophils, is constitutively active in *pcd1* leaves. However, a constitutively active RbohA enzyme remains to be demonstrated.

GER3 is another potential putative source of H_2O_2 whose transcript was found to be constitutively expressed in *pcd1* leaves (Figure 3.11). Three *Arabidopsis* genes (*ATGER1*, *ATGER2* and *ATGER3*) encoding germin-like proteins have previously been described (Membré *et al.*, 1997). However, no function has been described for these genes as yet. In wheat, germins have been found to possess an oxalate oxidase (oxalate:oxygen oxidoreductase, E.C. 1.2.3.4) activity, catalysing the oxidation of oxalate to CO_2 and H_2O_2 (Lane *et al.*, 1993). It is well established that certain plant pathogenic fungi secrete oxalic acid when invading plant tissues. Oxalic acid may have a number of functions in the infection process including the sequestration of Ca^{2+} and the acidification of the walls, thus facilitating the action of fungal-wall-degrading enzymes. Induction in oxalate oxidase of barley in response to fungal infection has previously been reported (Dumas *et* al., 1997). Thus, oxalate oxidase does not only degrade this potential toxin, but also directly generates H_2O_2 (Bolwell & Wojtaszek, 1997). Therefore, I propose that *GER3* might act as a third H_2O_2-generating enzyme that is constitutively activated by the *pcd1* mutation. Interestingly, *ATGER3* is subjected to circadian regulation; *ATGER3* transcripts are abundant in the evening but absent in the morning. Thus, and since Col-0 and *pcd1* tissue samples were collected in the morning, I speculate that the characteristic circadian regulation of *ATGER3* transcription is altered in *pcd1* background. However, since it was performed only once, this *ATGER3* Northern experiment will have to be reproduced with Col-0 and *pcd1* leaf tissue samples collected in both morning and evening. Moreover, assaying the oxalate oxidase activity in *pcd1* protein extracts would be a very informative experiment.

Taken together, I propose that there are at least three distinct enzymatic H_2O_2-generating mechanisms, that are constitutively active in *pcd1* leaves.

3.3.2.2 ROS detoxifying mechanisms in *pcd1*

ROS occur during normal metabolism in healthy plant cells. They are exploited by plant cells to serve several purposes including: killing pathogens, transducing and amplifying signal, and strengthening the cell wall (Levine *et* al., 1994; Baker & Orlandi, 1995). Moreover, their generation is a common feature of defence responses to challenge by microbial pathogens and elicitors (Lamb & Dixon, 1997). However, if not properly controlled, ROS may bring about irreversible destructive cellular damages including lipid peroxidation, modification or inactivation of proteins, and DNA damage leading to loss of cell viability (Adam *et al.*, 1989; Croft *et al.*, 1990).

One of the mechanisms contributing to oxidative signal-induced stress and pathogen tolerance is the activation of detoxifying and protection/defence gene expression. For example, *Arabidopsis* plants respond to oxidative stress with an increase in the production of antioxidant enzymes, including GSTs, PODs, CATs, and SODs (Baker & Orlandi, 1995). As stated before, PODs serve a dual role as they can both generate and indeed detoxify H_2O_2 to water. Interestingly, PODSs are active in the H_2O_2 - dependent polymerisation of hydroxycinnamyl alcohols (monolignols) during the final stages of lignin biosynthesis (Monties, 1989). Moreover, increases in peroxidase activity during incompatible plant-pathogen/elicitor interactions are often associated with a progressive incorporation of phenolic compounds within the cell wall and proteins (Fink *et al.*, 1991; Graham & Graham, 1991; Reimers *et al.*, 1992; Milosevic & Slusarenko, 1996; Iiyama *et al.*, 1994). Thus, cross-linking leads to strengthening of the cell wall against physical penetration by fungal pathogens and at the same time helps to dissipate H_2O_2 Therefore, I believe that one mechanism for *pcd1* plants to cope with the unusual constitutive accumulation of H_2O_2 is by increasing its POD activity. Demonstration of the peroxidase-mediated action in cell wall cross-linking in *pcd1* would be an interesting experiment.

Catalase was another enzyme whose activity was tested in *pcd1* leaves. Unexpectedly, no significant difference in CAT activity was found in *pcd1* leaves when compared to Col-0 plant (Figure3.7). This result is particularly surprising especially when I found out that the *CAT3* transcript are expressed to constitutive levels in *pcd1* plants. In *Arabidopsis*, catalases form a small multigene family that includes three genes encoding individual subunits which associate to form at least six isozymes that are readily resolved by non-denaturing gel electrophoresis (McClung, 1997). *Arabidopsis CAT3* transcripts is under tight circadian regulation; it accumulates in the late afternoon/early evening and is absent during the day (McClung, 1997). Hence, similar to the behaviour of *GER3,* I propose that the characteristic circadian regulation pattern of *CAT3* transcripts is altered in a *pcd1* background. Again, reproduction of this experiment is necessary to confirm this observation. Catalase plays a significant role in reducing high levels of H_2O_2 in peroxisomes. However, its importance as a H_2O_2-scavenger during plant-pathogen interactions is thought to be overestimated. Due to its high K_m, catalase is very inefficient at scavenging low levels of H_2O_2 produced in cells (Baker & Orlandi, 1995). Therefore, in situations such as that encountered in *pcd1*, where high levels of H_2O_2 accumulate, it is expected for catalase to play a more significant and efficient role as an H_2O_2 scavenger. Several explanations can be made for the observation that no changes in the overall CAT activity between *pcd1* and wild-type plants. Firstly, inhibition of CAT activity by SA. I demonstrated that *pcd1* accumulates high levels of the signal molecule SA and its conjugated form SAG (Figure 3.9). One of the proposed modes of action for SA, is binding and inhibiting catalase, which would then lead to an increase in the concentration of H_2O_2. This theory on SA mode of action has been further consolidated using transgenic plants deficient in catalase (Chen *et al.*, 1993; Takahishi *et al.*, 1997). However, this hypothesis is disputed as it could not be harmonised with subsequent observations that SA was required for induction of SAR proteins by H_2O_2 and that catalase inactivation had deleterious effects on plant health (reviewed in Mauch-Mani & Métraux, 1998). Therefore, catalase inhibition and the subsequent rise in H_2O_2 levels is unlikely to be the main mode of action of SA in the induction of defence responses.

Secondly, catalase inhibition might take place by other signal molecules or environmental conditions. For example, CAT inactivation has recently been reported to take place in response to light and different stress conditions that suppress protein synthesis (Schäfer & Feierabend, 2000). Moreover, O_2^- is known to inhibit CAT activity (Kono & Fridovich, 1982) and it has recently been reported that NO and $ONOO^-$ reversibly inhibit the activities of tobacco catalase and ascorbate peroxidase, the two major H_2O_2-scavenging enzymes of plant peroxisomes (Clark *et al.*, 2000). Histochemical staining of *pcd1* leaves with NBT, indicated no detectable O_2^- accumulation (data not shown). Thus, it is necessary to quantify endogenous O_2^- and NO level in *pcd1* plants, and examine the *in vitro* CAT inhibitory ability of *pcd1* crude protein extracts in order to confirm this hypothesis. Thirdly, it is plausible that activities of specific CAT isoforms are under extensive posttranslation regulation, similar to that reported for POD isoforms. Understanding of the role that different CAT isoforms play in *pcd1* would therefore be helpful in either refuting or accepting these speculations.

Glutathione (GSH), the tripeptide γ-glutamylcesteinglycine, plays a central role in protecting plants from environmental stresses, including oxidative stress due to the generation of ROS, xenobiotics, and some heavy metals (Alscher, 1989; Larson, 1988). Plants detoxify many xenobiotics and by conjugating them or their metabolites to GHS for storage or further metabolism. These reaction are catalysed by glutathione S-transferases (GSTs) (Alscher, 1989; Larson, 1988). *GST* has been reported to be a faithful marker for the oxidative stress exerted by H_2O_2 (Levine *et al.*, 1994; Grant *et al.*, 2000). Hence, *GST1* expression was examined and it was shown to be constitutive in *pcd1* leaves (Figure 3.11). Therefore, I believe that *GST1* plays an important role in ROS detoxification in *pcd1* leaves.

Taken together, it is believed that the constitutive activity and level of expression of the antioxidant components POD and *GST1* are part of a wider detoxification network that are activated in *pcd1* plants. Therefore it would be interesting to identify these other components. However, despite the activation of *GST1* expression and POD activity, the ROS level is above the antioxidant capacities in *pcd1* leaves

failing to prevent the progression of cell death. Understanding the role of PCD1 in cell death control and the establishment of SAR should help in finding some explanations to this intriguing observation.

3.3.3 SA-mediated signalling in pcd1 leaves

SA has previously been shown to increase after pathogen-induced necrosis (Ukness *et al.*, 1993) and to be required for SAR signal transduction (Gaffney *et al.*, 1993; Vernooij *et al.*, 1994). I found that *pcd1* accumulate approx. 8 and 15 times more SA and SAG, respectively, than Col-0 leaves (Figure 3.9). To investigate whether SA, ET, or JA are required for H_2O_2 accumulation and HR-like lesion formation in *pcd1*, the double mutants *pcd1::nahG*, *pcd1::coi1*, and *pcd1::etr1* were generated. Interestingly, visual examination of *pcd1::nahG* F1 progeny revealed that lesion formation and curled-leaf phenotypes were completely suppressed. Similarly, SA and SAG accumulation in *pcd1::nahG* plants was completely abolished (Figure 3.9). Moreover, H_2O_2 accumulation in these plants was also blocked. However, lesion formation, curliness and H_2O_2 accumulation was not affected in *pcd1::coi1* and *pcd1::etr1* plants F2 progeny (Figure 3.16). Hence, I conclude that PCD1 functions is in an SA-dependent pathway. Additionally, these results suggest that lesion formation and H_2O_2 accumulation occur as a result of SA accumulation. This occurs possibly through a feedback regulation of lesion formation in *pcd1* by SA or SA-dependent events. Similar behaviour has been described in some *lsd* mutants (Weymann *et al.*, 1995). This could be explained by the oxidative cell death (OCD) model in which a self-amplifying loop involving H_2O_2, SA and cell death is proposed to operate (Draper, 1997; Van Camp *et al.*, 1998; Shirasu *et al.*, 1997). In this scenario, a cycle of H_2O_2 accumulation, SA formation, and cell death, in concert with other signals such as NO and ET, contributes to the amplification of the H_2O_2 signal defence gene expression in a highly controlled manner. Hence, the removal of one of the essential components of the OCD cycle, for example, via disrupting a negative regulator of cell death, as it is the case in the *lsd1* mutant, would lead to the constitutive formation of this cycle (Kliebenstein *et al.*, 1999). This constitutive formation of the OCD cycle could then be abolished by the removal of SA, for

example via the introduction of the *nahG* gene. Examination of the SAR response and defence gene expression in *pcd1::nahG* as well as *pcd1::coi1* and *pcd1::etr1* should advance our understanding and give further insight into the role PCD1 plays in the establishment of SAR and the degree of cross-talk that might exist between SAR and for example the JA/ET-dependent pathway.

3.3.3.1 Biotic stress responses in *pcd1*

A common plant response to different abiotic and biotic stresses, such as heat, chilling, excessive light, drought, wounding, ozone exposure, UV-B irradiation, osmotic shock, and pathogens is the production of ROS (Inzé &Van Montagu; Allen, 1995; Blowell & Wojtaszek; 1997; Lamb & Dixon, 1997; Noctor & Foyer, 1998; Orozco & Ryan, 1999; Karpinski *et al.*, 1999). In many eukaryotes, the transduction of oxidative signals is controlled by protein phosphorylation involving MAPKs. MAPK and immediate upstream activators, MAPKK and MAPKKK, constitute a functionally interlinked MAPK cascade (Jonak *et al.*, 1994). Interestingly, several plant homologues of MAPK components have been identified indicating that MAPK cascades are also operational in plants. However, our knowledge as to their precise physiological functions is largely limited (Nishihama *et al.*, 1995). Elevation of MAPK activity has been detected in plants after exposure to various stimuli including ozone (Samuel *et al.*, 2000); UVB/UVA (Stratmann *et al.*, 2000); fungal elicitors (Romeis *et al.*, 1999); H_2O_2 (Grant *et al.*, 2000); and NO, SA, ET and JA (Kumar & Klessig, 2000). To this end, I detected a constitutive 46 and 48 kD MAPK activity in *pcd1* leaves (Figure 3.8). Hence, I conclude that a MAPK activity is operating in a constitutive manner in *pcd1* plants, presumably in response to H_2O_2 accumulation.

I have shown that *pcd1* plants display significantly high resistance level against the hemi-biotrophic bacterial pathogen *Pseudomonas syringae* (Figure 3.12), the biotrophic fungal pathogen *Erysiphe* (Figure 3.13) and the oomycete *Peronospora parasitica* (Figure 3.14) when compared to wild-type Col-0 plants. Resistance against these pathogens are generally believed to be conveyed via an SA-dependent

pathway. For example, the resistance level exhibited by *pcd1* plants could be mimicked by wild-type Col-0 exogenously treated by SA whereas SA-deficient *nahG* transgenics showed an enhanced disease susceptibility phenotype (Figure 3.14). Thus, SA plays a central role in conveying resistance to these biotic stresses. Recently, the isolation the *EDR1* gene of *Arabidopsis*, a MAPKK homologue, revealed that one possible function for some MAPK cascade components is to negatively regulate SA-dependent disease resistance pathways (Frye *et al.*, 2000). Accordingly, it is possible that the constitutive induction of MAPK activity in *pcd1* leaves also plays a role in the observed heightened resistance to biotic stresses. Examination of the expression level of some of these identified components in *pcd1* should contribute towards establishing the role MAPK cascade plays against biotic stresses.

3.3.4 Investigation of abiotic stress responses in pcd1

Many studies have shown that plant responses to both biotic and abiotic challenges are rather similar, which might be why plants resistant to one stress are sometimes cross-tolerant to others. Indeed, it has been shown that in some cases resistance to one type of stress brings about cross-tolerance to another (Grant *et al.*, unpublished; Park *et al.*, 2001). In this context, the enhanced resistance in *pcd1* against biotic stresses prompted us to investigate whether it is accompanied by cross-tolerance to abiotic stresses. It has been reported that the overexpression of *GST* and heat shock protein (HSP), known to be activated in response to oxidative stress, in transgenic tobacco and *Arabidopsis* has been shown enhance plant tolerance to low temperature, salt, or heat (Roxas *et al.*, 1997; Prandl *et al.*, 1998). Thus, tolerance to abiotic stresses, namely salt tolerance and abscisic acid insensitivity, was examined in *pcd1* plants. Interestingly, *pcd1* salt tolerance response, expressed as germination rate, mirrored that of wild-type Col-0 seedlings (Figure 3.15). Therefore, *pcd1* seedlings do not appear to have an enhanced tolerance when germinated on media containing high salt concentration. However, I know that the *pcd1* phenotype is suppressed in tissue culture conditions. Therefore, testing soil-grown mature plants for salt tolerance could be more informative and accurate.

It has been documented that the overexpression of a MAPKKK gene, known as *ANP* (*Arabidopsis NPK1*-like protein kinase, in which NPK is *Nicotiana* protein kinase), result in enhanced tolerance to multiple environmental stress condition including freezing, heat and salt stresses (Kovtun *et al.*, 2000). Therefore, I checked the transcription level of *ANP1* in *pcd1* plants. No hybridising signal was detected when a full length cDNA probe corresponding to the *ANP1* gene. However as no positive control was included, and the experiment was performed once, it is premature at this stage to make any conclusions. Furthermore, I envisage that the close examination of adult *pcd1* response to various abiotic stimuli, such as heat treatment, freezing, heavy metals, and ozone sensitivity, is crucial in progressing our understanding of the role of PCD1, if any, in abiotic stress tolerance.

CHAPTER IV

4 NITRIC OXIDE AND CALCIUM SIGNAL TRANSDUCTION IN *ARABIDOPSIS*

"While knowledge of $[Ca^{2+}]_{cyt}$ has gained apace, there are serious areas of ignorance. Characterisation of transduction component interaction and imaging of the spatial movement of transduction components in living cells represents the way forward and is where we predict most spectacular advances will now be made"

{A. J. Trewavas & R. Malho, 1998}.

4.1 Introduction

4.1.1 Calcium signalling in plant versus animal cells

Calcium (Ca^{2+}) is deemed to be one of the most important second messengers in many signal transduction networks in all living organisms, including animals and plants. In animal cells, Ca^{2+}-mediated signal transduction pathways have been shown to be enormously versatile and complex in the temporal and spatial organisation of the signal, as well as in the proteins that produce and intercept it (Berridge, 1993a). Equally, plants possess signal transduction networks that are highly conserved in terms of components which are also as sophisticated as that in their mammalian counterparts (Chrispeels *et al.*, 1999). In the resting (un-stimulated) state, the cytosolic free calcium concentration $[Ca^{2+}]_{cyt}$ is ~ 200nM and most of the cellular calcium is sequestered in cytoplasmic organelles such as the vacuole (100 mM), endoplasmic reticulum (ER) (1 mM), or the cell wall (1 mM) (Bush, 1995). This difference of many orders of magnitude in free Ca^{2+} concentrations between the cytoplasm and cytosolic compartments creates a large electrochemical calcium gradient (200-300 mV), across the PM, ER, and tonoplast that favours the energy-independent (downhill) movement of Ca^{2+} into the cytosol (influx). This movement is controlled by a diverse set of specialised Ca^{2+} channels and pores. Conversely, the movement of Ca^{2+} against this electrochemical gradient, from the cytoplasm into the stores (efflux), is energy-dependent, and, requires ATP or proton motive force and is provided by specialised Ca^{2+}-ATPase pumps. Both types of proteins, channels and pumps, are abundant in the plasma membrane and tonoplast and also occur in the ER, mitochondria and chloroplasts.

The channels that are responsible for Ca^{2+} influx into the cytosol are gated by either voltage, stretch, inositoltriphosphate (IP_3), cADPR or G-proteins. Calcium-mediated signalling takes place when some of these channels open, allowing Ca^{2+} to move down the electrochemical gradient (Ward *et al.*, 1995). A single channel can conduct 10^6 Ca^{2+} atoms per second; thus, $[Ca^{2+}]_{cyt}$ can increase rapidly. On the other hand,

subsequent activation of membrane-bound Ca^{2+}-ATPases (or Ca^{2+}/H^{+} exchange proteins) in the ER, vacuolar, mitochondrial, or plasma membrane ensures that most $[Ca^{2+}]_{cyt}$ signals are transients (Poovaiah & Reddy, 1993; Bush, 1995). In plants, Ca^{2+} or Ca^{2+} fluxes function in many biochemical and processes (reviewed in Malho *et al.*, 1998; Sanders *et al.*, 1999; Trewavas, 1999).

Ca^{2+} transients have been shown to take place in response to red light (Shacklock *et al.*, 1992), abscisic acid (McAinsh *et al.*, 1990), gibberellin (Bush & Jones, 1988), salinity/drought (Knight *et al.*, 1997), hypoosmotic stress (Taylor *et al.*, 1996), touch, cold (Knight *et al.*, 1991), heat shock (Gong *et al.*, 1998) and nodulation factors (Ehrhardt *et al.*, 1996). Moreover, Ca^{2+} fluxes play a pivotal role in developmental and physiological processes such as: egg cell fertilisation (Digonet *et al.*, 1997), pollen tube elongation (Pierson *et al.*, 1996), regulation of stomatal aperture (Gilroy *et al.*, 1991), circadian rhythms (Johnson *et al.*, 1995), oxidative stress (Price *et al.*, 1994; Levine *et al.*, 1996) and pathogen infection (Xu & Heath, 1998).

The ability of a plant cell to differentiate among various Ca^{2+} signals to activate the correct set of cellular responses is intriguing. Each signal creates its own Ca^{2+} fingerprint that is unique in the lag period, frequency and amplitude of the Ca^{2+} wave, and its spatial distribution. The targets of Ca^{2+} signal transduction can be divided into two categories: primary sensors and downstream substrates. Phosphorylation cascades regulated by protein kinases and phosphatases represent the primary transduction route interpreting the $[Ca^{2+}]_{cyt}$ signal. Ca^{2+}-dependent protein kinase (CDPK), Ca^{2+}/CaM-dependent protein kinase (CaM kinase) and a protein kinase C-type enzyme have all been shown to be present in plants with primary role in Ca^{2+} sensing and decoding. The ubiquitous Ca^{2+}-binding protein CaM is considered to be an essential player as a Ca^{2+} sensor or receptor and is highly conserved in all eukaryotes. When bound to Ca^{2+}, CaM activates over 100 proteins, most of which have not been characterised.

The activities of several enzymes including myosin V, kinesin, Ca^{2+}-ATPase, Ca^{2+} channels, glutamate carboxylase, NAD kinase, and a number of protein kinases are all calmodulin dependent in plant cells (reviewed in Trewavas & Malho, 1997; Trewavas & Malho, 1998).

In animal cells, NO is a well-known potent inducer of calcium transients. Recent reports have demonstrated the ability of NO or its donors sodium nitroprosside (SNP) and S-nitroso-N-acetylpenicillamine (SNAP) to elicit dose-dependent Ca^{2+} fluxes in human neutrophiles (Loitto *et al.*, 2000). In contrast, nothing whatsoever is known about the ability of NO to induce Ca^{2+} fluxes in plants. Indirect evidence for the involvement of NO in collaboration with ROS in Ca^{2+} signalling in plants was presented. Thus, ROS was reported to induce hypersensitive cell death by raising the $[Ca^{2+}]_{cyt}$ (Price *et al.*, 1994). In animals, NO was found to reduce the ROS threshold for calcium signalling via the modulation of cGMP-gated ion channels (Berridge, 1993b). This resulted in NO activation of cGMP-dependent pathway and potentiation of ROS-induced cell death (Delledonne *et al.*, 1998).

4.2 Results

4.2.1 Examining Ca^{2+} transients in response to nitric oxide

4.2.1.1 $Ca2^{+}$ transients follow a dose-dependent fashion in response to NO

The use of transgenic plants that have been transformed with the soluble, calcium-sensitive, luminescent protein aequorin has significantly contributed to the advancement of our knowledge of the signals that trigger increase in $[Ca^{2+}]_{cyt}$ levels (Knight *et al.*, 1991; Trewavas & Knight, 1994; Haley *et al.*, 1995). I have employed this approach in order to study the changes in $[Ca^{2+}]_{cyt}$ levels in response to the nitric oxide donor SNP. Transgenic two-week old *Arabidopsis* seedlings were used in all experiments. For detailed description on the experimental set-up, handling of seedlings and treatments refer to section 2.27. Increasing concentrations of SNP, between 0.1-10 mM, prepared in water, were injected via a syringe, fitted with a special needle, into the cuvette through a designated rubber-wrapped luminometer port. Luminescence counts were measured every 1 s for the duration of the experiment (generally 2 min). Previously, intracellular $[Ca^{2+}]$ could be quantified using a specific mathematical model (Chandra & Low, 1997). Alternatively, Price *et al.* (1994) have successfully used the luminescence response as a satisfactory parameter for qualitative analysis of changes in $[Ca^{2+}]_{cyt}$ in response to oxidative signals. Therefore, in this work I solely relied on the use of relative luminescence units (RLU) counts. Elevations in luminescence responses or RLU counts, hence, were interpreted as a faithful reporter of increases in $[Ca^{2+}]_{cyt}$ levels. Figure 4.1 illustrates the results obtained from the dose-response experiments between SNP and luminescent light.

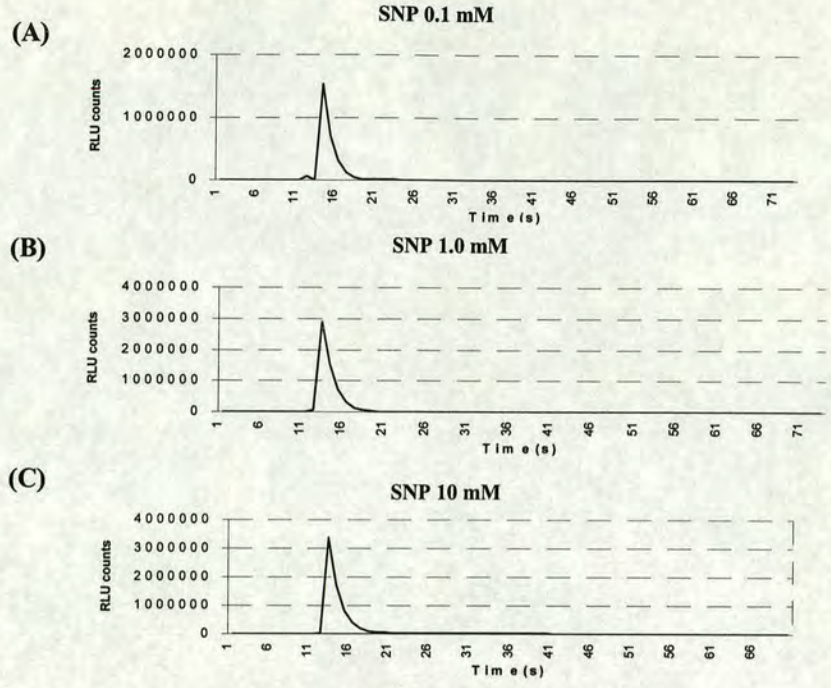

Figure 4.1: Dose dependency of the calcium transient induced by the NO donor SNP. SNP solutions were injected into the cuvette containing coelenterazine-reconstituted *35S::AEQUORIN* seedlings, floating in water, to give final concentrations of 0.1 mM (A), 1 mM (B) and 10 mM (C). Injections were normally done at approximately 12 s after the start of the measurement. Treatments were repeated at least three times with similar results.

Three independent experiments were performed and traces shown best represent the average size of response for each concentration. An instantaneous spike, with a maximum RLU value of ~ 1500000, was observed when a 0.1 mM SNP solution was injected (Figure 4.1 A). Moreover, the observed RLU counts almost doubled when the reconstituted aequorin seedlings were treated with a ten times more concentrated SNP solution (i.e. 1.0 mM) (Figure 4.1 B). Furthermore, the increase in the RLU value in response to increasing SNP concentrations was maintained, albeit to a lesser extent (only ~1/6 increase), when a solution of 10 mM SNP was administered (Figure 4.1 C). Taken together, I conclude that NO is capable of triggering an elevation in $[Ca^{2+}]_{cyt}$ that is dependent on SNP concentration. The observed dose-dependency was reproducible in several independent experiments. Irrespective of NO concentration, a single instantaneous transient spike of Ca^{2+}-dependent

luminescence was observed. Moreover, the overall increase in $[Ca^{2+}]_{cyt}$ was transient, lasting between 1 and 2 s, even though the seedlings remained immersed in the solution of SNP. Hence, I conclude that the induced increase in $[Ca^{2+}]_{cyt}$ in response to NO is subject to a rigorous control whereby the state of Ca^{2+} homeostasis within the cell is effectively recovered after the stimulating signal, i.e. NO, has been transduced. A similar pattern of changes in $[Ca^{2+}]_{cyt}$ was observed in transgenic aequorin tobacco seedlings in challenged with hydrogen peroxide (Price *et al.*, 1994). However, the average maximum spike value obtained with a 10 mM SNP solution was apparently ~500 and 60 times more than that obtained with H_2O_2 and cold shock treatments, respectively. Hence, NO is capable of triggering a much stronger elevation in $[Ca^{2+}]_{cyt}$ than either H_2O_2 or cold shock. It is, therefore, believed that the lag period length before the transient starts, the rise time to the transient peak and the decay time back to the resting level are all unique parameters to each signal (Trewavas & Malho, 1998).

4.2.1.2 SNP does not interact directly with aequorin

Aequorin is a Ca^{2+}-activated photoprotein normally produced by the marine jellyfish *Aequoria vectoria*. The protein consists of a single polypeptide chain, apoaequorin. Coelenterazine, a hydrophobic luminophore, converts apoaequorin into an active calcium-sensitive aequorin. When Ca^{2+} ions bind to this protein, the lumniphore is discharged (oxidised) and a finite amount of blue light is emitted in a dose-dependent manner (Campbell, 1983). To examine whether the observed Ca^{2+} spike is due to a direct reaction between aequorin and SNP, apoaequorin was *in vitro* reconstituted and its bioluminescence counts were integrated over 10 s upon treatment with 10 mM SNP. Typically, the reconstituted aequorin gave a luminescence value of ~150000 when treated with 25 mM $CaCl_2$, whereas a background luminescence value averaging around 30 was obtained when the reconstituted aequorin was treated with sterile water at room temperature. Moreover, when the reconstituted aequorin was treated with a 10 mM solution of SNP, luminescence values around 100 were consistently obtained. Furthermore, the 10 mM SNP solution in the absence of

aequorin gave similar values to that obtained in the presence of aequorin (i.e.100). Hence, I concluded that there is no evidence for direct interaction between SNP and aequorin.

4.2.1.3 SNP-induced $[Ca^{2+}]_{cyt}$ increase is partially contributed by PM channels

Lanthanum chloride (La^{3+}) is a well known plasma membrane channel blocker (Tester, 1990). To investigate the contribution of plasma membrane channels towards the observed elevation in $[Ca^{2+}]_{cyt}$, in response to SNP challenge, I pretreated seedlings with increasing concentrations of La^{3+} (Section 2.27). Figure 4.2 represents luminescence traces obtained upon La^{3+}-pretreated seedlings were subsequently challenged with a 1.0 mM SNP solution.

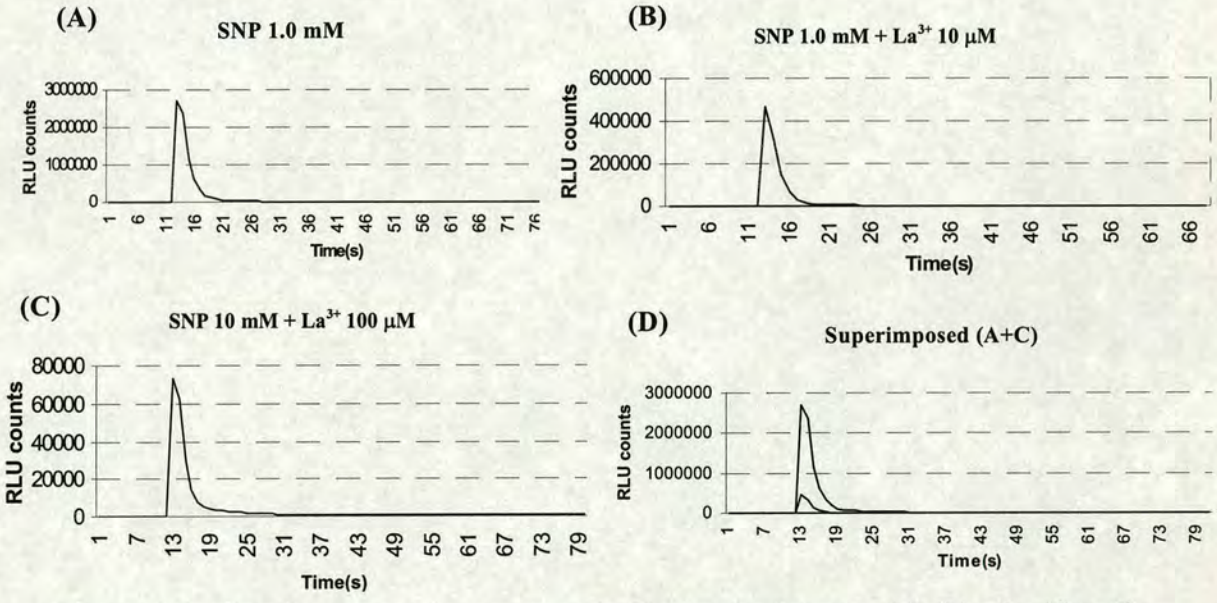

Figure 4.2: The plasma membrane channels blocker lanthanum chloride significantly diminishes the calcium transients induced by SNP. Coelenterazine-reconstituted *35S::APOAEQUORIN* seedlings, floating in the cuvette, were incubated with La^{3+} at concentrations of 10 µM (B) and 100 µM (C) for 4 hours before SNP injection. (D) is a superimposition of (A) and (C). SNP injections were normally conducted at approximately 12 s after the start of the measurement. Injections were done directly into the cuvette by means of a 1 ml syringe fitted with a needle Treatments were repeated at least three times with similar results.

A one-order-of-magnitude reduction was observed when seedlings were pretreated with a 10 µM La^{3+} (Figure 4.2 B). Moreover, a two order-of-magnitude inhibition was obtained when seedlings were treated with a ten-times more concentrated La^{3+}

solution (100 μM) (Figure 4.2 C). Therefore, the inhibition pattern observed in the magnitude of SNP-induced spike in response to La^{3+} treatment is concentration-dependent. No significant inhibitions in spike's magnitude were observed when more concentrated La solutions were tried (data not shown).

Taken together, it can be concluded that the observed elevation in $[Ca^{2+}]_{cyt}$ can partially be accounted for by a contribution from plasma membrane channels. Moreover, the observation that the inhibition in spike's magnitude is only partial suggests that there are, as yet unidentified, other sources of calcium giving rise to the observed SNP-induced increases in $[Ca^{2+}]_{cyt}$.

4.2.1.4 The SNP-induced $[Ca^{2+}]_{cyt}$ increase is NO-specific

To investigate whether the observed increase in $[Ca^{2+}]_{cyt}$ is associated with NO and not with SNP, I tested the effect of the SNP non-functional analogue potassium ferrocyanide $\{K_4Fe(CN)_6\}$, which does not release NO (Delledonne *et al.*,1998), on the induction of Ca^{2+} spikes. Potassium ferrocyanide induced only a weak spike that was three order-of-magnitude weaker than that induced by 1.0 mM SNP (Figure 4.3 A&B). Hence, I conclude that the observed increase in $[Ca^{2+}]_{cyt}$ is associated with NO that is released by SNP and not by its other degradation chemical products or components. Moreover, I have tested the effect of the NO scavenger 2-4-carboxyphenyl-4,4,5,5-tetramethylimidazoline-1-oxyl-3-oxide (C-PTIO) (Delledonne *et al.*, 1998) on the observed SNP-induced Ca^{2+} spike. A significant ~ 2 times reduction in the magnitude of the 1.0 mM SNP-induced Ca^{2+} spike was obtained when *Arabidopsis* seedlings were pre-treated with 150 μM C-PTIO (Figure 4.3 C &D). Approximately, a three-times reduction was observed when a two-times more concentrated C-PTIO solution was used (data not shown). Experiments were repeated twice with similar results. Moreover, in *in vivo* Ca^{2+} imaging experiments, infiltrating leaves of adult *Arabidopsis* plants with 1 mM SNP strongly induced a bioluminescence response. This observed bioluminescence was strongly blunted when leaves were pre-infiltrated with 150 μM C-PTIO (Figure 4.3 E&F). Leaves

infiltrated with sterile water exhibited an undetectable bioluminescent response (image not shown). Taken together, these results strongly demonstrate that the observed reduction in the magnitude of the Ca^{2+} spike correlates well with the NO-scavenging effect of C-PTIO. These data clearly present further evidence for the NO specificity of the observed elevation in $[Ca^{2+}]_{cyt}$.

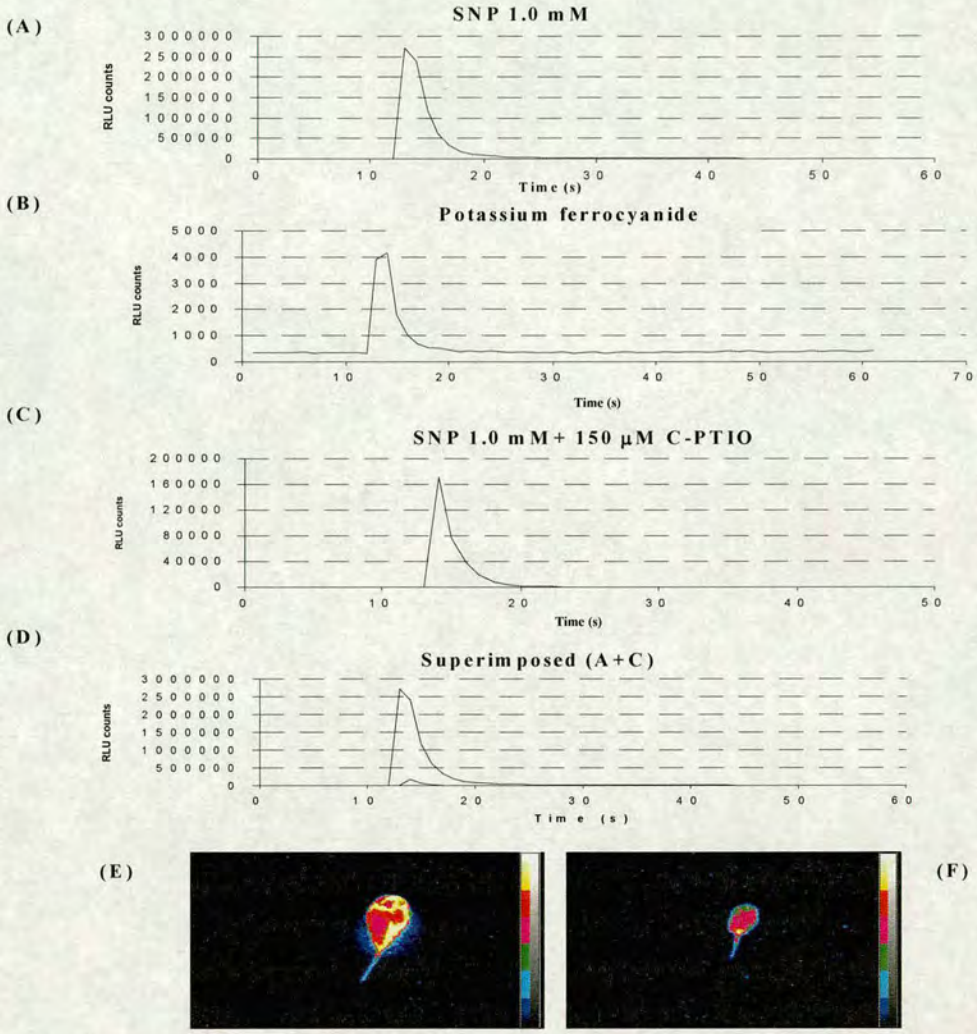

Figure 4.3: The calcium transient induced by SNP is specific to NO and is blocked by the NO scavenger C-PTIO. Potassium ferrocyanide, an SNP non-functional analogue, produces an insignificantly low calcium transient (B) when compared with the strong calcium transient induced by SNP (A). Pre-incubation of reconstituted seedlings with the NO scavenger C-PTIO (C) (significantly reduces the magnitude of SNP-induced calcium transient by at least one order of magnitude. (E) *In vivo* calcium imaging clearly confirms that the SNP induced calcium transient is specifically due to NO as C-PTIO significantly reduced the bioluminescence intensity (F). Image settings were: accumulation, 3 min; integration, 1.5 min. All images were taken within 1 min after leaf treatment.

4.2.1.5 Avirulent PstDC3000 (*AvrB*) does not induce oxidative burst-specific $[Ca^{2+}]_{cyt}$ spikes

It has previously been shown that treatment of soybean cell suspensions with an avirulent strain of *P. syringae* pv. *glycinea* (*Psg*) triggers a corresponding elevation in endogenous NO. This follows a biphasic pattern. A rapid and weak first peak in NO concentration by both virulent and avirulent *Psg* strains (after half an a hour) is followed by a stronger peak in NO concentration (~2 μM) at around 6 hrs post-inoculation (Delledonne *et al.*, 1998). Similarly, upon the plant's R-mediated successful recognition of cognate Avr protein, a burst in H_2O_2 concentration is observed at 6 hrs post-inoculation with avirulent *Psg* (Delledonne *et al.*, 1998). Moreover, in tobacco plants, hydrogen peroxide has previously been shown to trigger an instantaneous spike in $[Ca^{2+}]_{cyt}$ (Price *et al.*, 1994). In this work, I showed that the NO-releasing compound SNP is capable of triggering an instantaneous spike in $[Ca^{2+}]_{cyt}$ that is both dose-dependent and specific to NO. Therefore, I wanted to test the hypothesis whether a biphasic pattern in $[Ca^{2+}]_{cyt}$ preceeds the elevation in endogenous NO and/or H_2O_2 concentrations upon the infiltration of *Arabidopsis* leaves with *Pst*DC3000 (*AvrB*). In order to test this hypothesis, aequorin transgenic *Arabidopsis* adult plants were infiltrated with *Pst*DC3000 (A*vrB*) (OD= 0.2) via a syringe. Luminescence counts were scored every 5 s over a period of at least 3 hrs. A weak spike in $[Ca^{2+}]_{cyt}$ (~ 180 nM) was observed at around 30 min post-inoculation. No other spikes were detected over a ~3 hrs period (Figure 4.4 A). A similar response pattern was obtained in an compatible interaction where *Arabidopsis* leaves were inoculated with *Pst*DC3000 (OD= 0.2) (figure not shown). Each experiment was repeated at least three times with similar results. These results obtained with both compatible and incompatible interactions were additionally confirmed via *in vivo* calcium-dependent aequorin luminescence imaging. In time-course experiments, conducted with reconstituted transgenic aequorin plants treated with either virulent or avirulent bacterial strains, similar response was obtained. Both treatments gave rise to an early calcium-related bioluminescence at around 30 min post-inoculation.

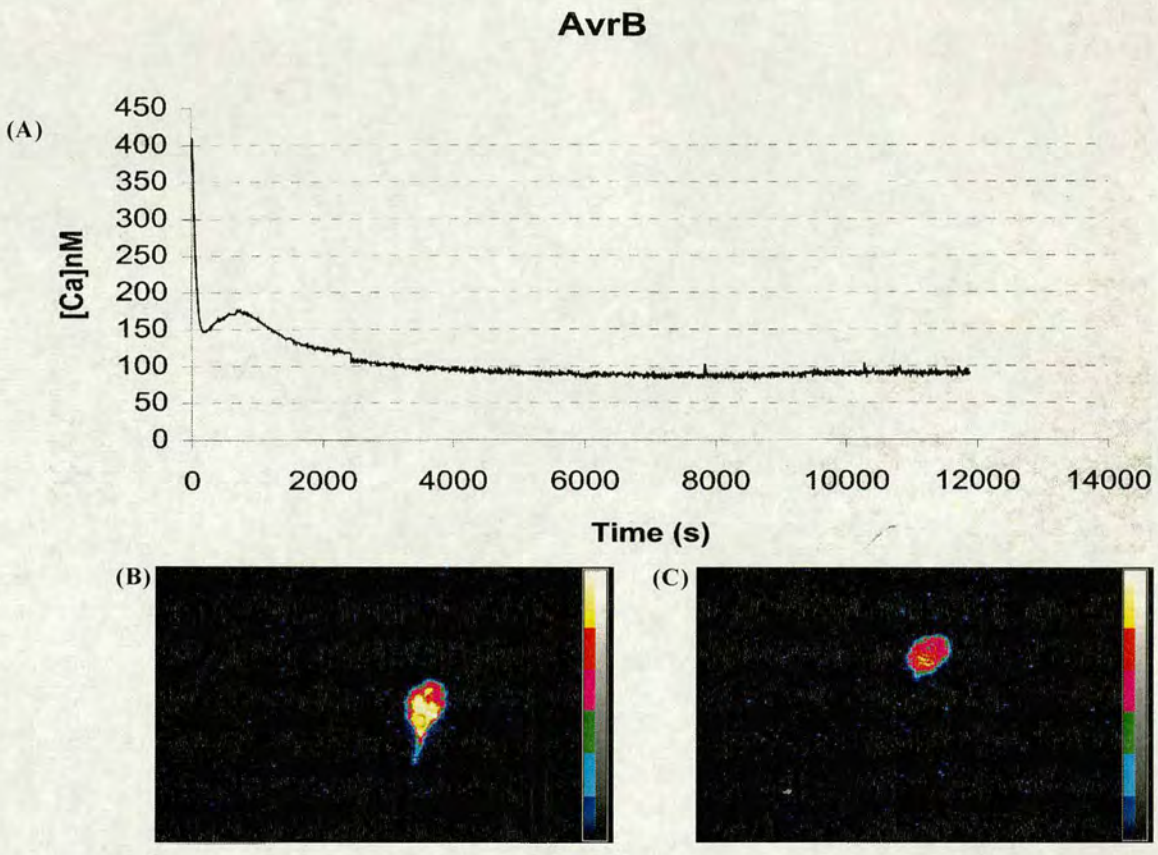

Figure 4.4: Elevation in cytosolic calcium concentration in response to challenge by avirulent bacteria. (A) The avirulent strain *Pst*DC3000 (*AvrB*) induces an immediate single strong calcium transient (monophasic). The strong luminescence produced as a result of *Pst*DC3000 (*AvrB*) inoculation (B) is blocked when leaves were pre-infiltrated with La^{3+} μM (C). In (A), leaves of four-week old coelenterazine-reconstituted *35S::AEQUORIN* plants infiltrated with *Pst*DC3000 (*AvrB*) were detached, placed in cuvettes. Then, cuvettes containing the detached leaves were put into the chemiluminometer's chamber and the RLU counts measurement began. In (B)&(C), treated leaves were detached, placed into a dark box and imaged by a low-light camera.

Figure 4.4 B shows a typical image depicting elevation in bioluminescence intensity taken 30 min post-inoculation with the avirulent *Pst*DC3000 (*AvrB*) strain. This observed strong bioluminescent intensity could be significantly blunted by La^{3+} (Figure 4.4 C). Therefore, the observed AvrB-mediated elevation in biolumiescence intensity is mediated by plasma membrane Ca^{2+} channels. Infiltration of aequorin

reconstituted leaves with $MgCl_2$ buffer resulted in no significant bioluminescence (data not shown). No other biolumenescent signal was detected in either incompatible or compatible interaction over a period of 8 hrs (images not shown).

4.2.1.6 $_L$-Arginine triggers an immediate $[Ca^{2+}]_{cyt}$ spike

In vertebrates, NO biosynthesis is believed to be accomplished by the enzymatic conversion of $_L$-arginine to $_L$-citrulline mediated by the action of nitric oxide synthase (NOS) (Nathan & Xie, 1994). By analogy, despite that fact that a plant *NOS* has not been isolated yet, both NOS -like activity and NO accumulation, based on the formation of $_L$-citrulline from $_L$-arginine and/or sensitivity to mammalian NOS inhibitors, has been reported in different plant species (reviewed in Wendehenne *et al.*, 2001). Moreover, using soybean cell suspensions, cytosolic NOS-like activity has been previously reported to be strictly dependent on the elevation in free calcium concentration (Delledonne *et al.*, 1998). Therefore, I tested whether $_L$-arginine uptake would triger a spike in $[Ca^{2+}]_{cyt}$. As predicted, 10 mM $_L$-arginine triggered a strong spike in $[Ca^{2+}]_{cyt}$ (Figure 4.5 A). The magnitude of the observed Ca^{2+} spike was on average equal to that induced by 10 mM SNP. Moreover, $_L$-arginine capability of inducing a strong Ca^{2+} spike was confirmed in *in vivo* Ca^{2+}-dependent aequorin bioluminescence imaging (Figure 4.5 B). However, in time-course luminometer or *in vivo* Ca^{2+} experiments, no other spikes or bioluminescence were detected over a period of 8 hrs, respectively (data not shown).

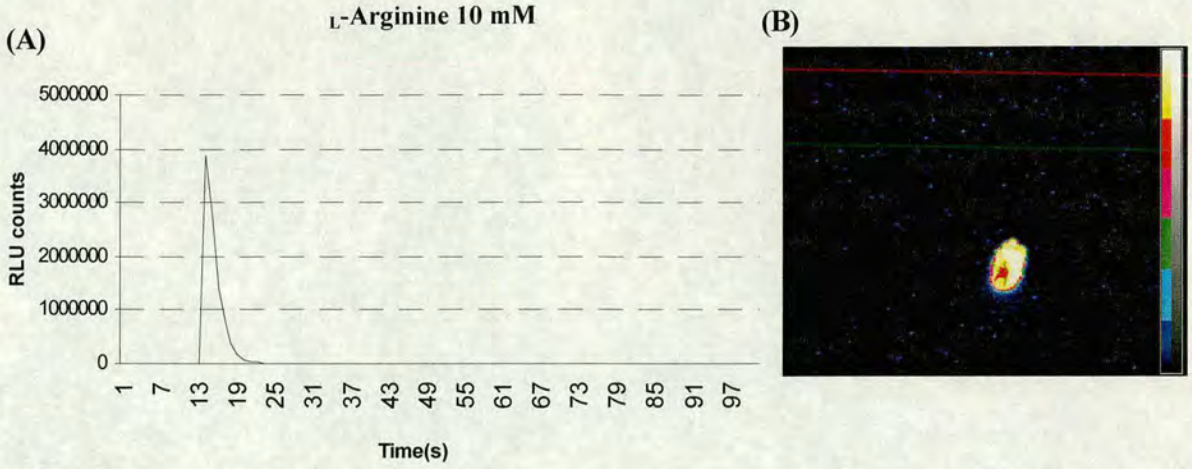

Figure 4.5: L-Arginine is potent inducer of cytosolic calcium spikes. L-Arginine induced an immediate strong calcium transient as reported by chemiluminometer (A) and *in vivo* imaging assays (B). In (A), coelenterazine-reconstituted two-week old *35S::AEQUORIN* seedlings, floating in water in the cuvette, were treated with 10 mM L-arginine by direct injection into the cuvette, via a 1 ml syringe fitted with a needle. In (B), leaves of reconstitued four-week old *35S::AEQUORIN* plants were infiltrated with 10 mM L-arginine, detached and imaged by a low-light camera.

4.2.1.7 Measurement of NO emissions using a photoacoustic CO-based laser spectroscopy

As previously stated, endogenous NO generation has been reported in intact plant and cell systems following gene-for-gene resistance during incompatible interactions (Delledonne *et al.*, 1998, Durner *et al.*, 1998). NO is a highly reactive lipophilic gaseous radical molecule that is soluble in water (1.6 mM at 37°C) but does not react with it. Moreover, it diffuses readily across cell membranes and through the cytoplasm (Poole & Hughes, 2000). Therefore, in this respect, due to its low molecular weight it can readily be transpired like many other gases (e.g. CO_2, O_2) and phytohormones (e.g. Me-JA, ET). Accordingly, I speculate that NO is transpired in minute concentrations during incompatible interactions from challenged plant tissues. Hence, once in the air, NO can serve many physiological roles including inducing defence responses in nearby plants.

In collaboration with Luc-Jan Laarhoven (Trace gas facility, Molecular & Laser physics department, University of Nijmegen), I conducted several experiments employing the power of photoacoustic laser spectroscopy for the quantification of NO emissions. The theoretical basis of this novel approach is based on the "photoacoustic effect". The photoacoustic effect is based on the generation of acoustic waves as a consequence of light absorption (Figure 4.6 A). Absorption of an infrared photon excites a molecule into higher rotational-vibrational state. The resulting molecular collisions transfer the rotational-vibrational energy to translational energy mainly in the form of heat. Modulation of the light intensity, via a chopper, results in periodic variations in temperature. This change in temperature is translated into a pressure variation which creates a sound wave. Then, the sound wave, generated in the closed space of a photoacoustic cell, is detected by a sensitive microphone generating a signal (Harren *et al.*, 1986; Bicanic *et al.*, 1989) (Figure 4.6 B). A liquid nitrogen cooled photoacoustic CO-based laser was employed to quantify NO emissions (Figure 4.6 C) (Bijnen *et al.*, 1992).

(A)

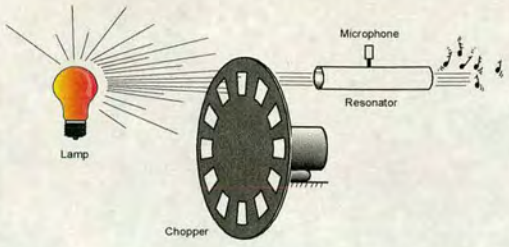

(B)

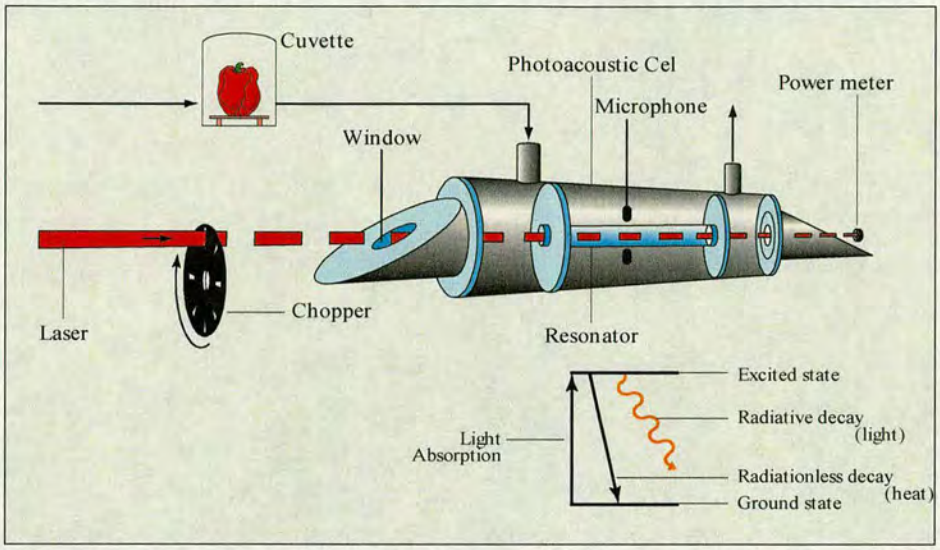

(C)

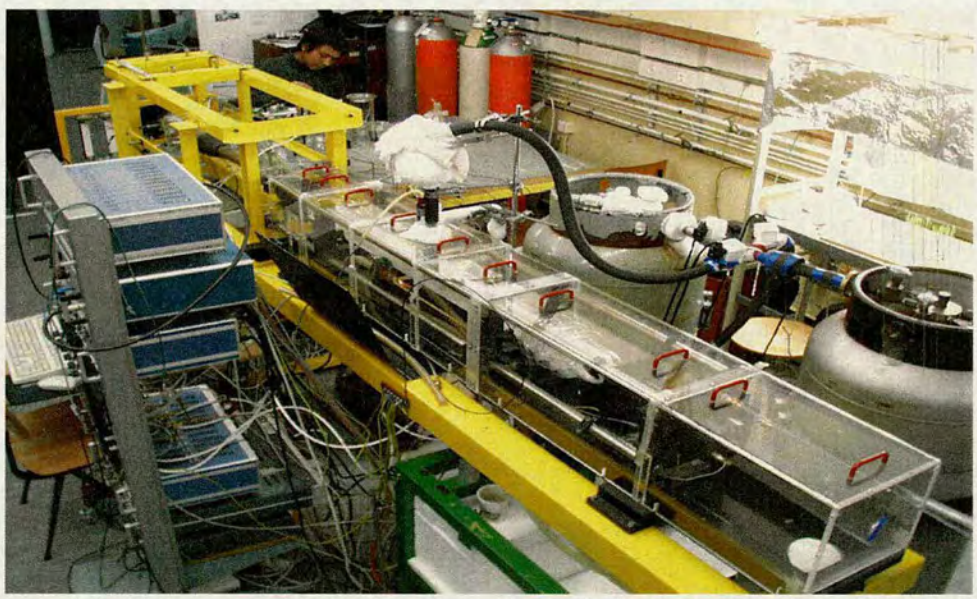

Figure 4.6: Photoacoustic spectroscopy. An artistic representation of the theoretical basis of the photoacoustic technique (A)&(B). Absorption of an infrared photon excites molecules into higher states. Upon relaxation energy is given off in the form of heat. By means of a chopper the light intensity is modulated resulting in temperature variation accompanied by variation in pressure. This pressure variation creates a sound that is detected by a sensitive microphone. (C) The full-scale photoacoustic CO laser employed for the detection of NO evolution.

In order to validate and optimise the photoacoustic laser machine for detecting NO emissions, an optimisation experiment using the NO-releasing agent SNP was undertaken. I utilised the property of SNP solutions to release NO in a pH dependent manner (the greatest quantity being released at pH 5.0 with decreasing amounts of NO released up to pH 7.4) (Gryglewski *et al.*, 1989). Figure 4.7 summarises the findings of this experiment.

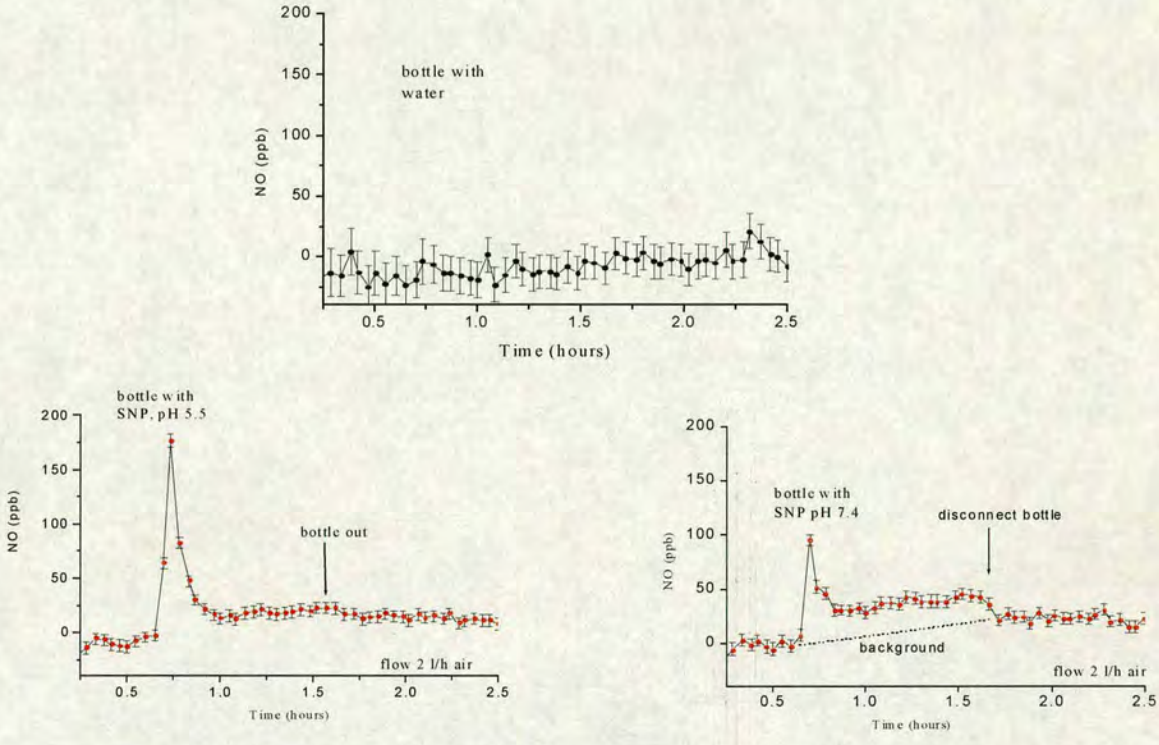

Figure 4.7: Measurement of pH-dependent NO evolution from SNP by photoacoustic CO-laser spectroscopy. SNP 1 mM was prepared in water whose pH was pre-adjusted to 5.5 and 7.4. The required pH of water was obtained using a 1 N solution of either HCl or NaOH. The bottles were sealed and left for 1 hr to allow for NO accumulation. Then, NO detection was started by allowing the carrier gas, composed of O_2, N_2, H_2, and CO (1:1:1:1), to flush the headspace. As a control, a bottle with water only under the same conditions was included. NO concentration is expressed as parts per billion (ppb).

Before I started the experiment, the laser machine was calibrated with 1 ppm pure NO gas, provided in commercially-available cylinders. NO emissions were recorded over a period of 2.5 hrs. Indeed as predicted, the CO photoacoustic laser could detect emissions of NO whose magnitude was pH dependent. At an acidic pH (~5.0), a strong spike in NO concentration was detected around ~175 ppb.

Conversely, at a neutral pH (~7.4), a 40% reduction in the concentration of released NO was observed. In the negative control bottle (i.e. containing sterile water only), no NO signal above the background was detected.

These results are in agreement with the pH dependent NO release known for SNP. Moreover, the calculated detection limit for NO was as low as 50 parts per billion (ppb). Therefore, the maximum concentration NO reported to be generated during incompatible interactions 6 hrs post-infiltration represents a 1200 times (2 μM = 60000 ppb) more than the calculated detection limit of the photoacoustic laser machine. Hence, with ability to integrate 100 measurements per μs, the use of this technology for detection of NO emissions from plants during incompatible interactions should be reliable and accurate.

The second experiment attempted was the detection of NO emissions released by *Arabidopsis* adult plants upon challenge by an avirulent as compared to virulent bacterial pathogen. The experimental set-up of this experiment is shown in Figure 4.8.

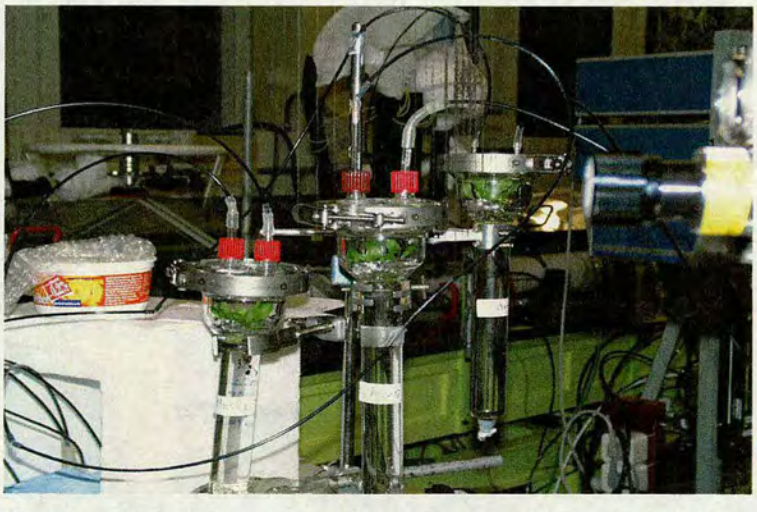

Figure 4.8: Experimental set up for the measurement of NO evolution from *Arabidopsis* plants during virulent and avirulent interactions by photoacoustic CO laser spectroscopy. Five-weeks old *Arabidopsis* plants were infiltrated with: 10 mM MgCl2 (as a negative control), avirulent *Pst*DC3000 (OD600=0.2) and virulent *Pst*DC3000 (OD600=0.0002).

As soon as plants where infiltrated by $MgCl_2$ buffer, *Pst*DC3000 or *Pst*DC3000(*avrB*), they were put in sealed cuvettes, one plant per cuvette, and NO monitoring begun. Emissions were monitored over a period of at least 6 hrs. Under this experimental set up, I failed to detect any NO from either avirulent or virulent bacteria-treated plants. Due to time limitation, I could not repeat this experiment. Similarly, in another experiment, I attempted to monitor NOS-based generation of NO upon treatment with 10 mM $_L$-arginine. Again, I was not able to detect any NO emissions (Figure 4.9).

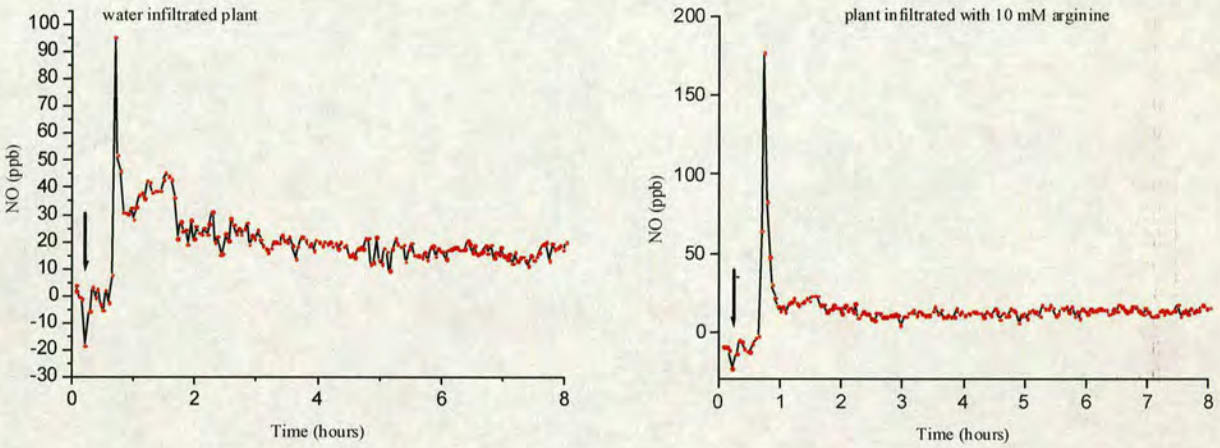

Figure 4.9: Measurement of NO evolution from *Arabidopsis* plants infiltrated with 10 mM $_L$-arginine. The infiltration was carried out on leaves of four-week old Col-0 wild-type plants by means of a 1 ml syringe. Arrows denote the start of measurement. Peaks around half an hour from the start of the measurement are due to an accidental unnoticed cuvette leakage. Experiment was repeated twice with similar results.

Several explanations are possible for the observed failure to detect NO in these experiments. Firstly, under this experimental set up, the actual NO concentrations released by plants are much lower than the detection limit (i.e.<50 ppb). In this context, it is worth noting that NO is a highly reactive radical with a theoretical life time of about 30 min, if it were oxidised to NO_2, when generated in a cellular environment at about 10^{-7} M (Poole &Hughes, 2000). But in practice, its lifetime is thought to be as low as 1 s. This could be explained by its rapid reactivity with a variety of targets (e.g. guanyl cyclase, thiols, superoxide ion) (Poole &Hughes,

2000). For example, the rate constant values k for NO reaction with O_2 and O_2^- are $1.2 \times 10^3 \times 10^{(230/T)}$ and $(2.0 \pm 0.4) \times 10^{10}$ $M^{-1}.s^{-1}$, respectively (Tsukahara *et al.*, 1999; Nauser & Koppenol, 2002). Therefore, this evidence might explain why NO could not be detected, as only a fraction of NO gas, not high enough to be detected by the laser spectroscopic machine, of what is actually produced within the cell is transpired into air. Experimental evidence still to be produced to support this speculation. Secondly, it is also possible that the big headspace in the cuvettes used causes significant dilutions to any released NO gas; hence it can not be detected. Therefore, more time is required to design suitable cuvettes with smaller headspaces to allow the detection of NO released by plants.

4.2.2 Overexpression of HMP/NOD bacterial gene in Arabidopsis

The second objective of this work was to generate transgenic lines that are compromised in their NO signal transduction pathway. In this context, the *E. coli* haemoprotein (*HMP*) gene was chosen to achieve our objective. The *HMP* gene has previously been shown to exhibit a dihydropteridine reductase (DHPR) activities (Vasudevan *et al.*, 1991). Moreover, this ubiquitous enzyme has recently been reported to possess a novel nitric oxide dioxygenase (NOD) activity. HMP/NOD has also been documented to exhibit NO-consuming activity, converting NO to NO^-_3, that is O_2-dependent, cyanide-sensitive and aconitase-protective (Gardner *et al.*, 1998a; Gardner *et al.*, 1998b).Therefore, I chose *HMP/NOD* as a candidate for my overexpression studies. The following sections present the results of these experiments.

4.2.2.1 ***In silico analysis of the HMP/NOD gene***

To express a bacterial (prokaryotic) gene into eukaryotic cells several considerations needed to be taken into account. Thus, before I embarked on the overexpression of *HMP/NOD* gene, it was of paramount importance to undertake computer analyses performed on the gene and its protein product. A genomic fragment containing two

open reading frames (ORF) of the *hmp* and *glnA* genes subcloned into the pALTER plasmid was donated by P. Gardner (University of Cincinnati, USA). Using the GENSCAN software, developed by Chris Burge (Stanford University; http://genes.mit.edu.GENSCAN.html), I scanned the bacterial genomic fragment sequence for any possible ORFs. In agreement with the composition of the bacterial genomic fragment, the output indicated the presence of two major ORFs that are transcribed in opposite orientations (Figure 4. 10).

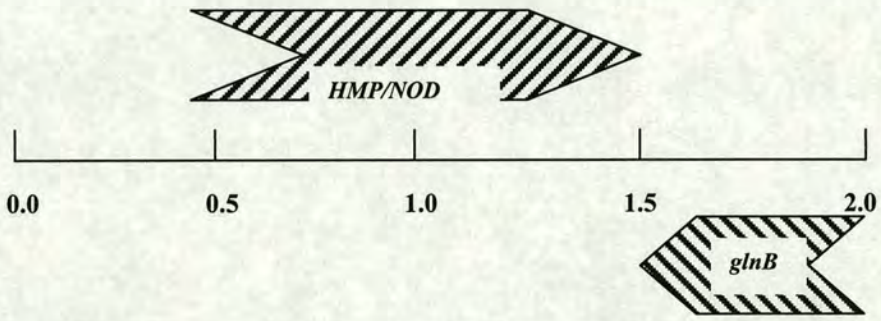

Figure 4.10: Output of GENSCAN analysis performed on *HMP/NOD* genomic fragment. Two major ORFs, in opposite orientations, are predicted within the 2.0 kb fragment. The *HMP/NOD* ORF (0.5-1.5 kb) has been associated with NOD activity in *E. coli.*

Moreover, I employed the NetGene2 software (provided by the Centre for Biological Sequence Analysis; http://www.cbs.dtu.dk), to scan the *HMP/NOD* gene sequence for any possible splicing sites with *Arabidopsis* codon system as a reference. The search output indicated that there is no functional splicing sites within the *HMP/NOD* gene. Furthermore, a manual comparison between *E. coli* and *Arabidopsis* codon usage lists indicated that there is no apparent discrepancies in codon usage for transcribing the *HMP/NOD* gene between the two systems. Hence, no codon usage optimisation was found necessary to undertake on the *HMP/NOD* gene sequence. Taken together, these results predict a faithful transcription of the bacterial *HMP/NOD* gene in *Arabidopsis.*

4.2.2.2 Phenotypic and molecular characterisation of *35S::HMP/NOD* transgenic lines

A promoterless *HMP/NOD* gene was cloned under the control of the CaMV 35S constitutive promoter followed by the termination and polyadenylation sequences from *ocs3'* in pART7 vector. Then, a *Not* I fragment containing the 35S-*HMP/NOD*-*ocs3'* transcriptional unit was subsequently subcloned into the transformation binary vector pGREEN containing the *bar* gene for selection of *bona fide* transformants on soil. A schematic representation of the transformation cassette used for *Agrobacterium*-mediated floral dip is shown in Figure 4.11.

Figure 4.11: The transformation cassette employed in generation of *Arabidopsis* transgenic lines overexpressing the bacterial *HMP/NOD* gene. Abreviations: RB. Right border; *P35S*, CaMV 35S constitutive promoter; *NOD*; promoterless *E. coli* nitric oxide dioxygenase gene; *Tocs3'*, *Agrobacterium* octopine synthase terminator sequence; *Pnos*; *Agrobacterium* nopaline synthase promoter sequence; *Bar*, Basta resistance gene; *Tnos*, *Agrobacterium* nopaline synthase terminator sequence.

The transformation was performed on both Col-0 wild-type and *35S::APOAEQUORIN* transgenic backgrounds to allow for investigation of changes in $[Ca^{2+}]_{cyt}$ in an NO-deficient background (i.e. *35S::HMP/NOD* background). *Bona fide* T1 transformants were selected by Basta spraying. Leaf PCR analysis was subsequently performed on selected *35S::HMP/NOD* transgenic lines to confirm the presence of the *HMP*/NOD gene. All tested lines tested positive for *HMP/NOD* gene as can be seen from the PCR-amplified product corresponding to the correct size of the gene (~1.2 kb). Samples from Col-0 leaves and aliquots from the pALTER(*HMP*) were used as negative and positive control, respectively (Figure 4.12 A).

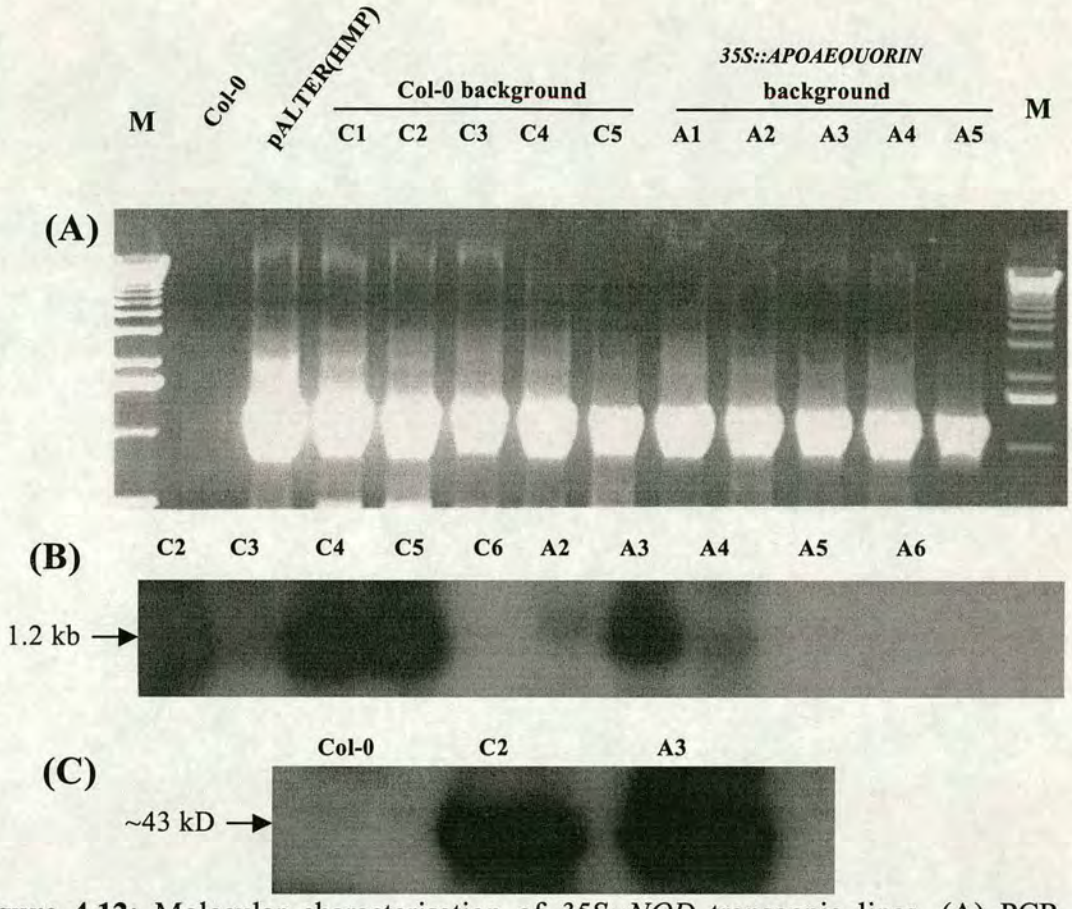

Figure 4.12: Molecular characterisation of *35S::NOD* transgenic lines. (A) PCR analysis performed on T1 transgenic lines to confirm the presence of the HMP gene. All lines tested positive for the 1.2 kb HMP gene. (B) Northern analysis of T1 transgenics using a full-length HMP DNA as a probe. (C) Western analysis of T1 transgenics. Out of 12 tested lines, only line C2 and C3 showed overexpression of the HMP protein at the expected molecular weight. Polyclonal anti-rabbit antibodies raised against HMP were used for the detection of HMP.

Moreover, northern analysis was performed on the selected *bona fide* transformants using the full-length promotorless *HMP/NOD* gene fragment as a probe. Transgenic lines C2, C4, C5, and A3 displayed a strong signal that corresponded well to the expected correct size for the *HMP/NOD* mRNA (Figure 4.14 B). Furthermore, these lines were tested for the expression of HMP/NOD protein via western analysis using a polyclonal anti-rabbit antibodies raised against HMP. Out of ten tested lines, only two (i.e. C2 & A3) lines displayed a signal at about 43 kD (the expected size of HMP) that was absent from Col-0 wild-type plants (Figure 4.14 C). I , therefore, based on the molecular evidence presented in Figure 4.14, selected lines C2 and A3 for further analysis.

In sobean cell suspensions, measurement of endogenous NO burst during incompatible interactions was undertaken using a haemoglobin-based assay (Delledonne *et al.*, 1998). The technique is based on the conversion of oxyhaemoglobin to methaemoglobin (Murphy & Noack, 1994). I wanted to test the changes in endogenous NO concentration in the selected *35S::HMP/NOD* lines C2 and A3 during incompatible interactions using this approach. But first, I embarked on a series of optimisation experiments using the NO-donor SNP. Oxyhaemoglobin was prepared as described by Murphy & Noack (1994). Increasing concentrations of SNP were added to oxyhaemoglobin (final concentration 5 μM), mixed and then incubated for 2 min. Then, the NO concentration in mM was calculated by measuring the shift in absorbance of the solution at 421 nm and 401 nm using the following formula: $C = \varepsilon (A_{401}-A_{421})$, where C is the NO concentration in mM; ε is the extinction coefficient for NO which 77 $mM^{-1}.cm^{-1}$. However, to my surprise, no apparent change in A_{401} and A_{421} was observed. Further investigation into the matter revealed that this shift in absorbance is so small that it requires a specialised diode-array dual-wavelength spectrophotometer in order to pick it up (Massimo Delledonne, personal communication; Murphy & Noack, 1994). Therefore, due to the non-availability of such a spectrophotometer, I could not optimise the assay and hence the NO burst responses in lines C2 and A3 could not be tested. Alternative approaches are currently being sought.

Due to the fact that HMP contains heme- and flavin-binding domains, the protein heme and FAD contents have previously been used as an indication of the correct folding and activity of the HMP/NOD (Gardner *et al.*, 1998a). Therefore, I attempted to use the same strategy on *35S::HMP/NOD* lines C2 and A3 protein extracts. As an indication of HMP heme contents, absorption of C2 and A3 lines protein extracts at λ_{427} nm and λ_{550} nm was examined compared to that of Col-0 wild-type. Interestingly, protein extracts of C2 ($A_{427} = 0.025$; $A_{550} = 0.049$) and A3 ($A_{470} = 0.016$, $A_{550} = 0.034$) lines exhibited relatively higher absorption values, at λ_{427} nm and λ_{550} nm, compared to Col-0 protein extract. Therefore, based on this biochemical evidence, I conclude that protein extracts from A2 and C3 lines appear to express high amounts of properly-folded and probably active HMP. Further biochemical

evidence, however, is required to confirm beyond doubt that the expressed HMP protein is active. Polarographic approach has previously been employed by Gardner *et al.* (1998a) in an NO consumption assay using a selective NO microelectrode. However, due to limited financial resources I could not employ this approach.

4.2.2.3 Examination of bacterial resistance response of selected *35S::HMP/NOD* lines

In *Arabidopsis*, it has previously been shown, using a selection of NOS inhibitors, that NO play a central role in plant disease resistance in plants (Delledonne *et al.*, 1998). Therefore, my next experiment was to examine disease resistance responses of the selected *35S::HMP/NOD* C2 and A3 lines towards the virulent bacterial pathogen *Pst*DC3000. Figure 4.13 displays the results obtained in this experiment. As the *35S::HMP/NOD* C2 exhibited higher heme contents (according to the spectrophotometric data), I chose it for this experiment.

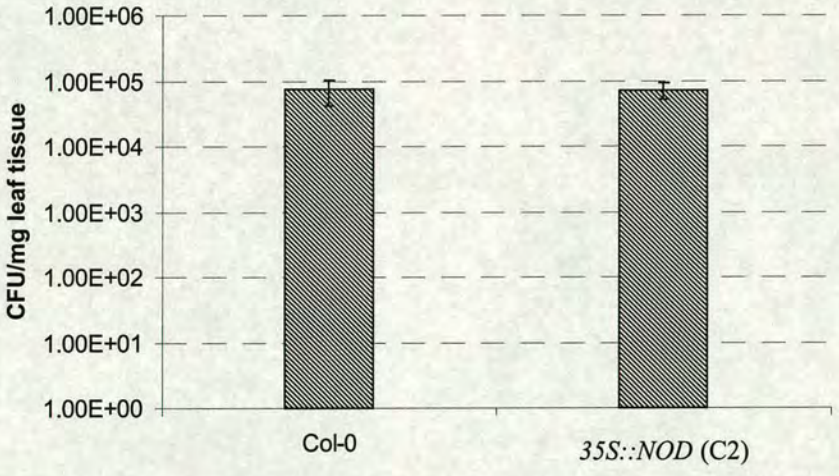

Figure 4.13: Growth of the virulent bacterial pathogen *Pst*DC3000 in selected *35S::NOD* transgenic line as compared to Col-0 wild-type. Leaves were infiltrated with a bacterial suspension (OD600=0.0002). Samples were collected and bacterial number scored at three days post-inoculation. The experiment was repeated three times with similar results. Error bars represent the standard deviation on the mean (n= 3).

Interestingly, no significant difference, with regard to endogenous virulent bacterial growth, between Col-0 wild-type and C2 plants at day 3 post-inoculation. The experiment was repeated three times with similar results. Several explanations for this observation are possible. Firstly, the overexpression level of the HMP/NOD protein is not enough to consume all NO that is being produced; resulting in a wild-type response in C2 transgenic lines. Secondly, the HMP/NOD protein is expressed to high enough levels but there is an alternative NO-generating system that is compensating for the NO deficiency caused by HMP/NOD activity. Thirdly, despite the fact that HMP/NOD protein is fully-expressed and properly-folded it is not 100% active. However, further experiments are still required to critically investigate each of the above mentioned assumptions. Moreover, more *35S::HMP/NOD* candidates need to be tested to assist in our investigation.

4.3 Discussion

4.3.1 Advantages of the aequorin system

As previously stated in the introduction (Section 4.1.1), Ca^{2+} is strongly believed to serve as a second messenger in several vitally important physiological processes in plants. Nevertheless, its accurate quantitation during cellular signalling events has until recently proven very difficult (Chandra & Low, 1997). In the $^{45}Ca^{2+}$ method, $^{45}Ca^{2+}$ binds avidly to cell walls, often masking the small changes in cytoplasmic $^{45}Ca^{2+}$ that could indicate its function as a second messenger. Moreover, signal transduction pathways that might trigger release of Ca^{2+} from internal cellular organelles are largely invisible to $^{45}Ca^{2+}$-based methodologies, because no net change in cellular $^{45}Ca^{2+}$ occurs (Demarty *et al.*, 1984). Furthermore, although methodologies based on the use of Ca^{2+}-sensitive fluorescent dyes have yielded useful information in a few plant systems, their general resistance to entry into plant cells has greatly limited their application (Bush & Jones, 1990). Indeed, most membrane-permeant esters of Ca^{2+}-dependent fluorophores hydrolyse to their impermeant forms in the cell wall, preventing their penetration to their intracellular destinations (Chandra & Low, 1995).

With the advent of molecular biology and plant transformation, studies of the molecular basis of the bioluminescence of jelly fish have yielded two proteins aequorin and GFP, showing their great potential in replacing many of the laborious and technically difficult fluorescent dye techniques (Gilroy, 1997). To this end, Knight *et al.* (1991), introduced, for the first time, the use of tobacco plants transformed with a calcium-sensitive protein termed aequorin; they demonstrated that stimulus-induced Ca^{2+} increases generated readily measurable levels of bioluminescence. Thus, aequorin technology allows the noninvasive visualisation of calcium dynamics and signalling event in living cells, functioning tissues, organs, and even whole plants. Transgenic aequorin has been successfully expressed in various cellular organells and compartments including the cytosol, nucleus, mitochondria, chloroplast, endoplastic reticulum, tonoplast, and plasma membrane

(Reviewed in Gilroy, 1997). Moreover, because the intensity of light emitted by aequorin is directly proportional to Ca^{2+} concentration, measurement of aequorin-derived biolulminescence enables direct quantitation of Ca^{2+} transients in the transformed cytoplasm of the cell (Chandra & Low, 1997). Thus, in contrast to the more conventional use of $^{45}Ca^{2+}$ and/or Ca^{2+}-sensitive fluorophores, the aequorin methodology is not toxic to the plant, allows for the collection of quantitative data at short (0.1 s) time intervals, thereby permitting accurate evaluation of the kinetics of a Ca^{2+} transient, and permits localisation of the Ca^{2+}-sensitive protein in desired internal organelles by use of organelle targeting sequences (Chandra *et al.*, 1997). Furthermore, due to its simplicity, aequorin technology has facilitated the measurement of the kinetics of $[Ca^{2+}]_{cyt}$ transients induction in response to some ten signals (Reviewed in Trewavas & Malho, 1998).

4.3.2 Examination of nitric oxide-mediated calcium signalling

In this work, I employed aequorin-transformed *Arabidopsis* plants to examine the involvement of Ca^{2+} in NO signal transduction and during avirulent pathogen interactions. Several chemical compounds have previously been reported to act as donor for NO. These include S-nitrosothiols (e.g. SNAP) and nitroprussides (e.g. SNP). The SNP anion $[Fe(CN)_5(NO)]^{2-}$, with an NO^+ nitrosyl group, is an effective nitrosating agent to S and N nucleophiles at neutral pH values. The product may then decompose to release NO and oxidised thiol RS, where R represents alkyl group (e.g. protein) (Poole & Hughes, 2000). Thus, SNP has been previously used as a potential NO donor to study NO-mediated signalling in mammalian and plant systems (Delledonne *et al.*, 1998; Durner *et al.*, 1998; Loitto *et al.*, 2000).

In this work, I demonstrated that NO is capable of triggering a strong monophasic Ca^{2+} pulse in a dose-dependent manner (Figure 4.1). Interestingly, the average amplitude of the bioluminescent signal exceeded that produced in response to both cold shock and hydrogen peroxide treatments. Precisely, the average amplitude of the calcium spike obtained upon treatment with 10 mM SNP was approximately 500 and

60 times greater than that observed upon either H_2O_2 or cold shock treatments, respectively (Price *et al.*, 1994). However, despite being different in amplitude, the patterns of the induced $[Ca^{2+}]_{cyt}$, in response to H_2O_2, cold shock and NO, are similar in that they are all monophasic. Conversely, it has previously been reported that hypo-osmotic shock induces a distinctively different elevation in $[Ca^{2+}]_{cyt}$, that is biphasic (Cessna *et al.*, 1998). Moreover, the observed $[Ca^{2+}]_{cyt}$ spike in response to NO challenge was similar to that obtained upon cold shock treatment, in the fact that it was instantaneous, with no apparent lag period (Figure 4.1). The reported $[Ca^{2+}]_{cyt}$ spike obtained upon H_2O_2 treatment has been shown to follow a definite lag period of 20-40 s lasting between 1-2 min (Price *et al.*, 1994). Furthermore, the decay time in the NO-induced luminescent signal was comparable with a shorter transient signal lasting only between 3-5 s. Taken together, I envisage that this apparent qualitative and quantitative differences in $[Ca^{2+}]_{cyt}$ dynamics, between different stimuli, underline the uniqueness of each $[Ca^{2+}]_{cyt}$ transient in transducing a distinct signal. This observation conforms to the general belief that the lag period length before the transient starts, the rise time to the transient peak and the decay time back to the resting level are all unique parameters to each Ca^{2+} signal (Trewavas & Malho, 1998).

As the NO-donor, SNP, was used in these experiments, it was conceivable that the observed luminescence emission was not brought about by NO but rather via a direct chemical modification of aequorin by SNP or one of its by-products. To evaluate this possibility, I employed a combination of an SNP non-functional analogue and NO scavenger. Any direct interaction between SNP and aequorin was ruled out by demonstrating that SNP was not capable of inducing any significant light emissions when added to *in vitro* reconstituted aequorin (section 4.2.1.2). Moreover, the SNP non-functional analogue potassium ferrocyanide was shown to induce negligible luminescence in chemiluminometer assay (Figure 4.3). Furthermore, the NO scavenger C-PTIO significantly blunted the SNP-induced $[Ca^{2+}]_{cyt}$ spike in both chemiluminometer and *in vivo* Ca^{2+} imaging assays (Figure 4.3). Taken together, these results suggest that the observed SNP-mediated spike in $[Ca^{2+}]_{cyt}$ is specific to NO.

In mammalian systems, the ability of NO to induce $[Ca^{2+}]_{cyt}$ spikes is now well-documented (Loitto *et al.*, 2000). Moreover, NO has been also shown to cause a cGMP-independent intracellular Ca^{2+} rise in porcine endothelial cells (Berkels *et al.*, 2000). Thus, as far as I know, based on the evidence in Figures 4.1 & 4.3, I believe that our work is the first of its kind to report that NO is capable of inducing $[Ca^{2+}]_{cyt}$ spikes in plants. Indeed, this evidence highlights further the fact that NO-mediated signal transduction in both animals and plants share great similarities.

Previously, pharmacological studies have been successfully employed to identify the sources of observed Ca^{2+} transients induced in response to several stimuli (Price *et al.*, 1994; Cessna *et al.*, 1998). In this regard, the use of a variety of calcium channel inhibitors has proved to be useful. I used La^{3+}, a plasma membrane channel blocker (acts as a potent Ca^{2+} antagonist), to assess the contribution of external Ca^{2+} pools towards the observed NO-induced $[Ca^{2+}]_{cyt}$ spike. La^{3+} treatment caused a concentration-dependent inhibition in $[Ca^{2+}]_{cyt}$ spike. However, complete abolition of the luminescent signal was not evident (Figure 4.2). Moreover, La^{3+} concentrations above 100 μM resulted in no further significant inhibition. Thus, it can be concluded that the NO-mediated elevation in $[Ca^{2+}]_{cyt}$ is only partially contributed by an external Ca^{2+} pool or source. In contrast, employing a combination of lanthanum chloride (a plasma membrane blocker) and ruthenium red (a mitochondrial channel blocker), Price *et al.* (1994) have shown that H_2O_2 is capable of mobilising Ca^{2+} from both external and internal pools, with a major contribution from the internal pools. Conversely, cold shock has been reported to mobilise Ca^{2+} primarily from external pools (Price *et al.*, 1998). Interestingly, hypo-osmotic shock has been reported to induce a biphasic $[Ca^{2+}]_{cyt}$ influx. The first influx has been shown to derive from external Ca^{2+} stores, whereas the second influx derives from internal ones (Cessna *et al.*, 1998). These results suggest that NO, H_2O_2, cold shock and hypo-osmotic shock mobilise different Ca^{2+} pools. In the future, it will be interesting to investigate the contribution of internal Ca^{2+} pools towards the observed NO-induced $[Ca^{2+}]_{cyt}$ spike. However, relying solely on calcium channel blockers could be misleading. For example, lanthanides at high concentration range (mM) may

penetrate the plasma membrane (Quiquampoix *et al.*, 1990), resulting in ambiguity in result interpretation.

One major limitation of the aequorin system is in determining the subcellular localisation of calcium. Ca^{2+} signals are often extremely localised and are probably influenced by cell-wall architecture and distribution of organelles (Miyawaki *et al.*, 1997 and references therein).To this end, a recent advancement in fluorescent microscopy has allowed the *in vivo* imaging of ROS and RNI bursts in elicitor-induced tobacco whole-tissue using specific fluorescent dyes (Allan & Fluhr, 1997; Foissner *et al.*, 2000). Hence, as a complementary approach, the use of one of the new generation of intracellular calcium indicators; such as the chameleon system can be useful in localising distinct Ca^{2+} sources. In chameleons, engineered variants of GFP are used to probe their ionic environment using intramolecular fluorescence-resonance-energy transfer (FRET) (Miyawaki *et al.*, 1997). In FRET analysis, two interacting cell components are labelled with different fluorochromes such that when one, the donor, is excited with its appropriate wavelength of light some part of its emission energy is transferred to the second fluorochrome, the acceptor, which then fluoresces. The efficiency in energy transfer is inversely proportional to the distance (i.e. the two fluorochromes must be within nanometers to show significant FRET). Thus, the technique provides the capability to image molecular interactions with super-resolution, well beyond the point-to-point resolution of conventional fluorescence microscopy (Gilroy, 1997). Interestingly, a pH-dependent, GFP-based calcium indicator, yellow cameleon, has been used to report cytoplasmic calcium dynamics in *Arabidopsis* guard cells (Allen *et al.*, 1999). Moreover, recently, two variants of GFP, cyan and yellow, has been employed to investigate the role of metallothionein in NO signalling (Pearce *et al.*, 2000). These approaches, in combination with aequorin-based technology and Ca^{2+} channel blockers, should prove useful in dissecting the sources of NO-mediated $[Ca^{2+}]_{cyt}$ influxes.

Pathogen recognition is a prerequisite for the induction of defence responses. In the widely studied gene-for-gene interaction the plant's resistance (*R*) gene product acts as a signalling adaptor for a cognate pathogen avirulence (*Avr*) gene product, leading to the elaboration of HR (Flor, 1971; Yang *et al.*, 1997). One of the most rapid responses identified during incompatible interactions is the OB marked by the generation of ROS- which include H_2O_2. (reviewed in Baker & Orlandi, 1995). Two phases of ROS induction by fungal and bacterial elicitors have been measured in plant cell suspension cultures. The pattern of ROS has been shown to follow biphasic kinetics: (i) a very rapid response (within minutes) has been termed phase I and is not associated with plant disease resistance; (ii) later ROS production (2-4 hours) is termed phase II and correlates with resistance (Baker & Orlandi, 1995). Similarly, during incompatible interactions, a rapid elevation in NOS activity and a subsequent burst in NO concentration leading to the induction of defence-related gene expression have been reported in plants (Delledonne *et al.*, 1998; Durner *et al.*, 1998). Moreover, the observed increase in NO concentration has also been shown to be biphasic; the second phase of this burst has been observed only during incompatible interactions (Delledonne *et al.* 1998).

In this work, I established that NO is capable of inducing $[Ca^{2+}]_{cyt}$ pulse in a dose-dependent fashion (Figure 4.3). Thus, I investigated whether a biphasic pulse in $[Ca^{2+}]_{cyt}$ takes place during incompatible interactions. Interestingly, a single early spike (within 30 min) in $[Ca^{2+}]_{cyt}$ was obtained in both compatible and incompatible interactions. No incompatible-interaction specific spike in $[Ca^{2+}]_{cyt}$ was evident over 8 hours (Figure 4.6 A). Moreover, these results were highly reproducible. Furthermore, the virulent and avirulent pathogens, employed during the course of these experiments, were successful in triggering clear chlorotic disease symptoms 3 days post-inoculation and visible HR within 24 hrs post-inoculation respectively. Therefore, based on the rigorous controls performed, I believe that this result is credible. Hence, I conclude that: (i) the observed early spike in $[Ca^{2+}]_{cyt}$ is independent of the presence or the successful delivery of AvrB; (ii) there is no apparent qualitative differences in $[Ca^{2+}]_{cyt}$ observed between compatible and incompatible interactions. Despite this apparent similarity in $[Ca^{2+}]_{cyt}$ kinetics during

compatible and incompatible interactions, it is conceivable that distinct Ca^{2+} pools are selectively mobilised. For example, the hypo-osmotic shock has been reported to trigger a biphasic cytosolic Ca^{2+} spike in which the first and second Ca^{2+} waves are recruited from external and internal pools, respectively. However, more experiments are required to explore this possibility (Cessna *et al.*, 1998).

Recently, using similar aequorin-mediated luminescence approach, RPM1 has been shown to facilitate a rapid and sustained biphasic increase in $[Ca^{2+}]_{cyt}$ that is necessary for the oxidative burst and HR (Grant *et al.*, 2000). Moreover, the AvrB protein has also been reported to a delayed but similarly prolonged increase in $[Ca^{2+}]_{cyt}$. Furthermore, temporal association between H_2O_2 accumulation at reaction sites and the changes in $[Ca^{2+}]_{cyt}$ has been established via electron microscopy. The authors, has placed calcium elevation upstream of the oxidative burst (Grant *et al.*, 2000). These results clearly conflict with my findings presented in Figure 4.4. Because Grant *et al.* (2000) have used a similar approach, these findings are difficult to reconcile.

Several colorimetric and polarographic approaches for NO measurement have previously been reported (Murphy & Noak, 1994; Ridnour *et al.*, 2000; Gardner *et al.*, 1998a). However, a major drawback in these approaches is that they are invasive and time consuming due to the requirement of rigorous sample preparation prior to the actual measurement. Alternatively, the photoacoustic trace gas detectors have been demonstrated to be indispensable in high quality research performed in agriculture and biology. The strength of the technique lies in its ability to perform sensitive, on-line, non-invasive detection of trace gases under rapidly changing environmental factors (e.g. temperature, light, humidity, O_2, N_2, and CO_2) with high accuracy and specificity (Harren & Reuss, 1997). Thus, the photoacoustic approach has been widely used in many agricultural and medical applications including: (i) getting information on fermentation and spoilage process during storage of fruits, via monitoring trace gas emissions such as ethanol and acetaldehyde; monitoring ethylene emissions from orchid flowers as an indication of wilting and abscission processes; (iii) understanding water loss and transpiration dynamics in insects; this is

accomplished through measuring water, carbon dioxide and methane emissions; and (iv) medical diagnostics through breath analysis of patients with pulmonary, heart and skin diseases. In this regard, measuring ethylene in the breath of UV-irradiated subjects, as an indication of lipid peroxidation and membrane damage, has been reported. Moreover, study of xenobiotic related by-products (i.e. NO, ethane, ethylene) and NO involvement in post-harvest fruit storage quality are another two important applications of this approach (http://www.sci.kun.nl/tracegasfac). Here I report the use of a photoacoustic CO-laser spectroscopy approach.

Historically, under different environmental and physiological conditions, high NO emission from plants have been reported to take place (Klepper, 1979; Wildt *et al.*, 1997). Moreover, measurement of NO emissions during senescence of pea leaves, via an NO-specific sensor, has been demonstrated (Leshem & Haramaty, 1996). Interestingly, photoacoustic-based monitoring of NO gaseous emissions during ripening of strawberries and avocados has been recently illustrated (Leshem & Pinchasov, 2000). Hence, the experimental rationale employed here was the application of the photoacoustic approach in monitoring NO emissions during incompatible interactions and in response to $_{L}$-arginine, the substrate for NOS, treatment in *Arabidopsis*. Thus, I successfully demonstrated that the photoacoustic system is capable of detecting NO emissions from the NO-releasing compound SNP. Moreover, the amount of NO released correlated well with the pH-dependent pattern of NO release known for SNP; more NO was released under acidic than neutral pH values (Figure 4.7). Accordingly, I concluded that the experimental set-up for the photoacoustic laser system (i.e. laser lines wave length, etc.) is well-suited for the selective detection and quantitation of NO emissions. However, to my disappointment, I failed to detect any NO emissions in either *Pst*DC3000/*Pst*DC3000 (*AvrB*) or $_{L}$-arginine treated *Arabidopsis* Col-0 plants (Figures 4.8 & 4.9). I already know that the system in hand is capable of detecting NO emissions, as high as 100-175 ppb, and responds in a concentration-dependent manner (Figure 4.7). Moreover, a NO burst has been already reported to take place in both compatible and incompatible interactions as reported by a haemoglobin-based approach (Delledonne *et al.*, 1998). I also demonstrated in this work that $_{L}$-arginine is capable of triggering

a spike in $[Ca^{2+}]_{cyt}$ as reported by chemiluminometer and *in vivo* Ca^{2+} imaging assays (Figure 4.5). Furthermore, $_L$-arginine treatment in mammalian cells has recently been shown to correlate with a corresponding increase in NOS activity (Stathopulos *et al.* 2001). NOS activity has been detected in several plant species and has been shown to increase in incompatible interactions (Wendehenne *et al.*, 2001; Durner *et al.* 1998). Therefore, based on the experimental evidence already presented (Figure 4.7), I believe that the failure in detecting NO emissions suggests that a refinement in expreimental design may be required. Several observations support my assumptions. During the NO detection experiments, I used a CO laser spectroscopic system. In this system, the carrier gas used was composed of O_2, N_2, H_2 and CO (1:1:1:1). However, the commercially-available air cylinders are known to contain some ozone as well. It is well known that NO decomposition rate (i.e. oxidation to NO_2 and NO_3) is very insignificant. However, this rate is dramatically accelerated in the presence of any traces of ozone gas (personal communication, Luc-Jan Laarhoven, Trace Gas Facility, Holland). Therefore, it is conceivable that, in the presence of ozone, the NO concentration is dramatically reduced so that its detection becomes difficult (i.e. NO concentration falls beyond the detection limit of 50 ppb). In order to mitigate the ozone problem, the implementation of special ozone filters should be sufficient. Secondly, the plant cuvette with big headspace (Figure 4.6) could have caused a diluting effect on NO emissions beyond its detection limit. Therefore, an alternative cuvettes design with smaller headspace should have a positive effect on the detection of NO emissions. Leshem & Haramaty (1996) took into account these considerations in their experimental set-up during monitoring NO emissions from pea leaves. In their simplified bell jar system, to reduce NO decomposition and erroneous measurements, an NO-sensitive probe was inserted through an adaptor inlet held in place directly over the pea foliage. Hence, with half life ca. 5 s, I think that an adaptation whereby the plant's cuvette is brought closer to the photoacoustic cell would overcome the inherent problem of NO decomposition; by simply shortening the time NO emissions has to travel before getting detected.

4.3.3 Overexpression of HMP/NOD in Arabidopsis and characterisation of selected transgenics

Bacterial genes have previously been expressed in plants to manipulate plant biochemistry. For example, the *nahG* gene of *Pseudomonas putida*, encoding a salicylate hydroxylase has been successfully overexpressed in tobacco. Salicylate hydroxylase mediates the catalytic conversion of the signal molecule SA to catechol, a compound unable to induce SAR. Thus, *nahG* transgenic plants are depleted in SA and hence are compromised in establishing SAR. Indeed, the use of these transgenics has proved central to our understanding of SAR and SA-dependent defence signal transduction pathways in plants (Gaffney *et al.*, 1993; Delaney *et al.*, 1994; Friedrich *et al.*, 1995). Moreover, this approach has also been deployed to demonstrate the link between ROS accumulation (i.e. H_2O_2) and disease resistance via engineering of catalase-deficient plants. Therefore, the rationale behind this work was to engineer NO-deficient transgenic *Arabidopsis* plants in order to further investigate the role of this gas in defence signal transduction.

To this end, I have successfully engineered transgenic *Arabidopsis* plants that constitutively express the *HMP/NOD* from *E. coli* under the regulation of the 35S promoter of CaMV (Figure 4. 11). Moreover, molecular analyses performed on selected T1 transgenics revealed that the gene is faithfully transcribed and translated (Figure 4. 12). Visual phenotypic examination revealed that *35S::HMP/NOD* plants do not exhibit any characteristics that are different from wild-type Col-0 plants. Furthermore, unexpectedly no significant difference in the growth of the virulent bacteria *Pst* DC3000, between a selected *35S::HMP/NOD* and wild-type Col-0 plants, was found (Figure 4.13). Hence, I concluded that the overexpression of *HMP/NOD,* in the selected transgenic line C2, appears to have no impact on cell death or defence responses towards bacterial pathogens. Based on the western analysis (Figure 4. 12 C) and the spectral absorption values, indicative to heme and FAD content, of protein extracts of C2 lines, I think that the HMP/NOD is likely to be expressed and folded correctly. Hence, I attempted to find an explanation for the observed unexpected disease response of *35S::HMP/NOD* C2 transgenics.

A plausible scenario is that an NO- generating mechanism, presumably enzymatic, was up-regulated to compensate for endogenous NO deficiency caused by *HMP/NOD* overexpression. With the physiological roles known for NO in plants in mind, it is likely for an alternative mechanism of NO generation to have taken over to compensate for the NO deficiency and to maintain a homeostatic basal NO level that is required to perform these functions. In support of this hypothesis is the results obtained with antisense suppression of 2-cysteine peroxiredoxin (*2*-CP) in *Arabidopsis*. 2-Cps are known as antioxidants enzymes in many organisms and have been described in plants. The nuclear-encoded plant homologue if animal thioredoxin peroxidases and bacterial alkyl hydroperoxide reductases was have been shown to be post-translationally targeted to chloroplasts where it protects photosynthetic membrane from oxidative damage. Antisense suppression of *2-CP* in *Arabidopsis* resulted in photosynthesis impairment and acceleration in chloroplast proteins degradation. Moreover, a peroxidase activity assay indicated that the antioxidant protection system was up-regulated to compensate for 2-CP deficiency. The transient phenotype was strongest in plants of 4 weeks of age. However, at 6 weeks, adaptation reactions had fully compensated the antisense effect, and analysis of chlorophyll a fluorescence revealed that the mutant had an even higher level of stress tolerance than control plants (Baier *et al.*, 2000). Taken together, I believe that more experiments are required to accept or refute this theory. These include: analysis of endogenous NOD enzymatic activity, and analysis of NOS-dependent and NOS-independent (e.g. nitrite reductase) NO-generating activities *35S::HMP/NOD* lines.

Intriguingly, Chris Lamb's group (John Innes Centre) has reported that *HMP/NOD* overexpression in tobacco plants resulted in apparent development of HR-like lesions (Gary Loake, personal communication). Clearly this report directly conflicts with our findings. Interestingly, it has previously been reported, by the same group, that in soybean cell suspension cultures NO was found to act synergistically with ROS to potentiate cell death (Delledonne *et al.*, 1998). Interestingly, in soybean cell suspensions and tobacco plants, NO has also been shown to induce the expression of the defence-related genes *PAL* and *PR-1*, independently of ROS (Delledonne *et al.*, 1998; Durner *et al.*, 1998). Therefore, I speculate that the overexpression of an NO-

degrading enzyme is expected to break the synergistic effect of NO and ROS on cell death; leading to an increase in the threshold leading to cell death. Another explanation for these conflicting findings could perhaps be attributed to the inherent differences between the two model systems (i.e. *Arabidopsis* and tobacco). In this regard, Clarke *et. al.* (2000) have recently highlighted significant differences in NO signalling between *Arabidopsis* and the soybean system. Firstly, kinetics of NO generation by *Arabidopsis* cells following challenge by an avirulent pathogen differ from those reported for soybean, in which NO production closely matched ROS production (Delledonne *et al.*, 1998). In *Arabidopsis* suspension cultures, however, NO production rapidly increased over a 6 hrs period, whereas significant levels of H_2O_2 production were not observed until around 5 hrs after inoculation (Clarke *et al.*, 2000). Secondly, treatment with NOS inhibitors did not reduce NO generation following pathogen challenge (Clarke *et al.*, 2000). In contrast to the situation with soybean cultures, in which NOS inhibitors where reported to to reduce NO generation (Delledonne *et al.*, 1998). Thirdly, there is no synergism between NO and ROS in inducing cell death in *Arabidopsis* suspension cultures. Moreover, the NO-induced cell death does not result from the production of the highly reactive free radical peroxinitrite formed by the reaction of $O_2^{\cdot-}$ and NO (Clarke *et al.*, 2000). This is distinct from data employing soybeans cultures, in which NO and ROS were reported to act synergistically in cell death induction (Delledonne *et al.*, 1998).

Taken together, these conflicting findings underline clear differences in kinetics of NO generation and its mechanism between different plant species. In this context, enzymatic mechanisms for NO generation, other than NOS, have been reported (e.g. nitrate reductase) that could account for the observed difference in the dynamics of NO generation between *Arabidopsis* and soybean (Yamasaki *et al.*, 1999). Hence, this could explain the differences in the *HMP/NOD* overexpression results obtained in this work with that of Chris Lamb group in *Arabidopsis* and tobacco, respectively.

4.3.4 Concluding remarks

Recent investigations into NO-mediated signalling in plants revealed great similarities to their mammalian counterparts. In this regard, initial analysis of NO signalling in plants suggested that the well established pathway by which NO activated guanylate cyclase and cGMP production in mammals is also operative in plants. In this context, it has been demonstrated that NO induces a transient increase in cGMP and a corresponding increase in the expression of the defence-related gene *PAL-1*. Moreover, both cGMP production and *PAL-1* gene expression were reduced by inhibitors of guanylate cyclase, and the inhibition of *PAL-1* gene expression was partly reversed by the cell-permeable cGMP analogue 8Br-cGMP (Durner *et al.*, 1998). Furthermore, it is likely that NO mediates its effects in a cGMP-independent fashion. In this context, one important cGMP-independent function of NO might be the regulation of iron homeostasis, because NO has been found to inhibit the activity of plant cytosolic aconitase through the binding at the catalytic centre (the Fe-S cluster) (Navarre *et al.*, 2000). Moreover, the observation that plant cytosolic aconitases share reasonably high homology to human iron regulatory protein (IRP-1) suggests that they might perform an analogous function to IRP-1 (in mammals aconitase converts, binding to NO, to IRP-1 that is involved in iron metabolism). Hence, a plant IRP-1 protein with a potential of increasing free iron levels in response to NO could provide a defensive function following pathogen attack. In the presence of ROS, excess free iron could lead to oxidative destruction and cell death by promoting the Fenton reaction, which generates the hydroxyl radical, the most destructive reactive species (Wendehenne *et al.*, 2000). In this regard, the use of a novel approach such as GFP-based FRET could prove useful in ascertaining the role of aconitase in the regulation of iron metabolism in response to NO. This approach has been successfully used in the examination of the role of metalothionein in NO signalling (Pearce *et al.*, 2000). Aconitase is not the only enzyme whose activity is modulated by NO. Similarly, NO has recently been shown to exert an inhibitory effect on the antioxidant enzymes catalase and ascorbate peroxidase (Clark *et al.*, 2000). Taken together, it appears that the inhibitory effect on these enzymes would help to create a lethal environment that would contribute to HR via accumulating

ROS. Thus, NO synthesis inhibits cytochrome C oxidase in the mitochondira leading to enhancement of the destructive potential of mitochondrial electron transport. This NO-mediated inhibition of cytochrome c oxidase greatly increases the probability of superoxide formation from the ubiquinone pool, leading to the formation of the formation of the highly reactive peroxinitrite and hydroxyl radicals (Millar & Day, 1997). As a defence mechanism, an alternative oxidase can act as an alternative electron sink and markedly decrease the production of superoxide whereby preventing the formation of the destructive peroxinitrite (Millar & Day, 1997). Alternatively, urate, might operate as a natural inhibitor of peroxynitrite-mediated toxicity without affecting the plant's ability to defend itself against bacterial pathogens (Alamillo & Garcia-Olmedo, 2001).

One potential intracellular target for NO is the interaction with MAPK signalling pathways. In mammals, NO have been shown to activate MAPK cascade (Browning *et al.*, 2000). Recently, reports from our group and several others have indicated a role for ROS-mediated oxidative burst in MAPK cascade activation in plants (Romeis *et al.*, 1999; Grant *et al.*, 2000; Taylor *et al.*, 2001). Equally, a recent role for NO in the activation of MAPK cascades has been described. Thus, Kumar and Klessig (2000) have reported that NO induced the activation of a SIPK, leading to the induction of defence responses in tobacco. Moreover, Clarke *et al.* (2000) documented that, in *Arabidopsis* cell cultures, NO is capable of inducing a MAPK activity and that NO-mediated programmed cell death occurs independently of PD98059-sensitive MAPKs. In a quest to identify novel MAPKs that are involved in ROS/RNI-mediated signal transduction pathways, Loake's group is currently undertaking a proteomics approach. Thus, with the advent of matrix-assisted laser desorption/ionisation mass spectroscopy (MALDI-MS) and electrospray ionisation mass spectroscopy (ESI-MS), high throughput peptide mapping and protein identification has now become a much easier task (Smith, 2000).

Many uncertainties remain regarding the NO-generating enzymes in plants. Although biochemical and immunological approaches strongly suggest the existence of a plant homologue of mammalian NOS (Barroso *et al.*, 1999), the corresponding protein has not yet been identified. Thus, plant NOS-like enzyme could be structurally different from mammalian NOS. Therefore, an approach involving biochemical purification may be necessary to identify the protein responsible for L-arginine-dependent synthesis of NO in plants. Alternatively, a reverse genetics approach employing the power of T-DNA mutagenesis to generate knock-out mutants in individual P450 enzymes with down or upregulated NO production is an exciting one. Followed by subsequent NOS enzymatic activity assays, this approach may prove fruitful. Recently, a screen for mutants that are involved in nitric oxide signalling or parallel pathways which can bypass the requirement for NOS in plant pathogen defence response has been described. Thus, *H*R *d*espite *N*OS inhibitor (*hdn*) mutants have been identified (Worley *et al.*, 2001).

Finally, I believe that the simultaneous application of forward and reverse genetics and biochemical approaches should together assist in advancing our basic understanding of NO-mediated signal transduction networks and in identifying its components in plants.

CHAPTER V

5 TRANSFORMATION OF *FUSARIUM OXYSPORUM* WITH *G*REEN *F*LUORESCENT *P*ROTEIN (*GFP*) VIA PARTICLE BOMBARDMENT

"The biolistic process employs high-velocity microprojectiles to deliver nucleic acids and other substances into intact cells and tissue. Diverse applications for this process are rapidly being found for both basic research and genetic engineering"

{J. C. Sanford *et al.*, 1993}

5.1 Introduction

5.1.1 Particle bombardment as a tool for transformation of filamentous fungi

By far the most common forms of plant pathogenic fungi are filamentous fungi (so-called because they exist as hyphae or filaments when they are colonizing host tissue). Transformation (i.e. introduction of exogenous DNA into living cells) is one approach of a paramount importance in the genetic, biochemical and physiological study of fungi in general and plant pathogenic fungi in particular.

Over the past few years, huge and rapid advancements in fungal transformation have taken place. The fungal transformation procedures have been described of which protoplast transformation has become the most commonly used. It is based on the observation that DNA can readily enter cells devoid of walls in the presence of $CaCl_2$ and polyethylene glycol (PEG) (Rambosek and Leach, 1987). However, despite of its popularity, this approach is time consuming and laborious as it entails cells preparation and modification prior to transformation. Alternatively, particle bombardment (or biolistic) transformation has been introduced (Klein *et al.*, 1987). It is based on the introduction of DNA (e.g. plasmid construct) into living cells through the penetration by DNA-coated inert microprojectiles (either tungestin or gold) at an explosive acceleration. As it does not include prior cells preparation and simplicity, particle bombardment has recently become widely used. In addition to its successful use to transform plants (Klein *et al.*, 1988), animal cells (Johnston, 1990) and bacteria (Shark *et al.*, 1991), it has been used to stabley transform filamentous fungi (Fungaro *et al.,* 1995; Armaleo *et al.*, 1990; Lorito *et al.*, 1993) and filamentous fungal pathogens (Bailey *et al.*, 1993; Chaure *et al.*, 2000).

5.2 Results

In collaboration with Lucy Harrier (Scottish Agricultural College) I attempted to transform intact conidia of *Fusarium oxysporum* via the particle bombardment approach. Figure 5.1 displays the gGFP plasmid used for *Fusarium* transformation.

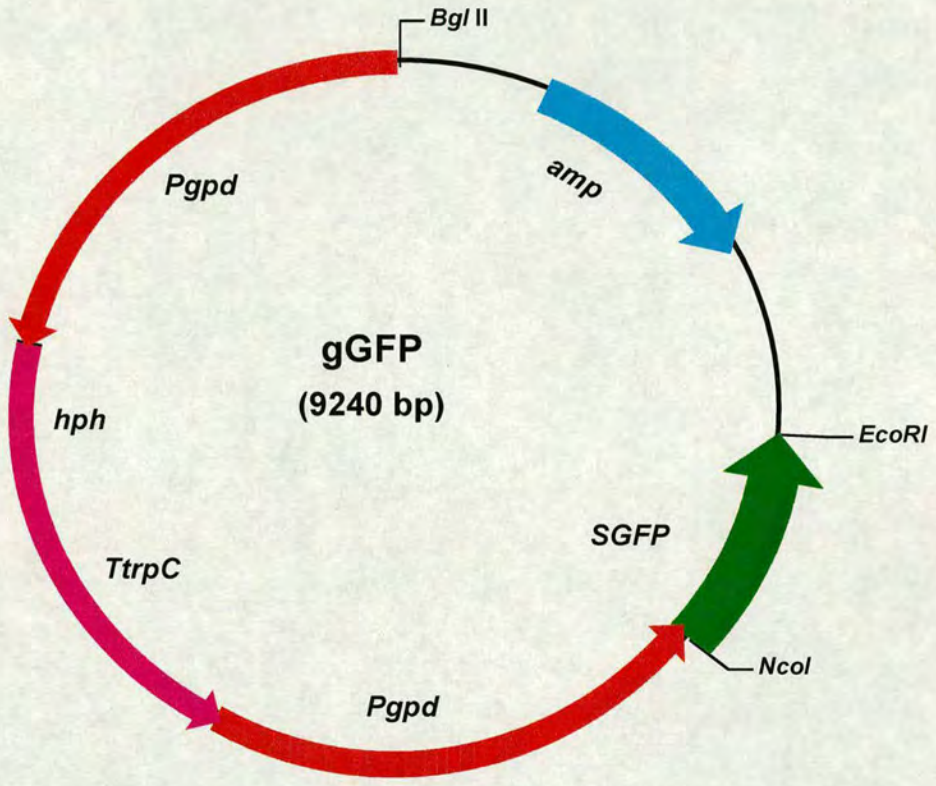

Figure 5.1: The gGFP plasmid used for *Fusarium oxysporum* transformation via particle bombardment (Maor *et al.*, 1998). Abbreviations: *Pgpd*, *Aspergillus nidulans* glyceraldehyde phosphodehydrogenase promoter; *SGFP*, codon-optimised (TYG) synthetic GFP; *hph*, hygromycin B phosphotransferase; *TtrpC*, *Aspergillus nidulans* terminator sequence of the tryptophan biosynthesis gene C; *amp*, *E. coli* ampicillin resistance gene.

By employing the optimised particle bombardment procedure outlined in chapter II, I obtained a transformation efficiency of 45.0 $\pm$5 *F. oxysporum* f. sp. *matthiolae* transformants per μg of gGFP plasmid DNA. A similar transformation efficiency was obtained in further independent experiments. The biolistic machine employed in *Fusarium* transformation is outlined in Figure 5.2.

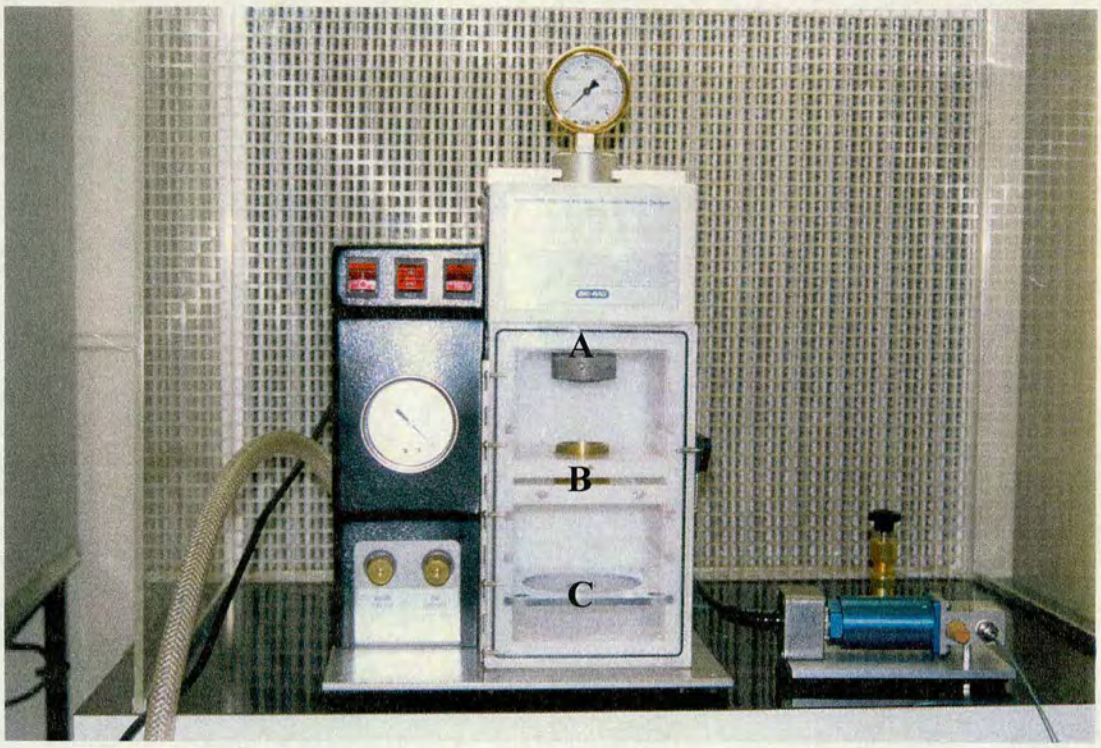

Figure 5.2: The Biolistic® PDS-100/He Particle Delivery System (Bio-Rad®) employed for the transformation of *Fusarium oxysporum.* The rupture disk retaining cap (A), microcarrier launch assembly (B), and target plate shelf (C) are indicated.

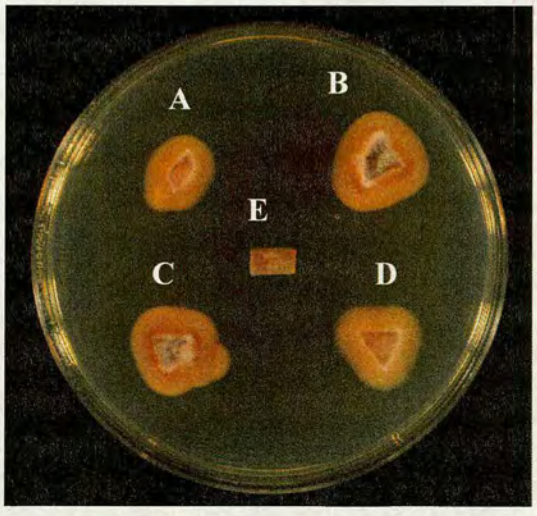

Figure 5.3: Growth of *Fusarium oxysporum* f sp *matthiolae* transformants (A, B, C, and D) after they were picked up and transferred to a new PAD medium supplemented with 50 μg per ml hygromycin B. Note that the growth of wild-type fungus is completely blocked (E).

Selected hygromycin-resistant transformants were transferred to fresh PAD supplemented with 50 μg ml^{-1} hygromycin B. Unlike wild-type *F. oxysporum* f. sp. *matthiolae*, whose growth was blocked, *bona fide* transformants grew well on 50 μg ml^{-1} hygromycin (Figure 5.3).

The vast majority of transformants maintained their characteristic parental morphotypes including their purple pigmentation. A number of transformants were screened for GFP expression by means of a GFP Leica fluorescence microscope. No GFP fluorescence was detected in wild-type *F. oxysporum* f. sp. *matthiolae*. A typical bright transformant was selected for further analysis (Figure 5.4).

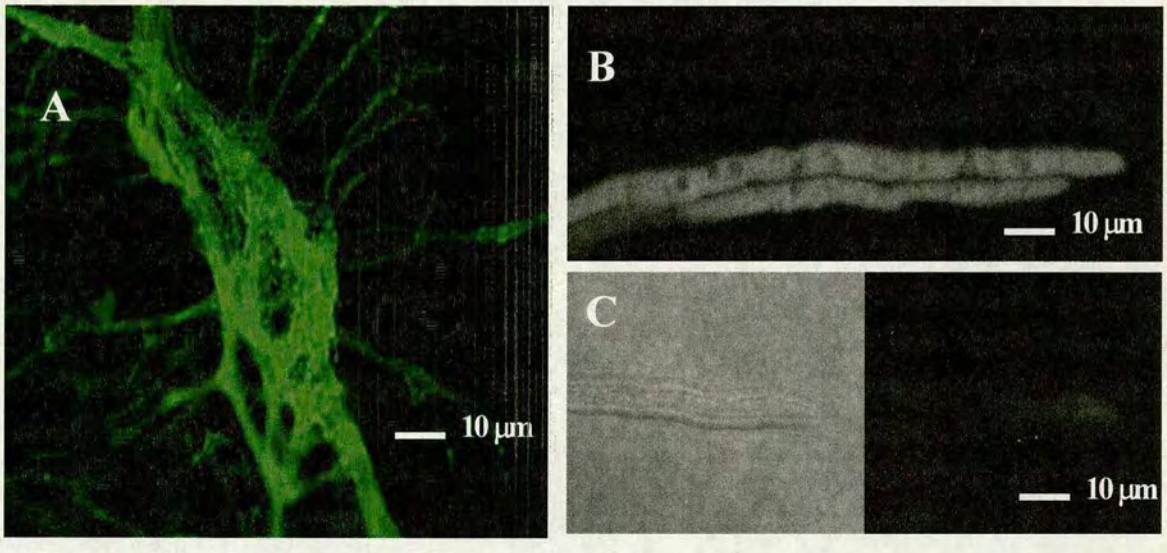

Figure 5.4: Fluorescence and confocal microscopic examination of GFP-transformed *Fusarium oxysporum*. (A) Fluorescence microscopy; note the high intensity and emerald-green brightness characteristic to GFP. No fluorescence signal was detectable in the wild-type fungal hyphae. Confocal imaging revealed that the transformant hyphae expresses GFP uniformly (B); negatively stained spots denote the nuclei. Again, no signal was detectable from wild-type fungal hyphae. No fluorescence signal was detectable in the wild-type fungal hyphae (C).

Confocal microscopic examination of the selected transformant indicated that GFP expression was uniformly distributed throughout the cytoplasmic space in the fungal hyphae. No GFP expression was detected in spores of the same transformant (data not shown). Therefore, the *Aspergillus nidulans Pgpd* promoter does not direct significant GFP gene expression during *F. oxysporum* f. sp. *matthiolae* spore development. GFP fluorescence quantification revealed a relative fluorescence of 38 RFU per µg total protein (Figure 5.5).

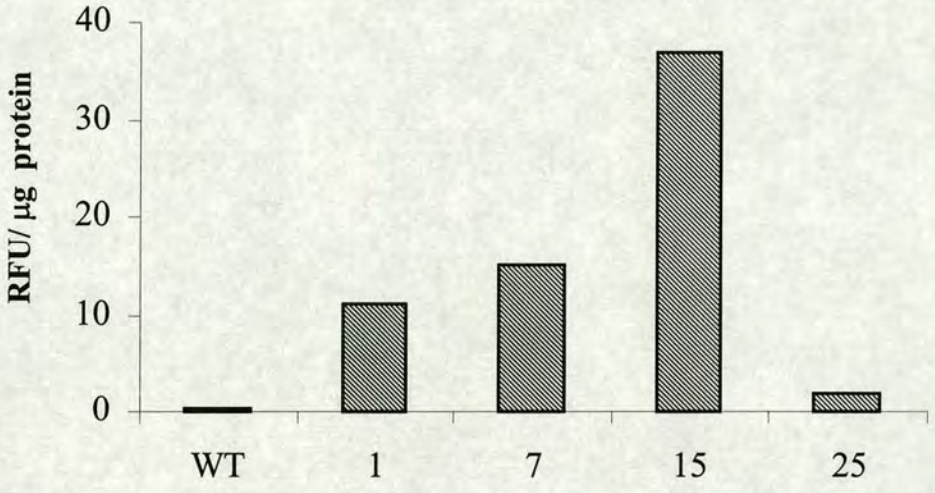

Figure 5.5: Spectrophotometric GFP fluorescence measurements in protein extracts of representative *Fusarium oxysporum* transformants. Negligible fluorescence value was obtained in the wild-type fungus (WT). Fluorescence values were expressed as relative fluorescence units (RFU) and normalised against protein contents of each sample.

Arabidopsis pathogenicity assays revealed that successful transformation did not significantly impact fungal virulence. The transformant under study produced clear disease symptoms, visualised as wilting and necrosis, in *Arabidopsis* leaves 4 days post inoculation. The extensive amount of fluorescent plant material produced during necrotic symptom development precluded visualisation of *F. oxysporum* f. sp. *matthiolae in planta* during infection of *Arabidopsis* leaves.

Virulent isolates of *F. oxysporum* have previously been shown to lead to the activation of a variety of plant defence responses including the expression of genes encoding antifungal peptides such as plant defensins (*PDF*). Infection of *Arabidopsis* Col-0 plants containing a *PDF1.2::LUC* transgene with a selected transformant resulted in a strong increase in LUC activity two days post *F. oxysporum* f. sp. *matthiolae* inoculation. In contrast, plants inoculated with a water control produced only a negligible increase in LUC activity (Figure 5.6).

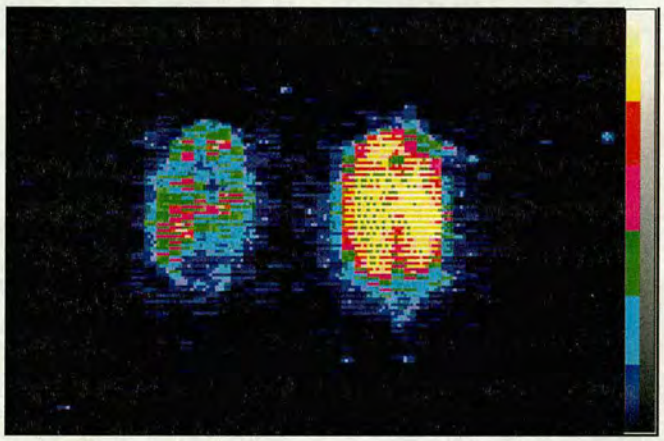

Figure 5.6: Pathogenicity assay and examination of transformant 15 ability of inducing plant defence responses by real-time luciferase imaging. The transformant was able to induce *Arabidopsis* defence response (plant defensin promoter) as reported by real time luciferase imaging transgenic *PDF1.2:: LUC* plants (leaf on the right). Shown is a pseudo-coloured image taken 48 h post-inoculation; note the high intensity of luciferase activity as shown by the colour index. Plants inoculated with sterile water had negligible bioluminescence (leaf on the left). Images were collected over a period of 10s.

Virulent isolates of *F. oxysporum* have previously been shown to lead to the activation of a variety of plant defence responses including the expression of genes encoding antifungal peptides such as plant defensins (*PDF*). Infection of *Arabidopsis* Col-0 plants containing a *PDF1.2::LUC* transgene with a selected transformant resulted in a strong increase in LUC activity two days post *F. oxysporum* f. sp. *matthiolae* inoculation. In contrast, plants inoculated with a water control produced only a negligible increase in LUC activity (Figure 5.6).

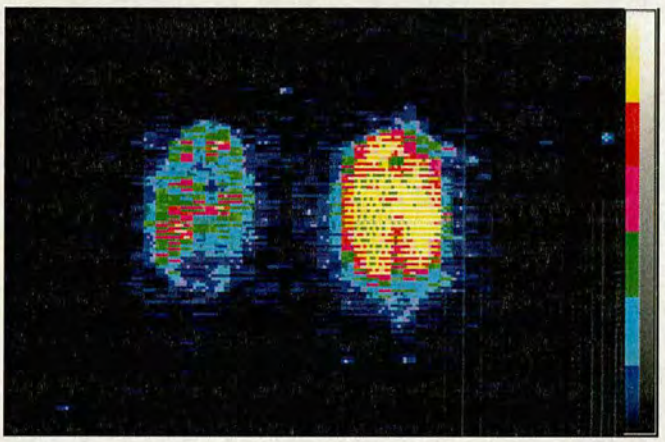

Figure 5.6: Pathogenicity assay and examination of transformant 15 ability of inducing plant defence responses by real-time luciferase imaging. The transformant was able to induce *Arabidopsis* defence response (plant defensin promoter) as reported by real time luciferase imaging transgenic *PDF1.2:: LUC* plants (leaf on the right). Shown is a pseudo-coloured image taken 48 h post-inoculation; note the high intensity of luciferase activity as shown by the colour index. Plants inoculated with sterile water had negligible bioluminescence (leaf on the left). Images were collected over a period of 10s.

5.3 Discussion

In this work, I have successfully demonstrated the utility of a particle bombardment technique as a valuable tool for gene transfer in *F. oxysporum* f. sp. *matthiolae*. I have optimised and developed an efficient and highly reproducible transformation system for this filamentous fungus (Section 2.29). The resulting transformants were found to be stable over at least six passages when grown on PDA medium without selective antibiotic pressure. Genetic analysis of these transformants is currently underway.

There are several reasons why I preferred to use GFP as a reporter gene over other previously reported reporter genes. Firstly, the fluorescence of GFP is resistant to photobleaching and remains stable under a wide variety of conditions (Cubitt *et al.*, 1995; Patterson *et al.*, 1997), permitting extended observation of GFP proteins. Secondly, GFP has no or little toxicity and its ability to fluoresce is preserved in fusion proteins (Cubitt *et al.*, 1995). Thirdly, it does not require exogenous substrate as the fluorescent GFP chromophore is formed through an autocatalytic mechanism. This makes GFP visualisation technique simple, fast and suitable to examine living organisms. Thus, GFP-transformed *Fusarium* may have significant utility as a tool to quantify fungal biomass. This application is particularly important as most currently available pathogenicity assays depend on qualitative disease index values. Moreover, the availability of a simple, robust and quantitative tool to score for disease symptoms is a prerequisite for large-scale genetic screens.

Plant resistance to necrotrophic fungal pathogens such as *F. oxysporum* is thought to be mediated via the jasmonate signalling pathway (Loake, 1996), which activates a number of genes including those encoding the antifungal defensin PDF1.2 and numerous thionins (Penninckx *et al.*, 1996; Epple *et al.*, 1997). Moreover, accessions of *Arabidopsis* that show resistance against *F. oxysporum* have been reported to show elevated thionin accumulation (Epple *et al.*, 1998). The inoculation of a transgenic *Arabidopsis* plant containing a *PDF1.2*::*Luc* gene fusion with a selected *F. oxysporum* f. sp. *matthiolae* transformant resulted in the activation of LUC

activity two days post inoculation, in a similar fashion to wild-type *F. oxysporum* f. sp. *matthiolae*. The detection of LUC activity via ultra low-light imaging preceded the development of disease symptoms and subsequent death. Thus, the transformation procedure and the expression of relatively high levels of GFP does not seem to negatively impact *F. oxysporum* f. sp. *matthiolae* virulence on *Arabidopsis*. I anticipate the GFP marked *F. oxysporum* f. sp. *matthiolae* in combination with this novel transgenic *Arabidopsis* line will have high utility for the identification of *Arabidopsis* mutants perturbed in the engagement of jasmonate based defence signalling in response to *F. oxysporum* f. sp. *matthiolae* infection.

To my knowledge, the only reports of *F. oxysporum* transformation required the time consuming production of fungal protoplasts and resulted in a relatively low transformation efficiency, typically one transformant per μg DNA (Kistler and Benny, 1988; Malardier *et al.*, 1989). The protocol described herein is significantly more rapid and straightforward than those reported previously. Moreover, at an average frequency of 45 transformants per μg of DNA the efficiency is also forty-five times greater. Thus, the transformation of *F. oxysporum* via particle bombardment has significant utility for gene transfer experiments in this agronomically important filamentous fungus. In this context, the sequencing of the *Fusarium* genome by the biotechnology industry has recently been completed and an expressed sequence tag (EST) database for *F. sporotrichioides* has been established within the public domain (http://www.genome.ou.edu/fsporo.html). Hence, exciting opportunities now exist for functional genomics in this phytopathogen. An endogenous active transposon has recently been described in *F. oxysporum* which could be exploited for gene tagging approaches (Migheli *et al.*, 1999). Moreover, insertional inactivation of genes via introduced DNA has also proved a powerful tool to ascribe gene function in filamentous fungi (Bölker *et al.*, 1995), and this approach has also recently been deployed in *F. oxysporum* (Namiki *et al.*, 2001). In addition to forward genetic screens, complementary reverse genetic strategies will also be required to assign gene function and this approach has also begun to be deployed in *F. oxysporum* (Di Pietro *et al.*, 2001). These functional genomic approaches are dependent upon an effective gene transfer system. Thus, the facile and efficient

transformation protocol described herein may help facilitate such gene function search based approaches.

It was my intention to use GFP-transformed *Fusarium* as a tool to be able to quantify fungal biomass on leaf surfaces. This application is particularly important as most currently available pathogenicity assay rather rely on a qualitative disease index values. Moreover, the availability of a simple, reliable and quantitative tools to score for disease symptoms is a prerequisite in any large-scale functional genomic mutant screen. However, the following practical difficulties were encountered which prevented me from accomplishing this task. Firstly, the selected *Fusarium oxysporum* GFP-transformant displayed a slower growth compared to wild-type. This can not be attributed to GFP expression as GFP protein was shown to be have little or no toxicity (Cubitt *et al.*, 1995). A plausible explanation of this is the possibility that gGFP plasmid has been integrated in a gene that is vital for growth and development. Secondly, pathogenicity assays with either wild-type or GFP-transformed *Fusarium* soil-grown *Arabidopsis* seedlings were extremely unreproducible and therefore results were difficult to interpret reliably. This could partially be explained by the inherent tendency of *Fusarium oxysporum* to mutate when grown for instance on rich medium or under unfavourable harsh conditions resulting in a less virulent or completely non-virulent strain (Nick Read, Personal communication). I am currently assessing the feasibility of extending the use of GFP transformation by particle bombardment to other *Arabidopsis* and crop plants necrotrophic fungal pathogens (e.g. *Botrytis cinerea*). This approach should contribute towards our further understanding of fungal-plant interactions and the development of quantitative tools for scoring disease symptoms.

CHAPTER VI

6 SUMMARY AND FUTURE WORK

6.1 Characterisation of *pcd1*

6.1.1 Summary

I have generated a library of 8000 T-DNA activation tagged lines using the activation tagging vector SKI15 (Figure 3.1). In this context, the *Arabidopsis* transgenic designer background *PR1a::LUC* was transformed by *Agrobacterium* harbouring the plasmid SKI15 via a standard floral dip protocol. Screening for gain-of-function mutants was our focus. Screening efforts resulted in the isolation of the *pcd1* mutant by virtue of its constitutive expression of luciferase activity (Figure 3.4 A&C). Phenotypic characteristics of *pcd1* include stunted stature, curly leaves, HR-like lesion formation in a mosaic-like fashion in the absence of pathogens, and accelerated cell death (Figure 3.5 A-D). Histochemical examination of *pcd1* leaves revealed that *pcd1* leaves accumulate high levels of H_2O_2 and phenolic compounds and camalexin (data was not shown) (Figure 3.5 H & K). Interestingly, biochemical analysis indicated that *pcd1* leaves accumulate high levels of the signal compound SA (Figure 3.9). However, when SA levels were blunted, in *pcd1::nahG* F1 progeny double crosses, the characteristic HR-like lesion formation and H_2O_2 was suppressed (Figure 3.9 & 3.16; Table 3.1). However, these typical phenotypic *pcd1* characteristics were maintained in the F2 progeny of *pcd1::coi1* and *pcd1::etr1* double mutants (Figure 3.16; Table 3.1). Hence, it was concluded that the *PCD1* gene functions in the SA-dependent signalling pathway upstream of SA (Figure 6.1). Further biochemical analysis revealed that *pcd1* exhibit heightened level of POD activity compared to wild-type Col-0 plants (Figure 3.6). However, no significant difference in CAT activity was detected (Figure 3.7 A & B). Moreover, a constitutive 46 and 48 kD MAPK activity was detected in *pcd1* leaves with or without lesions (Figure 3.8). Intriguingly, a reduction in total chlorophyll content of up to 50% was evident in *pcd1* plant exposed to high-light intensity (Figure 3.10 A&B). Hence, I concluded that chlorophyll catabolism rate is altered in *pcd1* plants in response to high light intensity.

Northern analysis indicated that *pcd1* leaves constitutively express key antioxidant and defence-related genes including *PR1*, *PR2* PR5, *PDF1.2*, *GST1*, *CAT3*, *GER3*, *PAL1* and *RbohA* (Figure 3.11). Additionally, *pcd1* plants exhibited significantly high resistance responses against several pathogens including the hemi-biotrophic bacteria *P. syringae* DC3000 (Figure 3.12), the biotrophic fungus *Erysiphe*, (Figure 3.13), and the oomycete *P. parasitica* (Figure 3.14). Moreover, *pcd1* abiotic stress tolerance response to salt and abscisic acid mirrored that of wild-type Col-0 seedling. Thus, I concluded that the *pcd1* mutation does not impact on salt tolerance and sensitivity to abscisic acid. Genetic analysis indicated that mode of inheritance for the *pcd1* mutation conforms to the classic Mendelian segregation for a dominant monogenic trait (Table 3.1). Molecular analysis revealed that the T-DNA linked to the *pcd1* mutation has undergone severe deletions in the CaMV 35S enhancer region and pSK fragment, and rearrangements in the *bar* gene (Figure 3.17). Accordingly, it is concluded that the *pcd1* is brought about by a T-DNA insertional event rather than gene enhancement. Moreover, because *pcd1* is a dominant gain-of-function mutation we envisage that a T-DNA insertion event in some part of the *PCD1* gene rendering it constitutively expressed. Thus, I propose that the PCD1 protein functions as a positive regulator of SAR in at two possible locations (Figure 6.1). Firstly, PCD1 could act early on in the signal transduction pathway immediately after pathogen recognition. Upon pathogen recognition, the *PCD1* gene becomes activated leading to subsequent activation of the signal transduction pathway culminating in *PR* gene expression and resistance (Figure 6.1). Secondly, PCD1 could function as a positive regulator of cell death. Upon PCD1 activation, enhancement of the self-amplifying OCD cycle takes place. In turn, a positive feed back regulation of NADPH oxidase via SA operates whereby maintaining the generation of ROS leading to the establishment of HR-like cell death and SA accumulation (Figure 6.1). Mapping experiments placed the *pcd1* gene on the lower arm of chromosome I in an 14 cM genetic interval between the SNP markers T12P18 (88 cM) and T1F15 (102 cM).

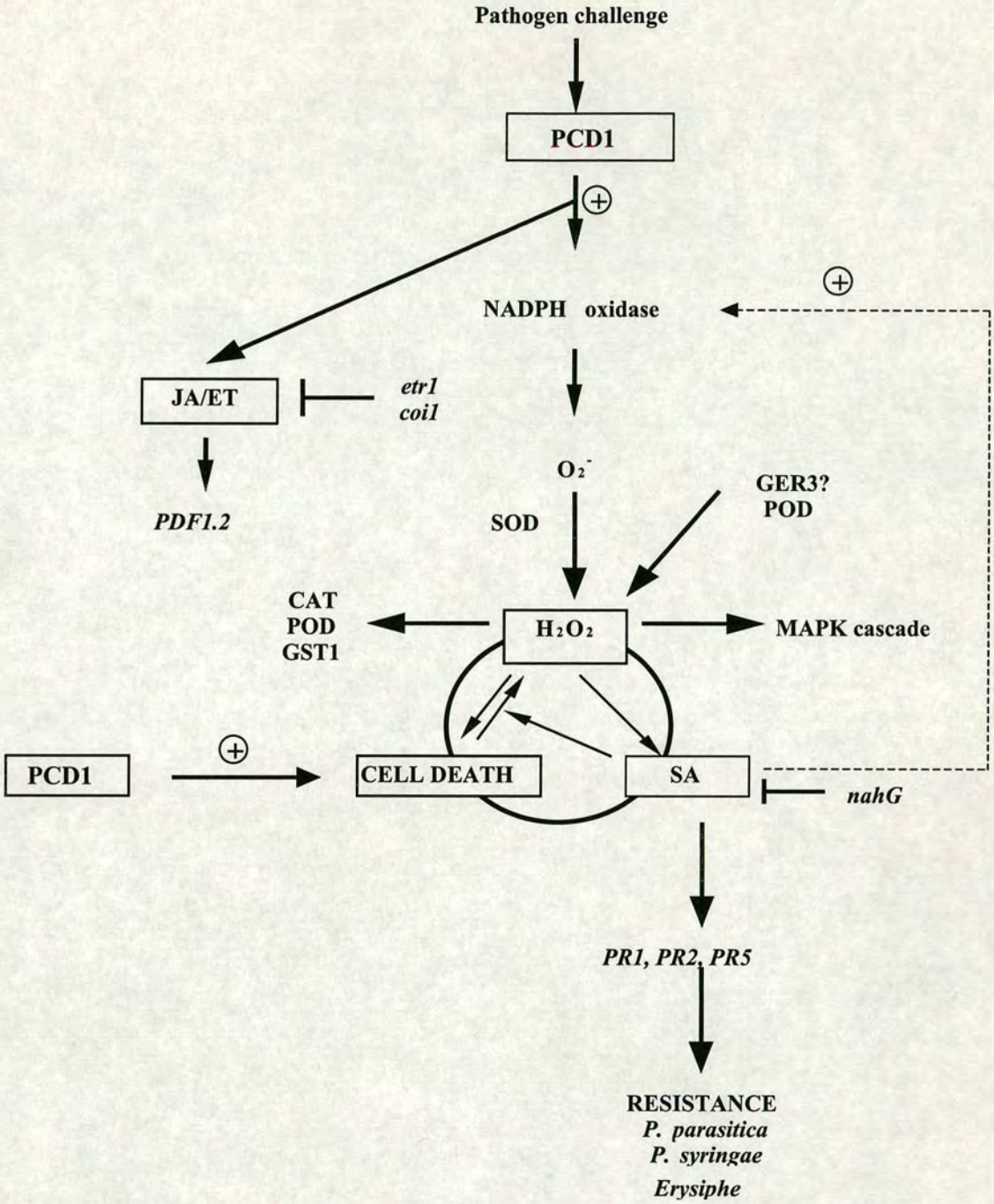

Figure 6.1: A proposed simplified model for the role of PCD1 in SAR signal transduction. The model is based on experimental evidence produced in this work and on our current knowledge of defence signal transduction pathways. According to this model, PCD1 is proposed to act as a positive regulator at least two points in the pathway leading to the establishment of SAR. The (?) symbol represents an assumption or uncertainty where no evidence from this work is supporting it. The cycle joining H_2O_2 generation, cell death execution and SA biosynthesis denotes the oxidative cell death cycle (OCD) (based on Van Camp *et al.*, 1998). The branching point for the JA-/ET-dependent pathway in relation to H_2O_2 accumulation is arbitrarily put upstream of the OCD cycle.

6.1.2 Future analysis of PCD1-mediated SAR

1) Fine mapping of the *pcd1* gene:

At this stage, approximately 600 (1200 chromosomes) of confirmed homozygous *pcd1::Ler* F2 recombinants have been collected by Xinwei Chen. Next, a high-throughput DNA isolation from these plants will be conducted using DNeasy® 96 Plant Kit. In this, a Mixer Mill MM 300 and centrifuge 4-15C with Plate Rotor 2x96 will be used. Thus, fine mapping of the *pcd1* gene will be significantly facilitated with the availability of extensive SNP markers (http::// http://godot.ncgr.org/Cereon). Using this strategy, the *pcd1* gene can be fine-mapped to an approximately 50-100 kb interval.

2) Map-based cloning of the *pcd1* gene:

As soon as it is successfully fine-mapped, cloning of the *pcd1* gene via its map position will be undertaken. Thus, different BACs overlapping the *pcd1* gene will be utilised. Moreover, the availability of transformation-competent artificial chromosome (TAC) vectors will be useful in speeding up the cloning process (Liu *et al.*, 1999). Furthermore, establishing the link between the phenotype and the genotype will be considered. In this regard, identifying a *pcd1* knock-out (i.e. loss-of-function) line from the publicly available T-DNA knock-out mutant libraries will be useful for establishing this link (http://afcg. stanford.edu; Galbiati *et al.* 2000; Krysan *et al.*, 1999). Moreover, modifying the levels of *PCD1* expression, through the generation of transgenic lines overepxressing the *PCD1* gene in a wild-type background, should also recapitulate the phenotypes associated with *pcd1*. In this, cloning of the *PCD1* cDNA behind the 35S Cauliflower Mosaic Virus constitutive promoter followed by the *ocs3'* terminator sequence in the binary vector pGREEN (John Innes Centre, UK) will be conducted.

3) Completion of the epistasis analysis of *pcd1*.:

Analysis of defence responses of *pcd1::eds1 and pcd1::ndr1* double mutant should help understanding whether PCD1 functions through an NDR1-, EDS1-dependent or another pathway. As to the generation of *pcd1::pad3* and *pcd1::pad4*, it should help understanding the importance of phytoalexins in *pcd1*-mediated disease resistance. Moreover, analysis of these double mutants should give insights into the role EDS1, NDR1, PAD3, and PAD4, if any, in the PCD1-mediated cell death control. Furthermore, analysis of *pcd1::npr1* mutants should unravel whether PCD1 functions in an SA-dependent/NPR1-dependent or SA-dependent/NPR1-independent pathway. And finally, examination of defence gene expression and disease resistance responses of these double mutants will be valuable.

4) Understanding the contribution of JA/ET-dependent signalling components and signalling molecules in *pcd1*:

I have demonstrated that in *pcd1* the HR-like lesion formation and H_2O_2 accumulation does not require COI1 and ETR1. But the question remains: is disease resistance and defence gene expression in *pcd1* affected by these mutations?. In this regard, quantification of endogenous levels of JA (both JA and Me-JA) and ET in *pcd1,* wild-type Col-0, *pcd1::coi1*, *pcd1::etr1*, and *pcd1::fad3/7/8* would prove informative. This will be accomplished via employing HPLC and GC-MS methods. Thus, analysis of JA/ET content in these unique genetic backgrounds should indicate whether *pcd1* plants accumulate JA/ET and require functional JA/ET signal transduction components to convey resistance to pathogens.

5) Understanding the scope of disease resistance in *pcd1*:

In this, I demonstrated that *pcd1* exhibits heightened resistance against biotrophic fungi and bacterial, and oomycete pathogens. Investigating whether the scope of this resistance extends to other necrotrophic fungi such as *Botrytis cinerea* and *Alternaria*

brassicicola is essential as it reflects on potential biotechnological applications of PCD1.

6) Functional genomic analysis of gene expression in *pcd1:*

In this regard, the Scottish Centre for Genomic Technology and Informatics (SCGTI) the University of Edinburgh) will provide access to high density arrays that is provided by Affymetrix. This genome-wide analysis approach should help providing a comprehensive knowledge of the scope of gene expression in a *pcd1* background (Schena *et al.*, 1998; Schenk *et al.*, 2000). One particular advantage of this approach is to pinpoint genes whose expression is up- or down-regulated in a *pcd1* background. Consequently, nonredundant genes will be selected and double-mutants of these genes with *pcd1* will be generated. Accordingly, analysis of these unique double mutants should shed some light on novel components in the *PCD1*-mediated SAR.

7) Investigating whether PCD1 plays a role in conveying abiotic stress tolerance:

My results indicated that *pcd1* seedlings are not significantly different in its tolerance to salinity and abscisic acid, compared to wild-type. However, I have not tested the response of *pcd1* adult plants. Therefore, I wish to investigate the abiotic stress responses of *pcd1* adult plants to a broad range of abiotic stresses including drought, salinity, freezing treatment, heat shock and heavy metals.

8) Isolation of modifiers of the *pcd1*-mediated cell death:

Interestingly, I demonstrated that the *pcd1* mutation is recessive in a L*er* background. Moreover, BTH was found to be capable of overriding this recessiveness. Therefore, I propose that the ecotype L*er* contain some negative regulators *pcd1* that are controlled by BTH. Thus, mapping these factors that are unique to the L*er* background could yield very interesting results. Alternatively, a mutagenesis approach will be undertaken to identify *pcd1* modifiers in Col-0 background. In this

regard, EMS mutagenises of homozygous *pcd1* plants will be conducted. Screening of these lines, for example, for suppressers of the *pcd1*-mediated cell death and pathogen resistance should help identifying genes that modify that action of *pcd1*.

9) Evaluation of potential biotechnological application of PCD1 for crop protection:

In this regard, database search for *PCD1* orthologues in economically-important crop plants, to ascertain its conservation in the plant kingdom, could yield some interesting findings. Moreover, as it is proposed that PCD1 acts possibly as a positive regulator of cell death, engineering crop plants that overexpress PCD1 should provide heightened resistance to pathogens. In this context, plants transformed with the *PCD1* cDNA under the control of a glucocorticoid- or ethanol- inducible promoter could be advantageous (Slater *et al.*, 1998; McNellis *et al.*, 1998). This inducible system should provide some flexibility whereby the magnitude of cell death in *iPromoter::PCD1* transgenic plants is controlled to avoid any harmful impact on the health of crop plants.

6.2 Investigation of NO-mediated $[Ca^{2+}]_{cyt}$ signalling in *Arabidopsis*

6.2.1 Summary

The first objective of this work was to investigate the Ca^{2+}-mediated NO signalling in *Arabidopsis*. Thus, transgenic plants transformed with the Ca^{2+}-sensitive, luminescent protein aequorin were employed. The NO-donor SNP induced a concentration-dependent luminescence peak (Figure 4.1). Moreover, I demonstrated that the SNP compound is capable of releasing NO in a pH-dependent manner (Figure 4.7). Treatment with the NO-scavenger C-PTIO significantly blunted the SNP-induced luminescence peak (Figure 4.3 C&D). Furthermore, water treatment (data not shown) and potassium ferrocyanide (Figure 4.3 B), a nonfunctional analogue of SNP that can not release NO, resulted in insignificant luminescence.

Taken together, it is concluded that the observed concentration-dependent spike in $[Ca^{2+}]_{cyt}$ is specific to NO. Treatment with increasing concentrations (up to 100 μM) of the general plasma membrane channels blocker La^{3+}, resulted in corresponding concentration-dependent inhibition in SNP-mediated luminescence (Figure 4.2). However, higher concentrations of La^{3+} had no further significant impact on SNP-mediated luminescence (data not shown). Thus, I concluded that both external and internal Ca^{2+} pools are recruited in response to SNP treatment.

The second objective of this work, was to engineer transgenic plants that were compromised in NO mediated signalling. To this end, I have successfully cloned the *E. coil* gene encoding a nitric oxide dioxygenase (NOD) under the control of the constitutive promoter CaMV 35S followed by the *ocs3'* terminator sequence from *Agrobacterium* in the binary transformation vector pART7 (Gleave, 1992) (Figure 4.11 & 4.12 A). Moreover, faithful transcription and translation of the *NOD* was confirmed in some of the tested *35S::HMP/NOD* F1 transgenic plants, namely C2 and A3 lines (Figure 4.12 B&C). Furthermore, protein extracts of these candidates exhibited relatively higher absorption values at λ427 and λ550, indicating the presence of higher heme contents, in these extracts compared to wild-type Col-0. In conclusion, this was taken as an indirect evidence for the proper folding of the HMP/NOD in the tested candidates. Phenotypic examination of lines C2 and A3 indicated no apparent phenotypes. Moreover, lines C2 exhibited a disease resistance response against the bacterial pathogen *Pst* DC3000 that is similar to that of wild-type Col-0 plants.

6.2.2 Future work

6.2.2.1 Further dissection of NO-mediated $[Ca^{2+}]_{cyt}$ signalling

Understanding the precise contribution of external as well as internal Ca^{2+} pools that are mobilised in response to SNP, and other NO donors, is important. This can be achieved through the use of a selection of several well-known external and internal Ca^{2+} channel blockers. Moreover, the importance of each individual Ca^{2+} pool for the expression of downstream defence-related gene expression, e.g. *PAL1* and *PR1*, will be assessed. Furthermore, the effect of known SAR-compromised and defence-response mutants on the observed NO-mediated $[Ca^{2+}]_{cty}$ will be evaluated. The use of the following double mutants should prove useful:

35S::Aequorin::pcd1,
35S::Aequorin::nahG,
35S::Aequorin::npr1,
35S::Aequorin::coi1,
35S::Aequorin::etr1,
35S::Aequorin::eds1,
and *35S::Aequorin::ndr1*

6.2.2.2 Further characterisation of *35S::HMP/NOD* transgenic lines

In this regard, assaying the *in vitro* NOD activity in the protein extracts of *35S::HMP/NOD* lines, by virtue of its NO consumption capacity, by means of an NO-specific electrode, is a straightforward approach in order to ascertain that the *NOD* gene product is active and functional (Gardner *et at.*, 1998a). Moreover, quantification of the build-up in endogenous NO levels in these lines during avirulent plant-bacterial interactions can also be informative (Delledonne *et al.*, 1998). Furthermore, the use of these lines can provide further information as to the

influence *HMP/NOD* overexpression might have on NO-mediated and antioxidant gene transcription.

6.3 Transformation of *Fusarium oxysporum* with *GFP* via particle bombardment

6.3.1 Summary

I have successfully transformed intact fungal spores of the vascular wilt fungus *Fusarium oxysporum* via particle bombardment. The optimised procedure employed herein has reproducibly yielded a transformation efficiency of approx. 45.0 ±5 *Fusarium* transfromants per μg of gGFP plasmid DNA. Emerging hygromycin-resistant transformants were detectable 3 days post-transformation (Figure 5.1). Phenotypic examination of the transformants indicated that the majority of them maintained their parental morphotypes. One transformant was selected and found to exhibit high GFP fluorescence as reported by both fluorescence and confocal microscopy (Figure 5.2). Moreover, the pattern of GFP expression in that transformant appears to be uniformly distributed in the cytoplasm. Furthermore, spectrophotometric examination of GFP fluorescence in protein extracts of selected transformants, further confirmed that the selected transformant exhibits the highest level of fluorescence per μg of total protein (Figure 5.3). Interestingly, the selected transformant maintained its pathogenic ability on wild-type Col-0 tissue culture-grown seedling, and it was able to induce *PDF1.2* gene expression, within 2 hrs post-inoculation, as reported with luciferase imaging (Figure 5.4). However, the transformant failed to develop any noticeable disease symptoms on soil-grown adults Col-0 plants (data were not shown).

6.3.2 Further work

1) Southern analysis on putative transformants:

This should provide an insight as to the mechanism the gGFP vector is maintained in *Fusarium oxysporum*; i.e. whether it is integrated into the fungal genome or maintained as an autosomal plasmid.

2) Employing GFP-transformed *Fusarium* in monitoring fungal growth:

Most of the transformants exhibited slow growth which made it difficult to develop any observable disease symptoms on soil grown plants. Hence, monitoring GFP expression as an indication of fungal growth on leaf surfaces was not possible. As an alternative, examining the infectivity of GFP-expressing transformants through the natural route, i.e. roots, could prove more relevant and successful (Di Pietro *et al.*, 2001).

3) Transformation of other fungi:

The possibility of extending this approach to transform several other necrotrophic fungi, such as *Botrytis cinerea* and *Alternaria brassicicola* will be sought and assessed.

CHAPTER VII

7 BIBLIOGRAPHY

Aarts, N.; Metz, M.; Holub, E.; Staskawicz, B. J.; Daniels, M. J. and Parker, J. E. (1998). Different requirements for the *EDS1* and *NDR1* by disease resistance genes define at least two *R* gene-mediated signaling pathways in *Arabidopsis*. *Proc. Natl. Acad. Sci. USA*, 95: 10306-10311.

Abei, H. (1984). Catalase *in vitro*. *Methods Enzymol.*, 105: 121-126.

Adam, A.; Farkas, T.; Somlyai, G; Hevesi, M. and Kiraly, Z. (1989). Consequence of O_2^- generation during becterially induced hypersensitive reaction in tobacco: deterioration of membrane lipids. *Physiol. Mol. Plant Pathol.*, 34: 13-26.

AGI, the *Arabidopsis* Genome Initiative (2000). Analysis of the genome sequence of the flowering plant *Arabidopsis thaliana*. *Nature*, 408: 796-85.

Agrios, G. N. (1997). Plant Pathology. Fourth Edition, Academic Press.

Agrios, G.N. (1988). Vascular wilts caused by ascomycetes and imperfect fungi. In *Plant Pathology,* pp. 408-422. San Deigo: Academic Press, London.

Alamillo, J. and Garcia-Olmedo, F. G. (2001). Effects of urate, a natural inhibitor of peroxinitrite-mediated toxicity, in the response of *Arabidopsis thaliana* to the bacterial pathogen *Pseudomonas syringae*. *Plant J.*, 25: 529-540.

Alexander, D.; Glascock, C.; Pear, J.; Stinson, J,; Ahl-Goy, P.; Gut-Rella, M.; Goodman, R. M. and Ryals, J. (1993). Systemic acquired resistance in tobacco: Use of transgenic expression to study the functions of PR proteins. In: Advances in Molecular Genetics of Plant-Microbe Interactions, eds. E. W. Nester and D. P. S. Verma, pp. 527-533. Kluwer Academic Publishers, Dordrecht.

Alfano, J. R. and Collmer, A. (1997). The type III (Hrp) secretion pathway of plant pathogenic bacteria: trafficking harpins, Avr proteins, and death. *J. Bacteriol.,* 179: 5655-62.

Allan ,C. A. and Fluhr, R. (1997). Two distinct sources of elicited reactive oxygen species in tobacco epidermal cells. *Plant Cell*, 9: 1559-1572.

Allen, G. I.; Kwak, J. M.; Chu, S. P.; Llopis, L.; Tsien, R. Y.; Harper, J. F. and Schroeder, J. I. (1999). Cameleon calcium indicator reports cytoplasmic dynamics in Arabidopsis guard cells. *Plant J.*, 19: 735-747.

Allen, R. D. (1995). Dissection of oxidative stress tolerance using transgenic plants. *Plant Physiol.*, 107: 1049-1054.

Alonso, J. M.; Hirayama, T.; Roman, G.; Nourizadeh, S. and Ecker, J. R. (1999). EIN2, a bifunctional transducer of ethylene and stress responses in *Arabidopsis*. *Science*, 284: 2148-2152.

Alscher, R. G. (1989). Biosynthesis and antioxidant function of glutathione in plants. *Physiol. Plant*, 77: 457-467.

Alvarez, M. E.; Pennell, R. I.; Meijer, P.-J.; Ishikawa, A.; Dixon, R. A. and Lamb, C. (1998). Reactive oxygen intermediates mediate a systemic signal network in the establishment of plant immunity. *Cell*, 92: 773-784.

Andre, D; Colau, D.; Schell, J. Van Montagu, M. and Hernalsteens, J.-P. (1986). Gene Tagging in Plants by a T-DNA insertion mutagen that generates APH(3')II-plant gene fusions. *Mol. Gen. Genet.*: 512-518.

Argueso, C. and Delaney, T. P. (2001). SAR-independent resistance mutants in *Arabidopsis*. In: Abstracts (poster 104) 10th International Congress on Molecular Plant-Microbe Interactions. Madison Wisconsin, July 10-14.

Armaleo, D.; Ye, G. N.; Klein, T. M.; Shark, K. B.; Sanford, J. C. and Johnston, S. A. (1990). Biolistic nuclear transformation of *Saccharomyces cerevisiae* and other fungi. *Curr. Genet.*, 17: 97-103.

Baier, M. and Dietz, K. J. (1997). The plant 2-Cys peroxiredoxin BAS1 is a nuclear-encoded chloroplast protein: its expressional regulation, phylogenetic origin, and implications for its specific physiological function in plants. *Plant J.,* 12:179-190.

Baier, M.; Noctor, G.; Foyer, C. H. and Dietz, K.-J. (2000). Antisense suppression of 2-cysteine peroxiredoxin in *Arabidopsis* specifically enhances the activities and expression of enzymes associated with ascorbate metabolism but not glutathione metabolism. *Plant Physiol.*, 124:823-32.

Bailey, A. M.; Mena, G. L. and Herrera-Estrela, L. (1993). Transformation of four pathogenic Phytophthora spp by microprojectile bombardment on intact mycelia. *Curr. Genet.*, 23: 42-46.

Baker, B.; Zambryski, P.; Staskawicz, B. and Dinesh-Kumar, S. P. (1997). Signaling in plant microbe interactions. *Science*, 267:726-733.

Baker, C. J. and Orlandi, E. W. (1995). Active oxygen species in plant pathogenesis. *Ann. Rev. Phytopathol.*, 33: 299-321.

Barroso, J. B.; Corpas, F. J.; Carreras, A.; Sandalio, L. M.; Valderama, R.; Palma, J. A.; Lupianez, J. A. and del Rio, L. A. (1999). Localization of nitric oxide synthase in plant peroxisomes. *J. Biol. Chem.*, 274: 36729-36733.

Barroso, J. B; Corpas, F. J.; Carreras, A.; Sandalio, L. M.; Valderrama, R.; Palma, J. M.; Lupianez, J. A. and del Rio, L. A. (1999). Localization of nitric oxide synthase in plant peroxisomes. *J. Biol. Chem.*, 274: 36729-36733.

Beachy, R. N. (1999). Coat-protein-mediated resistance to tobacco mosaic virus: discovery mechanisms and exploitation. *Philos. Trans. R. Soc. Lond. B. Biol. Sci.*, 354:659-664.

Beck, K. F.; Eberhardt, W.; Frank, S.; Huwiler, A.; Messmer, U. K.; Muhl, H. and Pfeilschifter, J. (1999). Inducible NO synthase: role in cellular signalling. *J. Exp. Biol.*, 202: 645-653.

Behringer, J.; and Medford, J. (1992). A Plasmid rescue technique for the recovery of plant DNA disrupted by T-DNA Insertion. *Plant Mol. Biol. Rep.*, 10(2): 190-198.

Beligni, M. W. and Lamattina, L. (2000). Nitric oxide stimulates seed germination and de-etiolation, and inhibits hypocotyl elongation, three light-inducible responses in plants. *Planta,* 210: 215-221.

Bell, C. J. and Ecker, J. R. (1994). Assignment of 30 microsatellite loci to the linkage map of *Arabidopsis*. *Genomics*, 19, 137-144.

Bendahmane, A.; Kohm, B. A.; Dedi, C. and Baulcombe, D. C. (1995). The coat protein of the potato virus X is a strain-specific elicitor of Rx1-mediated resistance in potato. *Plant J.*, 8: 933-941.

Berkels, R.; Surehoff, S.; Roesen, R. and Klaus, W. (2000). Nitric oxide causes a cGMP-independent intracellular calcium rise in porcine endothelial cells- a paradox?. *Microvascular Res.*, 59: 38-44.

Berna, A. and Bernier, F. (1999). Regulation by biotic and abiotic stress of a wheat germin gene encoding oxalate oxidase, a H2O2-producing enzyme. *Plant Mol. Biol.* 39:539-49.

Berridge, M. J. (1993a). Inositol triphosphate and calcium signalling. *Nature,* 361: 315-325.

Berridge, M. J. (1993b). A tale of two messengers. *Nature,* 365: 388-389.

Bhalla, U. and Iyengar, R. (1999). Emergent properties of networks of biological signaling pathway. *Science*, 283: 381-387.

Bicanic, D.D.; Harren, F.; Reuss, J.; Woltering, E.; Snel, J.; Voesenek, L.A.C.J.; Zuidberg, B., Jalink, H.; Bijnen, F.; Bolm, C.W.P.M.; Sauren, H.; Kooijman, M.; van Hove, L. and Tonk, W. (1989). Trace detection in agriculture and biology. In: Photoacoustic and Photochemical Processes in Gases (Ed. P. Hess). Springer Verlag Heidelberg, pp. 213-245.

Bijnene, F.G.C.; Brugman, T.; Harren, F.J.M. and Reuss, J. (1992). A liquid nitrogen cooled CO-laser in a photoacoustic set up monitors low gas concentrations. In: Springer Series in Optical Science 69 (Ed. D.D.Bicanic). Springer Verlag Heidelberg, pp. 12-15.

Bittner-Eddy, P. D. and Beynon, J. L. (2001). The *Arabidopsis* downy mildew resistance gene, *RPP13-Nd*, functions independently of NDR1 and EDS1 and does not require the accumulation of salicylic acid. *Mol. Plant Microbe Interact.*, 14: 416-421.

Bittner-Eddy, P. D; Crute, I. R.; Holub, E.B. and Beynon, J.L. (2000). *RPP13* is a simple locus in *Arabidopsis thaliana* for alleles that specify downy mildew resistance to different avirulent determinants in *Peronospora parasitica*. *Plant J.*, 21: 177-188.

Bokoch, G. M. (1994). Regulation of the human neutrophil NADPH oxidase by the Rac GTP-binding proteins. *Curr. Opin. Cell Biol.*, 6: 212-218.

Bolker, M.; Bonhert, H.U.; Braun, K.H.; Gorl, J. and Kahmann, R. (1995). Tagging pathogenicity genes in *Ustilago maydis* by restriction enzyme-mediated integration (REMI). *Mol. Gen. Genet.*, 248: 547-552.

Bolwell, G. P. and Wojtaszek, P. (1997). Mechanisms for the generation of reactive oxygen species in plant defence-a broad prespective. *Physiol. Mol. Plant Pathol.*, 51: 347-366.

Bonas, U. and Van den Ackerveken, G. (1999). Gene-for-gene interactions: bacterial avirulence proteins specify plant disease resistance. *Curr. Opin. Microbiol.*, 2: 94-98.

Borevitz, J. O.; Xia, Y.; Blount, J.; Dixon, R. A. and Lamb, C. (2000). Activation tagging identifies a conserved MYB regulator of phenylpropanoid biosynthesis. *Plant Cell*, 12: 2383-2394.

Bowell, G. P.; Butt, V. S.; Davies, D. R. and Zimmerlin, A. (1995). The origin of the oxidative burst in plants. *Free Radicals Res.*, 23: 517-532.

Bowling, S. A.; Clarke, J. D.; Liu, Y.; Klessig, D. F. and Dong, X. (1997). The *cpr5* mutant of *Arabidopsis* expresses both *npr1*-dependent and *npr1*-independent resistance. *Plant Cell*, 9: 1573-1584.

Bowling, S. A.; Guo, A.; Cao, H.; Gordon, A. S.; Klessig, D. F. and Dong, X. (1994). A mutation in *Arabidopsis* that leads to constitutive exspression of systemic acquired resistance. *Plant Cell*, 6: 1845-1857.

Boyes, D. C.; Nam, J. and Dangl, J. L. (1998). The *Arabidopsis thaliana* RPM1 disease resistance gene product is a peripheral plasma membrane protein that is degraded coincident with the hypersensitive response. *Proc. Natl. Acad. Sci. USA*, 95: 15849-15854.

Bradford, M. M. (1976). A rapid and sensitive method for the quantitation of microgram quantities of protein utilizing the principle of protein-dye binding. *Anal. Biochem.*, 72:248-254.

Brown, E. G. and Newton, R. P. (1992). Analytical procedures for cyclic nucleotides and their associated enzymes in plant tissue. *Phytochem. Anal.*, 3: 1-13.

Browning, D. D.; McShane, M. P.; Marty, C. and Ye, R. D. (2000). Nitric oxide activation of p38 mitogen-activated protein kinase in 293T fibroblasts requires cGMP-dependent protein kinase. *J. Biol. Chem.*, 275: 2811-2816.

Brüne, B., von Knethen, A. & Sandau, K. B. (1998). *Eur. J. Pharmacol.*, 351: 261-272.

Bryan, G. T.; Wu, K. S.; Farrall, L.; Jia, Y.; Hershey, H. P.; McAdams, S. A.; Faulk, K. N.; Donaldson, G. K.; Tarchini, R. and Valent, B. (2000). A single amino acid difference distinguishes resistant and susceptible alleles of the rice blast resistance gene Pi-ta. *Plant Cell*, 12:2033-2046.

Buschges, R. K.; Hollricher, K.; Panstruga, R.; Simons, G.; Wolter, M.; Frijters, A.; Van Daelen, R.; Van Der Lee, T.; Diergaarde, P.; Groenendijk, J.; Topsch, S.; Vos, P.; Salamini, F. and Schulze-Lefert, P. (1997). The barley *Mlo* gene: a novel control element of plant pathogen resistance. *Cell*, 88: 695-705.

Bush, D. S. (1995). Calcium regulation of in plant cells and its role in signaling. *Annu. Rev. Plant Physiol. Plant Mol. Biol.*, 46: 95-122.

Bush, D.S. and Jones, R.L. (1990). Measuring intracellular Ca^{2+} levels in plant cells using the fluorescent probes, Indo-1 and Fura-2. *Plant Physiol.* 93: 841-845.

Campbell, A. K. (1988). Chemiluminescence: Principles and Applications in Biology and Medicine. Chicester, UK: Horwood/VCH.

Campbell, A.K. (1983). Interacellular calcium-its universal role as regulator. Wiley, Chichester, UK. 556 pp.

Cao, H.; Bowling, S. A.; Gordon, A. S.and Dong, X. N. (1994). Characterization of an *Arabidopsis* mutant that is nonresponsive to inducers of systemic acquired resistance. *Plant Cell*, 6: 1583-1592.

Cao, H.; Glazebrook, J.; Clarke, J. D.; Volko, S. and Dong, X. (1997). The *Arabidopsis NPR1* gene that controls systemic acquired resistance encodes a novel protein containing ankyrin repeats. *Cell*, 88: 57-63.

Cao, H.; Li, X. and Dong, X. (1998). Generation of broad-spectrum disease resistance by overexpression of an essential regulatory gene in systemic acquired resistance. *Proc. Natl. Acad. Sci. USA*, 95: 6531-6536.

Century, K. S.; Shapiro, A. D.; Repetti, P. P.; Dahlbeck, D.; Holub, E. and Staskawicz, B. J. (1997). NDR1, a pathogen-induced component required for *Arabidopsis* disease resistance. *Science*, 278: 1963-1965.

Cessna, S.; Chandra, S. and Low, P. S. (1998). Hypo-osmotic shock of tobacco cells stimulates Ca^{2+} fluxes deriving first from external and then internal Ca^{2+} stores. *J. Biol. Chem.*, 273: 27286-27291.

Chandra, S. and Low, P. S. (1997). Measurement of Ca2+ fluxes during elicitation of the oxidative burst in aequorin-transformed tobacco cells. *J. Biol. Chem.*,272:28274-28280.

Chandra, S.and Low, P. S. (1995). Role of phosphorylation in elicitation of the oxidative burst in cultured soybean cells. *Proc. Natl. Acad. Sci. USA*, 92:4120-4123.

Chang, C.; Kwok, S. F.; Bleecker, A. B.; and Meyerowitz, E. M. (1993). Arabidopsis ethylene-response gene ETR1: similarity of product to two-component regulators. *Science*, 262:539-544.

Chaure, P.; Gurr, S. J. and Spanu, P. (2000). Stable transformation of *Erisiphe graminis*, an obligate biotrophic pathogen of barley. *Nature Biotech.*, 18: 205-207.

Chen, L., Xie, Q. W. & Nathan, C. (1998). Alkyl hydroperoxide reductase subunit C (AhpC) protects bacterial and human cells against reactive nitrogen intermediates. *Mol. Cell,* 1: 795-805.

Chen, Z.; Silva, H. and Klessig, D. F. (1993). Active oxygen species in the induction of plant systemic acquired resistance by salicylic acid. *Science*, 262: 1883-1885.

Chester, K. S.(1933). The problem of acquired physiological immunity in plants. *Q. Rev. Biol.*, 8: 275-324.

Cho, R. J.; Mindrinos, M.; Richards, D. R.; Sapolsky, R. .J.; Anderson, M.; Drenkard, E.; Dewdney, J.; Reuber, T. L.; Stammers, M.; Federspiel, N.; Theologis, A.; Yang, W. H.; Hubbell, E.; Au, M.; Chung, E. Y. Lashkari, D., Lemieux, B.; Dean, C.; Lipshutz, R. J.; Ausubel, F. M.; Davis, R. W. and Oefner, P. J. (1999). Genome-wide mapping with biallelic markers in *Arabidopsis thaliana*. *Nat. Genet.*, 23:203-207.

Chrispeels, M. J.; Holuigue, L., Latorre, R.; Luan, S.; Orellana, A. Pena-Cortes, H.; Raikhel, N. V.; Ronald, P. C. and Trewavas, A. (1999). Signal transduction networks and biology of plant cells. *Biol. Res.,* 32: 35-60.

Church, G. M. and Gilbert, W. (1984). Genomic sequencing. *Proc. Natl. Acad. Sci. USA*, 81: 1991-1995.

Clark, D.; Durner, J.; Navarre, D. A. and Klessig, D. F. (2000). Nitric oxide inhibition of tobacco catalase and ascorbate peroxidase. *Mol. Plant Microbe Interact.*, 13: 1380-1384.

Clarke, A.; Desikan, R.; Hurst, R. D.; Hancock, J. T. and Neill, S. J. (2000). NO way back: nitric oxide and programmed cell death in *Arabidopsis* suspension cultures. *Plant J.*, 24: 667-677.

Clarke, J. D.; Aarts, N.; Feys, B. J.; Dong, X. and Parker, J. E. (2001). Constitutive disease resistance requires EDS1 in the *Arabidopsis* mutants *cpr1* and *cpr6* and is partially EDS1-dependent in *cpr5*. *Plant J.*, 26: 409-420.

Clarke, J. D.; Liu, Y.; Klessig, D. F. and Dong, X. (1998). Uncoupling *PR* gene expression from *NPR1* and bacterial resistance: characterization of the dominant *Arabidopsis cpr6-1* mutant. *Plant Cell*,10: 557-569.

Clarke, J. D.; Volko, S. M.; Ledford, H.; Ausubel, F. M. and Dong, X. (2000). Roles of salicylic acid, jasmonic acid, and ethylene in *cpr*-induced resistance in *Arabidopsis*. *Plant Cell*, 12: 2175-2190.

Clough, S. J. and Bent, A. F. (1998). Floral dip: a simplified method for Agrobacterium-mediated transformation of *Arabidopsis thaliana*. *Plant J.*, 16:735-743.

Clough, S. J.; Fengler, K. A.; Yu, I. C., Lippok, B.; Smith, RK Jr., Bent AF. (2000). The *Arabidopsis dnd1* 'defense, no death' gene encodes a mutated cyclic nuceotide-gated ion channel. *Proc. Natl. Acad. Sci. USA* 97, 9323-9328.

Cohen, Y.; Guegler, K.; Moesinger, E. and Niderman, T. (1992). Plant pathogenesis-related proteins. *Inter. Patent Applic.* NO. WO92/20800.

Conrath, U.; Chen, Z.; Ricigliano, J. R. and Klessig, D. F. (1995). Two inducers of plant defense responses, 2,6-dichloroisonicotinec acid and salicylic acid, inhibit catalase activity in tobacco. *Proc. Natl. Acad. Sci. USA*, 92: 7143-7147.

Conrath, U.; Silva, H. and Klessig, D. F.(1997). Protein dephosphorylation mediates salicylic acid-induced expression of *PR-1* genes in tobacco. *Plant J.* 11, 747-757.

Cooley, M. B.; Pathirana, S.; Wu, H. J.; Kachroo, P. and Klessig, D. F. (2000). Members of the *Arabidopsis HRT/RPP8* family of resistance genes confer resistance to both viral and oomycete pathogens. *Plant Cell*, 12: 663-676.

Cooper, C. E. (ed.) (1999). Nitric oxide biochemistry. *Biochem. Biophys. Acta,* 1411: 217-488.

Creelman, R. A. and Mullet, J. E. (1997). Biosynthesis and action of jasmonate in plants. *Annu.Rev. Plant Pathol. Physiol. Plant Mol. Biol.*, 48: 355-381.

Croft, K. P. C.; Viosey, C. R. and Slusarenko, A. J. (1990). Mechanisms of hypersensitive cell collapse: correlation of increased lipoxygenase activity with membrane damage in leaves of *Phaseolus vulgaris* (L.) inoculated with an avirulent race of *Pseudomonas syringae* pv *phaseolicola*. *Physiol. Mol. Plant Pathol.*, 36: 49-62.

Cubitt, A. B.; Heim, R.; Adams, S. R.; Boyd, A. E.; Gross, L. A. and Tsien, R. Y (1995). Understanding, improving and using green fluorescent proteins. *Trends Biochem. Sci.*, 20: 448-455.

Dangl, J. (1998). Innate immunity. Plants just say NO to pathogens. *Nature,* 394: 525-526.

Dangl, J. L. (1994). The enigmatic avirulence genes of phytopathogenic bacteria. *Curr. Top. Microbiol. Immunol.*, 192: 99-118.

Dangl, J. L. R.; Dietrich, R. A. and Richberg, M. H.(1996). Death don't have mercy: cell death programs in plant-microbe interactions. *Plant Cell*, 8: 1793-1807.

Darvill, A.; Bergmann, C.; Cervone, F.; De Lorenzo, G.; Ham, K. S.; Spiro, M. D.; York, W. S. and Albersheim, P. (1994). Oligosaccharins involved in plant growth and host-pathogen interactions. *Biochem. Soc. Symp.*, 60:89-94.

de Wit, P. J. G. M. and Joosten, M. H. A. J. (1999). Avirulence and resistance genes in the *Cladosporium fulvum*-tomato interactions. *Curr. Opin. Microbiol.*, 2: 368-373.

De Lorenzo, G.; Ovidio, R. D.and Cervone, F. (2001). The role of polygalacturonase-inhibiting proteins (PGIPs) in defense against pathogenic fungi. *Annu. Rev. Phytopathol.*, 39:313-335.

del Pozo, O. and Lam, E. (1998). Caspases and programmed cell death in the hypersensitive response of plants to pathogens. *Curr. Biol.*, 8:R896.

Delaney, T. P.; Freidrich, L. and Ryals, J. A. (1995). *Arabidopsis* signal transduction mutant defective in chemically and biologically induced disease resistance. *Proc. Natl. Acad. Sci. USA*, 92: 6602-6606.

Delaney, T. P.; Uknes, S.; Vernooij, B.; Friedrich, L.; Weymann K.; Negrotto, D.; Gaffney, T.; Gut-Rella, M.; Kessmann, H.; Ward, E. and Ryals, J. (1994). A central role of salicylic acid in plant disease resistance. *Science*, 226: 1247-1250.

Delledonne, M.; Xia, Y.; Dixon, R. A. and Lamb, C. (1998). Nitric oxide functions as a signal in plant disease resistance. *Nature,* 394:585-588.

Demarty, M.R.; Morvan, C. and Thellier, M. (1984). Clacium and the cell wall. *Plant Cell Environ.*, 7: 441-448.

Dempsey, D. A.; Pathirana, M .S.; Wobbe, K. K. and Klessig, D .F. (1997). Identification of an Arabidopsis locus required for resistance to turnip crinkle virus. *Plant J.*, 11:301-311.

Despres, C.; DeLong, C.; Glaze, S.; Liu, E. and Fobert, P. R. (2000). The *Arabidopsis NPR1/NIM1* protein enhances the DNA binding activity of a subgroup of the TGA family of bZIP transcription factors. *Plant Cell*, 12: 279-290.

Dewdney, J.; Reuber, T. L.; Wildermuth, M. C.; Devoto, A.; Cui, J.; Stutius, L. M.; Drummond, E. P. and Ausubel, F. M. (2000). Three unique mutants of *Arabidopsis* identify *eds* loci required for limiting growth of a biotrophic pathogen. *Plant J.*, 278: 205-218.

Di Pietro, A.; García-Maceira, F.I.; Méglecz, E. and Roncero, I.G. (2001). A MAP kinase of the vascular wilt fungus *Fusarium oxysporum* is essential for root penetration and pathogenesis. *Mol. Microbiol.*, 39: 1140-1152.

Dietrich, R. A.; Delaney, T. P.; Uknes, S. J.; Ward, E. R.; Ryals, J. A. and Dangl, J. L. (1994). Arabidopsis mutants simulating disease resistance response. *Cell*, 77: 565-577.

Dietrich, R. A.; Richberg, M. H.; Schmidt, R.; Dean, C. and Dangl, J. L. (1997). A novel zinc finger protein is encoded by the *Arabidopsis LSD1* gene and functions as a negative regulator of cell death.. *Cell*, 88: 685-694.

Digonnet, C.; Aldon, D.; Leduc, N.; Dumas, C. and Rougier, M. (1998). First evidence of a calcium transient in flowering plants at fertilization. *Development,* 124: 2867-2874.

Ding, H. and Demple, B. (2000). Direct nitric oxide signal transduction via nitrosylation of iron-sulfur centrers in the SoxR transcription activator. *Proc. Natl. Acad; Sci. USA,* 9: 5146-5150.

Dixon, R. A.; Harrison, M. S. and Lamb, C. (1994). Early events in the activation of plant defence responses. *Annu. Rev. Phytopathol.*, 32: 479-501.

Dixon, R. A.; Lamb, C. J.; Masoud, S.; Sewalt, V. J. and Paiva, N. L. (1996). Metabolic engineering: prospects for crop improvement through the genetic manipulation of phenylpropanoid biosynthesis and defense responses--a review. *Gene*, 179:61-71.

Doares, S. H.; Narvaez-Vasquez, J.; Conconi, A. and Ryan, C. A. (1995). Salicylic acid inhibits synthesis of proteinase inhibitors in tomato leaves induced by systemin and jasmonic acid. *Plant Physiol.*, 108: 1741-1746.

Draper, J. (1997). Salicylate, superoxide synthesis and cell suicide in plant defence. *Trends Plant Sci.*, 2: 162-165.

Du, H. and Klessig, D. F. (1997). Identification of a soluble, high-affinity salicylic acid-binding protein in tobacco. *Plant Physiol.*, 113: 1319-1327.

Duijff, B. J.; Pouhair, D.; Alabouvette, C. and Lemanceau, P. (1998). Implication of systemic induced resistance in the suppression of fusarium wilt of tomato by *Pseudomonas fluorescens*

WCS417r and by nonpathogenic *Fusarium oxysporum* Fo47. *Eur. J. Plant Pathol.*, 104: 903-910.

Dumas, B. ; Freyssinet, G. and Pallet, K. E. (1997). Tissue-specific expression of germin-like oxalate oxidase during development and fungal infection of barley seedlings. *Plant Physiol.*, 107: 1091-1096.

Durner, J.; Wendehenne, D. and Klessig, D. F. (1998). Defense gene induction of tobacco by nitric oxide, cyclic GMP and cyclic ADP-ribose. *Proc. Natl. Acad. Sci. USA,* 95: 10328-10333.

Ehrhardt, D. W. (1996). Calcium spiking in plant root hairs responding to *Rhizobium* nodulcation signals. *Cell,* 85: 673-681.

Ellis, C. and Turner, J.G. (2001). The Arabidopsis mutant *cev1* has constitutively active jasmonate and ethylene signal pathways and enhanced resistance to pathogens. *Plant Cell*, 13:1025-1033.

Ellis, J. G.; Lawrence, G. J.; Luck, J. E. and Dodds, P. N (1999). Identification of regions in alleles of the flax rust resistance gene L that determine differences in gene-for-gene specificity. *Plant Cell*, 3:495-506.

Ellis, J.; Dodds, P. and Pryor, T (2000). Structure, function and evolution of plant disease resistance genes. *Curr. Opin. Plant Biol.*, 4:278-84.

Epple, P.; Apel, K. and Bohlmann, H. (1995). An *Arabidopsis thaliana* thionin gene is inducible via a signal transduction pathway different from that for pathogenesis-related proteins. *Plant Physiol.*,109: 813-820.

Epple, P.; Apel, K. and Bohlmann, H. (1997). Overexpression of an endogenous thionin ehances resistance of *Arabidopsis* against *Fusarium oxysporum*. *Plant Cell*, 9: 509-520.

Epple, P.; Vignutelli, A.; Apel, K. and Bohlmann, H. (1998). Differential inducation of the *Arabidopsis thaliana Thi*2.1 gene by *Fusarium oxysporum* f. sp. *matthiolae*. *Mol. Plant Microbe Interactions*, 11: 523-539.

Erickson, F. L.; Dinesh-Kumar, S. P.; Holzberg, S.; Ustach, C. V.; Dutton, M.; Handley, V.; Corr, C. and Baker, B. J. (1999). Interactions between tobacco mosaic virus and the tobacco *N* gene. *Phil. Trans. R. Soc. Lond.*, 354: 653-658.

Falk, A.; Feys, B. J.; Frost, L. N.; Jones, J. D.; Daniels, M. J. and Parker, J. E. (1999). EDS1, an essential component of R gene-mediated disease resistance in *Arabidopsis* has homology to eukaryotic lipases. *Proc. Natl. Acad. Sci. USA*, 9: 3292-3297.

FAO, Food and Aqricultural Organisation Production Year Book (1993).

Feldmann, K. A. (1991). T-DNA Insertion Mutagenesis in *Arabidopsis*: Mutational Spectrum. *Plant J.*, 1: 71-82.

Felton, G. W.; Korth, K. C.; Bi, J. L.; Wesley, S.V; Huhman, D. V.; Mathews, M. C.; Murphy, J. B.; Lamb, C. and Dixon, R. A. (1999). Inverse relationship between systemic resistance to microorganisms and to insect herbivory. *Curr. Biol.*, 9: 317-320.

Fink, W.; Deising, H. and Mendgen, K. (1991). Early defense responses of cowpeas (*Vigna sinensis* L.) induced by non-pathogenic rust fungi. *Planta*, 185: 246-254.

Flor, H. H. (1971). Current status of the gene-for-gene concept. *Ann. Rev. Phytopathol.*, 9: 275-296.

Foissner, I. *et al.* (2000). Imaging of an elicitor-induced nitric oxide burst in tobacco. *Plant J.,* 23: 817-824.

Forbes, P. J.; Millam, S.; Hooker, J. E. and Harrier, L. A. (1998). Transformation of the arbuscular mycorrhiza *Gigaspora rosea* by particle bombardment. *Mycol. Res.*, 102: 497-501.

Freialdenhoven, A.; Scherag, B.; Hollricher, K.; Collinge, D. B.; Thordal-Christensen, H. and Schulze-Lefert, P. (1994). *Nar-1* and *Nar-2;* two loci required for Mla_{12}-specified race-specific resistance to powedery mildew in barley. *Plant Cell*, 6: 983-994.

Friedrich, L.; Vernnoij, B.. Gaffney, T.; Morse, A. and Ryals, L. (1995). Characterization of tobacco plants expressing a bacterial salicylate hydroxylase gene. *Plant Mol. Biol.*, 29: 959-968.

Fry, S. C. (1986). Cross-linking of matrix polymers in the growing cell walls of angiosperms. *Annu. Rev. Plant Physiol.*, 37: 165-186.

Fry, W. E. (1982). Principles of plant disease management. Academic Press, New York.

Frye, C. A. and Innes, R. W. (1998). An *Arabidopsis* mutant with enhanced resistance to powdery mildew. *Plant Cell*, 10: 947-956.

Frye, C. A.; Tang, D. and Innes, R. W. (2000). Negative regulation of defense responses in plants by a conserved MAPKK kinase. *Proc. Natl. Acad. Sci. USA*, 98: 373-378.

Fungaro, M. H. P.; Rech, E.; Muhlen, G. S.; Vainstein, M. H.; Pascon, R. C.; de Queiroz, M. V.; Pizzirani-Kleiner, A. A. and de Azevedo, J. L. (1995). Transformation of *Apergillus nidulans* by microprojectile on intact conidia. *FEMS Microbiol. Lett.*, 125: 293-298.

Gaffney, T.; Friedrich, L.; Vernooij, B.; Negrotto, D.; Nye, G.; Ukness, S.; Ward, E.; Kessman, H. and Ryals, J. (1993). Requirement of SA for the induction of SAR. *Science*, 201: 754-756.

Galbiati, M.; Moreno, M. A.; Nazdan, G.; Zourelidou, M. and Dellaporta, S. L. (2000). *Funct. Integr. Genomics*, 1:25-34.

Gardner, P. R.; Gardner, A. M.; Martin, L. A. and Salzman, A. L. (1998). Nitric oxide dioxygenase: An enzyme function for flavohemoglobin. *Proc. Natl. Acad. Sci. USA,* 95: 10378-10383.

Gardner, P.R., Constantino, G. and Salzman, A.L. (1998b). Constitutive and adaptive detoxification of nitric oxide in *Escherichia coli*. Role of nitric-oxide dioxygenase in the protection of aconitase. *J. Biol. Chem.*, 273: 26528-26533.

Gardner, P.R.; Garnder, A.M.; Martin, L.A. and Salzman, A.L. (1998a). Nitric oxide dioxygenase: An enzymic function for flavohemoglobin. *Proc. Natl. Acad. Sci. USA*, 95: 10378-10383.

Genoud, T. and Metraux, J.-P. (1999). Crosstalk in plant cell signaling: structure and function of the genetic network. *Trends Plant Sci.*, 4: 503-507.

Gibson, S and Somerville, C. .R. (1993). Isolation of plant genes. *Trends Biotech.*, 11: 306-313.

Gilroy, S. (1997). Fluorescence microscopy of living plant cells. *Annu. Rev. Plant. Physiol. Plant Mol. Biol.* 48: 165-190. Nitric oxide induces dose-dependent Ca^{2+} transients and causes temporal morphological hyperpolarization in human neutrophils (2000). *J. Cell. physiol.*,182: 402-413.

Glazebrook, J. and Ausubel; F. M. (1994). Isolation of phytoalexin-deficient mutants of *Arabidopsis thaliana* and characterization of their interactions with bacterial pathogens. *Proc. Natil. Acad. Sci.* 91: 8955-8959.

Glazebrook, J.; Rogers, E. E.; and Ausubel F. M. (1997a). Use of Arabidopsis for genetic dissection of plant defense responses. *Annu. Rev. Genet.*, 31:547-69.

Glazebrook, J.; Zook, M.; Mert, F.; Kagan, I.; Rogers, E. E.; Crute, I. R.; Holub, E. B.; Hammerschmidt, R. and Ausubel, F. M. (1997b). Phytoalexin-deficient mutants of *Arabidopsis* reveal that *PAD4* encodes a requlatory factor and that four *PAD* genes contribute to downy mildew resistance. *Genetics*, 146: 381-392.

Gleave, A. P. (1992). A versatile binary vector system with a T-DNA organisational structure conductive to efficient integration of cloned DNA into the plant genome. *Plant Mol. Biol.*, 20: 1203-1207.

Gong, M. (1998). Heat-shock-induced changes in intracellular Ca^{2+} level in tobacco seedlings in relation to thermotolerance. *Plant Physiol.,* 116: 429-437.

Govrin, E. M. and Levine, A. (2000). The hypersensitive response facilitates plant infection by the necrotrophic pathogen *Botrytis cinerea*. *Curr. Biol.*, 10: 751-757.

Graham, M. Y. and Graham, T. L. (1991). Rapid accumulation of anionic peroxidases and phenolic polymers in soybean cotyleson tissues following treatment with *Phytophthora megasperma* f.sp. *glycinea* wall glucan. *Plant Physiol.*, 97: 1445-455.

Grant, J. J. and Loake, G. J. Role of reactive oxygen intermediates and cognate redox signaling in disease resistance (2000). *Plant Physiol.*, 124:21-9.

Grant, J. J.; Yun, B.-W. and Loake, G. J. (2000). Oxidative burst and cognated redox signalling reported by luciferase imaging; identification of a signal network that functions independently of ethylene, SA and Me-JA but is dependent on MAPKK activity. *Plant J.*, 24: 1-16.

Grant, M.; Brown, I.; Adams, S.; Knight, M.; Ainslie, A. and Mansfield, J. (2001). The RPM1 plant disease resistance gene facilitates a rapid and sustained increase in cytosolic calcium that is necessary for the oxidative burst and hypersensitive cell death. *Plant J.,* 23:441-450.

Gray, J. P.; Close, P. S.; Briggs, S. P. and Johal, G. S. (1997). A novel suppressor of cell death in plants encoded by the *Lls1* gene of maize. *Cell*, 89: 25-31.

Greenberg, J. T. (1996). Programmed cell death: A way of life for plants. *Proc. Natl. Acd. Sci. USA*, 93: 1204-12097.

Greenberg, J. T. (2000). Positive and negative regulation of salicylic acid-dependent cell death and pathogen resistance in *Arabidopsis lsd6* and *ssi1*. *Mol. Plant Microbe Interact.*, 13: 877-881.

Greenberg, J. T. and Ausubel, F. M. (1993). *Arabidopsis* mutants compromised for the control of cellular damage during pathogenesis and aging. *Plant J.* 4, 327-341.

Greenberg, J. T.; Silverman, F. P. and Liang, H (2000). Uncoupling salicylic acid-dependent cell death and defense-related responses from disease resistance in the Arabidopsis mutant acd5. *Genetics*, 156:341-350.

Greenberg, J.; Guo, A.; Klessig, D. F. and Ausubel, F. M. (1994). Programmed cell death in plants: a pathogen-triggered response activated coordinately with multiple defense functions. *Cell*, 77: 551-563.

Groom, Q. J.; Torres, M. A.; Fordham-Skelton, A. P.; Hammond-Kosack, K. E.; Robinson, N. J. and Jones, J. D. (1996). *rbohA*, a rice homologue of the mammalian gp91phox respiratory burst oxidase gene. *Plant J,* 10:515-522.

Gryglewski, R.J. *et al.* (1989). *Int. J. Tiss. Reac.*, 11: 269.

Gupta, V.; Willits, M. G. and Glazebrook, J. (2000). *Arabidopsis thaliana* EDS4 contributes to salicylic acid (SA)-dependent expression of defense responses: evidence for inhibition of jasmonic acid signaling by SA. *Mol. Plant Microbe Interact.*, 13: 503-511.

Haley, A.; Russel, A.; Wood, N.; Allan, A.; Knight, M. R.; Campbell, A.K.C. and Trewavas, A.J. (1995). Mechanical effects on cytoplasmic calcium. *Proc. Natl. Acad. Sci. USA*, *92:* 4124-4128.

Ham, J. H.; Bauer, D. W.; Fouts, D. E. and Collmer, A. (1998). A cloned *Erwinia chrysanthemi* Hrp (type III protein secretion) system functions in *Escherichia coli* to deliver *Pseudomonas syringae* Avr signals to plant cells andd to secrete Avr proteins in culture. *Proc. Natl. Acad. Sci. USA*, 95: 10206-10211.

Hammerschmidt, R. (1999). Phytoalexins: What have we learnes after 60 years?. *Annu. Rev. Phytopathol.*, 37: 285-306.

Hammerschmidt, R. and Dann, E. K (1999). The role of phytoalexins in plant protection. *Novartis Found. Symp.*, 223:175-87; discussion 188-90.

Hammond-Kosack, K. E. and Jones, J. D. G. (1996). Resistance gene-dependent plant defence responses. *Plant Cell*, 8: 1773-11791.

Hammond-Kosack, K. E. and Jones, J. D. G. (1997). Plant disease resistance genes. *Annu. Rev. Plant Physiol. Plant Mol. Biol.*, 48: 575-607.

Harren, F. and Reuss, J. (1997). Photoacoustic spectroscopy. In: Encyclopedia of Applied Pysics, Vol; 19. (ed. G. L. Trigg). VHC, Weinheim. pp. 413-435.

Harren, F.; Sikkens, C. and Bicanic, D. D. (1986). Photoacoustics in Agriculture. *SPIE* 701 (Bellingham, USA): 525-531.

Hausladen, A.; Privalle, C. T.; Keng, T.; DeAngelo, J. and Stamler, J.S (1996). Nitrosative stress: activation of the transcription factor OxyR. *Cell*, 86:719-29.

He, S. Y. (1996). Elicitation of plant HR by bacteria. *Plant Physiol.*, 112: 865-869.

He, S. Y.; Huang, H. C. and Collmer, A. (1993). *Pseudomonas syringae* pv. *syringae* harpinPss: a protein that is secreted via the Hrp pathway and elicits the hypersensitive response in plants. *Cell*, 73: 1255-1266.

Holmes, F. O. (1938). Inheritance of resistance to tobacco-mosaic disease in tobacco. *Phytopathol.*, 28: 553-561.

Hueck, C. J. (1998). Type III protein secretion systems in bacterial pathogens of animals and plants. *Microbiol. Mol. Biol. Rev.*, 62: 379-433.

Huertas-Gonzalez, M. D.; Ruiz-Roldan, M. C.; Di Pietro, A. and Rongero, M. I. G. (1999). Cross protection provides evidence for race-specific avirulence factors in *Fusarium oxysporum*. *Physiol. Mol. Plant Pathol.*, 54: 63-72.

Hunt, M. D.; Neuveschwander, L. B.; Lawton, K. A. Steiner, H.-Y. and Ryals, J. A. (1996). Recent advances in systemic acquired resistance research. *Gene*, 179: 89-95.

Hunt, M.; Delaney, T. P.; Dietrich, R. A.; Weymann, K. B.; Dangl, J. L. and Ryals, J. A. (1997). Salicylate-independent lesion fromation in *Arabidopsis lsd* mutants. *Mol. Plant Microbe Interact.*, 10: 531-536.

Ievinsh, G. (1992). Chracterization of the peroxidase system in winter rye seedlings: compartmentation and dependence on leaf development and hydrogen donors. *J. Plant Physiol.*, 140: 257-263.

Iiyama, K.; Lam, T. B. T. and Stone, B. A. (1994). Covalent cross-links in the cell wall. *Plant Physiol.*, 104: 315-320.

Inzé, D. and Van Montagu, M. (1995). *Curr. Opin. Biotechnol.*, 6: 153-158.

Jackson, P. and Ricardo, C. P. P. (1994). An examination of the peroxidases from *Lupinus albus* L. hypocotyls. *Planta*, 194: 311-317.

Jackson, R. W.; Athanassopoulos, E.; Tsiamis, G.; Mansfield, J. W.; Sesma, A.; Arnold, D. L.; Gibbon, M. J.; Murillo, J.; Taylor, J. D. and Vivian A. (1999). Identification of a pathogenicity island, which contains genes for virulence and avirulence, on a large native

plasmid in the bean pathogen *Pseudomonas syringae* pv. *phaseolicola*. *Proc. Natl. Acad. Sci. USA*, 96: 10875-10880.

Jaffrey, S. R. & Snyder, S. H. (1996). PIN: an associated protein inhibitor of neural nitric oxide synthase. *Science,* 274: 774-777.

Jarosz, A. M. and Davelos, A. L. (1995). Effects of disease in wild plant populations and the evolution of pathogen agressiveness. *New Pathologist*, 129: 371-387.

Jia, Y.; McAdams, S. A.; Bryan, G. T.; Hershey, H. P. and Valent, B. (2000). Direct interaction of resistance gene and avirulence gene products confers rice blast resistance. *EMBO J.*, 19:4004-4014.

Jin, Q and He, S. Y. (2001). Role of the Hrp pilus in type III protein secretion in *Pseudomonas syringae*. *Science*, 294: 2556-2558.

Jirage, D.; Tootle, T. L.; Reuber, T. L.; Frost, L. N.; Feys, B. J.; Parker, J. E.; Ausubel, F. M. and Glazebrook, J. (1999). *Arabidopsis thaliana PAD4* encodes a lipase-like gene that is important for salicylic acid signaling. *Proc. Natl. Acad. Sci. USA*, 96: 13583-13588.

Jirage, D.; Zhou, N.; Cooper, B.; Clarke, J. D.; Dong, X.and Glazebrook, J. (2001). Constitutive salicylic acid-dependent signaling in *cpr1* and *cpr6* mutants requires PAD4. *Plant J.*, 26: 359-407.

Johnson, C. H.; Knight, M. R.; Kondo, T.; Masson, P.; Sedbrook, J.; Haley, A. and Trewavas, A. (1995). Circadian oscillations of cytosolic and chloroplastic free calclium in plants. *Science,* 269: 1863-1865.

Johnston, S. A. (1990). Biolistic transformation: Microbes to mice. *Nature*, 346: 776-777.

Jonak, C.; Herbert-Bors, E. and Hirt, H. (1994). MAP kinases: universal multi-purpose signaling tools. *Plant Mol. Biol.*, 24: 407-416.

Jones, J. D. G. (2001). Putting knowledge of plant disease resistance genes to work.. *Curr. Opin Plant Biol.,* 4: 281-287.

Jorgensen, J. H. (1996). Effect of three suppressers on the expression of powdery mildew resistance in barley. *Genome* 39, 492-498.

Kachroo, P.; Yoshioka, K.; Shah, J.; Dooner, H. K. and Klessig, D. F. (2000). Resistance to turnip crinkle virus in *Arabidopsis* is regulated by two host genes and salicylic acid dependent but NPR1, ethylene, and jasmonate independent. *Plant Cell*, 12: 677-690.

Karpinski, S.; Reynolds, H.; Karpinska, B.; Wingsle, G.; Creissent, G. and Mullineaux, P. (1999). Systemic signaling and acclimation in response to excess excitation energy in Arabidopsis. *Science*, 284: 654-657.

Karrer, E. E.; Beachy, R. N. and Holt, C. A. (1998). Cloning of Tobacco Genes that Elicit the Hypersensitive Response. *Plant Mol. Biol.*, 36: 681-690.

Katavic, V; Reed, D. W.; Taylor, D. C.; Giblin, E. M.; Barton, D. L.; Mackenzie, S. L.; Covello, P. S. and Kunst, L. (1995). Alteration of seed fatty acid composition by an ethyl methanesulfonate-induced mutation in *Arabidopsis thaliana* affecting triacylglycerol acyltranseferase activity. *Plant Physiol.*, 108: 399- 409.

Kawasaki, T.; Henmi, K.; Ono, E.; Hatakeyama, S.; Iwano, M.; Satoh, H. and Shimamoto, K. (1999). The small GTP-binding protein rac is a regulator of cell death in plants. *Proc. Natl. Acad. Sci. USA,* 96: 10922-10926.

Keen, N. T.; Ersek, T.; Long, M.; Bruegger, B. and Holliday, M. (1981). Inhibition of the hypersensitive reaction of soybeans leaves to incompatible *Pseudomonas spp.* by blasticidin S, streptomycin or elevated temperature. *Physiol. Plant Pathol.*, 18: 325-337.

Keller, T.; Damude, H. G.; Werner, D.; Doerner, P.; Dixon, R. A. and Lamb, C. (1998). A plant homolog of the neutrophil NADPH oxidase gp91phox subunit gene encodes a plasma membrane protein with Ca2+ binding motifs. *Plant Cell*, 10:255-266.

Kenten, R. H. (1955). The oxidation of indole-3-acetic acid by waxpod bean root sap and peroxidase systems. *Biochem. J.*, 59: 110-121.

Kessmann, H.; Staub, T.; Hofman, C.; Maetzke, T.; Herzog, J.; Ward, E.; Ukness, S. and Ryals, J. (1994). Induction of systemic acquired resistance in plants by chemicals. *Ann. Rev. Phytopathol.*, 32: 439-459.

Kieber, J. J.; Rothenberg, M.; Roman, G.; Feldmann, K. A. and Ecker, J. R. (1993) CTR1, a negative regulator of the ethylene response pathway in Arabidopsis, encodes a member of the raf family of protein kinases. *Cell*, 72:427-441.

Kim, H. S.; Malamy, J. I. and Delaney, T. P. (2001). Identification and characterization of extragenic suppressors of the *Arabidopsis nim1-1* mutant. In: Abstracts (poster 144) International Congress on Molecular plant Microbe Interactions. Madison Wisconsin, July 10-14.

King, E. D.; Ward, M. K. and Raney, D. E. (1954). Two simple media for the demonstration of phycocyanin and fluorescin. *J. Lab. Clin.*, 44: 301-307.)

Kinkema, M.; Fan, W. and Dong, X. (2000). Nuclear localizaion of NPR1 is required for activation of PR gene expression. *Plant Cell*, 12: 2339-2350.

Kistler, H. C. and Benny, U. K. (1988). Genetic transformation of the fungal plant wilt pathogen, *Fusarium oxysporum*. *Curr. Genet.*, 13:145-149.

Kjemtrup, S.; Nimchuk, Z. and Dangl, J. L. (2000). Effector proteins of phytopathogenic bacteria: bifunctional signals in virulence and host recognition. *Curr. Opin. Microbiol.*, 3: 73-78.

Kleier, D. A. and Raskin, I. (1991). Salicylic Acid is a Systemic Signal and an Inducer of PR Proteins in Virus-Infected Tobacco. *Plant Cell*, 3: 809-818.

Klein, T. M.; Harper, E. C.; Svab, Z.; Sanford, J. C.; Fromm, M. E. and Maliga, P. (1988). Stable genetic transformation of intact *Nicotiana* cells by the particle bombardment process. *Proc. Natl. Acad. Sci. USA*, 85:8502-8505.

Klein, T. M.; Wolf, E. D.; Wu, R. and Sanford, J. C. (1987). High velocity microprojectiles for delivering nucleic acids into living cells. *Nature,* 327: 70-73.

Klepper, L. (1979). Nitric oxide (NO) and nitrogen dioxide (NO_2) emissions from herbicide-treated soybean plants. *Atmos. Environ.*, 13: 537-542.

Kliebenstein, D. J.; Dietrich, R. A.; Martin, A. C.; Last, R. L. and Dangl, J. L. (1999). LSD1 regulates salicylic acid induction of copper zince superoxide dismutase in *Arabidopsis thaliana*. *Mol. Plant Microbe Interact.*, 12: 1022-1026.

Knight, H.; Brandt, S. and Knight MR. (1997). Calcium signaling in *Arabidopsis thaliana* responding to drought and salinity. *Plant J.,* 12: 1067-1078.

Knight, M. R.; Campbell, A. K.; Smith, S. M. and Trewavas, A. J. (1991). Transgenic plant aequorin reports the effects of cold shock and elicitors on cytoplasmic calcium. *Nature,* 352: 524-526.

Knight, M. R.; Read, N. D.; Campbell, A. K. and Trewavas, A. J. (1993). Imaging calcium dynamics in living plants using semi-synthetic recombinant. aequorins. *J Cell Biol.*, 121:83-90.

Knoester, M.; Pieterse, C. M.; Bol, J. F. and Van Loon, L. C. (1999). Systemic resistance in *Arabidopsis* induced by rhizobacteria requires ethylene-dependent signaling at the site of application. *Mol. Plant Microbe Interact.,* 12: 720-727.

Knogge, W. (1996). Fungal infection of plants. *Plant Cell*, 8: 1711-1722.

Kondo, R. (1999); A point mutation in a plant calmodulin is responsible for its inhibitio of nitric oxide synthase. *J. Biol. Chem.,* 51: 36213-36218.

Kondo, R.; Tikunova, S. B.; Cho, M. J. and Johnson, J. D. (1999). A point mutation in a plant calmodulin is responsible for its inhibition of nitric-oxide synthase. *J. Biol. Chem.*,274:36213-36218.

Kono, Y. and Fridovich, L. (1982). Superoxide radical inhibits catalase. *J. Biol. Chem.*, 257: 5751-5754.

Koorneef, M. and Stam, P. (1992). Genetic analysis. In: Methods in *Arabidopsis thaliana* Research. pp. 83-99. C. Koncz, N. Chua, and J. Schell (eds.), 1st editions. World Scientific Publishing, Singapore.

Kovtun, Y.; Chiu, W.-L.; Tena, G. and Sheen, J. (2000). Functional analysis of oxidative stress-activated mitogen-activated protein kinase cascade in plants. *Proc. Natl. Acad. Sci. USA,* 97: 2940-2945.

Krysan, P. J.; Young, J. C. and Sussman, M. R. (1999). T-DNA as an insertional mutagen in Arabidopsis. *Plant Cell*, 11: 2283-2290.

Kumar, D. and Klessig, D. F. (2000). Differential induction of tobacco MAP kinase by the defense signals nitric oxide, salicylic acid, ethylene, and jasmonic acid. *MPMI*, 13: 347-351.

Kwak, S. S.; Kim, S. K.; Lee, M. S.; Jung, K. H.; Park, I. H. and Liu, J. R. (1995). Acidic peroxidase from suspension-cultures of sweet potato. *Phytochemistry*, 39: 981-984.

Lagrimini, L. M. (1991). Wound-induced deposition of polyphenols in transgenic plants overexpressing peroxidas. *Plant Physiol.*, 96: 577-583.

Lamb, C. and Dixon, R. (1997). The Oxidative burst in plant disease resistance. *Annu. Rev. Plant Physiol. Plant Mol. Biol.*, 48: 251-275.

Lamb, C. J.; Lawton, M. A.; Dron, M. and Dixon, R. A. (1989). Signals and transduction mechanisms for activation of plant defence against microbial attack. *Cell*, 56: 215-224.

Lamport, D. T. A. (1986). Roles for peroxidases in cell wall genesis. In: Molecular and Physiological Aspects of Peroxidase (eds. C. Panel, T. Gaspar, H Greppin). Université de Genéve, Geneva, Switzerland, pp. 199-208.

Lancaster, J. R. (1994). Stimulation of the diffusion and reaction of endogenously produced nitric oxide. *Proc. Natl. Acad. Sci. USA,* 91: 8137-8141.

Lane, B. G.; Dunwell, J. M.; Ray, J. A.; Schmitt, M. R. and Cuming, A. C. (1993). Germin, a potent marker for early plant development, is an oxalate oxidase. *J. Biol. Chem.*, 268: 12239-12242.

Larson, R. A. (1988). The antioxidants of higher plants. *Phytochem.*, 27: 969-978.

Lebel, E.; Heifetz, P.; Thorne, L.; Uknes, S.; Ryals, J; and Ward, E. (1998). Functional analysis of regulatory sequences controlling *PR-1* gene expression in *Arabidopsis*. *Plant J.*, 16: 223-233.

Leeman, M.; van Pelt, J. A.; den Ouden, F. M.; Heinsbroek, M.; Bakker, P. A. H. M. and Schippers, B. (1995). Induction of systemic resistance by *Pseudomonas fluorescens* in radish cultivars differing in susceptibility to fusarium wilt, using a novel bioassay. *Eur. J. Plant Pathol.*, 101: 655-664.

Leshem, Y. Y. and Kuiper, P. J. C. (1996). Is there a GAS (general adaptation syndrome) response to various types of environmental stress?. *Biol. Plant.,* 38: 1-18.

Leshem, Y. Y. and Pinchasov, Y. (2000). Noninvasive photoacoustic spectrophotometric determination of relative endogenous nitric oxide and ethylene content stoichiometry during the ripening of strawberries *Fragaria anannasa* (Duch.) and avocados *Persea amaricana* (Mill.). *J. Exp. Bot.*, 51: 1471-1473.

Leshem, Y. Y. and Haramaty, E (1996). The characterization and contrasting effects of the nitrci oxide free radical in vegetative stress and senescence of *Pisum sativum* Linn. foliage. *J. Plant Physiol.*, 148: 258-263.

Levine, A.; Pennell, R. I.; Alvarez, M. E.; Palmer, R. and Lamb, C. (1996). Calcium-mediated apoptosis in plant hypersensitive disease resistance response. *Curr. Biol.,* 6: 427-437.

Levine, A.; Tenhaken, R.; Dixon, R. and Lamb, C. (1994). H_2O_2 from the oxidative burst orchestrates the plant hypersensitive disease resistance response. *Cell*, 79: 583-593.

Li, X.; Zhang, Y.; Clarke, J. D.; Li, Y. and Dong, X. (1999). Identification and cloning of a negative regulator of systemic acquired resistance, SNI1, through a screen for supressors of NPR-1. *Cell*, 98: 329-339.

Lichtenthaler, H. K. (1987). Chrlorophylls and carotenoids: Pigments of photosynthetic biomembranes. *Methods Enzymol.*, 148: 350-382.

Lindgren, P. B.; Peet, R. C.and Panopoulos, N. J. (1986). Gene Cluster of *Pseudomonas syringae* pv. *phaseolicola* Controls Pathogenicity of Bean Plants and hypersensitivity on Non-Host Plants. *J. Bacteriol.*, 168: 512-522.

Linthorst, H. (1991). Pathogenesis related proteins of plants. *Crit. Rev. Plant Sci.*, 123-150.

Liu, D.; Kashchandra, G.; Raghothama, P.; Hasegawa, P. M. and Bressay, R. A. (1994). Osmotin overexpression in potato delays development of disease symptoms. *Proc. Natl. Acad. Sci. USA*, 91: 1888-1892.

Liu, Y.; Zhang, S. and Klessig, D. F. (2000). Molecular cloning and characterization of a tobacco MAP kinase kinase that interacts with SIPK. *Mol. Plant Microbe Interact.*, 13: 118-124.

Loake, G. J. (1996). Jasmonates: global regulators of plant gene expression. In Membranes: Specialised functions in plants. (eds. Smallwood, M.; Knox, J.P. and Bowles, D.J.), pp. 215-228. Bios. Oxford.

Loitto, V. M.; Nilsson, H.; Sundqvist, T.; and Magnusson, K. E. (2000). Nitric oxide induces dose-dependent Ca^{2+} transients and causes temporal morphological hyperpolarization in human neutrophils . *J. Cell. Physiol.*, 182: 402-413.

Lorito, M.; Hayes, C. K.; Pietro, A. D. L. and Harman, G. E. (1993). Biolistic transformation of *Trichoderma harzianum* and *Gilocladium virens* using plasmid and genomic DNA. *Curr. Genet.*, 24: 349-356

Lucas, J. A. (1998). Plant Pathology and Plant Pathogens. Third Edition. Published by Blackwell Science.

Luck, J. E.; Lawrence, G. L.; Dodds, P. N.; Shepherd, K. W. and Ellis, J. G. (2000). Regions outside the leucine-rich repeats of flax rust resistance proteins play a role in specificity determination. *Plant Cell*, 12: 1367-1377.

Mach, J. M.; Castillo, A. R.; Hoogstraten, R. and Greenberg, J. T. (2001). The *Arabidopsis* accelerated cell death gene *ACD2* encodes red chlorohpyll catabolite reductase and suppresses the spread of disease symptoms. *Proc. Natl. Acad. Sci. USA*, 98: 771-776.

Mäder, M. (1992). Compartmentation of peroxidase isoenzymes in plant cells. In: Plant Peroxidases 1980-1990, Topics and Detailed Literature on Molecular, Biochemical and Physiological Aspects (eds. C. Panel, T. Gaspar, H Greppin). Université de Genéve, Geneva, Switzerland, pp. 37-46.

Malamy, J.; Carr, J. P.; Klessig, D. F. and Raskin, I. (1990). Salicylic acid: a likely endogenous signal in the resistance response of tobacco to viral infection. *Science*, 250: 1002-1004.

Malardier, L.; Daboussi, M.J.; Julien, J.; Roussel, F.; Scazzocchio, C. and Brygoo, Y. (1989). Cloning of the nitrate reductase gene (*niaD*) of *Aspergillus nidulans* and its use for transformation of *Fusarium oxysporum*. Gene, 78: 147-156.

Malho, R.; Moutinho, A.; van der Luit, A.and Trewavas, A. J. (1998). Spatial characteristics of calcium signaling: The calcium wave as a basic unit in plant calcium signaling. *Phil. Trans. R. Soc. Lond.*, B 353: 1464-1473.

Maor, R.; Puyesky, M.; Horwitz, B. A. and Sharon, A. (1998). Use of green fluorescent protein (GFP) for studying development and fungal-plant interaction in *Cochliobolus heterostrophus*. *Mycol. Res.*, 102: 491-496.

Marletta, M. A. (1994). Nitric oxide synthase: Aspects concerning structure and catalysis. *Cell,* 78: 927-930.

Mauch-Mani, B. and Metraux, J.-P. (1998). Salicylic acid and acquired resistance to pathogen attack. *Anals Botany*, 82: 535-540.

Mayda, E.; Mauch-Mani, B. and Vera, P. (2000). *Arabidopsis dth9* mutation identifies a gene involved in regulating disease susceptibility without affecting salicylic acid-dependent responses. *Plant Cell*, 12: 2119-2128.

Mayer, B. & Hemmens, B. (1997). Biosynthesis and action of nitric oxide in mammalian cells. *Trends Biochem. Sci.,* 22: 477-481.

McAinsh, M. R. (1990). Abscisic acid-induced elevation of guard cell cytosolic Ca^{2+} precedes stomatal closure. *Nature,* 343: 186-188.

McClung, C. R. (1997). Regulation of catalases in Arabidopsis. *Free Radic. Biol. Med.*, 23: 489-496.

McConn, M.; Creelman, R. A.; Bell, E.; Mullet, J.E. and Browse, J. (1997). Jasmonate is essential for induced insect defense in *Arabidopsis*. *Proc. Natl. Acad; Sci. USA*, 94: 5473-5477.

McDougall, G. I. (1992). Plant peroxidases and cell differentiation. In: Plant Peroxidases 1980-1990, Topics and Detailed Literature on Molecular, Biochemical and Physiological Aspects (eds. C. Panel, T. Gaspar, H Greppin). Université de Genéve, Geneva, Switzerland, pp. 101-115.

McDowell, J. M.; Cuzick A.; Can, C.; Beynon, J.; Dangl, J. L. and Holub, E. B. (2001). Downy mildew (*Peronospora parasitica*) resistance genes in *Arabidopsis* vary in functional requirements for NDR1, EDS1, NPR1, and salicylic acid accumulation. *Plant J.*, 22: 523-529.

McNellis, T. W.; Mudgett, M. B.; Li, K.; Aoyama, T.; Horvath, D.; Chua, N.-H. and Staskawichz, B. J. (1998). Glucocorticoid-inducible expression of a bacterial avirulence gene in transgenic *Arabidopsis* induces hypersensitive cell death. *Plant J.*, 14: 247-257.

Meinke, D. W.; Cherry, J. M.; Dean, C.; Rounsley, S. D.and Koornneef, M. (1998). *Arabidopsis thaliana*: A Model Plant for Genome Analysis. *Science*, 282: 678-682.

Membré, N.; Berna, A.; Neutelings, G.; David, A.; David, H.; Staiger, D.; Vasquez, J. S.; Raynal, M.; Delseny, M. and Bernier, F. (1997). cDNA sequence, genomic organisation and differential expression of three *Arabidopsis* genes for germin/oxalate oxidase-like proteins. *Plant Mol. Biol.*, 35: 459-469.

Merritt, P.; Tornero, P.; Dangl, J. and Innes, R. W. (2001). The cloning of PBS2, an *Arabidopsis* disease resistance signaling gene. In: Abstracts (poster 155) Intenrational Congress on Molecular plant Microbe Interactions. Madison Wisconsin, July 10-14.

Mestre, P.; Brigneti, G. and Baulcombe, D. C. (2000). A Ry-mediated resistance response in potato requires the intact active site of the Nia proteinase from potato virus. *Plant J.*, 23: 653-661.

Metraux, J.-P.; Signer, H.; Ryals, J.; Ward, E.; Wyss-Benz, M.; Gaudin, J.; Raschdor, K.; Schmidt, E.; Blum, W. and Inverad, B. (1990). Increase in salicylic acid at the onset of the SAR in cucumber. *Science*, 250: 1004-1006.

Michelmore, R. W.; Paran, I. and Kesseli, R. V. (1991). Identification of markers linked to disease-resistance genes by bulked segregant analysis: a rapid method to detect markers in specific genomic regions by using segregating populations. *Proc. Natl. Acad. Sci. USA*, 88: 9828-9832.

Migheli, Q.; Laugé, R.; Daviere, J-M.; Gerlinger, C.; Kaper, F.; Langin, T. and Daboussi, M-J. (1999). Transposition of the autonomous Fot1 element in the filamentous fungus *Fusarium oxysporum*. *Genetics*, 151: 1005-1013.

Millar, A. H. and Day, D. A. (1997). Alternative solutions to radical problems. *Trends Plant Sci.*, 2: 289.

Milosevic, N. and Sulsarenko, A. J. (1996). Active oxygen metabolism and lignification in the hypersensitive response in bean. *Plant Physiol.*, 49: 143-158.

Minke, F. L. H. and Klessig, D. F. (2001). Molecular cloning and characterization of a tobacco nuclear-encoded chloroplast protein that interacts with salicylic acid-induced protein kinase (SIPK). In: Abstracts (poster 154) International Congress on Molecular plant Microbe Interactions. Madison Wisconsin, July 10-14.

Mitsuhara, I.; Malik, K. A.; Miura, M. and Ohashi, Y. (1999). Animal cell-death suppressors Bcl-X_L and ced-9 inhibit cell death in tobacco plants. *Curr. Biol.*, 9: 775-778.

Mittler, R. and Lam, E. (1996). Sacrifice in the face of foes: pathogen-induced programmed cell death in plants. *Trends Microbiol.*, 4: 10-15.

Mittler, R.; Shulaev, V. and Lam, E. (1995). Coordinated activation of programmed cell death and defense mechanisms in transgenic tobacco plants expressing a bacterial proton pumb. *Plant Cell* 7, 29-42.

Miyawaki, G.; Llopis, J.; Heim, R.; McCaffery, J. M.; Adams, J. A.; Ikura, M. and Tsien, R. Y. (1997). Fluorescent indicators for Ca^{2+} based on green fluorescent proteins and calmodulin. *Nature*, 388: 882-887.

Moerschbacher, B. M. (1992). Plant peroxidases; involvement in responses to pathogens. In: Plant Peroxidases 1980-1990, Topics and Detailed Literature on Molecular, Biochemical and Physiological Aspects (eds. C. Panel, T. Gaspar, H Greppin). Université de Genéve, Geneva, Switzerland, pp. 91-99.

Molina, A.; Volrath, S.; Guyer, D.; Maleck, K.; Ryals, J. and Ward, E. (1999). Inhibition of protoporphyrinogen oxidase expression in *Arabidopsis* causes a lesion-mimic phenotype that induces systemic acquired resistance. *Plant J.*, 17: 667-678.

Monties, B. (1989). Lignins. In: Methods of Plant Biochemistry (Vol I, eds: P. M. Dey; J. B. Harborne). Academics Press, London. pp. 113-157.

Morel, J.-B. and Dangl, J. L. (1997). The hypersensitive response and the induction of cell death in plants. *Cell Death Differ.*, 4: 671-683.

Murphy, M. E. and Noack, E. (1994). Nitric oxide assay using hemoglobin method. *Meth. Enzymol.*, 233: 241-250.

Namiki, F.; Matsunga, M.; Okunda, M.; Inoue, I.; Nishi, K.; Fujita, Y. and Tsuge, T. (2001). Mutation of arginine biosynthesis gene causes reduced pathogenicity in *Fusarium oxysporum* F. sp *melonsis*. *Mol. Plant Microbe Interact.*, 14: 580-584.

Nathan, C and Shiloh, M. (2000). Reactive oxygen and nitrogen intermediates in the relationship between mammalina hosts and microbial pathogens. *Proc. Natl. Acad. Sci.*, 97: 8841-8848.

Nathan, C. and Xie, Q-W. (1994). Nitric oxide synthases: roles, tolls and controls. *Cell,* 78: 915-918.

Nauser, T. and Koppenol, W. H. (2002). The rate constant of the reaction of superoxide with nitrogen monoxide: Approaching diffusion limit. *J. Physical Chem. A*, 106: 4084-4086.

Navarre, D. A.; Wendehenne, D.; Durner, J.; Noad, R. and Klessig, D. F. (2000). Nitric oxide modulates the activity of tobacco aconitase. *Plany Physiol.*, 122: 573-582.

Nawrath, C. and Métraux, J. P. (1999). Salicylic acid-deficient mutants of *Arabidopsis* express *PR-2* and *PR-5* and accumulates high levels of camalexin. *Plant Cell*, 11: 1393-1404.

Nawrath, C.; Heck, S.; Parinthawong, N. and Métraux, J.-P. (2001). EDS5, an essential component for salicylic acid accumulation after UV-C light exposure or pathogen attack in Arabidopsis, is a potenital transporter. In: Abstracts (poster 159) International Congress on Molecular plant Microbe Interactions. Madison Wisconsin, July 10-14.

Nimchuk, Z.; Rohmer, L.; Chang, J. H. and Dangl, J. L. (2001). Knowing the dancer from the dance: R-gene products and their interactions with other proteins from host and pathogen. *Curr. Opin. Plant Biol.,* 4: 288-294.

Nishihama, R.; Banno, H.; Shibata, W.; Hirano, K.; Nakashima, M.; Usami, S. and Machida, Y. (1995). Plant homologues of components of MAPK (mitogen-activated protein kinase) signal pathways in yeast and animal cells. *Plant Cell Physiol.*, 36: 749-757.

Nishimura, N.; Hayamizu, T. and Yanagisaw,A. Y. (1986). Reduction of NO_2 to NO by rush and other plants. *Environ. Sci. Technol.,* 20: 413-416.

Noctor, G. and Foyer, C. H. (1998). *Annu. Rev. Plant Physiol. Plant Mol. Biol.*, 49: 249-279.

Noritake, T.; Kawakita, K. and Doke, N. (1996). Nitric oxide induces phytoalexin accumulation in potato tuber tissues. *Plant Cell Physiol.,* 37: 113-116.

Norman-Setterblad, C.; Vidal, S. and Palva, E. T. (2000). Interacting signal pathways control defense gene expression in *Arabidopsis* in response to cell-wall degrading enzymes from *Erwinia corotovora. Mol. Plant Microbe. Interact.*, 13: 430-438.

O'Donnell, P. J.; Calvert, C.; Atzorn, R.; Westernack, C.; Leyser, H. M. O. and Bowels, D. J. (1996). Ethylene as a signal mediating the wound response in tomato plants. *Science* 274, 1914-1917.

Oereke, E.-C.; Dehne, H.-W.; Schönbeck, F. and Weber, A. (1994). Crop production and crop protection: estimated losses in major food and cash crops. Elsevier, Amsterdam.

Ono, E.; Wong, H. L.; Kawasaki, T.; Hasegawa, M.; Kodama, O. and Shimamoto, K. (2001). Essential role of the small GTPase Rac in disease resistance of rice. *Proc. Natl. Acad. Sci. USA,* 98: 759-64.

Orbach, M. J.; Farrall, L.; Sweigard, J. A.; Chumley, F. G. and Valent, B. (2000). A telomeric aviulence gene determines efficacy for rice blast resistance gene *Pi-ta. Plant Cell,* 12:2019-2032.

Orozco-Cardenas, G. and Ryan, C. A. (1999). Hydrogen peroxide is generated systemically in plant leaves by wounding and systemin via the octanoid pathway.. *Proc. Natl. Acad. Sci. USA*, 96: 6553-6557.

Osbourn, A. E. (1996). Preformed antimicrobial compounds and plant defences against fungal attack. *Plant Cell*, 8: 1821-1831.

Padgett, H. S.; Watanabe, Y. and Beachy, R. N. (1997). Identification of the TMV replicase sequence that activateS the *N* gene-mediated resistance. *Mol. Plant-Microbe Interact.*, 10: 709-715.

Park, J.-M.; Park, C.-J.; Lee, S.-B.; Ham, B.-K.; Shin, R. and Paek, K.-H. (2001). Overexpression of the tobacco *Tsi* gene encoding an EREBP/AP2-type transcription factor enhances resistance against pathogen attack and osomotic stress in tobacco. *Plant Cell*, 13: 1035-1046.

Parker, J. E.; Szabo, B. J.; Staskawicz, C.; Lister, C.; Dean, C.; Daniels, M. J. and Jones, J. D. G. (1993). Phenotypic characterization and molecular mapping of the *Arabidopsis thaliana* locus *RPP5*, determining disease resistance to *Peronospora parasitica. Plant J.*, 4: 821-831.

Patterson, G. H.; Knobel, S. M.; Sharif, W. D.; Kain, S. R. and Piston, D. W. (1997). Use of the green fluorescent protein and its mutants in quantitative fluorescence microscopy. *Biophysic. J.*, 73: 2782-2790.

Pearce, L. L.; Gandley, R. E.; Han, W.; Wasserloos, K.; Stitt, M.; Kanai, A. J.; McLaughlin, M. K.; Pitt, B. R. and Levitan, E. S. (2000). Role of metallothionein in nitric oxide signaling as revealed by a green fluorescent fusion protein. *Proc. Natl. Acad. Sci. USA*, 97: 477-482.

Pedroso, M. C.; Magalhaes, J. R. and Durzan, D. (2000). Nitric oxide burst precedes apoptosis in angiosperm and gymnosperm callus cells and foliar tissues. *J. Exp. Bot.,* 51: 1027-1036.

Penacortes, H.; Albrecht, T.; Prat, S.; Weiler, W. and Willmitzer, L. (1993). Aspirin prevents wound-induced gene-expression in tomato leaves by blocking jasmonic acid biosynthesis. *Planta* 191, 123-128.

Penninckx, I. A. M.; Eggermont, K.; Terras, F. R.; Thomma, B. P.; De Samblanx, G. W.; Buchala, A.; Metraux J.-P.; Manners, J. M. and Broekaert, W. F. (1996). Pathogen-induced systemic activation of a plant defensin gene in *Arabidopsis* follows a salicylic acid-independent pathway. *Plant Cell*, 8: 2309-2323.

Penninckx, I. M. A. .A.; Thomma, B. P.; Buchala, A.; Metraux, J.-P. and Broekaert, W. F. (1998). Concomitant activation of jasmonate and ethylene response pathways is required for induction of a plant defensin gene. *Plant Cell*, 10: 2103-2114.

Penson, S. P.; Schuurink, R. C.; Fath, A.; Gubler, F.; Jacobsen, J. V. and Jones, R. L. (1996). cGMP is required for gibberellic acid-induced gene expression in barley aleurone. *Plant Cell*, 8: 2325-2333.

Peterhänsel, C.; Freialdenhoven, A.; Kurth, J.; Kolsch, R. and Schulze-Lefert, P. (1997). Interaction analyses of genes required for resistance responses to powdery mildew in barley reveal distinct pathways leading to leaf cell death. *Plant Cell* 9, 1397-1409.

Petersen, M.; Brodersen, P.; Naested, H.; Andreasson, E.; Lindhart, U.; Johansen, B.; Nielsen, H.B.; Lacy, M.; Austin, M. J.; Parker, J. E.; Sharma, S. B.; Klessig, D. F.; Martienssen, R.; Mattsson, O.; Jensen, A. B.and Mundy, J.(2000). Arabidopsis map kinase 4 negatively regulates systemic acquired resistance. *Cell*, 103:1111-1120.

Pfeiffer, S.; Janistyn, B.; Jessner, G.; Pichorner, H. and Ebermann, R. (1994). Gaseous nitric oxide stimulates guanosine-3',5'-cyclic monophosphate (cGMP) formation in spruce needles. *Phytochemistry,* 36: 259-262.

Pierson, E. S.; Miller, D. D.; Callaham, D. A.; van Aken, J.; Hackett, G. and Hepler, P. K. (1996). Tip-localized calcium entry fluctuates during pollen tube growth. *Developmental Biol.* 174, 160-173.

Pieterse, C. M. J., Van Wees, S. C. M. Hoffland, E.; Van Pelts, J. A. and Van Loon, L. C. (1996). Systemic resistance in *Arabidopsis* induced by biocontrol bacteria is independent of Salicylic acid accumulation and pathogenesis-related gene expression. *Plant Cell*, 8: 1225-1237.

Pieterse, C. M.; Van Wees, S. C. M.; Van Pelt, J. A.; Knoester, M.; Laan, R.; Gerrits, H.; Weisbeek, P. J. and Van Loon, L. C. (1998). A novel signalling pathway controlling induced systemic resistance in *Arabidopsis*. *Plant Cell*, 10: 1571-1580.

Poole, R.K. and Hughes, M.N. (2000). New functions for the ancient globin family: bacterial responses to nitric oxide and nitrosative stress. *Mol. Microbiol.*, 36: 775-783.

Poovaiah, B. W. & Reddy, A. S. N. (1993). Calcium and signal transduction in plants. *Cri. Rev. Plant Sci.,* 12: 185-211.

Prandl, R.; Hinderhofer, K.; Eggers-Schumacher, G. and Schoffl, F. (1998). HSF3, a new heat shock factor from Arabidopsis thaliana, derepresses the heat shock response and confers thermotolerance when overexpressed in transgenic plants. *Mol. Gen. Genet.*, 258:269-278.

Price, A. H.; Taylor A.; Ripley, S. J.; Griffiths, A.; Trewavas, A. J. and Knight, M. R. (1994). Oxidative signals in tobacco increase cytosolic calcium. *Plant Cell,* 6: 1301-1310.

Pruite, R. E. and Meyerowitz, E. M. (1986). Characterization of the genome of *Arabidopsis thaliana*. *J. Mol. Biol.*, 187: 169-183.

Quiquampoix, H.; Ratcliffe, R. G.; Ratkovic, S. and Vucinic, M. (1990). ^{1}H and ^{31}P NMR investigation of gadolinium uptake in maize roots. *J. Inorg. Biochem.*, 265-275.

Rambosek, J. and Leach, J. (1987). Recombinant DNA in filamentous fungi: progress and prospects. *CRC Critical Rev. Biotech.*, 6: 357-393.

Rao, M. V.; Lee, H.; Creelman, R. A.; Mullet, J. E. and Davis, K. R. (2000). Jasmonic acid signaling modulates ozone-induced hypersensitive cell death. *Plant Cell*, 12: 1633-1646.

Rasmussen, J. B.;Schmidt, R.and Zook, M. N. (1991). Systemic induction of SA accumulation in cucumber after inoculation with *Pseudomonas syringae* pv. *syringae*. *Plant Physiol.*, 97: 1422-1437.

Rate, D. N.; Cuenca, J. V.; Bowman, G. R.; Guttman, D. S. and Greenberg, J. T. (1999). The gain-of-function- *Arabidopsis acd6* mutant reveals novel regulation and function of the salicylic acid signaling pathway in controlling cell death, defenses, and cell growth. *Plant Cell*, 11: 1695-1708.

Reimers, P. J.; Guo, A. and Leach, J. E. (1992). Increased activity of a cationic peroxidase associated with an incompatible interaction between *Xanthomonas oryzae* pv *oryzae* and rice (*Oriza sativa*). *Plant Physiol.*, 99: 1044-1050.

Ren, T.; Qu, F. and Morris, T. J. (2000). *HRT* gene function requires interaction between a NAC protein and viral capsid protein to confer resistance to urnip crinkcle virus. *Plant Cell.*, 12: 1917-1925.

Reuber, T. L.; Plotnikova, J. M.; Dewdney, J.; Rogers, E. E.; Wood, W. and Ausubel, F. M. (1998). Correlation of defense gene induction defects with powdery mildew susceptibility in *Arabidopsis* enhanced disease suscebtibility mutants. *Plant J.*, 16: 473-385.

Ribeiro, E. A.; Cunha, F. Q.; Tamashiro, W. M. S. C. and Martins, I. S. (1999). Growth phase-dependent subcellular localization of nitric oxide synthase in maize cells. *FEBS Lett.*, 455: 283-286.

Ridnour, L.; Sim, J. E.; Hayward, M. A.; Wink, D. A.; Martin, S. M.; Buettner, G. R. and Spitz, D. R. (2000). A spectrophotometric method for the direct detection and quantitation of nitric oxide, nitrite and nitrate in cell culture media. *Anal. Biochem.*, 281: 223-229.

Roine, E.; Wei, W.; Yuan, J.; Nurmiaho-Lassila, E.-L.; Kalkkinen, N.; Romantschuk, M. and He, S. Y. (1997). Hrp pilus: a *hrp*-dependent bacterial surface appendage produced by *Pseudomonas syringae* pv. *tomato* DC3000. *Proc. Natl. acad. Sci. USA*, 94: 3459-3464.

Romeis, T.; Piedras, P.; Zhang, S.; Klessig, D. F.; Heribert, H. and Jones, J. D. (1999). Rapid Avr9-Cf-9-dependent activation of MAP kinases in tobacco cell cultures and leaves: convergence of resistance genes, elicitors, wound, and salicylate responses. *Plant Cell*, 11: 273-287.

Ross, A. F. (1952). Studies on mosaic resistance in potato. In *Proceedings of the Conference on Potato Virus Diseases.* Wageningen: Lisse, pp. 40-47.

Ross, A. F. (1961a). Local acquired resistance to plant virus infection in hypersensitive hosts. *Virology*, 14: 329-339.

Ross, A. F. (1961b). Systemic acquired resistance induced by localized virus infection in plants. *Virology*, 14: 340- 358.

Roxas, V. P.; Smith, R. K.; Allen, E. R.and Allen, R. D. (1997). Overexpression of glutathione S-transferase/glutathione peroxidase enhances the growth of transgenic tobacco seedlings during stress. *Nat. Biotechnol.*, 15: 988-991.

Ryals, J. A.; Neuenschwander, Y. H.; Willits, M. G.; Molina, A.; Steiner, H.-Y.; and Hunt, M. D. (1996). Systemic acquired resistance. *Plantt Cell*, 8: 1809-1819.

Ryals, J.; Ukness, S.; and Ward, E. (1994). Systemic acquired resistance in plants. *Plant Physiol.*, 104: 1109-1112.

Ryals, J.; Weymann, K.; Lawton, K.; Friedrich, L.; Ellis, D.; Steiner, H. Y.; Johnson, J.; Delaney, T. P.; Jesse. T.; Vos. P. and Uknes, S. (1997). The *Arabidopsis NIM1* protein shows homology to the mamalian transcription factor inhibitor IB. *Plant Cell*, 9: 425-439.

Ryan, C. (1990). Protease inhibitors in plants: genes for improving defenses against insects and pathogens. *Annu. Rev. Phytopathol.*, 28: 425-449.

Ryerson, D. E.; and Heath, M. C.(1996). Cleavage of nuclear DNA into oligonucleosomal fragments during cell death by fungal infection and abiotic treatments. *Plant Cell*, 8: 393-402.

Sambrook, J.; Fritsch, E. F. and Maniatis, T. (1989). Molecular Cloning: A Laboratory Manual. Second Editon. Cold Spring Harbor Laboratory Press (CSH).

Samuel, M. A.; Miles, G. P. and Ellis, B. E. (2000). Ozone treatment rapidly activates MAP kinase signalling in plants. *Plant J.*, 22: 367-76.

Sanders, D. (1999). Communicating with calcium. *Plant Cell,* 11: 691-706.

Schäfer, L. and Feierabend, J. (2000). Photoinactivation and protection of glycolate oxidase *in vitro* and in leaves. *Z. Naturforsch.*, 55c: 361-372.

Schena, M.; Heller, R. A.; Theriault, T. P.; Konrad, K.; Lachenmeier, E. and Davis, R. W. (1998). Microarrays: biotechnology's discovery platform for functional genomics. *Trends Biotechnol.*, 16: 301-306.

Schenk, P. M.; Kazan, K.; Wilson, I.; Anderson, J. P.; Richmond, T.; Somerville, S. C. and Manners, J. M. (2000). Coordinated plant defense responses in *Arabidopsis* revealed by microarray analysis. *Proc. Natl. Acad. Sci. USA*, 97: 11655-11660.

Schmidt, H. H. H. W. & Walter, U. (1994). NO at work. *Cell*, 78: 919-925.

Sembdner, G. and Parthier, B. (1993). The biochemical, physiologcial and molecualr actions of JA. *Annu. Rev. Plant Physiol. Plant Mol. Biol.*, 44: 569-589.

Shacklock, P. S. (1992). Cytosolic free calcium mediates red light induced photomorphogenesis. *Nature,* 358: 153-155.

Shah, J.; Kachroo, P. and Klessig, D. F. (1999). The *Arabidopsis ssi1* mutation restores pathogenesis-related gene expression in *npr1* plants and renders defensin gene expression salicylic acid dependent. *Plant cell*, 11: 191-206.

Shah, J.; Tsui, F. and Klessig, D. F. (1997). Characterization of a salicylic acide-insensitive (*sai1*) mutant of *Arabidopsis thaliana*, identified in a selective screen utilizing the SA-inducible expression of *tms2* gene. *Mol. Plant Microbe Interact.*, 10: 69-78.

Shan, L.; Thara, V. K.; Martin, G. B.; Zhou, J.-M. and Tang, X. (2000). The *Pseudomonas* AvrPto protein is differentially recognized by tomato and tobacco and is localized to the plant plasma membrane. *Plant Cell*, 12: 2323-2337.

Shark, K. B.; Smith, F. D.; Harpending, P. R.; Rasmussen, J. L. and Sanford, J. C.(1991). Biolistic transformation of a procaryote, *Bacillus megaterium*. *Appl. Environmen. Microbiol.*, 57: 480-485.

Sharma, Y. K.; Leon, J.; Raskin, I. and Davis, K. R. (1996). Ozone-induced responses in *Arabidopsis thaliana*: The role of salicylic acid in the accumulation of defense-related transcripts and induced resistance. *Proc. Natl. Acad. Sci. USA*, 93: 5099-5104.

Shiloh, M. U.; MacMicking, J. D.; Nicholson, S.; Brause, J. E.; Potter, S.; Marino, M.; Fang, F.; Dinauer, M. and Nathan, C. (1999). . Phenotype of mice and macrophages deficient in both phagocyte oxidase and inducible nitric oxide synthase. *Immunity,* 10: 29-38.

Simon, A. E.; Li, X. H.; Lew, J. E.; Stange, R.; Zhang, C.; Polacco, M. and Carpenter, C. D. (1992) Susceptibility and resistance of *Arabidopsis thaliana* to turnip crinkle virus. *Mol. Plant-Microbe Interact.*, 5:496-503.

Shirasu, K.; Dixon, R. A. and Lamb, C. (1996). Signal transduction in plant immunity. *Curr. Opin. Immunol.*, 8: 3-7.

Shirasu, K.; Lahaye, T.; Tan, M. W.; Zhou, F.; Azevedo, C. and Schulze-Lefert, P. (1999). A novel class of eukaryotic zinc-binding proteins is required for disease resistance signaling in barley and development in *C. elegans*. *Cell*, 99: 355-366.

Shirasu, K.; Nakajima, H. and Krishnamachari, R. V. (1997). Salicylic acid potentiates an agoinst-dependent gain control that amplifies signals in the activation of defence mechanisms. *Plant Cell*, 9: 261-270.

Siegel-Itzkovich, J. (1999). Viagra makes flowers stand up straight. *West J. Med.*, 171: 38.

Silva, H.; Yoshioka, K.; Dooner, H. K. and Klessig, D. F. (1999). Characterization of a new Arabidopsis mutant exhibiting enhanced disease resistance. *Mol. Plant Microbe Interact.*,12: 1053-1063.

Slater, M. G.; Paine, J. A.; Riddell, K. V.; Jepson, I.; Greenland, A. J.; Caddick, M. X. and Tomsett, A. B. (1998). Characerisation of the ethanol-inducible *alc* gene expression system for transgenic plants. *Plant J.*, 16: 127-132.

Slaymaker, D.; Navarre, D. A. and Klessige, D. F. (2001). Identification of a salicylic acid-binding protein in tobacco chloroplast. In: Abstracts (poster 174) International Congress on Molecular plant Microbe Interactions. Madison Wisconsin, July 10-14.

Slazer, P.; Hebe, G.; Reith, A.; Zitterell-Haid, B.; Stransky, H.; Gaschler, K. and Hager, A. (1996). Rapid reactions of spruce cells to elicitors released from the ectomycorrhizal fungus *Hebeloma crustuliniforme*, and inactivation of these elicitors by extracellular spruce enzymes. *Planta*, 198: 118-126.

Smith, H. B. (2000). Proteomics: broad strokes of expression?. *Plant Cell*, 12: 303-304.

Snedecor, G. W. and Cochran, W. G. (1989). *Statistical Methods, Eighth Edition*, Iowa State University Press.

Stamler, J. S. (1992). Biochemistry of nitric oxide and its redox-activated forms. *Science,* 258: 1898-1902.

Stamler, J. S. (1994). Redox signaling: nitrosylation and related target interactions of nitric oxide. *Cell,* 78: 931-936.

Staskawicz, B. J.; Ausubel, F. M.; Baker, B. J.; Ellis, J. G.and Jones, J. D. (1995). Molecular genetics of plant disease resistance. *Science*, 268: 661-667.

Staswick, P. E.; Yuen, G. Y. and Lehman, C. C. (1998). Jasmonate signaling mutants of *Arabidopsis* are susceptible to the soil fungus *Pythium irregulare*. *Plant J.*, 15: 747-754.

Stathopulos, P. B.; Lu, X.; Shen, J.; Scott, J. A.; Hammond, J. R.; McCormack, D. G.; Arnold, J. M. and Feng, Q (2001). Increased L-arginine uptake and inducible nitric oxide synthase activity in aortas of rats with heart failure. *Am. J. Physiol. Heart Circ. Physiol.*, 280: H859-H867.

Stratmann, J. W.; Stelmach, B. A.; Weiler, E. W. and Ryan, C. A. (2000). UVB/UVA radiation activates a 48 kDa meyelin basic protein kinase and potentiates wound signaling in tomato leaves. *Photochem. Photobiol.*, 71: 116-123.

Swiderski, M. R. and Innes, R. W. (2001a). The Arabidopsis *PBS1* resistance gene encodes a member of a novel protein kinase subfamily. *Plant J.*, 26:101-112.

Swiderski, M. R. and Innes, R. W. (2001b). PBS1 resistance kinase-where does it play a role?. In: Abstracts (poster 621) Intenrational Congress on Molecular plant Microbe Interactions. Madison Wisconsin, July 10-14.

Takahashi, H.; Chen, Z.; Du, H.; Liu, Y. and Klessig, D. (1997). Development of necrosis and activation of disease resistance in transgenic tobacco plants with severely reduced catalase levels. *Plant J.*, 11: 993-1005.

Tang, X.; Frederick, R. D.; Zhou, J. .Halterman, D. A.; Jia, Y. and Martin, G. B. (1996). Physical interaction of avrPto and Pto kinase defines a recognition event involved in plant disease resistance. *Science*, 2060-2063.

Taylor, A. R. (1996). Spatial organization of calcium signaling involved in cell volume control in *Fucus rhizoid. Plant Cell,* 8: 2015-2031.

Taylor, A. T. S.; Kim, J. and Low, P. S. Low (2001). Involvement of mitogen-activated protein kinase activation in the signal-transduction pathways of the soya bean oxidative burst. *Biochem. J.*, 355: 795-803.

Tenhaken, E.; Levine, A.; Brisson, L.; Dixon, R. A. and Lamb, C. (1995). Function of the oxidatvie burst in hypersensitive disease resisntace. *Proc. Natl. Acad. Sci. USA*, 92: 4158-4163.

Terras, F. R. G.; Eggermont, K.; Kovaleva, V.; Raikhel, N. V.; Osborn, R. W.; Kester, A.; Rees, S. B.; Torrekens, S.; Van Leuven, F.; Vanderleyden, J.; Cammue, B. P. A. and Broekaert, W. F. (1995). Small cysteine-rich antifungal proteins from radish: Their role in host defense. *Plant Cell*, 7: 573-588.

Tester, M. (1990). Plant ion channels-Whole cell and single channel studies. *New Phytol.,* 114: 305-340.

Thomma, B. P. H. J.; Eggermont, K.; Broekaert, W. F. and Cammue, B. P. A.(2000). Disease development of several fungi in *Arabidopsis* can be reduced by treatment with methyl jasmonate. *Plant Physiol. Biochem.* 38, 421-427.

Thomma, B. P. H. J.; Eggermont, K.; Penninckx, I. A. M. A.; Mauch-Mani, B.; Vogelsang, R.; Cammue, B. P. A. and Broekaert, W. F. (1998). Separate jasmonate-dependent and salicylate-dependent defense response pathways in *Arabidopsis* are essential for resistance to distinct microbial pathogens. *Proc. Natl. Acad. Sci. USA*, 95: 15107-15111.

Thomma, B. P. H. J.; Eggermont, K.; Tierens, K. F. and Broekaert, W. F. (1999a). Requirement for functional *EIN2* (ethylene insensitive 2) gene for efficient resistance of *Arabidopsis thaliana* to infection by *Botritis cinerea. Plant Physiol.*, 121: 1093-1101.

Thomma, B. P. H. J.; Nelissen, I.; Eggermont, K. and Broekaert, W. F. (1999b). Deficiency in phytoalexin production causes enhanced susceptibility of *Arabidopsis thaliana* to the fungus *Alternaria brassicicola. Plant J.*, 19: 163-171.

Thordal-Christensen, H. ; Zhang, Z.; Wei, Y. and Collinge, D. B. (1997). Subcellular localization of H_2O_2 in plants. H_2O_2 accumulation in papillae and hypersensitive response during the barley-powdery mildew interaction. *Plant J.*, 11: 1187-1194.

Ton, J.; Davison, S.; Van Wees, S. C.; Van Loon, L. and Pieterse, C. M. (2001). The *Arabidopsis isr1* locus controlling rhizobacteria-mediated induced systemic resistance is involved in ethylene signaling. *Plant Physiol.*, 125:652-661.

Ton, J.; Pieterse, C. M. and Van Loon, L. C. (1999). Identification of a locus in *Arabidopsis* controlling both expression of rhizobacteria-mediated induced systemic resistance (ISR) and basal resistance against *Pseudomonas syringae* pv. *tomato. Mol. Plant Microbe Interact.,* 12: 911-918.

Torp, J. and Jorgenesen, J. H. (1986). Modification of barley powdery mildew resistance gene *Mla12* by induced mutation. *Can. J. Genet. Cytol.*, 28: 725-731.

Torres, M. A.; Onouchi, H.; Hamada, S.; Machida, C.; Hammond-Kosack, K. E. and Jones, J. D. G. (1998). Six *Arabidopsis thaliana* homologues of the uman respiratory burst oxidase *gp91* (*phox*). *Plant J.*, 14: 365-370.

Trewavas, A. (1999). Le calcium, C'est la Vie: Calcium makes waves. *Plant Physiol.,* 120: 1-6.

Trewavas, A. J. & Malho, R. (1997).Signal perception and transduction: The origin of the phenotype. *Plant Cell,* 9: 1181-1195.

Trewavas, A. J. & Malho, R. (1998). Ca^{2+} signalling in plant cells: the big network!. *Curr. Opinion Plant Biol.,* 1: 428-433.

Trewavas, A.J. and Knight, M.R. (1994). Mechanical signaling, calcium and plant form. *Plant Mol. Biol.,* 26: 1329-1341.

Tsiamis, G.; Mansfield, J. W.; Hockenhull, R.; Jackson, R. W.; Sesma, A.; Athanassopoulos, E.; Bennett, M. J.; Stevens, C.; Vivian, A. and Taylor, J. D. (2000). Cultivar-specific avirulence and virulence functions assigned to *avrPphF* in *Pseudomonas syringae* pv. *phaseolicola*, the cause of bean halo-blight disease. *EMBO J.*, 19: 3204-3214.

Tsukahara, H.; Ishida, T. and Mayumi, M. (1999). Gas-phase oxidation of nitric oxide: Chemical kinetics and rate constant. *Nitric oxide-Biol. & Chem.*, 3: 191-198.

Uknes, S.; Mauch-Mani, B.; Moyer, M.; Potter, S.; Williams, S.; Dincher, S.; Chandler, D.; Slusarenko, A.; Ward, E. and Ryals, J. (1992). Acquired resistance in *Arabidopsis*. *Plant Cell*, 4: 656.

Uknes, S.; Winter, A.; Delaney, T.; Vernooij, B.; Morse, A.; Friedrich, L.; Potter, S.; Ward, E. and Ryals, J. (1993). Biological induction of systemic acquired resistance in Arabidopsis. *Mol. Plant Microbe Interact.*, 6: 680-685.

Valent, B. (1997). The rice blast fungus, *Magnoporthe grisea*. Plant relationships. In G.C.Carroll and P.Tudzynoski (eds.), The *Mycota V Part B*, Springer-Verlage, Heidelberg, Germany, pp. 37-54.

Valvekens, D.; Van Montagu, M. and Lijsbettens, M. V. (1988). *Agrobaterium tumefaciens*-Mediated Transformation of *Arabidopsis thaliana* Explants by Using Kanamycin Selection. *Proc. Natl. Acad. Sci. USA*, 85: 5536-5540.

Van Camp, W.; Van Montagu, M. and Inzé, D. (1998). H_2O_2 and NO: redox signals in disease resistance. *Trends Plant Sci.*, 3: 330-334.

Van der Hoorn, R. A. L.; Roth, R. and De Wit, P. J. G. M. (2001). Identification of distnict specificity determinants in resistance protein Cf-4 allows construction of a *Cf-9* mutant that confers recognition of avirulence protein AVR4. *Plant Cell*, 13: 240-250.

Van Kan, J. A. L.; Van den Ackerveken, G. F. J. M. and De Wit, P. J. G. M. (1991). Cloning and characterization of cDNA of avirulence gene *avr9* of the fungal tomato pathogen *Cladosporium fulvum*, casual agent of tomato leaf mold. *Mol. Plant-Microbe Interact.*, 4: 52-59.

Van Peer, R.; Nieman, G. J. and Schippers, B. (1991). Induced resistance and phytoalexin accumulation in biological control of fusarium wilt of carnation by *Pseudomonas* sp. strain WCS417r. *Phytopathol.*, 81: 728-734.

Van Wees, S. C. M.; De Swart, E. A.; Van Pelt, J. A.; Van Loon, L. C. and Pieterse, C. M. (2000). Enhancement of induced disease resistance by simultaneous activation of salicylate- and jasmonate-dependent defense pathways in *Arabidopsis thaliana*. *Proc. Natl. Acad. Sci. USA*, 97: 711-8716.

Van Wees, S. C.; Luijendijk, M.; Smoorenburg, I.; Van Loon, L. C. and Pieterse, C. M. (1999). Rhizobacteria-mediated induced systemic resistance (ISR) in *Arabidopsis* is not associated with a direct effect on expression of known defense-related genes but stimulated the expression of the jasmonate-inducible gene *Atvsp* upon challenge. *Plant Mol. Biol.*, 41: 537-549.

Vasudevan, S.G.; Armarego, W.L.F.; Shaw, D.C.; Lilley, P.E.; Dixon, N.E. and Poole, R.K. (1991). Isolation and nucleotide sequence of the *hmp* gene that encodes a haemoglobin-like protein in *Escherichia coli* K-12. *Mol. Gen. Genet.*, 226: 49-58.

Verhagen, B. W. M.; Glazebrook, J.; Chang, H.-S.; Zou, G.; Zhu, T.; Van Loon, L. C. and Pieterse, C. M. V. (2001). Expression profiling of *Arabidopsis* genes during *rhizobacteria*-mediated induced systemic resistance (ISR). In : Abstracts (poster 281) 10th International Congress on Molecular Plant-Microbes Interactions. Madison, Wisconsin July 10-14.

Vernooij, B.; Friedrich, L.; Morse, A.; ReisT, R.; Kolditz-Jawhar, R.; Ward, E.; Ukness, S.; Kessman, H.and Ryals, J. (1994). Salicylic acid is not the translocated signal responsible for inducting SAR but is required in signal transduction. *Plant Cell*, 6: 959-965.

Viard, M.-P.; Martin, F.; Pugin, A.; Ricci, P. and Blein, J.-P. (1994). Protein phosphorylation is induced in tobacco cells by the elicitor cryptogein. *Plant Physiol.*, 104: 1245-1249.

Vijayan, P.; Shockey, J.; Levesque, C. A.; Cook, R. A. and Browse, J. (1998). A role for Jasmonate in pathogen defense of *Arabidopsis*. *Proc. Natl. Acad. Sci. USA*, 95: 7209-7214.

Walbot, V. D. A. *et al.* (1983). Disease leasion mimics in maize. In: Genetic Engineering of Plants (eds T. Kosuge and C. Meredith. Plenum Publishing Company, New York.

Walden, R.; Fritze, K.; Hayashi, H.; Miklashevichs, E.; Harling, H and Schell, J. (1994). Activation tagging: A mean of isolating genes implicated as playing a role in plant growth and development. *Plant Mol. Biol.*, 26: 1521-1528.

Wallace, G. and Fry, S. C. (1999); Action of diverse peroxidases and laccases on six cell wall-related phenolic compounds. *Phytochem.*, 52: 769-773.

Wanner, L. A.; Li, G.; Ware, D.; Somssich, I. E. and Davis, K. R. (1995). The phenylalanine ammonia-lyase gene family in *Arabidopsis thaliana*. *Plant Mol. Biol.*, 27: 327-338.

Ward, E. R.; Uknes, S. J.; WiliamS, S. C.; Dincher, S. S.; Wiederhold, D. L.; Alexander, D. C.; Ahl-Goy, P.; Metraux, J. P., and Ryals, J. A. (1991). Cooridnated gene activity in response to agents that induce systemic acquired resistance. *Plant Cell*, 3: 1085-1094.

Ward, J. M.; Pei, Z. M. and Schroeder, J. I. (1995). Roles of ion channels in initiation of signal transduction in higher plants. *Plant Cell,* 7: 833-844.

Warren, R. F.; Merritt, P. M.; Holub, E.; and Innes, R. W. (1999). Identification of three putative signal transduction genes involved in R gene-specified resistance in *Arabidopsis*. *Genetics*,152: 401-412.

Weigel, D.; Ahn, J. H.; Blazquez, M. A.; Borevitz, J. O.; Christensen, S. K.; Fankhauser, C.; Ferrandiz, C.; Kardailsky, I.; Malancharuvil, E. J.; Neff, M. M.; Nguyen, J. T.; Sato, S.; Wang, Z. Y.; Xia, Y.; Dixon, R. A.; Harrison, M. J.; Lamb, C. J.; Yanofsky, M. F. and Chory, J. (2000). Activation tagging in Arabidopsis. *Plant Pysiol.*, 122:1003-1013.

Welinder, K. G. (1992). Plant peroxidases: structure, function relationships. In: Plant Peroxidases 1980-1990, Topics and Detailed Literature on Molecular, Biochemical and Physiological Aspects (eds. C. Panel, T. Gaspar, H Greppin). Université de Genéve, Geneva, Switzerland, pp. 1-24.

Welinder, K. G.; Jespersen, H. M.; Kjaersgard, I. V. H.; Ostergaard, L.; Abelskov, A. K.; Hansen, L. N.; Rasmussen, S. K. (1996). What can we learn from Arabidopsis peroxidases?. In: Plant Peroxidases: Biochemistry and Physiology (eds. C. Obinger, U. Burner, R. Ebermann, C. Penel, H. Greppin). Université de Genéve, Geneva, Switzerland, pp. 173-178.

Wendehenne, D.; Pugin, A; Klessig, D. F. and Durner, J. (1998). Nitric oxide: comparative synthesis and signaling in animal and plant cells. *Trends Plant Sci.,* 6:177-183.

Weymann, K.; Hunt, M.; Uknes, S.; Neuenschwander, U.; Lawton, K.; Steiner, H.-Y. and Ryals, J. (1995). Suppression and restoration of lesion formation in *Arabidopsis lsd* mutants. *Plant Cell*, 7: 2013-2022.

Whalen, M. C.; Innes, R. W.; Bent, A. F. and Staskawicz, B. J. (1991). Identification of *Pseudomonas syringae* pathogen of *Arabidopsis* and a bacterial locus determining avirulence on both *Arabidopsis* and soybean. *Plant Cell,* 3: 49-59.

Whitham, S.; Denish-Kumar, S. P.; Choi, D.; Hehl, R.; Corr, C. and Baker, B. (1996). The product of the tobacco mosaic virus resistance gene *N*: similarity to Toll and the interleukin-1 receptor. *Cell*, 78: 1101-1115.

Wilde, M. C.; Dewdney, J.; Wu, G. and Ausubel, F. (2001). Isochorismate synthase is required to synthesize salicylic acid for plant defence. *Nature*, 414: 562-565.

Wildermuth, M. C.; Dewdney, J.; Wu, G. and Ausubel, F. M. (2001). Isochorismate synthase is required to synthesize salicylic acid for plant defence. *Nature*, 414: 562-565.

Wildt, I. *et al.* (1997). Emission of NO from several higher plant species. *J. Geo. Res.* 102: 5919-5927.

Willmott, N.; Sethi, J. K.; Walseth, T. F.; Lee, H. C.; White, A. M. and Galione, A. (1996). Nitric oxide)induced mobilization of intracellular calcium via the cyclic ADP-ribose pathway. *J. Biol. Chem.,* 271: 3699-3705.

Wobbe, K. K. and Zhao, Y. (1998). Avirulence determinant of turnip crinkle virus localized to the N-terminus of the coat protein. In Abstracts of the 17th Annual Meeting of American Society for Virology (Vancouver: American Society for Virology), p. 169, P6–20.

Wolter, M. K.; Hollricher, K.; Salamini, F. and Schulze-Lefert, P. (1993). The *mlo* resistance alleles to powdery mildew infection in barley trigger a developmentally controlled defence mimic phenotype. *Mol. Gen. Genetics* 239, 122-128.

Worley, C. K.; Maliszewski, L. E.; Hubner, J. H. and Shapiro, A. D. (2001). Genetic screen to identify *hdn Arabidopsis* mutants: *H*R *d*espite *N*OS inhibitor. Abstracts: 10th International Congress on Molecular Plant-Micribe Interactions, Wisconsin (July 10-14).

Wulff, B. B.; Thomas, C. M.; Smoker, M. ;Grant, M. and Jones, J. D. (2001). Domain swapping and gene suffling identify sequences required for induction of an avr-dependent hypersensitive response by the tomato cf-4 and cf-9 proteins. *Plant Cell*, 13: 255-272.

Xiao, S.; Ellwood, S.; Calis, O.; Patrick, E.; Li, T.; Coleman, M. and Turner, J. G. (2001). Broad-specturm mildew resistance in *Arabidopsis thaliana* mediated by RPW8. *Science*, 291: 118-120.

Xie, D.-X.; Feys, B. F.; James, S., Nieto-Rostro, M. and Turner, J. G. (1998). *COI1*: An *Arabidopsis* gene required for jasmonate-regulated defense and fertility. *Science*, 280: 1091-094.

Xu, H. & Heath, M. C. (1998). Role of calcium in signal transduction during the hypersensitive response caused by basidiospore-derived infection of the cowpea rust fungus. *Plant Cell,* 10: 585-597.

Xu, L.; Liu, F.; Wang, Z.; Peng, W.; Huang, R.; Huang, D. and Xie, D.(2001). An Arabidopsis mutant *cex1* exhibits constant accumulation of jasmonate-regulated *AtVSP*, *Thi2.1* and *PDF1.2*. *FEBS Lett.*, 494:161-164.

Xu, Y.; Linda-Chang, P.-F.; Liu, D.; Narasimhan, M. L.; Raghothama, K. G.; Hasegawa, P. M. and Bressan, R. A. (1994). Plant defense genes are synergistically induced by ethylene and methyle jasmonate. *Plant Cell* 6, 1077-1085.

Yalpani, N.; Leo, J.; Lawton, M. and Raskin, I. (1993). Pathway of SA biosynthesis in healthy and virus-inoculated tobacco. *Plant Physiol.*, 103: 315-321.

Yalpani, N.; Silverman, P.; Wilson, T. M. A.; Kleier, D. A. and Raskin, I. (1991). Salicylic acid is a systemic signal and an inducer of pathogenesis-related proteins in virus-infected tobacco. *Plant Cell*, 3: 809-818.

Yamasaki, H.; Sakihama, Y. and Takahashi, S. (1999). An alternative pathway for nitric oxide production in plants; new features of an old enzyme. *Trends Plant Sci.*, 4: 128-129.

Yamasaki, H.; Sakihama, Y. and Takahashi, S. (1999). An alternative pathway for nitric oxide production in plants: new features of an old enzyme. *Trends Plant Sci.*, 4: 128-129.

Yang, K. Y.; Kim, E. Y.; Kim, C. S.; Guh, J. O.; Kim, K. C. and Cho, B. H. (1998). Characterization of a glutathione S-transferase gene *ATGST1* in *Arabidopsis thaliana*. *Plant Cell Reports*, 17: 700-704.

Yang, Y.; Shah, J. and Klessig, D. F. (1997). Signal perception and transduction in plant defencse responses. *Genes rev.*, 11: 1621-1639.

Yazazi, K.; Heide, L. and Tabata, M. (1991). Formation of *p*-hydroxy benzoic acid from *p*-commaric acid by cell free extracts of *L. erythrorhizon* cell cultures. *Phytochem.*, 7: 2233:2236.

Yoshioka, K.; Kachroo, P.; Tsui, F.; Sharma, S. B.; Shah, J. and Klessig, D. (2001). Environmentally sensitive, SA-dependent defense responses in the *cpr22* mutant of *Arabidopsis*. *Plant J.*, 26: 447-459.

Yu, I. C.; Fengler, K. A.; Clough, S. J. and Bent, A. F. (2000). Identification of *Arabidopsis* mutants exhibiting an altered hypersensitive response in gene-for-gene resistance. *Mol. Plant Microbe Interact.*, 13: 277-286.

Yu, I.-C.; Parker, J. and Bent, A. F. (1998). Gene-for-gene resistance without the HR in *Arabidopsis dnd1* mutant. *Proc. Natl. Acd. Sci. USA*, 95: 7819-7824.

Zhang, S. & Klessig, D. F. (1997). Salicylic acid activates a 48 kD MAP kinase in tobacco. *Plant Cell* 9, 809-824.

Zhang, Y.; Fan, W.; Kinkema, M.; Li, X. and Dong, X. (1999). Interaction of NPR1 with basic leucine zipper protein transcription factors that bind sequences required for salicylic acid induction of the PR-1 gene. *Proc. Natl. Acad. Sci. USA*, 96: 6523-6528.

Zheng, M.; Aslund, F. and Storz, G. (1998). Activation of the OxyR transcription factor by reversible disulfide bond formation. *Science,* 279:1718-1721.

Zhong, H. H. and McClung, C. R. (1996). The circadian clock gates expression of two *Arabidopsis* catalase genes to distinct and opposite circadian phases. *Mol. Gen. Genet.*, 251: 196-203.

Zhou, J. M.; Trifa, Y.; Silva, H.; Pontier, D.; Lam, E.; Shah, J. and Klessig, D. F. (2000). NPR1 differentially interacts with memebers of the TGA/OBF family of transcription factors that bind an element of PR-1 gene required for induction by salicylic acid. *Mol. Plant Microbe Interact.*, 13: 191-202.

Zhou, N.; Tootle, T. L. and Glazebrook, J. (1999). *Arabidopsis PAD3*, a gene required for camalexin biosynthesis, encodes a putative cytochrome P450 monooxygenase. *Plant Cell*, 11: 2419-2428.

Zhou, N.; Tootle, T. L.; Tsui, F.; Klessig, D. F. and Glazebrook, J. (1998). PAD4 functions upstream from salicylic acid to control defense responses in *Arabidopsis*. *Plant Cell*, 10: 1021-1030.

Zhu, Q.; Maher, E. A.; Masoud, S.; Dixon, R. A. and Lamb, C. J. (1994). Enhanced protection against fungal attack by constitutive co-expression of chitinase and glucanase genes in transgenic tobacoo. *Biotechnology*, 12: 807-812.